MOLECULAR MECHANISMS IN P25/CDK5-MEDIATED NEUROINFLAMMATION AND SUBSEQUENT NEURODEGENERATION: THERAPEUTIC IMPLICATIONS FOR ALZHEIMER'S DISEASE

JEYAPRIYA RAJAMEENAKSHI SUNDARAM

(MSc., MPhil)

A THESIS SUBMITTED FOR THE DEGREE OF DOCTOR OF PHILOSOPHY

DEPARTMENT OF PHARMACOLOGY

NATIONAL UNIVERSITY OF SINGAPORE

2013

DECLARATION

I hereby declare that the thesis is my original work and it has been written by me in its entirety. I have duly acknowledged all the sources of information which have been used in the thesis.

This thesis has not been submitted for any degree in any university previously.

Jeyapriya Rajameenakshi Sundaram

31st July 2013

i

ACKNOWLEDGEMENTS

TABLE OF CONTENTS

SUMMARY

Alzheimer's disease (AD) is a progressive neurodegenerative disorder that leads to irreversible memory loss. An escalating burden of AD, with an ever growing aging population, will lead to an extensive increase in healthcare costs. AD is characterized by the presence of pathological features including intracellular neurofibrillary tangles, extracellular amyloid plaques, extensive neuroinflammation and neuronal/synaptic loss in selected areas of the brain. Although several studies have specified that neuroinflammation is associated with AD pathology, the exact mechanisms have not been fully elucidated. Moreover, a better understanding of the mechanisms behind the initiation and progression of AD pathology will guide future studies to develop effective treatment strategies.

Deregulation of Cyclin-dependent kinase 5 (Cdk5) by production of its hyperactivator p25 (a fragment of its normal activator, p35), is involved in the formation of tau and amyloid pathology reminiscent of AD. Recent studies have shown that p25/Cdk5 hyperactivation is also associated with robust neuroinflammation. Therefore, the transgenic mouse that overexpresses p25 has the potential to be used as a mechanistic model to investigate the neuroinflammation and associated neurodegenerative changes *in vivo*. Although several studies supported the role of Cdk5 in neurodegeneration, the actual mechanism behind the initiation of p25/Cdk5-mediated neuroinflammation and its role in the progression of neurodegeneration has not been clearly demonstrated. Hence, this thesis aims to investigate the p25/Cdk5-mediated neuroinflammatory mechanisms using *in vitro* p25 overexpressing neurons and to translate this *in vivo* in the CamK2a-p25 inducible transgenic (p25Tg) mice. The first half of this thesis deals with the characterization of the neuroinflammatory pathways regulated by p25 overexpression and the second half covers the investigation of beneficial effects of early intervention of p25-mediated neuroinflammation in the progression of neurodegeneration in p25Tg mice using a potent natural anti-inflammatory agent, curcumin.

Results showed the onset of neuroinflammation in p25Tg mice and the involvement of astrogliosis as an early event in the absence of microgliosis, tau and amyloid pathology. Subsequent *in vitro* characterization identified that neuronal cytosolic phospholipase 2 (cPLA2) upregulation-mediated production of a soluble lipid, lysophosphatidylcholine (LPC) was crucial for the initiation of p25 overexpression-mediated neuroinflammation and the progression of neurodegeneration. In addition, results from *in vitro* gene silencing experiments clearly showed that the inhibition of p25-induced neuroinflammation reduced the progression of tau/amyloid pathology and subsequent neurodegeneration.

These novel findings were then validated further *in vivo* in p25Tg mice using curcumin, a multipotent natural compound that can cross the blood-brain barrier without any adverse side effects. Results showed an obvious reduction in the major events of inflammatory pathways including astrocyte activation, cPLA2 upregulation and LPC production. Moreover, this curcumin-mediated suppression of neuroinflammation efficiently limited the progression of p25-induced tau/amyloid pathology and in turn ameliorated the p25-induced cognitive impairments.

Together, results from this study have identified a novel pathway behind p25-induced neuroinflammation and subsequent neurodegeneration. Data from this study could open exciting avenues of research to find effective therapeutic interventions against neuroinflammation and subsequent neurodegeneration that could be utilized in neurodegenerative diseases especially AD.

LIST OF TABLES

LIST OF FIGURES

LIST OF ILLUSTRATIONS

LIST OF ABBREVIATIONS

AACOCF3	Arachidonyl trifluoromethyl ketone
Aβ	amyloid-β
AchE	Acetylcholinesterase
AD	Alzheimer's disease
ALS	Amyotrophic lateral sclerosis
ApoE	Apolipoprotein E
APP	Amyloid precursor protein
ATP	Adenosine-5'-triphosphate
BACE	β-secretase
BBB	Blood–brain barrier
BCA	Bicinchoninic acid
BEL	Bromoenol lactone
BME	Beta-mercaptoethanol
BSA	Bovine serum albumin
CaMK II	Ca2+/calmodulin-depedent protein kinase II
Cdk5	Cyclin dependent kinase 5
cDNA	Complementary DNA
CIP	Cdk5 inhibitory peptide
CNS	Central nervous system
cPLA2	Cytosolic phospholipase A2
CSF	Cerebrospinal fluid

DAPI	4′,6-Diamidino-2-phenylindole dihydrochloride
DH5α	Douglas Hanahan bacterial strain 5α
DIC	Days in culture
DMEM	Dulbecco's minimal essential medium
DMSO	Dimethyl sulphoxide
DNA	Deoxyribonucleic acid
DNase	Deoxyribonuclease
dNTP	Deoxyribonucleotide triphosphate
DTT	Dithiothreitol
EBSS	Earle's balanced salt solution
ECL	Enhanced chemiluminescence
EDTA	Ethylenediaminetetraacetic acid
EGTA	Ethylene glycol-bis (β-amino ethyl Ether)-N, N, N', N' -tetra-acetic acid
EV	Empty vector
FAD	Familial Alzheimer's disease
FBS	Fetal bovine serum
GFAP	Glial fibrillary acidic protein
GFP	Green fluorescent protein
GSK-3β	Glycogen synthase kinase-3 beta
HEK	Human embryonic kidney
HEPES	4-(2-hydroxyethyl)-1-piperazineethanesulfonic acid
HPLC	High-performance liquid chromatography

IgG	Immunoglobulin subtype gamma
IL-1β	Interleukin-1β
iPLA2	Calcium-independent phospholipase A2
kDa	Kilodalton
LB	Luria Bertani
LC-MS	Liquid chromatography-mass spectrometry
LPC	Lysophosphatidylcholine
LV	Lentivirus
MAP	Microtubule associated protein
MCI	Mild cognitive impairment
MIP-1α	Macrophage inflammatory protein-1α
mRNA	Messenger RNA
NaCl	Sodium chloride
NaF	Sodium fluoride
Na$_3$VO$_4$	Sodium orthovanadate
NF-H	Neurofilament-heavy chain
NF-κB	Nuclear factor-kappa B
NFT	Neurofibrillary tangles
NMDA	N-methyl-D-aspartate
NSAID	Nonsteroidal anti-inflammatory drug
NSE	Neuron-specific enolase
PBMC	Peripheral blood mononuclear cells
PBS	Phosphate suffer saline

PC	Phosphatidylcholine
pCMV	Cytomegalovirus promoter
PCR	Polymerase chain reaction
PD	Parkinson disease
PFA	Paraformaldehyde
PHF	Paired helical filament
RBC	Red blood cells
RNA	Ribonucleic acid
RNase	Ribonuclease
ROS	Reactive oxygen species
RT-PCR	Real-time PCR
SDS	Sodium dodecyl sulphate
SDS-PAGE	Sodium dodecyl sulphate polyacrylamide gel electrophoresis
shRNA	Short hairpin RNA
SLCP	Solid lipid curcumin particle
SOD	Superoxide dismutase
SPE	Solid phase extraction
sPLA2	Secretory phospholipase A2
STAT3	Signal transducer and activator of transcription 3
TAE	Tris-Acetate-EDTA
TBST	Tris buffered saline and Tween 20
TER	Tetracycline-responsive promoter element

Tg	Transgenic
TGF-β	Transforming growth factor-β
TNF-α	Tumor necrosis factor-alpha
tPA	Tissue plasminogen activator
TRIS	Tris(hydroxymethyl)aminomethane
tTA	Tetracycline-controlled transactivator
TUNEL	Terminal deoxynucleotidyl transferase dUTP nick end labeling
WT	Wild-type

LIST OF PUBLICATIONS AND AWARDS

Research Articles

1. Charlene P. Poore,*** Jeyapriya Raja Sundaram**,* Tej K. Pareek, Amy Fu, Niranjana Amin, Nur Ezan, Mohamed,Ya-Li Zheng, Angeline X. H. Goh, Mitchell K. Lai, Nancy Y. Ip, Harish C. Pant, and Sashi Kesavapany (**2010**) Cdk5-mediated phosphorylation of delta-catenin regulates its localization and GluR2-mediated synaptic activity, *Journal of Neuroscience*. June 23rd 2010, 30:8457–8467 (* Equal contribution).

2. **Jeyapriya Raja Sundaram**, Elizabeth S Chan, Charlene P Poore, Tej K Pareek, Wei Fun Cheong, Guanghou Shui, Ning Tang, Chian-Ming Low, Markus R Wenk and Sashi Kesavapany, (**2012**) p25/Cdk5-Induced Cytosolic PLA2-Mediated Lysophosphatidylcholine Production Regulates Neuroinflammation and Triggers Neurodegeneration, *Journal of Neuroscience*. January 18 2012, 32(3):1020-1034.

3. **Jeyapriya Raja Sundaram,** Charlene Priscilla Poore, Noor Hazim Bin Sulaimee, Tej Pareek, ABMA Asad, Ramamoorthy Rajkumar, Wei Fun Cheong, Markus R Wenk Gavin Stewart Dawe, Kai-Hsiang Chuang, Harish C Pant and Sashi Kesavapany (**2013**) Specific Inhibition of p25/Cdk5 Activity by the Cdk5 Inhibitory Peptide (CIP) Reduces Neurodegeneration *in vivo, Journal of Neuroscience*. January 2nd 2013, 33(1): 334-43.

Abstracts

1. **Jeyapriya Raja Sundaram**, Wang Jun Yen, Charlene P. Poore, Ramasamy Tamizhselvi, Tej Kumar Pareek, Harish C. Pant, Madhav Bhatia and Sashi Kesavapany, Studying p25/Cdk5-mediated neuroinflammation and its effect *in vivo*, **Society for Neuroscience 39th Annual Meeting**, 2009, USA.

2. **Jeyapriya Raja Sundaram**, Elizabeth S Chan, Charlene P Poore, Noor Hazim Sulaimee, Tej K Pareek, Wei Fun Cheong, Guanghou Shui, Ning Tang, Chian-Ming Low, Markus R Wenk and Sashi Kesavapany, p25/Cdk5 induced neuroinflammation triggers neurodegeneration via a novel pathway independent of amyloid and tau pathology, **Society for Neuroscience 42nd Annual Meeting**, 2012, USA.

3. Low, C-M., Chan, S-Y., **Sundaram J.R**. and Kesavapany, S. (2013). Targeting cPLA2 inhibition to reduce lysophosphatidylcholine (LPC) production induced by Cdk5/p25: An anti-inflammatory strategy in

neurodegeneration. *Acta Pharmacologica Sinica* 34 (Suppl July): 110. (http:www.chinaphar.com/1671-4083/34/34(7)suppl.htm)

Oral Presentation

1. **Jeyapriya R Sundaram**, Elizabeth S Chan, Charlene P Poore, Tej K Pareek, Wei Fun Cheong, Guanghou Shui, Ning Tang, Chian-Ming Low, Markus R Wenk and Sashi Kesavapany, p25/Cdk5 Production of lysophosphatidylcholine Causes Neuroinflammation and Neurodegeneration, **YLL-SOM Graduate Scientific Congress,** 25th January 2011.

Award

1. Merck Millipore Young Scientist Award Singapore, 2011 (4th Place).

CHAPTER 1

CHAPTER 1: Introduction

1.1 Alzheimer's disease (AD)

Alzheimer's disease (AD), the most common form of dementia, is a chronic, progressive and irreversible degenerative disorder of the brain that will eventually lead to memory loss. Dementia is a group of symptoms that is coupled with a decrease in mental abilities such as thinking, reasoning and memory. Even though the precise cause of AD is unknown, the possible risk factors are increasing age, life style factors, genetic predisposition and previous head injuries. AD is definitively diagnosed only after autopsy and there is currently no cure for AD. However, promising research is underway for early diagnosis and effective treatment of AD.

1.1.1 History of AD

The presence of dementia (Latin: "de mens", without mind) in old people has been reported thousands of years ago by Greek and Roman scholars. Alzheimer's disease was first discovered by a German neurologist and psychiatrist, Dr. Alois Alzheimer (1864–1915) in 1906 (Dahm, 2006). AD was first observed in a female patient, Auguste D. on November 26th , 1901 and she displayed spatial and temporal disorientation, general confusion, anxiety, memory loss, impaired comprehension, psychosocial inaptitude and progressive aphasia (Maurer et al., 1997). Dr. Alzheimer followed her care for five years, until her death in 1906. Later, an autopsy was performed on her brain by Dr. Alzheimer and his colleagues and they found a massive loss of neurons throughout the brain. Furthermore, they observed peculiar thick fibrils and deposits of an unidentified substance throughout the cerebral cortex. Dr. Alzheimer presented his results of the case of Auguste D. for the first time in the 37th meeting of South-West German psychiatrists in Tübingen, Germany on November 3rd, 1906 and he published the Auguste D. case in 1911 (Alzheimer, 1911). Dr. Alzheimer's mentor, Dr. Emil Kraepelin, first renamed this presenile dementia as Alzheimer's disease (AD) in a text book (Kraepelin, 1910; Moller and Graeber, 1998).

1.1.2 Epidemiology of AD

Currently, it is estimated that 6.8 million people in the United States have dementia. Nearly, two-thirds of total cases are women and 4% have younger-onset AD. On average, the estimated annual incidence is approximately 170 new cases per 1,000 people between the ages of 75 to 84. In addition, the aggregate payments for healthcare and long-term care for people with dementia in America are projected to increase from $203 billion in 2013 to $1.2 trillion in 2050 (Hebert et al., 2001; Hebert et al., 2013; Thies and Bleiler, 2013).

According to the World Alzheimer Report 2009, there are an estimated 35.6 million people living with AD and other dementias worldwide. This number will nearly double and reach 66 million by the year 2030 and 115 million by 2050. One new case of dementia is diagnosed every 4 seconds, or 7.7 million cases per year. Based on this global incidence report, more than 600 million people in the world are expected to live with this disease in the next 40 years. According to the World Alzheimer Report 2010, the estimated worldwide cost of dementia in 2010 was US$ 604 billion, nearly equivalent to the cost of the 1% of the world's gross domestic product figure (Wortmann, 2012).

In Singapore, with the ever growing aging population, the escalating burden of AD and the others forms of dementia poses a huge problem for sufferers, families of patients and the healthcare industry. According to dementia statistics in the Asia pacific region in 2006, the prevalence of dementia in Singapore was approximately 22,000 in the year 2005 and this figure would reach 53,000 by 2020 (Alzheimer's Disease Association Singapore). A recent epidemiological study in Singapore reported that nearly 3-8% of people between the ages of 69-75 suffer from dementia and 60% of dementia cases over the age of 69 were AD (Sahadevan et al., 2008).

1.1.3 Types of AD

Sporadic or late onset AD is the most common form of AD, making up 90% of AD cases. It mainly affects people over 65 years of age and is caused by a chronic, nonlinear and dynamic pathophysiological cascade that leads to

neurodegeneration and late-stage clinical dementia (Hampel and Lista, 2012). Early-onset AD without a clear inheritance pattern, accounting for less than 10% of all AD cases, is a rare form of the disease in which individuals are diagnosed before age 65. Early-onset AD is mainly caused by mutations in one of three genes: *presenilin 1 (PS1), presenilin 2 (PS2)* or *amyloid precursor protein (APP)* (Miyoshi, 2009). In addition, Familial AD (FAD), a form of entirely inherited disease, accounts for less than 1% of all cases of AD. It is extremely rare and has a much earlier onset, often starts in the 40s (Bateman et al., 2012).

1.1.4 Risk factors for AD

Advancing age is the best known risk factor for AD and the probability of developing AD doubles every five years after the age of 65. Many studies have investigated the factors that increase the risk of developing AD and some examples are gender (Vina and Lloret, 2010), genetic predisposition (Bertram et al., 2007), family history (Breitner et al., 1986), education (Addae et al., 2003), hypertension (Kalaria et al., 2008), diabetes (Kroner, 2009) and a history of head trauma (Guo et al., 2000). Studies also reported that certain lifestyle factors can decrease the progress of AD and these include diet (Solfrizzi et al., 2011), happiness (Berger et al., 1999) and exercise (Larson et al., 2006).

1.1.5 Diagnosis of AD

Although a brain autopsy is a definitive method of diagnosing AD, comprehensive diagnostic workup such as mental and behavioral tests and physical examinations by skilled physicians can diagnose AD with 90% accuracy. A medical history taken from the patient and from an informant is important in identifying the rate of mental deterioration (McKhann et al., 1984). In addition, physical and neurological examination should be conducted to rule out the other causes of symptoms such as chronic infection, vitamin deficiency, thyroid disorders and problems with the nervous system. Furthermore, recent studies suggested that combined measurements of tau protein, Aβ peptide species and inflammatory molecules from cerebrospinal

fluid (CSF) could provide detailed information on disease progression (Blennow and Zetterberg, 2009; Perrin et al., 2009).

Recently, neuroimaging techniques such as magnetic resonance imaging (MRI) (Teipel et al., 2010), positron emission tomography (PET) (Jia et al., 2011), single-photon emission computerized tomography (SPECT) & fluorodeoxyglucose-PET (FDG-PET) (Jagust et al., 2001; Herholz, 2011), functional MRI (fMRI) (Gountouna et al., 2010), amyloid-PET (Forsberg et al., 2008) and diffusion tensor imaging (DPI) (Beaulieu, 2002) have been widely applied to diagnose AD and discover early changes in brain structure. Additionally, neuropsychological tests may provide further information for the diagnosis of AD. Cognition tests including simple screening tests like the Mini-Mental State Examination (MMSE), the cognitive part of the Alzheimer's Disease Assessment Scale (ADAScog), the Severe Impairment Battery, the Neuropsychiatric Inventory (NPI) and the scale for assessment of behavioral symptoms in AD (Behave-AD) were also conducted to investigate impairments in mental abilities (Folstein et al., 1975; Rosen et al., 1984; Khachaturian, 1985; Harrison et al., 2007; Ito et al., 2007).

1.1.6 Clinical features of AD

AD usually starts with slight memory loss that slowly reduces thinking skills and ultimately erodes the ability to perform daily tasks. Other major symptoms include problems with attention, confusion, impaired judgment, language disturbance, restlessness, hostility, withdrawal, irritability and impulsivity (Bird, 1993). Although the cause of spread of the disease is still poorly understood, the pattern of spreading has been studied extensively by several clinical studies (Locascio et al., 1995). Predicting the course of the disease is a key component that often forms the basis of treatment and healthcare decisions. The clinical features of AD are commonly classified into three stages: pre-clinical AD, mild cognitive impairment, and severe stage dementia. This is based on a set of criteria published by the working group of the National Institute on Aging (NIA) and the Alzheimer's Association (AA) to define the progressive pattern of cognitive and functional impairments (Croisile et al., 2012). However, highly variable individual patterns of

cognitive decline may affect these predictions (Tandon et al., 2006; Komarova and Thalhauser, 2011).

1.1.6.1 Pre-clinical or early stage AD

The pre-clinical stage of AD refers to a period of cognitive decline that precedes the onset of clinical AD. The pre-clinical AD stage consists of a slight decline in cognitive abilities with moderate neuronal damage (Sperling et al., 2011). Pathological changes associated with AD begin in the entorhinal cortex and then proceed to the hippocampus which explains early symptoms such as failing short-term memory (Figure 1.1A). This mild stage usually lasts 2 to 4 years and common symptoms include difficulty retaining new information, difficulty with problem solving or decision making, inappropriate use of words, mood swings, decreased motivation and attention, repeated questions or statements, trouble managing finances or other instrumental activities of daily living, personality changes, misplacing belongings or getting lost and difficulty navigating in familiar surroundings (Forstl and Kurz, 1999; Amieva et al., 2008).

1.1.6.2 Moderate or mild cognitive impairment (MCI) stage AD

The subsequent stage is the longest stage of the disease, lasting for 2 to 10 years. This stage is referred to as mild cognitive impairment (MCI) due to AD and defined by the presence of clear memory impairment and biomarker evidence for AD (Albert et al., 2011). Brain damage has spread to most of the areas of the cerebral cortex that control language and memory (Figure 1.1B). Subsequently, atrophy of the affected areas of the cerebral cortex produces clinical symptoms that are more pronounced and widespread. Patients often experience greater difficulty with memory and may need help with daily activities. Symptoms reported during this stage are greater memory loss, difficulty completing complex tasks, increasing difficulty finding the right words, poor judgment, greater confusion, hallucinations, delusions, suspiciousness, restlessness, agitation, anxiety and sleep disturbances (Mariani et al., 2007; Monastero et al., 2009).

1.1.6.3 Severe stage or dementia due to AD

The final stage is conceptualized as dementia due to AD where brain damage is widespread and most of the vital areas of the brain have atrophied further (Figure 1.1C) (McKhann et al., 2011). Patients might not recognize their own family members or loved ones and are totally dependent on others for all of their care. This stage may last between 1 and 3 years. Common symptoms in this stage include the complete loss of ability to communicate, unresponsiveness to stimuli, weight loss, seizures, difficulty swallowing, oversleeping and loss of bladder and bowel control. Patients may be in bed much or all of the time and death is often the result of other illnesses.

A   **B**   **C**
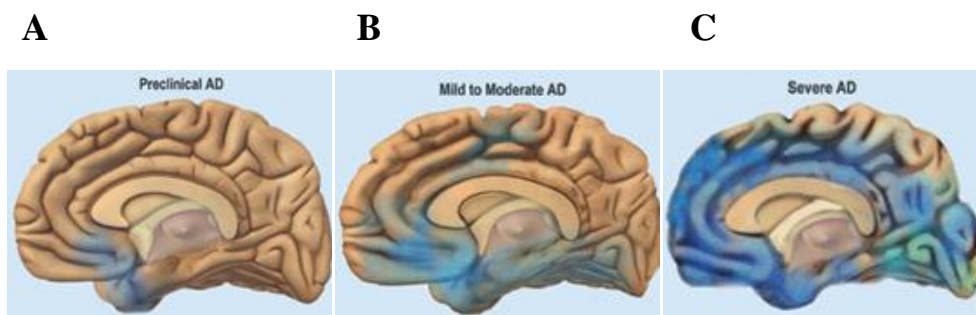
Figure 1.1: Stages of AD pathology

In human AD, pathological accumulations including amyloid plaques and neurofibrillary tangles (shown in blue) start in the transentorhinal region (A), then spread to the hippocampus and amygdala (B) and finally to most of the areas of the neocortex (C). This pattern of spreading strongly coincides with AD clinical presentation and cognitive impairments. Adapted from: (Rodgers et al., 2002)

1.1.7 Pathophysiology of AD

AD is characterized by three pathological features: intracellular neurofibrillary tangles (NFT), extracellular amyloid plaques and neuronal death. Plaques and tangles, first discovered by Dr. Alois Alzheimer in 1906, are usually localized in the brain areas that correspond to the clinical symptoms (Dickson, 1997). The following sections discuss some of the principal theories thought to cause neurodegeneration in AD.

1.1.7.1 The amyloid hypothesis

Amyloid-β plaques are thought to be major contributors to AD pathogenesis with severe and complicated pathophysiological processes. According to the amyloid hypothesis, generation and aggregation of amyloid is the principal causative factor behind the pathogenesis and progression of AD (Hardy and Selkoe, 2002). Amyloid beta precursor protein (APP), a ubiquitous transmembrane receptor-like protein has a critical role in neuronal growth and cell signaling (Thinakaran and Koo, 2008). Studies reported that APP is processed by three enzymes, i.e. β-secretase, γ-secretase and α-secretase (Chow et al., 2010). Under normal conditions, APP is cleaved first by α-secretase, followed by γ-secretase and release a soluble 40 amino acid peptide (Aβ 1-40). In contrast, in the amyloidogenic pathway, APP is cleaved by β-secretase first and then by γ-secretase and release an insoluble 42 amino acid peptide (Aβ 1-42) (Figure 1.2). Subsequently, amyloid-β (Aβ) monomers combined into dimers and oligomers, which in turn self-organized into fibrils and plaques (Zhang et al., 2011). The discovery of the three major genes (*APP, PS1* and *PS2*) in the formation of Aβ in Familial AD gave additional support to the amyloid hypothesis. *APP* gene mutation is the first discovered mutation found to cause Familial AD and there are at least 20 known mutations in the *APP* gene studied so far, located on chromosome 21 (Goate et al., 1991). Subsequently, *PS1* and *PS2* mutations were found to be the most common causes of Familial early-onset AD.
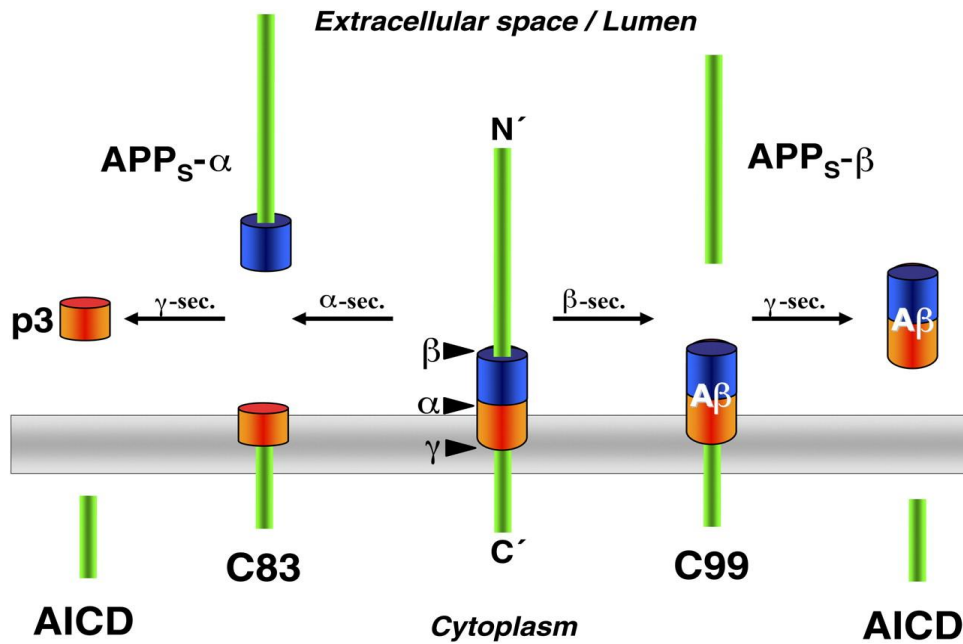
Figure 1.2: APP processing by secretases

In the non-amyloidogenic pathway, amyloid beta precursor protein (APP) is processed first by α-secretase followed by γ-secretase and generates APP intracellular domain (AICD) and extracellular large APP_s-α/p3 fragments. However, in the amyloidogenic pathways, a shorter APP_s species (APP_s-β) is secreted upon the first cleavage by β-secretase. The resulting C99 fragment is further cleaved by γ-secretase to produce Aβ and AICD which may be involved in nuclear signaling. Adapted from : (Kaether and Haass, 2004).

PS1 and *PS2* genes code for the catalytic subunit of γ-secretase and so far 140 and 10 mutations have been studied in *PS1* and *PS2* genes respectively (Rohan de Silva and Patel, 1997). Apolipoprotein E (ApoE) is a cholesterol transport protein abundantly expressed in the liver and the central nervous system (Mahley, 1988). In 1993, the role for ApoE E4 allele in AD was first reported and ApoE E4 allele was found to be more than 3 times as common in AD patients as in age-matched, cognitively-intact controls (Strittmatter et al., 1993). However, how ApoE affects the AD disease process is still unknown. Several studies indicated that ApoE binds directly to the Aβ peptide and promotes fibrillogenesis (Wisniewski et al., 1994; Castano et al., 1995). Aβ plaques were first observed in the temporal neocortex in the initial stage of AD and then progressively spread to the hippocampus and adjoining neocortical areas (Braak and Braak, 1991). The principle argument against the amyloid hypothesis has been the observation that neurofibrillary tangles

correlated more strongly with cognition scores than amyloid plaques (Arriagada et al., 1992; Giannakopoulos et al., 2003; Guillozet et al., 2003). However, other discoveries specified that soluble Aβ oligomers rather than the solid plaques are correlated to the clinical severity of disease and synapse loss (Naslund et al., 2000; Kirkitadze et al., 2002).

1.1.7.2 The tau hypothesis

Besides amyloid-β accumulation, many neurons in AD-affected brain regions also exhibit intracellular inclusions with bundles of abnormal fibers. These inclusions are neurofibrillary tangles (NFTs) which consist primarily of hyperphosphorylated tau (Kosik et al., 1986; Wang et al., 2007). Tau is a part of the microtubule associated protein (MAP) family, which is mainly implicated in microtubule stabilization (Kosik et al., 1986). Hence, tau protein is vital to crucial processes such as cytoskeletal organization, axonal transport and mitotic division (Cuchillo-Ibanez et al., 2008). There are six tau isoforms expressed by alternate splicing from the gene *MAPT*, found on chromosome 17 (Lace et al., 2007). The well-described post-translational modification of tau is phosphorylation and a list of serine (Ser) and threonine (Thr) sites were reported previously (Buee et al., 2000). In addition, protein kinases such as glycogen synthase kinase (GSK-3β), cyclin-dependent kinase 5 (Cdk5) and MAP kinases that phosphorylate tau were also well documented previously (Mandelkow et al., 1995). Conversely, protein phosphatase 2A (PP2A) is the principle enzyme involved in the dephosphorylation of tau (Liu et al., 2005). Hyperactivation of protein kinases such as Cdk5 and significant reductions in PP2A activity were believed to be the reasons behind the tau pathology in AD (Wang et al., 2007). In AD, tau is hyperphosphorylated mainly at Ser 214 and Ser 202 sites and loses its ability to bind to microtubules. This in turn causes microtubule disassembly and defective axonal transport (Li et al., 2007). Additionally, the hyperphosphorylated tau is more prone to aggregate and form NFTs (Figure 1.3). Eventually, this microtubule disassembly and aggregation of NFTs leads to defective synaptic function and then neuronal death (Ihara et al., 1986; Kosik et al., 1986).

In human AD, the pattern of spreading of tau pathology strongly coincides with clinical presentations of AD and cognitive impairments (Braak and Braak, 1991). In contrast, the lack of genetic linkage to the tau pathology has weakened the hypothesis of hyperphosphorylation of tau as a primary process in AD. However, some prominent *tau* gene mutations was discovered to cause neurodegeneration in familial frontotemporal dementia with Parkinsonism linked to chromosome 17 (Spillantini et al., 2000). Hyperphosphorylated tau has been thought to be secondary to Aβ peptide accumulation in AD (Blurton-Jones and Laferla, 2006; Iqbal et al., 2009). However, some studies reported that the tau protein is responsible for the initiation of the neurodegeneration, due to its ability to be predictive of dementia severity (Arriagada et al., 1992; Lace et al., 2007; Iqbal et al., 2009). Therefore, it is clear that the contributions of Aβ and tau to the progression of AD are closely linked and both should be considered in models of the disease.
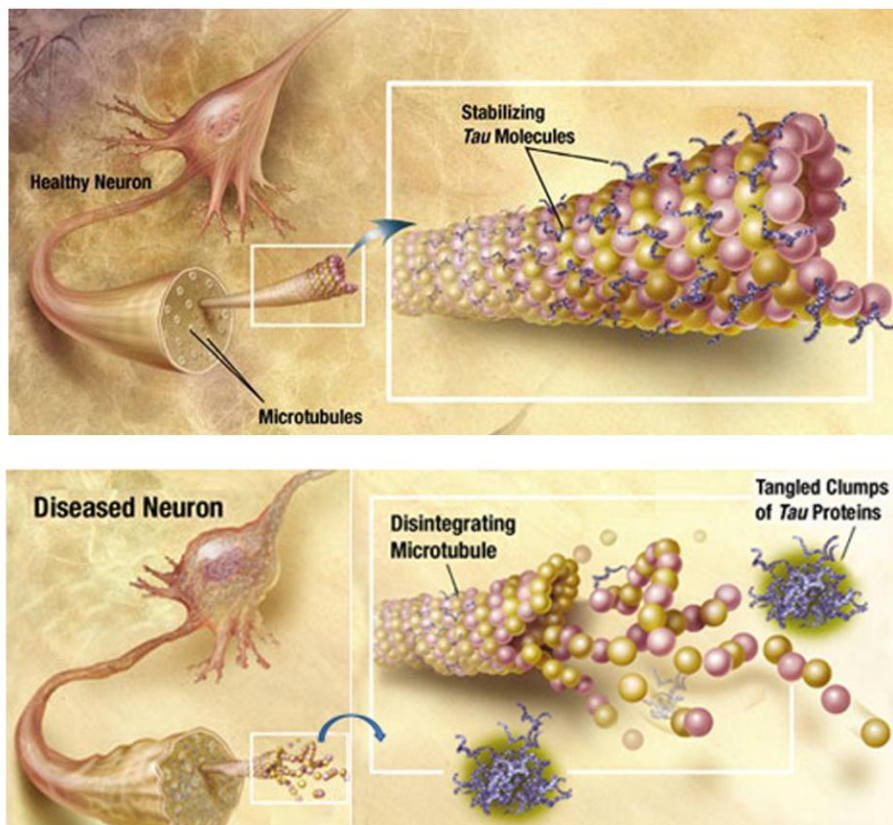
Figure 1.3: Tau pathology in AD

Under normal condition, tau protein binds and stabilizes microtubules. This is important for axonal morphology and function. However, hyperphosphorylation of

tau by hyperactivated protein kinases reduces its ability to binds to microtubules and causes microtubule disassembly. Hyperphosphorylated tau eventually then aggregates to form paired helical filaments (PHF) and NFTs. This leads to microtubule disassembly, defective synaptic function and then finally neuronal death. Adapted from : (National Institute on Aging and Health and Human Services Department, 2003)

1.1.7.3 Potential molecular mechanisms in AD

Cholinergic abnormalities are one of the oldest causal theories of AD where the number of cholinergic neurons and level of acetylcholine (Ach) are drastically reduced during the late stage of AD (Whitehouse et al., 1981; Arendt et al., 1983). Various studies indicated that the most viable therapeutic approach to increase the Ach levels in the brain is to inhibit the enzyme responsible for the degradation of Ach, acetylcholinesterase (AchE). Although currently available AchE inhibitors (donepezil and rivastigmine) effectively increase the level of Ach in AD brain, they failed to provide appreciable improvement in delaying clinical symptoms of the disease (Benzi and Moretti, 1998; Bentham et al., 1999; Jacobson and Sabbagh, 2008). Thus, collective data suggest that cholinergic abnormalities are not the only pathway dysregulated in an AD brain and hence the focus of AD research has now diverged into other causal theories to aid the development of new treatment strategies (Doraiswamy, 2002).

In addition, the endogenous systems for protection against reactive oxygen species (ROS) and oxidative stress are found to be insufficient in early AD. An augmented level of lipid peroxidation has also been observed in human AD brain (Pratico and Sung, 2004). Moreover, key antioxidant enzymes such as glutathione peroxidase and superoxide dismutase (SOD) are depleted in animal models of AD (Smith et al., 1991). Aβ peptides have been proposed as a source and a consequence of oxidative stress in an animal model of AD (Butterfield, 1997). It has been shown that an increased load of ROS is associated with amyloid plaques (McLellan et al., 2003). Furthermore, increased brain deposition of Aβ plaques was also reported in mice generated by crossing APP mutant mice with manganese SOD heterozygous knockout mice (Li et al., 2004). Studies also indicated that there is a close association

between oxidative stress and mitochondrial dysfunction at the early stages of AD (Lin and Beal, 2006).

Programmed cell death (apoptosis) is an important biological process during development and under pathological conditions. Several different triggers of neuronal apoptosis have been documented in AD such as oxidative stress, excitotoxicity caused by an overstimulation of N-methyl-D-aspartate (NMDA) receptors, DNA damage and accumulation of damaged proteins (Lipton and Rosenberg, 1994; Yuan and Yankner, 2000). Amyloid-β exposure can lead to neuronal death through direct or indirect interaction with number of cellular signaling proteins. These include mainly the components of the apoptotic signaling pathways, such as activation of c-Jun N-terminal kinase (JNK), resulting in down regulation of anti-apoptotic proteins (Yao et al., 2005) and the activation of calpain and caspase-3 through an increase in intracellular $Ca2+$ concentrations (Kuwako et al., 2002). Studies also indicated that inflammatory processes with the simultaneous release of pro-inflammatory mediators contributed to neuronal death (Boje and Arora, 1992; Block et al., 2007). Therefore, it is likely that a number of overlapping and interacting factors are involved in the mechanisms of neuronal cell loss in AD.

1.1.8 Neuroinflammation in AD

A wide variety of neurodegenerative diseases share a common conspicuous feature, neuroinflammation, which is a complex event of self-defensive response to injurious stimuli in the CNS (Saez et al., 2004). Pro-inflammatory mediators released by activated glial cells during brain inflammation have been proposed to contribute to neuropathology underlying cognitive deficits (Figure 1.4) (Frank-Cannon et al., 2009). Neuroinflammation in AD can be considered as a double-edged sword which has both beneficial effects by degrading toxic substances including Aβ and adverse effects by producing cytotoxic substances that contribute to disease progression (Akiyama et al., 2000). Optimal activation of immune cells are important for phagocytosis of Aβ, whereas hyperstimulation may eventually lead to neuronal death (Koistinaho et al., 2004; Simard et al., 2006). Studies over several years have indicated that neuroinflammation is indeed associated with AD pathology. In

fact, Dr. Alois Alzheimer himself noticed and reported the sign of inflammatory changes in the demented brain. Studies have found that pro-inflammatory cytokines are found at or near sites of pathological lesions in the AD brain (Johnston et al., 2011). Moreover, numerous epidemiological studies have found that the use of nonsteroidal anti-inflammatory drugs (NSAID) may be associated with reduced risk of AD development (Rogers et al., 1993; McGeer et al., 1996; Hirohata et al., 2008). Hence compelling evidences clearly suggest that there is a strong correlation between neuroinflammation and AD disease progression. However, the exact mechanism behind the link is not fully elucidated; whether it is a secondary process or directly involved in the initiation of the AD pathology is still unclear.
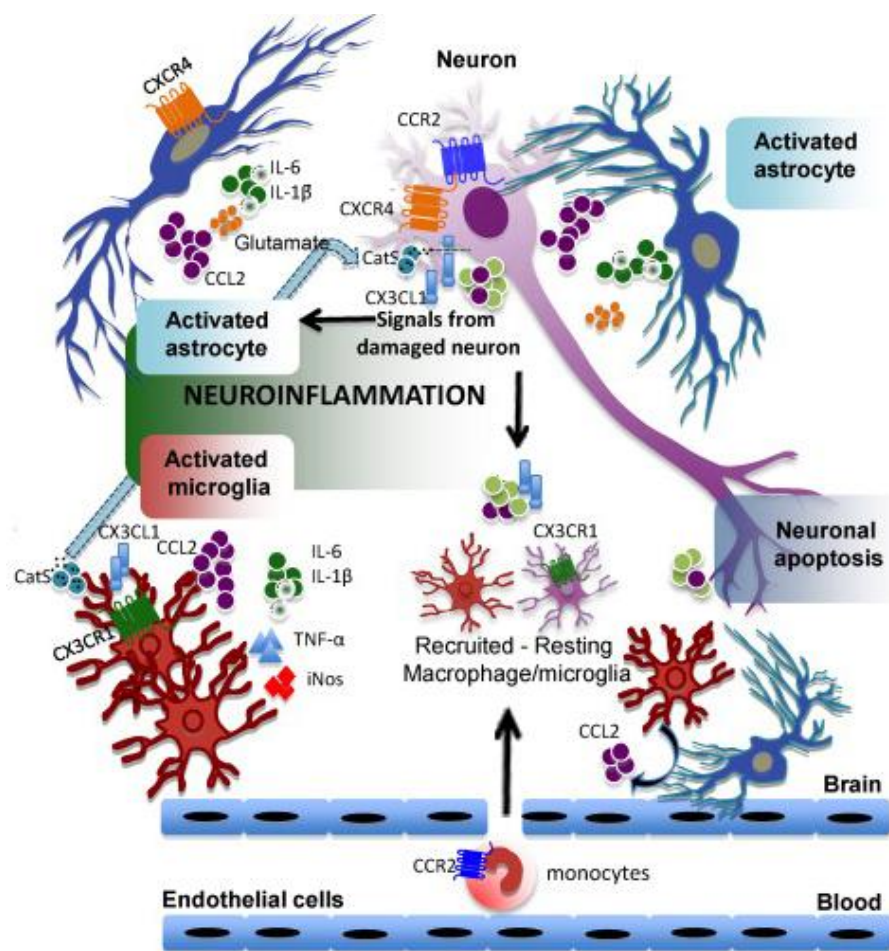
Figure 1.4: Schematic diagram showing the pathogenesis of chronic neuroinflammation

Chronic activation of resident immune cells (astrocytes and microglia) and macrophage recruitment by signals from injured neurons lead to the copious secretion of pro-inflammatory chemokines/cytokines which in turn causes neuroinflammation and subsequent neuronal cell death. Adapted from : (Reaux-Le Goazigo et al., 2013)

1.1.8.1 Role of glia in AD

1.1.8.1.1 Astrocytes

Astrocytes are the most abundant non-neuronal cells in the brain and act as the main element of the homoeostatic system of the brain (Simard and Nedergaard, 2004). They protect the microarchitecture of the brain and regulate the blood-brain barrier (BBB). Astrocytes also control the microenvironment of the central nervous system and defend the nervous system against various insults (Zonta et al., 2003; Kofuji and Newman, 2004; Takano et al., 2006). Astroglial cells form the first line of brain defense by limiting the intrinsic excitotoxicity of the neurons and provide the main antioxidant system in the brain (Rothstein et al., 1996). At the same time, astroglial cells can contribute to neuronal damage when severe insults compromise astrocyte metabolism by the reversal of glutamate uptake system (Vesce et al., 2007). In addition, neurotoxic insults elicit a defensive glial reaction, known as reactive astrogliosis, which facilitates the remodelling of brain circuits in areas surrounding the damaged region with a permanent glial scar (Alonso and Privat, 1993; Pekny and Nilsson, 2005; Sofroniew, 2005). Astrogliosis is also characterized by the robust synthesis of glial fibrillary acidic protein (GFAP) intermediate filaments and several studies have shown that GFAP is a specific marker for astrocytic activation (Eng and Ghirnikar, 1994; Jones et al., 1996). Prominent astrogliosis surrounding amyloid plaques is the main astroglial reaction found in the human AD brain (Nagele et al., 2004). Interestingly, increases in GFAP-mRNA and immunoreactivity have also been observed previously in the human AD brain (Harpin et al., 1990; Le Prince et al., 1993). The role of astrogliosis in the development of AD pathology was also reported in several animal models of AD (Muyllaert et al., 2008; Olabarria et al., 2010; Beauquis et al., 2012). In addition, reactive astrogliosis with altered GFAP expression was observed in other neurodegenerative diseases such as Amyotrophic lateral sclerosis (ALS), Parkinson's disease (PD) and Huntington's disease (Maragakis and Rothstein, 2006). Reactive astrogliosis in AD can be initiated by several factors, which include signals from damaged neurons as well as extracellular deposition of the amyloid-β peptide (Meda et al., 2001). The activated astrocytes in AD

brain are intimately involved in the progression of neuroinflammation through the release of cytokines, pro-inflammatory factors and nitric oxide/reactive oxygen species (Mrak and Griffin, 2005).

It is still under debate whether astrogliosis has a role in the initiation of AD pathology or it is just a secondary event in AD pathology. Recent studies showed that the treatment of cultured glial cells with aggregated amyloid-β triggered reactive astrogliosis (Paradisi et al., 2004). The role of astrocyte responses in Aβ-induced neuronal loss was reported in another recent study using co-culture systems with rat primary astrocytes and neurons (Garwood et al., 2011). At the same time, studies also demonstrated that cytokines released from astroglia could trigger Aβ production through the activation of astrocytic β-site APP cleaving enzyme 1 (BACE 1) (Zhao et al., 2011). Moreover, astroglial BACE 1 was significantly increased in activated astrocytes surrounding Aβ plaques in several transgenic AD mice models, such as Tg2576 and the double mutated K670N-M671L APP model (Heneka et al., 2005; Rossner et al., 2005). In summary, for a long time, astrocytes were thought to be merely "brain glue" and the role of astroglial activation in AD progression still remain largely unexplored. Hence, more studies are needed to unravel this mystery (Maragakis and Rothstein, 2006).

1.1.8.1.2 Microglia

Microglia are the primary innate immune cells in the CNS and represent 10% of all brain cells (Hughes, 2012). In addition, microglial cells show various phenotypes depending on the age and brain region (Hart et al., 2012). In their resting state, they display a ramified morphology with long and dynamic processes. The main role of resting microglia is to constantly move and scan the environment for harmful agents (Nimmerjahn et al., 2005). Upon activation, microglia proliferate, migrate to the site of lesion and undergo a drastic change to an amoeboid morphology with short processes (Ayoub and Salm, 2003). These reactive microglial cells then start to express surface antigens such as major histocompatibility complex (MHC)-II and subsequently release pro-inflammatory mediators including cytokines and complement factors (Heneka and O'Banion, 2007). The main role of this

process is to remove the toxic debris and protect neurons from damage (Schlachetzki and Hull, 2009). However, under chronic neurotoxic insults in various neurodegenerative disease states, prolonged release of inflammatory mediators is thought to cause neurodegenerative changes (Block et al., 2007). In particular, sustained neurotoxic insults in AD brains shift microglia towards a pro-inflammatory phenotype with reduced phagocytic abilities (Luo and Chen, 2012). However, it is still not clear why and when microglia switch from being beneficial to detrimental in the course of AD.

Marked increases in reactive astrocytes and microglia, especially around Aβ plaques, have been observed in many AD mouse model studies (Frautschy et al., 1998). In addition, Aβ has been shown to attract and activate microglia leading to the clustering of microglial cells around Aβ deposits (Combs, 2009; Cameron and Landreth, 2010). Furthermore, studies suggested that clustering of activated microglial cells in the brains of mice with deposited amyloid is a phagocytic attempt to clear the Aβ deposits (Bornemann et al., 2001). Nevertheless, more studies are required to delineate the role of microglial activation in AD whether it is a primary trigger or a secondary consequence to the Aβ pathology (Lautner et al., 2011). Together, findings from several studies emphasized that proper understanding of the complex role of innate immune processes in neurotoxicity will help future therapeutic development.

1.1.8.2 Role of inflammatory chemokines and cytokines in AD pathology

The role of bi-directional communication between microglia and astrocytes through the release of inflammatory cytokines and chemokines in the course of AD has been well studied previously (Tuppo and Arias, 2005). Cytokines and chemokines are small, soluble signaling molecules secreted by microglia and astrocytes to mediate the immune response. Likewise, neurotoxic insults including Aβ are able to induce cytokine production through the stimulation of the nuclear factor-kappa B (NF-κB) dependent pathway (Combs et al., 2001). Upregulation of various chemokines and their receptors has been observed in the AD brain (Xia and Hyman, 1999). Detection of macrophage inflammatory protein-1α (MIP-1α) in reactive astrocytes near Aβ plaques strongly supported the role of astrocytes-mediated response in the pathological progression of

AD. In addition, an *in vitro* study found a remarkable increase in the expression of chemokines such as interleukin 8 (IL-8), monocyte chemotactic protein-1 (MCP-1) and MIP-1α from the astrocytes after treatment with Aβ (Lue et al., 2001; Smits et al., 2002). In the same manner, changes in levels of many cytokines have also been described in AD brains (Tuppo and Arias, 2005). Based on their biological activity, cytokines are classified as pro-inflammatory (IL-6, IL-1β and TNF-α) and anti-inflammatory (IL-4, IL-10 and TGF-β) (Luster, 1998). In general, cytokines such as IL-1β (interleukin-1β), IL-6 (interleukin-6), TNF-α (tumor necrosis factor-alpha), IL-8 (interleukin-8) and TGF-β (transforming growth factor-β) seem to be up regulated during the course of AD (Akiyama et al., 2000). Moreover, neuron-mediated production of IL-1 (interleukin-1), IL-6, and TNF-α under stress conditions has also been reported. Indeed, these neuronal cytokines act as messengers between neurons and glial cells. Both IL-1 and IL-6 were found to be effective in the induction of astrogliosis and activation of microglia (Castell et al., 1989; Mrak and Griffin, 2001). Clinical evidence showed that there was a tremendous elevation in levels of TNF-α, the "master regulator" of the immune response in the cerebrospinal fluid of AD patients (Tarkowski et al., 2003). Additionally, the finding of TNF-α-mediated beta-amyloid-induced inhibition of long-term potentiation further supported the association of TNF-α with the memory impairment in AD (Wang et al., 2005). Various studies have determined that TNF-α contributes to neuronal dysfunction via its interactions with glutamate (Zou and Crews, 2005) and amyloid (Floden et al., 2005).

In addition, anti-inflammatory cytokines like IL-4 (interleukin-4), IL-10 (interleukin-10), TGF-β and IL-13 (interleukin-13) are also elevated in AD as a regulatory response to maintain homeostasis in the brain (Chao et al., 1994; Rota et al., 2006). These anti-inflammatory cytokines have been observed as inhibitory agents to the Aβ-induced neurotoxicity-mediated activation of microglial cells. In particular, IL-4 and TGF-β were found to reduce the expressions and activities of CD40 and class II major histocompatibility complex (MHC) (O'Keefe et al., 1999). More recently, decreased expression of TGF-β receptor and subsequent reduced neuronal TGF-β signaling were observed in both human AD cases and in AD mouse models (Das and Golde,

2006). In summary, it is crucial to preserve the balance between pro- and anti-inflammatory cytokines/chemokines in the brain for the maintenance of optimal neuronal function. Chronic inflammation can result from imbalances between the levels of these inflammatory mediators (Lue et al., 2010).

1.1.8.3 Peripheral leukocyte infiltration in neurodegenerative diseases

Recent studies provide evidence that discrete populations of peripherally-derived immune cells traffic to the CNS during disease states (Rezai-Zadeh et al., 2009). Although peripheral leukocyte migration and infiltration into the brain parenchyma is tightly regulated at the level of the BBB (Engelhardt, 2008), neuroimmune surveillance by peripheral leukocytes does occur in instances of disease. Indeed, this peripheral leukocyte migration is influenced by inflammatory cytokines and chemokines such as MIP-1α and TNF-α (Ramos et al., 2005). The occurrence of brain infiltration of significant number of bone marrow-derived macrophages has been observed in murine models of AD. It has also been reported that these cells were effective in the clearance of Aβ accumulations from the brain (Stalder et al., 2005; Simard et al., 2006). Although there have been some concerns about the occurrence of brain infiltration of peripheral monocytes (Ajami et al., 2007; Mildner et al., 2007), two recent reports provided positive evidence that peripheral monocytes/macrophages can act to restrict amyloid-β plaques (Town et al., 2008; Hawkes and McLaurin, 2009). Hence, further studies are required to clearly understand the role of peripheral leukocyte infiltration in the course of AD.

1.1.9 Transgenic mice models of AD

Multiple transgenic mouse models have been developed using familial AD mutations as a basis. Although these models do not completely replicate all aspects of the disease, they have been useful in understanding some of the mechanisms involved in the progression of AD (Spires and Hyman, 2005; Torres-Aleman, 2008). Mice are a particularly attractive model system due to their relatively easy genetic manipulation, short lifespan and ease of breeding. They can be engineered to develop specific pathological features which closely mimic aspects of human AD. However, there are a number of caveats

and limitations including ageing, environmental factors and genetic variability which must be considered (Jucker, 2010). Although mice models harboring mutations found in familial AD have led to the development of unique therapeutic strategies, none of the preclinical findings have translated into clinical success. This translational failure of promising animal studies is mainly due to the inadequate internal and external validity of preclinical studies. Hence, the external validity of mouse studies could be obtained by including more than one mouse model, testing at multiple sites and using adequately powered designs to confirm treatment effects (van der Worp et al., 2010).

1.1.9.1 Transgenic mice with Alzheimer's-like amyloid pathology

The first APP transgenic mouse (PDAPP) was generated with the Indiana mutation (V717F) using the platelet derived growth factor (PDGF) B chain promoter. This PDAPP mouse exhibited plaque pathology by 6-9 months and it is one of the few models with hippocampal atrophy (Games et al., 1995). Subsequent research done by various other groups using Morris water maze experiments reported age-dependent behavioral deficits in PDAPP mice (Chen et al., 2000). The next widely used APP model is the Tg2576 mice which expresses the APP 695 isoform with the Swedish mutation (K670N/M671L) using hamster PrP promoter. Tg2576 mice produced both $A\beta$ (1-40) and $A\beta$ (1-42) peptides and plaques usually developed at 12-18 months in both cortex and hippocampus (Hsiao et al., 1996). However, there was a lack of correlation between the late onset of deposition of amyloid plaques and memory deficits in these Tg2576 mice (Westerman et al., 2002). Subsequently, another *APP* 695 isoform expressing model (CRND8) was generated with both the K670N/M671L (Swedish) and V717F (Indiana) mutations and these mice developed early $A\beta$ deposition (at the age of 3 months) with premature mortality (Chishti et al., 2001). In addition, studies also reported prominent cognitive deficits, reduced basal synaptic transmission and increased long-term potentiation (LTP) in these mice (Jolas et al., 2002; McCool et al., 2003).

Presenilin mouse models have also been developed using various mutations in the *PS1* gene (M146V, M146L, PS1exon 9 deleted, and A246E). Selective overexpression of Aβ 1-42 peptide without plaque or tangle pathology was reported in PS1 transgenic mice (Sudoh et al., 1998). However, these mice exhibited increased susceptibility to excitotoxicity via abnormal intracellular Ca2+ signaling (Guo et al., 1999; Stutzmann et al., 2006). Furthermore, the cross of APP transgenic mice (Tg2576) with the PS1 transgenic mice (PS1 M146V) resulted in bi-transgenic mice (PSAPP) where accelerated Aβ pathology with robust elevated Aβ 1-42 levels were observed early at 3 months due to the presence of the *PS1* mutation (McGowan et al., 1999). 5X FAD Tg mice were made with multiple FAD mutations (Swedish, Florida and London) that additively increased Aβ production. Accordingly, 5X FAD mice represented a very aggressive amyloid deposition model that developed intraneuronal Aβ at 1.5 months, plaques at 2 months, memory deficits at 4 months and neuron loss at 9 months of age (Eimer and Vassar, 2013). Interestingly, levels of the hyperactivation subunit of Cdk5, p25, were significantly elevated at 9 months in 5X FAD brain (Oakley et al., 2006).

Transgenic mice expressing huBACE under the control of PrP promoter (SwAPP) or the neuron-specific mouse Thy1.2 promoter have also been developed to study the consequence of BACE overexpression on APP processing (Mohajeri et al., 2004; Ozmen et al., 2005). AD-like pathologies including Aβ production were massively increased in double transgenic mice expressing both BACE and SwAPP. At two months of age, early signs of extracellular Aβ deposition and reactive astrocytes were found in these double transgenic mice (Ozmen et al., 2005).

1.1.9.2 Tau mutant transgenic mice

Several transgenic models expressing familial tau mutations have been developed to study important aspects of AD pathology. JNPL3 mouse, which expresses the tau P301L mutation under the mouse PrP promoter, developed several features which mimic those observed in AD. Hyperphosphorylation of tau occurred at several AD-related epitopes, such as the AT8 epitope, and tau deposition was observed in the cortex, hippocampus and amygdala (Gotz et

al., 2001a). The JNPL3 mouse has also been used in the study of tau filament formation (Gotz et al., 2001a). In addition, tau transgenic mice have been used to investigate the interactions between Aβ and tau in AD research. For example, injection of Aβ fibrils exacerbated pathology in the JNPL3 mouse, resulted in a 5-fold increase in tangles in the amygdala (Gotz et al., 2001b). In another study, a cross between Tg2576 and the JNPL3 mouse resulted in an enhancement of neurofibrillary tangle pathology when compared to the tau mutants alone (Lewis et al., 2001), suggesting that Aβ overexpression can interact with tau protein to cause an enhancement of tangle pathology.

Triple transgenic (3X Tg) mouse was generated by the microinjection of cDNA constructs with hAPP (K670N/M671L) Swedish mutation and P301L tau mutation into the embryos of homozygous PS1M146V mutant mice with Thy1.2 neuronal-specific promoter. Robust elevation of APP, intraneuronal Aβ 1-42 and tau proteins were observed in these 3X Tg mice compared to the respective single transgenic mice. Studies reported that 3X Tg mice developed extracellular Aβ plaques before tangle pathology, as in human AD (Oddo et al., 2003). In addition, recent studies detected increased phosphorylation of tau in multiple phospho-tau sites, AT100 (Thr 212/Ser 214), AT8 (Ser 202, Thr 205) and AT180 (Thr 231) in the amygdala and cortex (Oh et al., 2010).

1.2 Cyclin dependent kinase 5 (Cdk5)

1.2.1 Discovery of Cdk5

Cyclin-dependent kinases (Cdks) are a family of proline-directed protein-serine/threonine kinases (30-35 kDa) with a well-established role in the timing of the various phases of cell cycle such as DNA synthesis phase (S), mitosis phase (M) and the two gap phases (G1 and G2) (Hengst et al., 1994; Morgan, 1997). There have been 20 Cdk-related proteins studied so far and they are involved mainly in the regulation of proliferation, differentiation, senescence and apoptosis of many cells (Satyanarayana and Kaldis, 2009). In general, Cdks need to bind to regulatory subunits, called cyclins, in order to be activated. However, activities of Cdks are also regulated through various mechanisms like post-translational modifications such as phosphorylation and endogenous inhibition by Cdks inhibitors (Tannoch et al., 2000). Even though,

most Cdks have been associated with the regulation of the cell cycle, certain Cdks are involved in other important cellular processes. An important example is Cyclin-dependent kinase 5 (Cdk5), a peculiar member of the Cdk family of serine/threonine kinases. Cdk5 is neither activated by any known cyclins nor involved in cell cycle regulation (Dhavan and Tsai, 2001). Cdk5 was first isolated from bovine brain and named as neuronal Cdc2 like kinase (NCLK) because of its sequence homology (58%) to the human cell cycle regulatory kinase Cdc2 (Hellmich et al., 1992; Lew et al., 1992; Meyerson et al., 1992). Cdk5 is the fifth Cdk in the line of discovery and the nomenclature was first fixed in 1993. Human and mouse *Cdk5* genes have been located on Chromosome 7 and 5 respectively and both encode for a 33 kDa protein with 292 amino acids (Demetrick et al., 1994).

1.2.2 Expression and activity of Cdk5

Although Cdk5 is ubiquitously expressed in all mammalian tissues, its activity is mainly present in the central nervous system (CNS) and plays a crucial role in neuronal migration (Hellmich et al., 1994; Huang et al., 1999). However, studies have also reported the low level activity of Cdk5 in lens epithelial cells, Leydig cells of the testis and β-cells of the pancreas (Gao et al., 1997; Musa et al., 1998; Lilja et al., 2001). In neurons, Cdk5 is predominantly present in the cytoplasm and neurite terminals (Nikolic et al., 1996; Nikolic et al., 1998). Cdk5 phosphorylates a large number of target proteins in post-mitotic neurons and the consensus phosphorylation site of Cdk5 is S/T-P-X-R/H/K (X can be any amino acid except Aspartate and Glutamate) (Beaudette et al., 1993; Lew et al., 1995). Activation of Cdk5 requires association with neuronally-enriched binding partners p35 and p39 and therefore its function is mainly restricted to post-mitotic neurons (Dhavan and Tsai, 2001). It has been reported previously that the phosphorylation of activation loop is required for optimal activation of most of the Cdks. However the activation of Cdk5 is not associated with the phosphorylation of its activation loop and studies have shown that the binding of a regulatory subunit with Cdk5 is enough to stretch the activation loop into a fully extended active state (Russo et al., 1996; Poon et al., 1997; Brown et al., 1999; Tarricone et al., 2001).

1.2.3 Regulation of Cdk5 activation

1.2.3.1 Cdk5 activators

Cdk5 activity is mainly regulated by association with its activators p35 and p39. p35 (NCK5a, neuronal Cdk5 activator comprising of 307 amino acids with 35 kDa mass) is the first Cdk5 binding partner to be identified and has been well-studied. Studies determined that association of p35 itself is sufficient to activate Cdk5 (Tsai et al., 1994). p39 (NCK5ai, neuronal Cdk5 activator isoform comprised of 367 amino acids with 39 kDa mass), another activator for Cdk5, was identified by its sequence homology (57% amino-acid identity) to p35 (Tang et al., 1995). Both p35 and p39 showed limited sequence homology to cyclins, suggesting that they belong to a non-cyclin family of Cdk5-activating proteins (Tang and Wang, 1996).

Cdk5 null mice died just before or after birth and displayed massive disruptions in the cortical lamination (Gilmore et al., 1998; Ohshima et al., 1999). In contrast, p35 knockout mice were viable, but have increased susceptibility to seizures (Kwon and Tsai, 1998). In addition, p35 knockout mice displayed moderate disruption in the organization of the CNS. Hence, it is clear from these studies that p39 could compensate to an extent for the absence of p35. Studies acknowledged that p39/p35 double knockout mice were phenotypically identical to Cdk5 knockout mice and further established that p35 and p39 are the primary activators of Cdk5 (Ko et al., 2001). Indeed, p35 and p39 display an overlapping, but distinct temporal and spatial pattern of expression in the synapse and neuronal growth cones (Delalle et al., 1997). Although there is no specific pattern of distribution of Cdk5, the sub-cellular distribution of Cdk5 and the choice of physiological substrates of Cdk5 are mainly dictated by the distribution pattern of p35/p39 (Pavletich, 1999).

One of the most direct ways of regulating Cdk5 activity is to regulate p35 levels in cells. p35 has been observed to be a short-lived protein with a half-life of 20-30 minutes (Patrick et al., 1998). A possible mechanism for the degradation of p35 is the autophosphorylation by Cdk5 (Lew et al., 1994; Tsai et al., 1994). The possibility of a negative feedback regulation by Cdk5 was supported by previous studies where mutations of potential Cdk5

phosphorylation sites in p35 increased the stability of p35 (Patrick et al., 1998).

1.2.3.2 Transcriptional regulation of Cdk5 and p35

Previous studies reported that chronic administration of cocaine to rats enhanced the expression of Cdk5. This cocaine-induced augmentation of Cdk5 expression was mainly due to the increased expression of transcription factor δFosB, a member of the c-jun family of proteins (Bibb et al., 2001). Converging evidence from various studies revealed that Cdk5 activity can be altered through the transcriptional regulation of p35 protein by various factors like extracellular matrix glycoprotein laminin and neurotrophic factors (Paglini et al., 1998; Tokuoka et al., 2000).

1.2.3.3 Binding with other partners

Previous studies suggested that proteins such as casein kinase 2, DNA binding protein (dbpA) and the ribosomal protein L34 regulated Cdk5 activity by binding directly with Cdk5 or with p35 (Moorthamer and Chaudhuri, 1999; Ching et al., 2002; Lim et al., 2004). Furthermore, the involvement of a nuclear protein SET in the activation of p35/Cdk5 has also been reported (Qu et al., 2002).

1.2.4 Physiological role of Cdk5 in central nervous system development

The significant role of Cdk5 in the development and maintenance of the cytoarchitecture of the CNS has been well studied previously. Major neuronal functions of Cdk5 have been addressed by various experimental approaches including the production of transgenic knockout mice, *in vitro* studies using dominant negative constructs, and finally the identification of various substrates. Some of the major functions of Cdk5 are summarized in the following sections.

1.2.4.1 Cdk5-mediated regulation of corticogenesis and neurite outgrowth

The formation of cortical laminar structure, proper corticogenesis and viability of neurons require an optimal level of p35/Cdk5 kinase activity. Cdk5 knockout mice studies suggested that Cdk5 activity was important for

neuronal survival during development. Cdk5 knockout mice exhibited lesions in the CNS, abnormal corticogenesis, inverted layering of cortical neurons and cerebellar defoliation that contribute to prenatal mortality (Ohshima et al., 1996). Furthermore, p35 knockout mice studies suggested that p35 was the crucial activator for Cdk5 during corticogenesis. p35 null mice showed similar inverted layering of cortical neurons, with little disruptions in the hippocampus (Kwon and Tsai, 1998). Many studies have demonstrated the indispensable role of Cdk5 in cell motility and neurite outgrowth. *In vitro* inhibition of Cdk5 using Cdk5 dominant negative constructs prevented neurite outgrowth, whereas overexpression of p35/Cdk5 promoted the extension of neurites. Thus, evidence collectively suggested that Cdk5 activity is critical for neurite outgrowth (Nikolic et al., 1996; Xiong et al., 1997). Cdk5 induced hyperphosphorylation of PAK1 (p21 (Cdc42/Rac)-activated kinase) and subsequent downregulation of PAK1 kinase activity were likely to have an impact on the regulation of actin cytoskeleton dynamics in neurons and in turn promote neuronal migration and neurite outgrowth (Nikolic et al., 1998). Additionally, studies also reported that neurite outgrowth is regulated by the phosphorylation of Cdk5 by the nonreceptor tyrosine kinase *c*-Abelson (*c*-Abl) at Tyr 15 (Zukerberg et al., 2000).

1.2.4.2 Modulation of axonal transport and microtubule dynamics

It has been well-documented that Cdk5 regulates neuronal migration by phosphorylating numerous microtubule-associated proteins (MAPs). Cdk5-mediated phosphorylation of the intermediate and heavy chain of neurofilaments especially at the carboxy-terminal KSP-rich domains influences the integration of neurofilaments into the cytoskeleton and also regulates its association with microtubules (Hisanaga et al., 1993; Grant et al., 2001). In addition, Cdk5-mediated phosphorylation of microtubule-associated protein 1B (MAP1B) in cerebellar macroneurons was implicated in neurite extension (Paglini et al., 1998). Moreover, phosphorylation of tau protein by Cdk5 regulated the binding of tau to microtubules and in turn modulated the stability of microtubule assembly (Ahlijanian et al., 2000; Grant et al., 2001). Nudel is a cytoplasmic dynein-associated protein that is highly expressed in

the brain. It has been reported that Cdk5 regulates dynein-mediated axonal transport through the phosphorylation of Nudel (Niethammer et al., 2000).

1.2.4.3 Role of Cdk5 in neurosignaling and neuronal survival

Numerous studies have investigated the role of Cdk5 in the regulation of neuronal signal transduction pathways. Cdk5 altered the efficacy of dopamine signaling pathways through the phosphorylation of DARPP-32 (dopamine- and cAMP-regulated phosphoprotein, 32 kDa), a key player in dopamine signaling. The role of Cdk5 in the MAPK (mitogen-activated protein kinase) and JNK (*c*-Jun N-terminal kinase) pathways have also been extensively studied earlier. Cdk5 phosphorylates JNK-3 at Thr131 and inhibits the JNK-3 activity to modulate neuronal apoptosis (Li et al., 2002). In addition, it has been reported that Cdk5 downregulates the MAPK signaling pathway via the phosphorylation of MAPK kinase 1 (MEK1) at Thr286. Subsequently, Cdk5-mediated inhibition of MEK1 downregulates the activity of ERK1/2 (Sharma et al., 2002). Moreover, Cdk5 has recently been reported to be involved in Ras and Rac signaling pathways through the phosphorylation of Ras guanine nucleotide releasing factors (RasGRF1 and RasGRF2) (Kesavapany et al., 2004; Kesavapany et al., 2006). Cdk5 activity was also found to be involved in the regulation of neuronal survival through the neuregulin/PI3-kinase/Akt signaling pathway (Li et al., 2003). Recent identification of B-cell lymphoma 2 (Bcl-2) protein as a Cdk5 substrate suggested that Cdk5-mediated regulation of Bcl-2 is essential for the maintenance of neuronal survival (Cheung et al., 2008).

1.2.4.4 Cdk5-mediated regulation of synapses, neurotransmission and learning and memory

Cdk5 plays a critical role in the regulation of neurotransmission through the modulation of synaptic vesicle exocytosis, endocytosis and neurotransmitter synthesis (Tomizawa et al., 2002; Bibb, 2003). Recent studies showed that Cdk5 regulates exocytosis by phosphorylating exocytosis-associated proteins like Pctaire 1, Munc18, Sept5 and Synapsin 1. In addition, Cdk5 also binds and phosphorylates endocytosis-associated proteins including synaptojanin 1, amphiphysin 1 and dynamin I at the synaptic terminals (Tan et al., 2003;

Tomizawa et al., 2003). Increasing evidence has pointed out that Cdk5 activity is associated with the regulation of cholinergic and glutamatergic neurotransmitter systems (Fu et al., 2001). In particular, p35/Cdk5 activity was found to be associated with acetylcholine receptor trafficking. The glutamatergic neurotransmitter system is also regulated by Cdk5 through the modulation of NMDA receptor activity (Fu et al., 2001; Hawasli et al., 2007). Cdk5 regulates the structural and functional plasticity of neurons through the phosphorylation of NMDA receptor subunit NR1 and NR2 (Li et al., 2001; Zhang et al., 2008). In addition, Cdk5-mediated regulation of calpain-induced NR2B degradation has been reported previously (Lai and Ip, 2009). Recently, many studies have emerged to study the role of Cdk5 in the modulation of learning, memory and pain response. Elevated Cdk5 activity was observed during associative learning and fear conditioning (Fischer et al., 2002). In fact, long-term depression induction and spatial learning were both altered in p35 knockout mice (Ohshima et al., 2005). Furthermore, p35 knockout mice exhibited abnormalities in pain signaling, where evident hypoalgesia was observed in response to thermal activation (Pareek et al., 2006).

1.2.4.5 Role of Cdk5 in transcriptional regulation

The localization of p35/Cdk5 in the nucleus and its role in transcriptional regulation has been recently investigated by various studies. Cdk5-mediated regulation of transcription factors including Egr-1 and signal transducer and activator of transcription 3 (STAT3) was identified previously and are mainly involved in dendrite outgrowth (Nikolic et al., 1996). In addition, Cdk5-mediated regulation of p53 transcriptional activity has also been reported previously (Zhang et al., 2002). Members of the myocyte enhancer factor 2 (MEF2) was recently identified as a Cdk5 substrate and phosphorylation of MEF2 by Cdk5 resulted in the inhibition of MEF2 transactivation activity (Gong et al., 2003). It has recently been reported that Cdk5 hyperactivation inhibits histone deacetylase 1 (HDAC1) which in turn impaired DNA integrity and finally caused neuronal death (Kim et al., 2008).

1.2.5 Cdk5 in neurodegeneration

1.2.5.1 Mechanism behind Cdk5 deregulation

Although Cdk5 activity is crucial for a proper CNS development, the deregulation of Cdk5 activity has been reported to be closely associated with the development of neurodegenerative processes in various neurodegenerative diseases (Nguyen et al., 2003; Tsai et al., 2004; Lopes et al., 2007; Alvira et al., 2008; Slevin and Krupinski, 2009). The tight regulation of Cdk5 is disrupted under many neurotoxic conditions like hydrogen peroxide exposure, ischemic brain damage, oxidative stress, excitotoxicity and Aβ exposure which lead to an abnormal increase in the intracellular Ca2+ levels (Lee et al., 2000). Cdk5 deregulation is mainly caused by the calpain-mediated cleavage of Cdk5 activator, p35 which releases a C-terminal p25 fragment with 209 amino acids and a small p10 fragment with 100 amino acids (Patrick et al., 1999; Kusakawa et al., 2000; Lee et al., 2000; Camins et al., 2006). Calpain activity is more vulnerable to Ca2+ homeostasis changes which makes calpain an important element in numerous neurodegenerative disease including AD (Vosler et al., 2008; Araujo et al., 2010). In fact, both NMDA and AMPA (α-amino-3-hydroxy-5-methyl-4-isoxazolepropionic acid) receptors were found to be involved in the abnormal influx of Ca2+ under neurotoxic insults (Alberdi et al., 2010). Calpain-mediated Cdk5 deregulation was further supported by recent findings where production of p25 was blocked by calpain-specific inhibitors (Sato et al., 2008).

The half-life of truncated Cdk5 activator p25 is considerably longer than that of their original precursor p35. Studies also indicated that the truncated Cdk5 activator p25 was more resistant to phosphorylation-induced proteasomal degradation (Patrick et al., 1998). In addition, it has been shown that binding of p25 to Cdk5 displayed much stronger activation profile of Cdk5 compared to p35/Cdk5 or p39/Cdk5 (Amin et al., 2002). Furthermore, the p25 fragment (without amino-terminal myristoylation site) freely moved around the neuronal compartments and associated with Cdk5 to form a p25/Cdk5 complex. This p25/Cdk5 complex exhibited abnormal subcellular localization and altered substrate specificity and eventually led to devastating effects for

cells such as destabilization of cytoskeleton, production of intra-cellular aggregates and finally modulation of nuclear function (Patrick et al., 1999; Kusakawa et al., 2000; Asada et al., 2008; Kim et al., 2008). A similar fragment, p29, produced from p39 cleavage has also been reported to move Cdk5 from its usual compartments, but p29/Cdk5 was detected mainly in the cell soma and the proximal neurites. However, the role of p29 in the progression of neurodegeneration has not been reported previously (Patzke and Tsai, 2002b).

1.2.5.2 Altered Cdk5 substrate specificity

p25-mediated altered Cdk5 substrate specificity might be the major event behind the neuropathological effects of Cdk5. Studies have shown that the expression of p25 in cortical neurons induced neurite retraction, microtubule collapse and apoptosis (Patrick et al., 1999). Although the mechanism behind this was not fully elucidated, p25 might mediate this through an altered Cdk5 substrate specificity. An *in vitro* study using primary neuronal culture revealed that the p25/Cdk5 complex more efficiently phosphorylated tau than the p35/Cdk5 complex. Furthermore, *in vivo* evidence indicated that transgenic mice overexpressing p25 displayed robust hyperphosphorylation of tau, whereas p35 overexpressing mice did not exhibit increased tau phosphorylation (Takashima et al., 2001; Bian et al., 2002). This hyperactive p25/Cdk5 complex also caused aberrant hyperphosphorylation of various cytoskeletal components including neurofilaments (medium/heavy, NF-M/H) (Ahlijanian et al., 2000; Lee and Tsai, 2003; Noble et al., 2003). Even though several *in vitro* and *in vivo* studies confirmed that tau and NF-H were not the physiological substrate for Cdk5,   p25/Cdk5-mediated altered substrate specificity induces the hyperphosphorylation of Tau and NF-H, eventually leading to cytoskeletal disruption and cell death (Dhavan and Tsai, 2001).
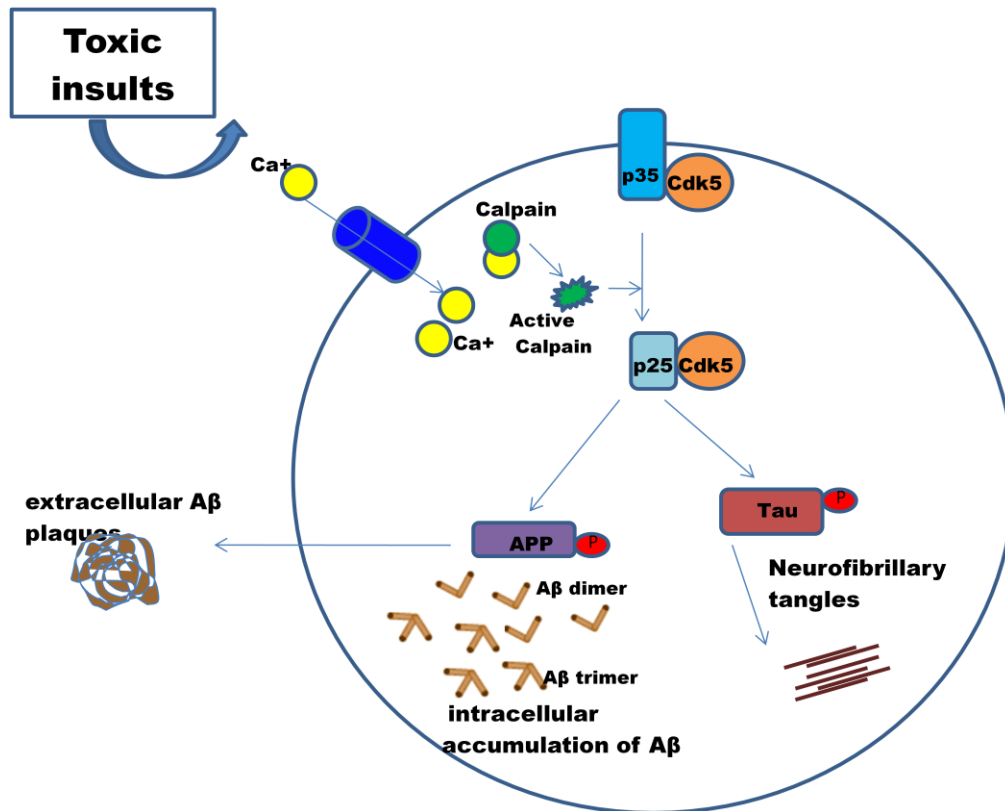
Figure 1.5: p25/Cdk5 deregulation-mediated neurodegeneration

Exposure of neurons to toxic insults activated the calcium-dependent protease calpain, which then cleaved the Cdk5 activator, p35, into p25 fragment. Deregulation of Cdk5 by the binding of p25 caused the hyperphosphorylation of tau and abnormal processing of APP, leading to the formation of intracellular neurofibrillary tangles and extracellular amyloid-β plaques.

In addition, p25/Cdk5-meditated altered phosphorylation has also been reported to be involved in abnormal processing of the amyloid precursor protein (APP) (Iijima et al., 2000). In particular, elevated APP Thr668 phosphorylation was found during increased p25/Cdk5 activity in transgenic mice (Cruz et al., 2003). p25/Cdk5 hyperactivation-mediated neurodegenerative changes are summarized in Figure 1.5.

However, not all Cdk5 substrates were affected by p25/Cdk5 hyperactivation. For example, the phosphorylation levels of Nudel, mDab1 or PSD95 were not impaired during p25 overexpression (Cruz et al., 2003) possibly due to their cellular localization. Moreover, p25-mediated alteration in substrate specificity of Cdk5 is also partly due to its biochemical properties. Crystal

structure studies for p25/Cdk5 indicated that certain residues on p25 might be responsible for the altered substrate specificity (Tarricone et al., 2001).

1.2.6 Role of p25/Cdk5 hyperactivation in neurodegenerative diseases

Numerous studies have found that Cdk5 deregulation is associated with the development of neuropathology in various neurodegenerative diseases including AD, ALS, PD, cerebral ischemia and Huntington's disease. The following sections summarize some of the key findings on the Cdk5-mediated neuropathological mechanisms underlying various neurodegenerative diseases.

1.2.6.1 Role of Cdk5 in Alzheimer's disease (AD)

Substantial evidence now support a model in which the p25-mediated Cdk5 deregulation is involved in the regulation of many of the signaling pathways that led to the development of AD-like neuropathology. Since Cdk5 deregulation has a close connection with Aβ toxicity, tau pathology, and synaptic abnormalities, it may be an effective and novel therapeutic candidate for AD. Although there have been some controversy concerning the detection of p25 in postmortem samples of AD patients (Tandon et al., 2003), studies observed significant accumulations of p25 along with striking elevation of Cdk5 activity in the human AD cases compared to age-matched control brains (Patrick et al., 1999; Tseng et al., 2002). In addition, increased levels of active calpain were also observed in the human AD brains (Saito et al., 1993; Lee et al., 1999; Patrick et al., 1999; Tseng et al., 2002).

1.2.6.1.1 Role of Cdk5 in Aβ accumulation

Aβ has long been proposed as the toxic instigator of the cascade of pathological events that eventually leads to synaptic dysfunction and neuronal loss in AD. As mentioned earlier, Aβ peptide is formed from the sequential cleaving of APP by β-secretase (BACE1) and then by γ-secretase in the transmembrane region. Subsequently, senile plaques are formed due to an accumulation of Aβ aggregates (Shoji et al., 1992). The main link between Cdk5 and AD was supported by studies showing that hyperactivated Cdk5 increased Aβ production through the phosphorylation-mediated abnormal processing of APP (Iijima et al., 2000; Lee and Tsai, 2003). Interestingly,

inhibition of Thr668 phosphorylation using Cdk5 inhibitors displayed marked reduction in Aβ peptides in cultured neurons (Lee et al., 2003). Additionally, elevated APP Thr668 phosphorylation has also been reported in p25 transgenic mice compared to controls (Cruz et al., 2006). Studies also reported the role of Cdk5 deregulation in the alteration of presenilin (PS1) metabolism and stability (Kesavapany et al., 2001; Lau et al., 2002).

Further studies specified that Cdk5-mediated phosphorylation of the transcription factor STAT3 resulted in elevation of transcription of BACE1, which then increased the generation of Aβ (Wen et al., 2008). Cdk5-mediated regulation of Aβ pathology was further supported by various studies where both *in vitro* and *in vivo* administration of Aβ peptide significantly elevated p25 levels (Patrick et al., 1999; Lopes et al., 2007, 2010). Moreover, studies have also shown that the direct or indirect inhibition of Cdk5 significantly reduced Aβ-mediated neurotoxicity (Lopes et al., 2007; Granic et al., 2010). These studies together strongly suggested that Cdk5 hyperactivation and subsequent abnormal processing of APP might be an early event in AD that led to the production of toxic Aβ peptide accumulation.

1.2.6.1.2 Role of Cdk5 in Tau pathology

Tau hyperphosphorylation and the presence of neurofibrillary tangles are among the major hallmarks of AD. Numerous studies showed that Cdk5 was co-purified with tau protein from microtubule preparations (Sobue et al., 2000). Various studies using phosphoepitope-specific antibodies and mass spectrometric analysis revealed that the Cdk5-specific phosphorylation sites on tau (S202, T205, S396 and S404) were also hyperphosphorylated in AD brains (Flaherty et al., 2000). Moreover, immunohistochemical analyses on the human brains discovered the apparent co-localization of increased Cdk5 immunoreactivity with both pretangle and NFT-bearing neurons (Yamaguchi et al., 1996). Results from *in vitro* studies indicated that p25/Cdk5 hyperactivity is involved in the hyperphosphorylation of tau (Hashiguchi et al., 2002). Likewise, p25 overexpressing mice displayed hyperphosphorylation of both neurofilaments and tau (Ahlijanian et al., 2000). Tau protein is thought to be degraded via the ubiquitin-proteasome mechanism (David et al., 2005;

Oddo, 2008). However, hyperphosphorylated tau is more resistant to this proteasome-mediated degradation and further causes the intracellular accumulation of tau fibers in neurons (Khatoon et al., 1992).

Plenty of recent emerging evidence further supported the significance of Cdk5-mediated phosphorylation in tau pathology. An interesting study using triple-transgenic AD mice showed that knockdown of Cdk5 expression reduced the abnormal tau phosphorylation and neurofibrillary tangle formation (David et al., 2005). Furthermore, Aβ-induced activation of Cdk5 was found to be responsible for the phosphorylation of tau that is missorted to the somato-dendritic compartment, which resulted in dissociation of tau from microtubules (Zempel et al., 2010). Cdk5 also facilitated tau phosphorylation by inhibiting phosphatase PP1 through phosphorylation (Lu et al., 2011).

1.2.6.2 Role of Cdk5 in Amyotrophic Lateral Sclerosis (ALS)

Amyotrophic lateral sclerosis (ALS), an adult-onset neurodegenerative disease, is mainly characterized by a selective loss of motor neurons in the spinal cord, brainstem and cerebral cortex, ultimately resulting in paralysis, respiratory failure, and death (Cleveland, 1999). ALS has been attributed to point mutations in the copper/Zinc *superoxide dismutase* (*SOD1*) gene that induce a series of neuropathological effects including excitotoxicity (Cudkowicz et al., 1997). An interesting discovery of elevated levels of p25 expression and subsequent Cdk5 hyperactivation was the first evidence that supported the involvement of Cdk5 in ALS (Nguyen et al., 2003). This p25-mediated Cdk5 hyperactivation induced hyperphosphorylation of the neurofilament H (NF-H) and made them insoluble. Subsequently, this insoluble hyperphosphorylated NF-H formed perikaryal aggregates, which disrupted axonal transport and eventually resulted in neuronal death (Nguyen et al., 2001; Patzke and Tsai, 2002a). In addition, co-localization of Cdk5 and NF-H aggregates was also noticed in the ALS patients' brain (Bajaj et al., 1999). The role of Cdk5 in ALS pathology was further supported by a recent study where minocycline treatment with mutant SOD1 mice drastically reduced Cdk5 immunoreactivity and subsequent disease progression (Kriz et al., 2003).

1.2.6.3 Role of Cdk5 in Parkinson Disease (PD)

Parkinson's disease (PD) is a progressive debilitating neurodegenerative disorder characterized by the selective loss of dopaminergic neurons in the substantia nigra (Dauer and Przedborski, 2003). The intracellular accumulation of α-synuclein aggregates named Lewy bodies is one of the major hallmark features of PD pathology (Spillantini et al., 1997; Baba et al., 1998; Venda et al., 2010). Interestingly, recent reports have shown the changes in level and activity of Cdk5 in the brain of PD patients (Alvira et al., 2008). Moreover, elevated levels of Cdk5 activation along with the increased levels of p25 expression were reported during treatment with the neurotoxin, 1-methyl-4-phenyl-1, 2, 3, 6-tetrahydropyridine (MPTP). This could be due to MPTP-induced glutamate toxicity and subsequent calpain activation (Smith et al., 2003; Alvira et al., 2006). In addition, another study demonstrated that MPTP-induced Cdk5-mediated phosphorylation of MEF2 contributed to neuronal death in dopaminergic neurons in the substantial nigra region of a PD mouse model (Smith et al., 2006). Moreover, MPTP-mediated Cdk5 hyperactivation also induced the downregulation of peroxidase activity of Prx2 (peroxiredoxin) and in turn reduced the elimination rate of ROS (reactive oxygen species), which eventually led to neuronal loss (Qu et al., 2007). The involvement of Cdk5 in PD pathology is further supported by recent findings where MPTP-induced neuronal loss and behavioral deficits were effectively reduced by the inhibition of Cdk5 activity (Smith et al., 2003; Smith et al., 2006; Qu et al., 2007). Findings of Cdk5-mediated phosphorylation of α-synuclein and parkin further supported the critical involvement of Cdk5 in the pathogenesis of PD (Avraham et al., 2007; Rubio de la Torre et al., 2009).

1.2.6.4 Role of Cdk5 in cerebral ischemia

Cerebral ischemia (stroke) is a condition in which loss of brain function occurs as a result of insufficient blood flow to the brain (Hou and MacManus, 2002). In particular, inflammatory reactions and excitotoxicity are the main events that contributes to neurodegeneration during cerebral ischemia (Mehta et al., 2007; Nakka et al., 2008). Recent *in vivo* studies have clearly demonstrated that Cdk5 overactivation-mediated regulation of NMDA receptors (Wang et

al., 2004) and phosphorylation of tau (Wen et al., 2007) play a major role in the induction of neuronal death.

1.2.6.5 Role of Cdk5 in Huntington's disease

Huntington's disease is an autosomal-dominant inherited genetic neurodegenerative disorder caused by a mutation in the *huntingtin* gene (*HTT*) that encodes for the protein, huntingtin (Htt) (Rubinsztein and Carmichael, 2003). Numerous recent studies showed a protective role of Cdk5 in Huntington's disease pathology, in contrast to the emerging detrimental role of p25/Cdk5 hyperactivation in various neurodegenerative diseases. Cdk5-mediated phosphorylation of huntingtin was found to be neuroprotective against DNA damage and polyglutamine expansion (Anne et al., 2007). Moreover, reduced p35/Cdk5 levels and activity were observed in postmortem samples of Huntington's disease patients (Anne et al., 2007) as well as in a Huntington's disease mouse model (Luo et al., 2005). Furthermore, Cdk5 phosphorylation at Ser434 abolished htt aggregation by reducing caspase-mediated cleavage (Luo et al., 2005). Collectively, findings suggested that Cdk5 activity offered a protective role in Huntington's disease by limiting the mutant htt toxicity.

1.2.7 Modelling p25-induced neurodegeneration - p25 transgenic mice

Several transgenic mouse lines overexpressing p25 have been generated and characterization of different p25 transgenic (p25Tg) mice lines has facilitated the investigation of mechanism behind p25/Cdk5-mediated neuropathology. However, these p25 transgenic mice lines exhibited variation in distribution pattern and expression levels of p25 and some are unsuitable for investigating the contribution of p25 formation in the development of AD-like pathology (Giese et al., 2005). For example, a mouse line developed with the platelet derived growth factor (PDGF) B chain promoter expressed relatively high amounts of p25 in the spinal cord. These mice exhibited profound dyskinesia, central axonal degeneration, but no neurofibrillary tangles. Moreover, this severe phenotype displayed semiparalysis of the hind limbs and early death occurred, preventing the investigation of memory formation and age-dependent processes (Bian et al., 2002). In addition, even though p25Tg

mouse generated using a cytomegalovirus promoter (pCMV) showed the accumulation of p25, neither hyperphosphorylation of tau nor neuronal death was seen (Takashima et al., 2001). Another p25Tg mouse generated using neuron-specific enolase (NSE) promoter exhibited hyperphosphorylation of tau/neurofilament, positive silver staining, and cytoskeletal disturbances that were similar to several neurodegenerative diseases including AD. In addition, mice displayed increased spontaneous locomotor activity compared to control mice (Ahlijanian et al., 2000). Furthermore, NSE p25Tg mice in a p35 knockout background were generated by another group and results reported that p25 can compensate partially for p35/Cdk5 under some conditions during development (Patzke et al., 2003). Additional support for the effect of Cdk5 on the progression of tau pathology comes from another study where NSE-p25-P301L-tau bi-transgenic mice displayed elevated formation of neurofibrillary tangles compared to their parent mice (P301L-tau transgenic mice and NSE p25Tg mice) (Noble et al., 2003).

Taken together, the variations in phenotypes as well as the spatial distribution of the p25 transgene in p25 overexpressing mice could be mainly due to the use of different promoters during the generation of transgenic mice. In addition, the intensity of p25 expression in these transgenic mice may possibly have a role in determining the rate of neurodegeneration (Cruz and Tsai, 2004). Thus, it is critical to confine p25 expression to appropriate brain regions, such as the forebrain, to fully investigate the pathological role of p25 production in AD. In addition, it is important to avoid the embryonic expression of p25 in order to prevent potential developmental consequences. Accordingly, mouse lines with the CaM kinase IIA promoter to drive p25 expression fulfill these criteria. Importantly, this promoter is not active during the embryonic stage and expression of p25 is directed primarily to the hippocampus and cerebral cortex (Giese et al., 2005). Initially, p25 expressing transgenic mice were generated in the C57BL/6 background using the forebrain-specific CaM KIIA promoter in order to study whether and how p25 formation affects learning and memory. This low level p25 expressing transgenic mice exhibited reduced contextual conditioning paired with enhanced tone conditioning in conjunction with improved reversal learning in

the Morris water maze (Angelo et al., 2003). In contrast, a later study indicated that low levels of p25 did not always improve learning (Mizuno et al., 2006). Absence of neurodegeneration with only slight increases in total tau protein was observed in these mice. Thus, results concluded that a high level of p25 expression was required to cause neuronal death.

1.2.7.1 CK-p25 bi-transgenic mice

To determine whether robust expression of p25 itself can trigger neurodegeneration, bi-transgenic p25 overexpressing mice (CK-p25Tg mice), that overexpress human *p25* gene under the control of the CaM KIIA promoter, were generated using tetracycline-controlled transactivator (tTA) system (Cruz et al., 2003). Initially, these CK-p25Tg mice were conceived and raised on a doxycycline supplemented diet. After normal development of the CNS (6-week postnatal), they were given a doxycycline-free diet to induce the expression of p25 specifically in the forebrain. Characterization of these CK-p25Tg mice demonstrated that these mice exhibited progressive neuronal loss especially in the cerebral cortex, widespread astrogliosis, and prominent brain atrophy that strongly correlated with p25 expression pattern (Cruz et al., 2003).

Gradual progression of tau-associated pathology was observed in these CK-p25Tg mice and p25-mediated hyperphosphorylation of endogenous tau at multiple epitopes emphasized the key role of p25/Cdk5 hyperactivation in the progression of neurofibrillary pathology in AD (Cruz et al., 2003). Subsequent characterization of these mice by the same group in 2006 demonstrated the occurrence of noticeable intracellular amyloid-β accumulations in the perinuclear regions within the forebrain (Cruz et al., 2006). They further claimed that apparent elevation of BACE 1 levels might be the mechanism behind the Aβ accumulation caused by the deregulation of Cdk5 in CK-p25Tg mice. However, these studies have not shed light on the precise molecular mechanisms by which p25/Cdk5 mediate neuronal death.

1.2.7.2 Behavioral studies in CK-p25Tg mice

In order to investigate the effects of deregulated Cdk5 activity on learning and memory, *in vivo* behavioral studies were performed with CK-p25 mice and results showed that sustained p25 expression severely impaired hippocampal LTP and memory along with profound synaptic loss. In contrast, transient p25 expression facilitated learning and memory with improved hippocampal LTP. Thus, these observations concluded that a sustained or prolonged p25 expression could have the ability to modify the normal physiological function of Cdk5 into a pathological one (Fischer et al., 2007).

1.2.7.3 Neuroinflammation in CK-p25Tg mice

Recently, Muyllaert et al. generated a new p25 overexpressing transgenic mouse line using the same strategy as in CK-p25 inducible Tg mice to investigate further the mechanism behind the role of p25 production in neurodegeneration (Muyllaert et al., 2008). They observed extensive neurodegeneration with severe brain atrophy, as reported previously (Cruz et al., 2003; Cruz et al., 2006). However, neither an apoptosis-mediated neuronal death nor elevated phosphorylation of tau was noticed even in later stages. Conversely, neuroinflammation was observed as the most prominent event with considerable activation of microglia in and around the specific brain regions with p25-expressing neurons (Muyllaert et al., 2008).

Collectively, findings from the characterization of inducible p25Tg mice (summarized in Table 1.1) delineated a novel pathological mechanism involving both neurofibrillary pathology and abnormal APP processing by aberrant p25/Cdk5 hyperactivity contributing to the development of AD pathologies. Although the occurrence of intense neuroinflammation was reported recently in these mice, the actual mechanism behind the p25-mediated neuroinflammation and subsequent neurodegeneration was not yet fully elucidated. Hence, further investigation of Cdk5-mediated effects on many stress-induced signaling pathways including neuroinflammation will be necessary to fully elucidate the role of Cdk5 deregulation in neurodegeneration (Giese et al., 2005).

Table 1.1 Summary of characterization of various p25 transgenic mice

Mouse line & Reference	Transgene, Promoter & mouse strain	Tau pathology	Amyloid pathology	Behavioral changes	Neuroinfla mmation
p25Tg mice (Ahlijanian et al., 2000)	Human *p25*; rat NSE promoter; FVB/N strain	Hyper p-tau and NFT	Not assessed	Increased locomotor activity	No glial staining
p25Tg mice (Takashima et al., 2001)	Bovine *p25*; pCMV/PDG F promoter	No neuronal loss and no p-tau	Not assessed	Unable to stand up-right and died at 6 months	Not assessed
p25Tg mice (Bian et al 2002)	Human *p25*; PDGF promoter; FVB/ N strain	Hyper p-tau; no NFTs	Not assessed	Hind limb semiparalysis and mild forelimb dyskinesia	Not assessed
p25/mutant tau Bi-Tg mice (Noble et al., 2003)	p25 mouse line (rat NSE) X Tau mutant mouse line (P301L)	Hyper p-tau and NFT	Not assessed	Pre-paralysis with neuronal loss in spinal cord	Not assessed
p25Tg mice (Angelo et al., 2003)	Mouse *p25*; CaMKIIa; C57BL6 Strain	Hyper p-tau and NFT	Not assessed	Impaired LTP and fear conditioning	No glial staining
Inducible p25 Bi-Tg mice (Cruz et al., 2003, 2006, Fischer et al., 2007)	Mice with human *p25*, (TetO) X CaMKII-tTA mice; C57BL/6 strain	Hyper p-tau and NFT	Intracellular Aβ aggregates	Impaired hippocampal LTP	Prominent astrogliosis
Inducible p25 Bi-Tg mice (Muyllaert et al., 2008)	Mice with human *p25* in pBI-Tet vector (TetO) X CaMKII- Tg mice; C57BL/6 strain	no p-tau	No Aβ aggregates	Not assessed	prominent astrogliosis

1.3 Objectives of this study

AD is a complicated neurodegenerative disorder and the exact mechanism behind the disease pathology is not yet clear. Neuroinflammation is a prominent characteristic of AD pathology and is thought to induce neurodegeneration. However, the precise mechanism behind neuroinflammation and its significance in the initiation of the pathogenesis of AD has not been fully elucidated. Increase in p25 expression with subsequent deregulation of Cdk5 activity has been shown to be a key causative agent for AD pathogenesis. Even though there are many studies available addressing the role of p25/Cdk5 hyperactivation in neurodegeneration, there has not been clear evidence for the mechanism behind p25/Cdk5-mediated neuroinflammation and its significance in neurodegenerative disease progression. Hence, this study aims to elucidate the p25/Cdk5-mediated neuroinflammatory mechanism using the CamK2a-p25 transgenic (p25Tg) mice, a mouse model that exhibits pathological hallmarks seen in AD. The thesis is broadly split into two parts: firstly, characterization of the neuroinflammatory cascade in the p25Tg line, and secondly, determining the biological benefit when these mice are treated with curcumin, an anti-inflammatory compound.

The objectives for the first part of this thesis are:

- To determine the onset of neuroinflammatory events such as astrogliosis, microgliosis and chemokine production in p25Tg mice.
- To determine the role of brain infiltration of leukocyte in p25-mediated neuroinflammation in p25Tg mice.
- To investigate the mechanism of p25-mediated robust increases in neuroinflammation *in vitro.*
- To determine whether this p25/Cdk5-mediated neuroinflammation is the initial trigger for neurodegeneration.

Disappointing failures of recent clinical trials of anti-inflammatory agents in neurodegenerative disorders has meant that a better understanding of the complex roles in the neuroinflammatory process is required to unravel its link

with neurodegeneration. Curcumin, a well-studied anti-inflammatory, antioxidant, anti-amyloidogenic and anti-oncogenic drug can be efficacious without any apparent side effects. However, its oral bioavailability is poor. To counter this, the laboratory of Sally Frautschy (UCLA) developed LONGVIDA-curcumin, a proprietary optimized formulation that showed promise in both human and animal studies with increased bioavailability in the brain as well as plasma (Begum et al., 2008; Frautschy and Cole, 2010). Hence, this study used this special formulation of curcumin to investigate whether early intervention to modulate inflammation will result in changes in later formation of pathological hallmarks in the p25 transgenic mice.

The objectives of the second part of this thesis are:

- To investigate the effect of curcumin on the p25-mediated neuroinflammation
- To investigate whether inhibition of p25-mediated neuroinflammation by treatment with curcumin affects neuropathological progression (tau and amyloid pathology formation) in p25Tg mice.

Taken together, data from this study will open avenues of research into inhibiting neuroinflammation in the AD paradigm and will also unveil potential therapeutic targets to treat AD effectively.

CHAPTER 2

CHAPTER 2: Materials and methods

2.1 Materials

2.1.1 Materials used for animal maintenance

- **<u>Doxycycline</u>**

  Doxycycline (Sigma, D9891)

Table 2.1: Doxycycline Preparation

Stock solution	Working dilution
20 mg/ml	**200 µg/ml**
1g of doxycycline in 50 ml of sterile ultra-pure water	2 ml of stock solution was mixed with 200 ml of sterile ultra-pure water
(18.2 MΩ·cm at 25°C, Arium 611VF, Sartorius)	

- **<u>Sucrose</u>**

  Sucrose (Sigma, S8501)

Table 2.2: Sucrose solution

Stock solution	Working dilution
40% solution	**1% solution**
40 g of sucrose in 100 ml of sterile ultra-pure water	5 ml of stock solution in 200 ml of sterile ultra-pure water

- **<u>Curcumin feed</u>**

  Longvida optimized Curcumin (Verdure Sciences) was mixed with regular rodent diet (Harlan, 4 g Curcumin/kg feed)

2.1.2 Genotyping

2.1.2.1 Tail clipping

- **Ethyl chloride Spray**
- Ethyl chloride spray (Walter Ritter GmbH & co) was used before tail clip to reduce pain in mice.
- **Super clot**

  Super clot (Synergy Labs) was used immediately after tail clip to stop bleeding in mice.

2.1.2.2 Genomic DNA Extraction

- **DNeasy tissue kit** (Qiagen, 69506) contains buffer ATL (Tissue lysis buffer), Proteinase K solution (> 600 mAu/ml), buffer AL (Lysis buffer), buffer AW1 & AW2 (Wash buffers) and buffer AE (elution buffer).
- **Absolute Ethanol** (Fisher Chemicals, E/0650DF/17)

2.1.2.3 PCR reagents

- **AccuPrime Pfx SuperMix**

  AccuPrime Pfx SuperMix (Invitrogen, 12344-040) was used for *p25* transgene PCR. It contains 22 U/ml thermostable polymerase, 66 mM Tris-SO4 (pH 8.4), 30.8 mM $(NH_4)_2SO_4$, 11 mM KCl, 1.1 mM $MgSO_4$, 330 µM dNTPs and stabilizers.

- **GoTaq Green Master Mix**

  GoTaq Green Master mix (Promega M712) was used for *Camk2a* transgene PCR. It contains GoTaq DNA polymerase, 400 µM dNTPs, 3 µM $MgCl_2$, reaction buffer (pH 8.5) and tracking dyes (Blue and yellow).

- **Primers**

Table 2.3: Primers for genotyping

Primers	Primer sequences
p25 **transgene:**	
p25 Forward	5' CCATCGATCTAGTACAGCTCGTCCATGC 3'
p25 Reverse	5' AGGGACGACGGCAACTAC 3'
IC Forward	5' CAAATGTTGCTTGTCTGGTG 3'
IC Reverse	5' GTCAGTCGAGTGCACAGTTT 3'
Camk2a **transgene:**	
Camk2a Forward	5' CGCTGTGGGGCATTTTACTTTAG 3'
Camk2a Reverse	5' CATGTCCAGATCGAAATCGTC 3'
IC Forward	5' CAAATGTTGCTTGTCTGGTG 3'
IC Reverse	5' GTCAGTCGAGTGCACAGTTT 3'

IC – Internal control

- **Genomic DNA**

1 µl with 10 ng of DNA extracted from mouse tail.

- **Water**

Nucleases, proteases and pyrogen free sterilized water (First Base, BUF-1180-1L).

2.1.2.4   Agarose gel electrophoresis

- **1X TAE (Tris-Acetate-EDTA) buffer**

50X TAE (First Base, BUF-3000) buffer was diluted into 1X with distilled water.

- **1.5 % Agarose gel**

2.25 g of Agarose powder (Invitrogen, 15510-027) was dissolved in 150 ml of 1X TAE buffer by heating in a microwave oven.

- **GelRed** (10,000X, Biotium, 41003-1)
- **Blue 6X loading dye** (Promega, G190A)
- **1000 bp DNA ladder** (Promega, G210A)

2.1.3 Mammalian cell culture

2.1.3.1 <u>Primary Neuron culture</u>

- **Neuron culture medium**

  Neurobasal medium (Invitrogen, 21103-049)

  B27 supplement (1:50, Invitrogen, 17504-044)

  100 IU/ml penicillin and 100 µg/ml streptomycin (Gibco, Life Technologies, 15070-063)

  2 mM glutamine (Gibco, Life Technologies, 25030-081)

- **Papain solution**

  Papain (Worthington Biochemical Corp, 3176) in 5 ml Earle's Balanced Salt Solution (EBSS, Sigma E2888) was mixed with 250 µl of 0.1% DNAse/EBSS (Worthington Biochemical Corp, LK003172).

- **Stop solution**

  600 µl of Papain Inhibitor (Worthington Biochemical Corp, LK003182) with 5.4 ml of EBSS was mixed with 250 µl of 0.1% DNAse/EBSS.

- **10/10 solution**

  0.1 g bovine serum albumin (BSA) (Sigma, A2153) and 0.1 g Trypsin Inhibitor (Sigma, T9253) was dissolved in 10 ml of EBSS.

- **Poly-L-lysine** (Sigma P6282)

  Stock - 5mg in 2.5ml of sterile ultra-pure water (2 mg/ml)

  Working - 1:100 in sterile ultra-pure water (20 µg/ml)

2.1.3.2 <u>Primary glia culture</u>

- **Glial cell culture media**

  Dulbecco's Minimal Essential Medium (DMEM) (GIBCO by Life Technologies, 12430-054)

  Fetal Bovine Serum (FBS) (GIBCO by Life Technologies, 10270-106)

  200 mM glutamine (GIBCO by Life Technologies, 25030-081)

  100 mM sodium pyruvate (GIBCO by Life Technologies, 11360-070)

  100 IU/ml penicillin and 100 μg/ml streptomycin (Gibco, Life Technologies, 15070-063)

- **3.0 μm tissue culture inserts** (Greiner bio-one, 657630)
- **Coverslips** (25 mm, 0111650, Marienfeld GmBH)

2.1.3.3 <u>Mammalian cell line</u>

- **Human Embryonic Kidney (HEK) FT cell line** (Life technologies, Invitrogen, R700-07)

- **HEK FT cell culture medium**

  DMEM (GIBCO by Life Technologies, 12430-054)

  Fetal Bovine Serum (FBS) (GIBCO by Life Technologies, 10270-106)

  200 mM glutamine (GIBCO by Life Technologies, 25030-081)

  10 mM non-essential amino acid (NEAA) solution (GIBCO by Life Technologies 1140050)

  100 mM sodium pyruvate (GIBCO by Life Technologies, 11360-070)

  Geneticin (G418 Sulphate, 500 μg/ml, GIBCO by Life Technologies, 10131-035)

- **1X Trypsin-EDTA**

  1X trypsin-EDTA solution was prepared from 10X stock (Biowest, X0930-100) using 1X Phosphate buffer saline (PBS)

- **Freezing Media**

  80% DMEM (GIBCO by Life Technologies, 12430-054)

  10% Dimethyl sulphoxide (DMSO) (MP Biomedicals, 191418)

  10% FBS (GIBCO by Life Technologies, 10270-106)

2.1.4 Plasmids

- **p25-LV-CMV** (a gift from Dr. Harish Pant (NINDS, NIH, USA)

  Carboxy terminal fragment (*p25*) of human cyclin-dependent kinase 5 regulatory subunit 1 (*CDK5R1*) coding region was cloned after PCR into LV-CMV-link (third generation self-inactivating vector) between Asc1 and BsiW1 (Zheng et al., 2005).

- **EV-LV-CMV** (a gift from Dr. Harish Pant (NINDS, NIH, USA)

  Empty Vector DNA-LV-CMV was constructed without the p25 coding region.

2.1.5 Transformation and Plasmid DNA Scaling up

- **DH5α ultra competent cells** (Invitrogen, 18265-017)
- **QIAprep Spin Miniprep Kit** (Qiagen, 27106)
- **Luria Bertani (LB) broth** (Novagen, EMD Millipore, 71753-5)

  25 g of LB powder was dissolved completely in 1 litre of ultra-pure water and sterilized by autoclaving (121°C, 15 psi for 20 minutes).

- **LB Agar** (BD Difco-244520)

  40 g of LB agar powder was dissolved completely in 1 litre ultra-pure water and sterilized by autoclaving (121°C, 15 psi for 20 minutes).

- **Ampicillin**

  Stock ampicillin solution was prepared by dissolving ampicillin powder (Sigma, A0166) in sterile water as 100 mg/ml, filter sterilized

and stored in aliquots at -20°C. This stock solution was mixed with LB broth or LB agar plates as 100 µg/ml concentration.

- **Glycerol stock**

Bacteria containing the plasmid of interest in LB-ampicillin broth were mixed with an equal volume of sterile glycerol (Invitrogen, 15514-011) solution to make glycerol stock and stored at -80°C.

2.1.6 Transduction and lentivirus production

- **Lipofectamine 2000** (Invitrogen by Life Technologies, 11668-019)
- **ViraPower Lentiviral packaging mix** (Invitrogen, K4975-00)
- **Syringe Filter** 0.4 µM (Millex, Millipore, SLCR025NS)
- **Ultracentrifugation tube** (Millipore, Amicon Ultra 100K, UFC910008)

2.1.7 Factor removal experiments

- DNAse (8 µg/ml) (Sigma, D4527)
- RNAse (50 µg/ml) (Sigma, R5125)
- Proteinase K (50 µg/ml) (Sigma, P2308)
- Solid phase extraction column (SPE-C18 column, Waters, 186004620)

2.1.8 Immunocytochemistry

- **Fixative**

4% Formaldehyde solution was prepared from 37% Formaldehyde stock (Calbiochem, 344198) in 1X phosphate buffered saline (PBS).

- **1X Phosphate buffer saline (PBS)**

10X PBS ((First Base, BUF-2040) (137 mM sodium chloride, 2.7 mM potassium chloride and 10 mM phosphate buffer) solution was diluted into 1X with distilled water.

- **Permeabilizing solution**

0.1% Triton-X-100 (BDH, 306324N) in 1X PBS

- **Blocking solution**

  5% FBS in 1X PBS

- **Antibody incubation solution**

  5% FBS in 1X PBS

- **DAPI**

  Stock DAPI (4', 6-diamidino-2-phenylindole dihydrochloride) (Sigma, D8413) solution was prepared by reconstituting the content provided in water as per manufacturer's instruction and used at a 1:1000 dilution.

- **Anti-fade fluor-mounting medium**

  DAKO faramount aqueous mounting medium, S3025

2.1.9 Immunohistochemistry

2.1.9.1 <u>Perfusion</u>

- **Mouse Anesthesia**

  A mixture of ketamine (75 mg/kg) and medepomidin (1 mg/kg) (provided by MD2 animal holding unit, Comparative Medicine, NUS).

- **Ringer's Solution (in 1 litre of ultra-pure water)**

  Sodium Chloride (NaCl) (First Base, Bio-1111) - 8.5 g,

  Potassium Chloride (KCl) (BDH, 101985 M) - 0.25 g,

  Calcium Chloride (CaCl$_2$) (Sigma, C1016) - 0.3 g

  Sodium Bicarbonate (NaHCO$_3$) (Sigma, S6297) - 0.2 g

- **Fixative solution (for 1 litre)**

  4% Paraformaldehyde (PFA) (Sigma, P6148)/1X PBS

  40 g of PFA powder was dissolved in 900 ml of ultra-pure water by heating slowly and pH was adjusted to 7.4 followed by addition of 100

ml of 10X PBS. The solution was allowed to cool before filtered through 0.2 μM filter and stored at 4°C.

- **Sucrose/1X PBS solution**

  10%, 20% and 30% sucrose (Sigma, S8501) solutions were prepared in 1X PBS.

- **Cryoprotectant for sectioning**

  Shandon M1 Embedding Matrix (Thermo Scientific, APD1310)

- **Superfrost ultra plus adhesion slides** (Thermo Scientific, 1014356145)

2.1.9.2 <u>Staining Reagents</u>

- *In situ* **cell death detection kit, TMR red (TUNEL kit)** (Roche, 12156792910)
- **Thioflavin solution**

  0.05% thioflavin-S (Sigma, T1892) in 50% ethanol

- **Bielschowsky Silver staining**

  20% Silver Nitrate (AgNO$_3$)

  4 g of Silver Nitrate (Sigma, 209139) was dissolved in 20 ml of distilled water.

  Ammoniacal Silver Nitrate Solution

  Ammonia solution (Sigma, 341428) was added to silver nitrate solution until the brown precipitate disappeared.

  Ammonia water solution

  20 μl of strong ammonia was added in 10 ml of distilled water.

  Developer Solution

2 ml of formaldehyde (37% formaldehyde, Calbiochem, 344198), 5 µl of concentrated nitric acid (Sigma, 258121) and 50 mg of citric acid (Sigma, 251275) in 10 ml of distilled water.

Hypo solution

5% Sodium thiosulphate (Sigma, 563188)

- **Absolute Ethanol** (Fisher Chemicals, E/06050DF/17)
- **Xylene** (Sigma, 534056)
- **Shandon-Mount permanent mounting medium** (Thermo Scientific, 1900331)

2.1.10 Western blot analyses

2.1.10.1 Protein quantification assay

- **Protein Standards**

  1 mg/ml of bovine serum albumin (BSA) (98% pure Sigma, A7906) was serially diluted in lysis buffer.

- BCA (Bicinchoninic acid) protein assay kit (Thermo Scientific, Pierce, 23225)

2.1.10.2 Buffers

- **Lysis buffer**

  50 mM Tris pH 7.0 (First Base, 1415)

  150 mM Sodium Chloride (NaCl) (First Base, BUF-1112)

  1% Triton-X-100 (BDH, 28817.295)

  1 mM Ethylenediamine tetra acetic acid (EDTA) (First Base, BUF 1052)

  1 mM Ethylene glycol-bis (β-amino ethyl ether)-N, N, N', N'-tetraacetic acid (EGTA) (Sigma, E8145)

  1 mM Sodium Fluoride (NaF) (Sigma, 201154)

- **Protease inhibitor cocktail solution**

  Complete EDTA-free protease inhibitor cocktail tablet (Roche, 11873580001) was prepared as 50X solution in lysis buffer and stored in aliquots at -20°C freezer and used at 1X dilution.

- **Laemmli sample buffer (2X)**

  4% Sodium dodecyl sulphate (SDS) (First Base, BUF-2051)

  20% glycerol (Invitrogen, 15514-011)

  125 mM Tris HCl pH 6.8 (First Base, BUF-1415)

  0.04% Bromophenol blue (Sigma, B6131)

  5% Beta-mercaptoethanol (BME) (BDH, 441435C) (add just prior to use)

- **1X Tris-glycine-SDS-running buffer**

  10X Tris-glycine-SDS-running buffer (First Base, BUF-2030) (0.025 M Tris, 0.192 M glycine and 0.1% SDS) was diluted to 1X with distilled water.

- **1X Tris-glycine-transfer buffer**

  100 ml of 10X-Tris-glycine-buffer (First Base, BUF-2020) (0.025 M Tris and 0.192 M glycine) was mixed with 200 ml of methanol (Schedelco, M0106) and 700 ml of distilled water.

- **TBST (Tris buffered saline and Tween 20) (For 1 litre)**

  50 mM Tris pH 7.0 (First Base, BUF-1415)

  150 mM NaCl (First Base, BUF-1112)

  1 ml of Tween 20 (Sigma, P1379)

- **Stripping buffer**

  0.5% SDS (First Base, BUF-2051)

62.5 mM Tris pH 7.0 (First Base, BUF-1415)

100 mM beta-mercaptoethanol (BME) (BDH, 441435C)

2.1.10.3 Blocking solution

10% milk (blotting grade blocker, BioRad-170-6404) in TBST

2.1.10.4 Antibody incubation solution

5% milk in TBST

2.1.10.5 Sodium dodecyl sulphate polyacrylamide gel electrophoresis (SDS-PAGE)

- **Pre-cast gels**

  Novex 4-20% Tris-Glycine mini gels, 1.0 mm, 10 well (Novex by Life technologies, EC6025)

- **Protein ladder**

  See Blue plus pre-stained standard (LC5925, Life Technologies)

- **Nitrocellulose Membrane**

  Amersham Hybond ECL, 0.45 µM (RPN68D, GE Healthcare)

- **Protein staining solution- Ponceau Red**

  0.1% Ponceau (Sigma, P3504) was prepared in 5% glacial acetic acid (Merck Millipore, 100063).

- **Detection solution**

  ECL detection kit (Amersham-ECL-prime-Western blot detection reagent, RPN 2232, GE Health care)

- **Film**

  Amersham hyperfilm, (28-9068-43, GE Health care)

2.1.11 Antibodies

Antibodies used are listed in the following tables

Table 2.4: Primary antibodies

Name	Source & Catalogue number	Clone	Dilution	Experiments
Mouse monoclonal anti-GFP	Roche, 11814460001	(7.1 & 3.1)	1:500	WB and IHC
Rabbit polyclonal anti-p35(C-19)	Santa Cruz Biotechnology, SC 820	-	1:200	WB
Rabbit polyclonal anti-Cdk5 (C-8)	Santa Cruz Biotechnology, SC 173	-	1:500	WB
Mouse monoclonal anti-GFAP	Sigma, G3893	G-A-5	1:1000	ICC and IHC
Rabbit polyclonal anti-GFAP	Sigma, G9269	-	1:3000	WB
Mouse monoclonal anti-Cd11b	Millipore, CBL1512	OX-42	1:200	WB
Mouse monoclonal anti-cPLA2	Santa Cruz Biotechnology, SC454	4-4B-3C	1:200	WB
Mouse monoclonal anti-CD8	Biolegend, 100702	53-6.7	1:200	IHC
Mouse monoclonal anti-CD4	Biolegend, 100506	RM45	1:200	IHC
Mouse monoclonal anti-α tubulin	Sigma, T9026	DM1A	1:10,000	WB
Mouse monoclonal anti-PHF-Tau	Pierce, MN1020	AT8	1:50	WB, ICC and IHC
Mouse monoclonal anti-PHF-Tau	Pierce, MN1060	AT100	1:100	WB, ICC and IHC
Mouse monoclonal anti-PHF-Tau	Pierce, MN1040	AT180	1:100	WB, ICC and IHC

Mouse monoclonal anti-PHF-Tau	Pierce, MN1050	AT270	1:200	WB, ICC and IHC
Rabbit polyclonal anti-tPA	Molecular Innovations ASMTPA-GF-HT	-	1:500	IHC
Mouse monoclonal anti-beta amyloid (1-16)	Covance, SIG-39300	6E10	1:100	WB, ICC and IHC
Rabbit polyclonal anti-beta amyloid (1-42)	Millipore, AB5078P	-	1:100	WB, ICC and IHC
Rabbit polyclonal anti-cleaved-caspase-3	Cell Signaling Technology, 9661L	-	1:200	WB and IHC
Rabbit Polyclonal anti-NF-κB	FIVEphoton Biochemicals NFKB-2	-	1:400	WB

WB-Western blot analyses, IHC-Immunohistochemistry and ICC-Immunocytochemistry

Table 2.5: Secondary antibodies

Name	Source & Catalogue number	Dilution	Experiment
Amersham ECL anti-mouse IgG, HRP-linked whole antibody (from Sheep)	GE Healthcare, NXA931	1:1000	WB
Amersham ECL anti-rabbit IgG, HRP-linked whole antibody (from donkey)	GE Healthcare, NA934	1:1000	WB
Alexa Fluor 488, Goat anti-Rabbit IgG	Invitrogen, A11008	1:200	ICC and IHC
Alexa Fluor 488, Goat anti-Mouse IgG	Invitrogen, A11001	1:200	ICC and IHC
Alexa Fluor 594, Goat anti-Rabbit IgG	Invitrogen, A11012	1:200	ICC and IHC
Alexa Fluor 594, Goat anti-Mouse IgG	Invitrogen, A11005	1:200	ICC and IHC

HRP-Horseradish peroxidase, WB-Western blot analyses, IHC-Immunohistochemistry and ICC-Immunocytochemistry

2.1.12 Kinase assay

- **Protein A-Sepharose beads** (Sigma P9424)
- **Kinase buffer**

20 mM Tris-HCL (pH 7.4) (First Base, BUF 1415)

10 mM Magnesium chloride ($MgCl_2$) (Sigma, M8266)

1 mM EDTA (First Base, BUF-1052)

10 µM Sodium fluoride (NaF, 131675.1210, Panreac)

1 μM Sodium orthovanadate (Na$_3$VO$_4$) (Alexis Biochemicals, A400-032-G005)

- **5X kinase assay mixture**

  100 mM Tris-HCl (pH 7.4) (First Base, BUF 1415)

  50 mM MgCl$_2$ (Sigma, M8266),

  5 mM EDTA (First Base, BUF 1052)

  50 μM NaF (Panreac, 131675.1210)

  5 μM Na$_3$VO$_4$ (Alexis, 400-032-G005)

  5 mM DTT (Pierce, Thermo scientific, 20290)

- **5 μCi of (γ-32P)ATP** (PerkinElmer, BLU002A100UC)
- **Histone H1** (Millipore, 14-155)
- **NF-H peptide** (VKSPAKEKAKSPVK) (Sigma Proligo)
- **Trichloroacetic acid** (Sigma 522082)
- **P81 phosphocellulose squares** (Millipore, 20-134)
- **Bio-safe II scintillation fluid** (111195, Research Products International, Mount Prospect, IL)

2.1.13 Real-Time PCR (RT-PCR)

- **Trizol** (Invitrogen, 15596-018)
- **Chloroform** (J. T. Baker – 9180-68)
- **70% ethanol**

  70 ml of 100% ethanol (Ethanol-Fisher Chemicals, E/06050DF/17) in 30 ml water

  RNeasy Mini Kit (Qiagen, 74106)

- **High capacity cDNA reverse transcription kit** (Applied Biosystems, 4368814)
- **Power SYBER green PCR master mix** (Applied Biosystems, 4367659)

- **Primers** (Sigma Proligo)

Table 2.6: Primers used in RT-PCR

Primers	Primer sequences
MIP-1α Forward	5' TTGAGCCCCGGAACATTC 3'
MIP-1α Reverse	5' GCAGCAAACAGCTTATAGGAGATG 3'
TNF-α Forward	5' AGCACAGAAAGCATGATCCG 3'
TNF-α Reverse	5' GGAGTAGACAAGGTACAACC 3'
TGF-β Forward	5' CTTTAGGAAGGACCTGGGTT 3'
TGF-β Reverse	5' CAGGAGCGCACAATCATGTT 3'
IL-1β Forward	5' ACCTGCTGGTGTGTGACGTTC 3
IL-1β Reverse	5' CAGCACGAGGCTTTTTTGTTGT 3'
iPLA2 Forward	5' TAACCTGAAGCCACCGACTC 3'
iPLA2 Reverse	5' TAGTGTTGATCTCTGATATG 3'
cPLA2 Forward	5' CTGCAAGGCCGAGTGACA 3'
cPLA2 Reverse	5' TTCGCCCACTTCTCTGCAA 3'

2.1.14 <u>Radial Maze</u>

Radial maze for mice: 5 cm lane width x 35 cm arm length x 9 cm wall height, Stoelting ANY-maze, IL, USA (60150) (**Software**: EthoVision 3.1)

Novel food: Kellogg's fruit loops

2.1.15 <u>Lipid Analyses</u>

- 1-Butanol (J.T. Backer, JT9189-01)
- Chloroform (J.T. Baker, JT9180-68)
- Methanol (Schedelco, M0106)

2.1.16 <u>Cytosolic Phospholipase A2 (cPLA2) analyses</u>

- **PLA2 Inhibitor studies**

  0.3 µM of BEL (Bromoenol Lactone) (iPLA2 inhibitor) (Sigma, B1552)

  10 µM of AACOCF3 (Arachidonyl trifluoromethyl ketone) (cPLA2 inhibitor) (Biomol, 149301-79-1)

- **cPLA2 silencing**

  cPLA2 shRNA lentivirus (Santa Cruz Biotechnology, sc-35098-V)

  Polybrene (hexadimethrine bromide) (3 µg/ml) (Sigma, 107689)

- **cPLA2 activity Assay**

  cPLA2 assay kit (Cayman Chemical, 765021)

  Ice cold buffer

  50 mM HEPES pH 7.4 (Thermo Scientific, SH 30237.01)

  1 mM EDTA (First Base, BUF-1052)

2.2 Methods

2.2.1 Animal Handling

All animal procedures were carried out according to protocols approved by the Institutional Animal Care & Use Committee (IACUC) of the National University of Singapore (IACUC protocol number: 078/09). The animals were housed in standard cages (19.1 x 29.2 x 2.7 cm) with corncobs bedding at constant room temperature (22 ± 1°C) and 46-48% relative humidity. They were under a regular light-dark schedule (lights on from 7AM to 7PM), had free access to food (Irradiated 18% protein rodent diet, Teklad global, 2918, Harlan) and water ad labitum.

2.2.2 p25 transgenic mice

Breeding pairs of p25 single transgenic mice (C57BL/6-Tg (tetO-CDK5R1/GFP) 337Lht/J, Stock No: 005706) and CaM KIIα single transgenic mice (B6; CBA-Tg (Camk2a-tTA) 1Mmay/DboJ, Stock No: 007004) were obtained from The Jackson Laboratory (Bar Harbor, Maine, USA). All transgenics were heterozygous. p25 transgenic mice had the transgenic vector that encodes the carboxy terminal proteolytic fragment (*p25*) of human cyclin-dependent kinase 5, regulatory subunit 1 (*CDK5R1*) sequence with a green fluorescent protein (GFP) tag under the control of a tetracycline-responsive promoter element (TRE; tetO). Transgenic construct in CaM KIIα mice was designed with mouse CaM KIIα promoter placed upstream of the tetracycline-regulated transactivator (*tTA*) gene. p25 single transgenic mice were crossed with CaM KIIα mice to generate bi-transgenic offsprings (p25Tg mice) that inducibly overexpress human *p25* gene under the control of the CaM KIIα promoter-regulated tet-off system. In this system, tTA binds to the TRE and activates transcription of the *p25* gene in the absence of repressor (tetracycline-derivative, doxycycline). All mice in this study were conceived and raised in the presence of doxycycline in drinking water, for 6 weeks postnatal to avoid any potential developmental consequences from the expression of p25. Water containing doxycycline (200 µg/ml) was mixed with 1% sucrose to reduce the bitter taste. p25 expression was induced by the removal of doxycycline in water and samples (brain/blood) were collected at

different weeks of p25 induction periods. p25Tg mice were initially characterized by Cruz et al., in 2003 and various studies suggested that p25Tg mice recapitulate most of the pathological features of AD including tau hyperphosphorylation, amyloid accumulation and neuronal loss. Wild-type littermates were used as control groups in all the experiments and mice of the same sex were used for comparison whenever possible.

2.2.3 Curcumin treatment in p25 transgenic mice

p25Tg mice were fed with a natural anti-inflammatory compound, curcumin, orally via in feed (4 g/kg of feed, Harlan). LONGVIDA, a novel curcumin formulation prepared under a novel method called SLCP (solid lipid curcumin particle) (Verdure Sciences), was used in this study which has greater bioavailability in both the brain and blood as compared to the unformulated curcumin powder (Gota et al., 2010).

2.2.4 Genotyping

The offsprings generated from mice under different breeding strategies were weaned and tails clipped to collect small pieces of tails (0.5 cm) at the age of 21 days. Genomic DNA was isolated from these tails using DNeasy tissue kit. Mice tails were first digested with 180 µl of buffer ATL and 20 µl of Proteinase K at $56^{o}C$ until the tissue was completely lysed. Digested tail samples were mixed with 200 µl of lysis buffer AL and 200 µl of 100% ethanol. This mixture was then transferred into mini spin column and washed with buffer AW1 and AW2. Finally, genomic DNA was eluted using the elution buffer AE. Purity as well as the concentration of the eluted DNA was assessed using NanoDrop (Spectrophotometer, ND 1000 Biofrontier Technology). Genotyping was done by independent PCRs with the extracted genomic DNA using primers specific for Camk2a-tTA and p25-GFP (see section 2.1.2.3). Details about the preparation of reaction mixtures and cycling parameters are shown in the following tables.

Table 2.7: Detection of *p25* transgene

Reaction Mixture			Cycle parameter			
Components	Amount (µl)	Conc (µM)	Step	Temp (°C)	Time	Remarks
p25 Forward primer	0.5	20	1	94	1.5 min	-
p25 Reverse primer	0.5	20	2	94	30 sec	-
IC Forward primer	0.5	20	3	58	1 min	-
IC Reverse primer	0.5	20	4	72	1 min	Repeat steps 2-4 for 30 cycles
Accuprime Master Mix	11	-	5	72	2 min	-
water	-	-	6	10	-	hold

Table 2.8: Detection of *Camk2a* transgene

Reaction Mixture			Cycle parameter			
Components	Amount (µl)	Conc (µM)	Step	Temp (°C)	Time	Remarks
Camk2a Forward primer	0.5	20	1	94	3.0 min	-
Camk2a Reverse primer	0.5	20	2	94	20 sec	-
IC Forward primer	0.5	20	3	60	30 sec	0.5°C drop in each cycle
IC Reverse primer	0.5	20	4	72	35 sec	Repeat steps 2-4 for 12 cycles
Promega master mix	6	-	5	94	20 sec	-
water	6	-	6	58	30 sec	-
			7	72	35 sec	Repeat steps 5-7 for 12 cycles
			8	72	2 min	-
			9	10	-	hold

IC –Internal control

1.5% Agarose gel prepared in 1X Tris-acetate-EDTA (TAE) buffer was used to resolve the PCR products at 124 V for 1 hour. GelRedTM, a red fluorescent nucleic acid dye, added during agarose gel preparation step (1:10,000, Biotium) was used to visualize the bands under UV in Chemidox GelDoc XRS system (BioRad). Mice were labeled according to the genotyping results and separated in different groups as single and bi-transgenic mice to use for further experimental procedures.

2.2.5 Mammalian Cell culture

2.2.5.1 Primary mouse cortical neuron culture

Cortices from the embryos of C57BL/6 wild-type or p25Tg mice at days 16-18 (E16-18) were dissected out under the microscope. Cortices were then snipped into smaller pieces and digested in papain solution for 40 minutes at 37°C, followed by centrifugation at 201 x g (Eppendorf, 5810R) for 5 minutes at 4°C. Pellet was resuspended in STOP solution to neutralize papain action and then filtered using 10/10 solution and centrifuge at 129 x g for 10 minutes at 4°C to get the homogenous single cell cortical neurons (Eppendorf, 5810R). Cortical neurons were then cultured in different densities (100,000 cells per 12-well plate, 1 x10^6 cells per 6-well plate and 6 x10^6 cells per 10 cm dish) in neurobasal medium with B27 supplement containing 100 IU/ml penicillin, 100 µg/ml streptomycin and 2 mM glutamine in plates/dishes coated with poly-L-Lysine. Coating was done by adding Poly-L-Lysine to the plates and kept at room temperature overnight. Plates were washed twice with sterile ultra-pure water and dried completely before plating the neurons. Cortical neurons from the p25Tg mice were cultured in neurobasal media with doxycycline (10 µg/ml) until the neurons fully differentiated. Samples were collected after 5 days induction of p25 expression by the removal of doxycycline from the media.

2.2.5.2 Primary mouse glial cell culture

Glial cells (mixed) were extracted from the pups at P0 (the day of birth)-P2 (2 days old). The same procedure as primary mouse cortical neuron culture was followed except the final 10/10 filtration step. Glial cells were cultured in

DMEM supplemented with 2 mM penicillin streptomycin glutamine, 10% FBS and 10 mM sodium pyruvate at 37°C with 5% CO_2.

2.2.5.3 Human embryonic kidney FT (HEK-FT) cell line

HEK-FT cells were cultured in DMEM containing 200 mM glutamine, 10 mM NEAA, 100 mM sodium pyruvate, geneticin (500 µg/ml) and 10% FBS at 37°C with 5% CO_2. Sub-culturing was performed by splitting the fully confluent cell culture flask into two or more flasks using 1X trypsin. Excess cells were frozen using freezing media.

2.2.6 Transformation and plasmid DNA extraction

Frozen DH5α (Douglas Hanahan bacterial strain 5α) ultra-competent cells were gently thawed on ice and 50 µl of the cells were transferred to a pre-chilled sterile round-bottom tube (352059, BD Falcon). Subsequently, 1-2 µl of plasmid DNA (2-10 ng) was mixed gently with the cells and incubated on ice for 30 minutes. Cells were heat shocked at 42°C for 30 seconds and placed back on ice for 2 minutes. Cells were then mixed gently with 950 µl of pre-warmed LB medium and incubated at 37°C for 1 hour with constant shaking at 225 rpm. Later, 100 µl of transformed cells were spread onto LB/Ampicillin (100 µg/ml) plates using a plate spreader under sterile conditions. Petri dishes were dried for 10 minutes with cover and incubated overnight at 37°C. On the next morning, 4 ml of LB/Amp starter culture was inoculated with the colonies grown on the plates and incubated at 37°C for 4-5 hours with shaking at 225 rpm. At the end of the day, the starter culture was mixed with 100 ml of pre-warmed LB/Ampicillin media and incubated overnight at 37°C with constant shaking at 225 rpm. Plasmid DNA from these bacterial cultures was then extracted following the QIAprep Spin Miniprep Kit protocol. Eluted plasmid DNA was then quantitated using a NanoDrop (Spectrophotometer, ND 1000 Biofrontier Technology) and stored at -20°C until further use.

2.2.7 Lentivirus production and transduction

Lentiviruses of empty vector (EV-LV) and p25-LV enhanced green fluorescent protein (EGFP) plasmids were prepared as per protocol published previously with slight changes (Zheng et al., 2005). EV-LV/p25-LV plasmids,

Virapower Packaging mix and Lipofectamine 2000 complexes were prepared according to manufacturer's instructions (Invitrogen, K4975-00) and added dropwise to HEK293-FT cells plated at 90-95% confluence in 10 cm dishes. Cells were incubated at 37°C with 5% CO_2 for 48 hours. Cell-free viral supernatants were collected by centrifuging the media at 1811 x g (Eppendorf, 5810R) for 15 minutes at 4°C followed by filtering with 0.45 μm filter and then concentrated using Amicon Ultra-15 centrifugal filter units at 1811 x g (Eppendorf, 5810R) for 20 minutes at 4°C. 7 days in culture (DIC) cortical neurons were treated with various dilutions of EV-LV/p25-LV virus to find out the optimal viral titre to get approximately 80% transduction efficiency. GFP-fluorescence was visualized and quantitated by counting the number of GFP positive cells (minimum 75 cells per field) and normalized against the number of DAPI signals in 10 independent fields.

2.2.8 Co-culture and supernatant transfer experiments

15 mm poly-L-Lysine-coated coverslips with the p25 overexpressing/control neurons (lentivirus-transduced neurons or primary neurons from p25Tg/control mice) were placed on tissue culture inserts (3.0 μm, Greiner bio-one, 657630). Inserts were then positioned inside the 6-well plates with the glial cells (plated either on the 18 mm coverslips or at the bottom of the plates) and co-cultured at 37°C with 5% CO_2 for 48 hours.

Alternatively, cell-free supernatants from p25 overexpressing neurons were collected by centrifugation (1811 x g (Eppendorf, 5810R) for 15 minutes) and then transferred directly onto the glial cells for 48 hours. Glial cells from co-culture and supernatant transfer experiments were processed for immunocytochemistry and Western blot experiments.

2.2.9 Factor removal experiments

Media supernatants from EV-LV/p25-LV transduced neurons were treated individually with DNAse (8 μg/ml), RNAse (50 μg/ml) and Proteinase K (50 μg/ml) for 60 minutes at 37°C. Subsequently these enzyme-treated supernatants were heated at 95°C for 10 minutes and then cooled to 37°C to arrest enzyme activity before adding onto glial cells. In parallel, major lipids

were removed from the untreated supernatants by passing through the solid phase extraction column and glial cells were also treated with these eluted supernatants. Finally, all the treated glial cells were processed further for Western blot analyses and immunocytochemistry after 48 hours.

2.2.10 Immunocytochemical analyses

Glial cells on 18 mm coverslips (300,000 cells/coverslip) were washed twice with 1X PBS for 5 minutes each and then fixed with 4% formaldehyde/1X PBS followed by permeabilization with 0.1% Triton-X-100/1X PBS for 20 minutes each. Subsequently, cells were incubated with blocking solution (5% FBS in 1X PBS) for 30 minutes followed by the primary antibody GFAP (1:1000) in 5% FBS/PBS for 1 hour at room temperature. The cells were then washed 3 times for 5 minutes before and after incubation with appropriate secondary antibodies for 1 hour at room temperature in the dark. Later, cells were stained with DAPI (nuclei stain) (1:1000) and mounted on glass slide with anti-fade fluor-mounting medium. Confocal images were taken with Zeiss LSM-510 laser-scanning confocal microscope at 40X magnification.

2.2.11 Histochemical studies

2.2.11.1 Perfusion and brain sectioning

Mice were anesthetized with mixtures of ketamine (75 mg/kg) and medepomidin (1 mg/kg) and placed on their backs on the paraffin block. Forelimbs were spread widely and each paw was secured with pins to the block. A cut was made along the sternum and on both sides of the diaphragm laterally to expose the heart. The mice were perfused first with Ringer's Solution by inserting a cannula into the left ventricle and the right auricle was punctured to allow the escape of return circulation. Once the colour of the releasing circulation turned clear, fixative line clamp was opened to perfuse the mice with freshly made pre-chilled 4% PFA/PBS until the limbs, liver and the rest of the body hardened. Perfusion instruments were removed and brain samples were collected from mice heads. Perfused brains were then immersed in fixative overnight at 4°C. Subsequently, brain samples were placed in a series of sucrose/1X PBS solutions at 10%, 20% and 30%. In each solution,

brain samples had to sink to the bottom of the tube before transfer to the next solution. Brain samples were frozen in liquid nitrogen using the cryoprotectant Shandon M1 Embedding Matrix and sectioned into sagittal sections of 16 μm thickness using a cryostat (CM 3050S, Leica).

2.2.11.2 Immunofluorescence staining

Immunofluorescence staining was carried out by rinsing the brain sections with wash buffer (1X PBS with 0.1% Trition-X-100) two times at 5 minutes each, followed by incubation of the sections with blocking solution (5% FBS in 1X PBS) to prevent non-specific staining. Subsequently, sections were incubated with respective primary antibodies prepared in 5% FBS in 1X PBS overnight at 4°C and then rinsed three times at 5 minutes each with wash buffer to remove excess and unbound primary antibodies. Secondary antibodies prepared in 5% FBS in 1X PBS were added onto the sections for 1 hour at room temperature and then sections were washed 3 times with 1X PBS for 5 minutes each. Nuclei were counter-stained with DAPI (1:1000 in 1X PBS) and washed two times with 1X PBS. Lastly, sections were mounted with Dako anti-fade fluor-mounting medium and allowed to dry in the dark until viewing with a confocal microscope.

2.2.11.3 Thioflavin staining

Thioflavin staining was performed according to the published protocol with some changes (Sun et al., 2002). Sections were incubated with 0.05% Thioflavin-S solution in 50% ethanol for 10 minutes in the dark followed by rinsing in 50 % ethanol two times for 10 seconds each and two washes with large volumes of water. Finally, sections were mounted with anti-fade fluor-mounting medium and allowed to dry in the dark. Confocal images were taken at 40X magnification.

2.2.11.4 Bielschowsky Silver staining

Clean glass wares and all the reagents were cooled to 4°C before staining. Firstly, sections were incubated with 20% silver nitrate (AgNO$_3$) solution and then with ammoniacal silver solution for 20 minutes each in the dark at 4°C, followed by washing with distilled water. Sections were then immersed

serially in ammonia water (2 minutes), developer solution (2 minutes) and distilled water (5 minutes). Staining was stopped by incubating with 5% sodium thiosulphate (hypo Solution) for 5 minutes and rinsed thoroughly with water. Finally, sections were dehydrated by immersing in graded series of ethanol solutions (50%, 95% and 100%) and then in xylene before mounting.

2.2.11.5 TUNEL staining

TUNEL staining was performed as per the instructions from the In situ cell death detection kit with some modifications. Briefly, slides with brain sections were rinsed twice in 1X PBS and then treated with 0.1% Trito-X-100/1X PBS solution for 2 minutes on ice. Slides were then washed immediately with 1X PBS twice for 5 minutes each and incubated with 50 μl of TUNEL mixture (mixture of 450 μl solution from Vial 2 and 50 μl of enzyme from vial 1) in a humidified chamber at 37°C for one hour. Lastly, sections were washed again with 1X PBS three times followed by nuclei DAPI staining. The slides were mounted and dried in a dark place until viewed with a confocal microscope.

2.2.12 Western blot analyses

2.2.12.1 Lysate preparation

- **Mice brain lysates**

Mice brain samples were homogenized in an ice cold lysis buffer using a Dounce homogenizer on ice. Homogenates were then kept on ice for 20 minutes followed by centrifugation at 18,800 x g (Thermo Electron Corporation, Legend Micro21R) for 30 minutes at 4°C. Clear supernatants were then stored in aliquots at -80°C until further use.

- **Soluble cell lysates**

Cells were gently scraped into ice-cold 1X PBS, centrifuged at 18,800 x g for 30 minutes at 4°C. Pellets were resuspended thoroughly in ice cold lysis buffer. Cell homogenates were kept on ice for 20 minutes followed by centrifugation at 18,800 x g for 30 minutes at 4°C. Clear supernatants were then stored in aliquots at -80°C before use.

2.2.12.2 Protein Quantitation/Bicinchoninic acid (BCA) Assay

50 µL of each standard (range from 8 to 48 µg/ml of BSA in lysis buffer) and test samples (5 µl of lysate with 45 µl of lysis buffer) were mixed and incubated with 1 ml of working reagent mixture (Reagent A and B in the ratio 50:1) at 37°C for 30 minutes. The intensity of the purple colour developed was read at 562 nm using a spectrophotometer (DU 800 Spectrophotometer, Beckman Coulter). Later, a standard curve plotted using the average blank-corrected readings for each standard *vs.* its respective concentration (µg/ml) was used to calculate the protein concentration for unknown samples.

2.2.12.3 Sample preparation

An equal volume of 2X Laemmli sample buffer (with 5% BME) was mixed with brain/cell lysates and heated at 95°C for 5 minutes before loading onto the SDS-PAGE gels. Total cell lysates were prepared by scraping the cells directly in 2X sample buffer and heated at 95°C for 5 minutes.

2.2.12.4 SDS-PAGE gel electrophoresis

30 µg of lysates were separated on Novex 4-20% Tris-glycine mini gels at 120 volts until the dye front reached the bottom of the gel and transferred onto the nitrocellulose membrane using the Novex XCell II blotting module with 1X Tris-glycine transfer buffer for 2 hours at 100 mA. Quality of protein transfer was confirmed by reversible staining of membrane using Ponceau S staining solution followed by adequate washing with Tris buffered saline and Tween 20 (TBST) buffer. Blocking of non-specific binding of primary antibodies was achieved by incubating the membranes in blocking solution (10% milk in TBST) for 1 hour at room temperature. Membranes were then probed with respective primary antibodies (listed in table 2.1.1) overnight at 4°C followed by 3 washes with TBST buffer for 5 minutes each. Subsequently, membranes were incubated with horseradish peroxidase-conjugated mouse or rabbit secondary antibodies (listed in table 2.1.2) for 1 hour at room temperature and then washed 3 times with TBST for 5 minutes each. Immunoblots were developed using ECL (enhanced chemiluminescence) detection kit as per the instructions of the manufacturer. Membranes were finally stripped using

stripping buffer for 30 minutes at 50°C with agitation and then reprobed with other primary antibodies.

2.2.13 (γ-32P) ATP Kinase Assay

(This work was done in collaboration with Dr. Tej Kumar Pareek, Case Western Reserve University, Cleveland, OH, USA)

Kinase assay was performed using 500 μg of brain/cell lysates in order to determine the changes in Cdk5 activity. Lysates were first pre-cleared with protein A-Sepharose beads slurry (50%) for 1 hour at 4°C. Subsequently, 10 μg of rabbit polyclonal anti-Cdk5 (C8) antibody was added to the pre-cleared lysates and incubated for 3-4 hours with constant mixing at 4°C. Later, protein A-Sepharose beads slurry (50%) was added to this mixture prior to overnight incubation at 4°C. Immunoprecipitates were then washed 3 times with lysis buffer, once with kinase buffer and then resuspended in 30 μl of water followed by the addition of 10 μl of 5X kinase assay mixture, 10 μg of histone H1 and 0.2 μM of NF-H peptide. Later, immunoprecipitates were incubated with 5 μCi of (γ-32P) ATP for 30 minutes at 30°C and then 50% trichloroacetic acid was added to precipitate out the proteins, followed by centrifugation at 18,800 x g (Thermo Electron Corporation, Legend Micro21R) for 10 minutes at 4°C. 10 μl of trichloroacetic acid supernatants were added onto the P81 phosphocellulose paper squares and air-dried. These paper squares were washed 5 times with 75 mM phosphoric acid for 15 minutes each and then once in 95% ethanol. Finally, these squares were transferred to vials containing bio-safe II scintillation fluid for counting in a Beckman Coulter scintillation counter.

2.2.14 Real-Time PCR

RNA samples were extracted using the RNeasy mini kit as per instructions from the manufacturer. Briefly, brain samples/cell pellets were homogenized with 1 ml of Trizol and kept at room temperature for 5 minutes. Subsequently, this solution was mixed vigorously with 200 μl of chloroform and centrifuged for 15 minutes at 13,800 x g (Thermo Electron Corporation, Legend Micro21R) at 4°C. The upper aqueous phase was separated and mixed with

70% ethanol and then added to the mini columns followed by centrifugation at 6,200 x g for 15 seconds at 4°C. Wash buffers RW1 and RPE were used to wash the columns before eluting the RNA with RNase free water. Later, RNA concentration was measured using Nanodrop (Spectrophotometer, ND 1000 Biofrontier Technology). cDNA was synthesized from RNA samples using high capacity cDNA reverse transcriptase kit and quantitative real-time PCR was performed using ABI Prism 7900 HT Fast 9 detection system and results were analyzed using software AB 7500 version 2.0.5.

2.2.15 Radial maze

The radial arm maze paradigm was carried out as described previously (Zou et al., 1998; Schmitt et al., 2003) with some changes. The radial maze with 8 arms extended radially from the central area was used and arms were numbered from 1 to 8. Visual cues (black and white images) were positioned at the end of the arms 2, 4, 6 and 8 and a video camera was placed just above the maze in the ceiling to capture the training and test session trials. Video images were sent to the computer equipped with EthoVision 3.1, software that can track the animal's path and measures a number of useful parameters such as number of visits to each arm, time spent within each arm, number of attempts needed to finish the task and so on. EthoVision was used to specify different zones of interest from the video image of the test arena to automatically measure parameters related to these zones. In the training phase, mice were given 7 minutes to explore all the arms and allowed to consume the novel food (fruit loops) that were placed in only one arm in the order of 2, 4, 6 or 8 each session. The apparatus was cleaned with 70% ethanol and dried in between trials. Novel food was also placed outside of all the arms to minimize the possibility of smell as a cue. During the test phase, all the four arms (2, 4, 6 and 8) were baited and trial continued until all baits had been consumed or until 5 minutes had lapsed. Reference memory errors (entering a non-baited arm) and working memory errors (number of re-entry in baited arms) were calculated and analyzed between the groups. Mice were given a maximum of two test sessions per day, 6 days per week during the period of behavioural testing. The test and training sessions were conducted approximately at the

same time of the day in a moderately lit room with standard conditions of temperature and free from any stray noise.

2.2.16 Lipid extraction from cell culture media

Lipid extraction from cell culture media was performed using a protocol described previously with slight modifications (Bremer and Norum, 1982). In brief, the cell culture media/supernatant was incubated with 6 ml of 1-butanol with agitation at 4 x g (Eppendorf, 5424) for 2 hours at 4^oC. After equilibration and phase separation, the upper layer of the butanol extract was saved and mixed with 5 ml of chloroform to facilitate the second extraction. Later, bottom phase of both the chloroform and the butanol extracts were mixed together and dried under the nitrogen stream and kept at -80^oC.

2.2.17 Lipid extraction from the brain samples

Lipids were extracted from the brain samples according to the protocol described previously (Sharman et al., 2010). Briefly, approximately 26 mg of brain tissue was homogenized with 900 µl of Chloroform: Methanol (1:2) using a PRO 200 Homogenizer (PRO Scientific Inc) and incubated at 4^oC with agitation at 4 x g (Eppendorf, 5424) for 2 hours. After incubation, 300 µl of chloroform and 300 µl of distilled water were added into the homogenates and mix thoroughly by vortex. Later, the homogenates were centrifuged at 7,800 x g (Thermo Electron Corporation, Legend Micro21R) at 4^oC for 2 minutes to break phase and the bottom organic phase was collected into a new tube. Re-extraction was carried out by adding another aliquot of 500 µl of chloroform and the organic phase obtained was pooled together, dried under a nitrogen stream and kept at -80^oC.

2.2.18 Lipids analysis using High-Performance Liquid Chromatography/Mass Spectrometry

(This work was done in collaboration with A/Prof. Markus Wenk's Lipidomics lab)

Agilent 1200 high-performance liquid chromatography (HPLC) system and a 3200 Q-trap mass spectrometer were used to quantify individual lipids extracted from brain/cell culture supernatants samples. The HPLC systems

contain an Agilent 1200 binary pump, an Agilent 1200 thermo sampler and an Agilent 1200 column oven. HPLC conditions are Luna 3u silica column (i.d.150x2.0 mm); mobile phase A (chloroform: methanol: ammonium hydroxide, 89.5:10:0.5), B (chloroform: methanol: ammonium hydroxide: water, 55:39:0.5:5.5); flow rate 350 µl/min; 5% B for 3 minutes, then linearly changed to 30% B in 24 minutes and maintained for 5 minutes, and then linearly changed to 70% B in 5 minutes and maintained for 7 minutes. Eluents were changed to the original ratio in 5 minutes and maintained for 6 minutes. Multiple Reaction Monitoring (MRM) transitions for individual lipid species such as phosphatidylethanolamine (PE), Phosphatidylcholine (PC), phosphatidylserine (PS), phosphatidylinositol (PI), ceramide (Cer) and sphingomyelin (SM) were set up for quantitative analyses. PC-14:0/14:0, PE-14:0/14:0, PS-14:0:14:0, ceramide, C12-SM and LPC 20:0 (4 µM) (Avanti Polar Lipids) were used as internal standards to quantitate the individual lipids.

2.2.19 Stereotactic injection of lipids into mouse brain

Mice were anesthetized and positioned in a stereotactic frame. Midline incision of the scalp was made and the vertex area was exposed. Later, a small hole was drilled according to the coordinates: caudal to bregma 2 mm, 2 mm lateral to the midline and 1.8 mm from the surface of the cortex. 1 µl of solution containing lipids (2 µM) was injected at a constant rate for 5 minutes using a microsyringe (Hamilton) inserted stereotactically through the opening. The needle was slowly withdrawn and the scalp sutured. After recovery from anesthesia, mice were returned to their cages and observed closely for normal food and water intake. Later, these mice were perfused with 4% PFA 48 hours post-injection and then brain samples were collected for sectioning and further immunostaining experiments.

2.2.20 Phospholipase A2 (PLA2) Inhibitor studies

Inhibitor studies were performed by transducing the neurons with p25-LV together with 0.3 µM of BEL (iPLA2 inhibitor) or 10 µM of AACOCF3 (cPLA2 inhibitor) for 48 hours at 37°C with 5% CO_2. Later, cell-free

supernatants from these neurons were transferred to glial cells for 48 hours and glial cells were processed for further analyses.

2.2.21 Cytosolic Phospholipase A2 (cPLA2) silencing

Silencing of *cPLA2* gene expression was performed in cortical neurons using shRNA lentivirus transduction. cPLA2 shRNA (mouse) lentiviral particles have a target-specific construct that encodes a 19-25 short hairpin RNA designed to knock-down *cPLA2* gene expression (Santa Cruz Biotechnology, SC-35098-V). Cortical neurons plated on 6-well plates were incubated with an aliquot of p25-LV along with the cPLA2 shRNA lentiviral particles in neurobasal medium with polybrene (3μg/ml) for 48 hours at $37^{o}C$ with 5% CO_2. Subsequently, glial cells were treated with the cell-free supernatants from these cPLA2-silenced cortical neurons and then fixed with 4% formaldehyde after 48 hours for further analyses.

2.2.22 cPLA2 activity assay

cPLA2 activity was measured using cPLA2 activity assay kit according to the manufacturer's instructions. Brain samples from different mice groups or cell pellets from neurons transduced with p25-LV/EV-LV were homogenized with ice cold buffer and lysates collected (10 μl) were diluted with 5 μl of assay buffer and added to the 96 well plate provide by the manufacturer. 15 μl of assay buffer was used as the blank and 10 μl of PLA2 standard (Bee venom included in the kit) diluted with 5 μl of assay buffer was added as a standard. Enzymatic reaction was initiated by incubating with 200 μl of substrate solution for 60 minutes. Subsequently, 10 μl of DTNB (5, 5'-dithiobis-(2-nitrobenzoic acid) solution was added to stop the enzyme reaction and allow colour development. Finally, intensities of the reactions, a marker of activity, were read at 414 nm using a Tecan Infinite M200 microplate reader. cPLA2 activity was calculated according to the formula suggested by the manufacturer and the results were normalized to total protein concentrations calculated by the BCA method.

2.2.23 Statistics

Data are expressed as the mean of at least three values $\pm$ standard error (s.e.m). Statistical significance was determined using student's t-test (Chapter 3 and Chapter 4), one-way analysis of variance (ANOVA) followed by post-hoc tukey's test (Chapter 5) and repeated measures ANOVA followed by post-hoc tukey's test (Behavioural studies in Chapter 5). P-value for statistical significance is defined as $P < 0.05$.

CHAPTER 3

CHAPTER 3: Investigation of p25/Cdk5-mediated neuroinflammation using *in vivo* (p25Tg mice) as well as *in vitro* (p25-LV virus-transduced cortical neurons) p25 overexpressing systems

3.1. Introduction

Neuroinflammation is one of the key pathological features of many neurodegenerative diseases, including AD, and is thought to contribute to neurodegeneration (Aisen, 1996; Rogers et al., 1996; Tuppo and Arias, 2005). However, the exact mechanisms behind neuroinflammation and its significance in the initiation of AD pathogenesis are not completely understood (Zilka et al., 2006; Agostinho et al., 2010).

Several studies suggested that Cyclin-dependent kinase 5 (Cdk5) hyperactivation could contribute to cytoskeletal abnormalities and neuronal death in AD (Pei et al., 1998; Patrick et al., 1999; Lopez-Tobon et al., 2011; Cheung and Ip, 2012). Although the potential role of Cdk5 deregulation by its hyperactivator p25 in the development of the pathogenesis of AD has been described by earlier studies (Ahlijanian et al., 2000; Yoo and Lubec, 2001; Cruz et al., 2003), the actual mechanisms behind the early changes in neuroinflammation that cause the progression of neurodegeneration during p25 overexpression remains obscure. Therefore, the experiments detailed in this chapter aim to investigate the mechanisms behind p25-mediated neuroinflammation by employing *in vivo* (p25Tg mice) & *in vitro* (cortical neurons transduced with p25-LV virus) p25 overexpression systems and co-cultures of cortical neurons/astrocytes.

3.2. Methods

3.2.1 p25 transgenic mouse model

C57BL/6-Tg (tetO-CDK5R1/GFP) 337Lht/J mice (The Jackson laboratory) were crossed with B6; CBA-Tg (Camk2a-tTA) 1Mmay/J mice (The Jackson laboratory) to generate bi-transgenic mice (p25Tg mice) that inducibly overexpress human *p25* transgene under the regulatory control of tetracycline analogue, doxycycline. Whenever possible, littermates of same sex mice were used for comparison. Brain samples were collected from p25 transgenic (p25Tg) mice at different induction periods of p25 expression such as 1, 4, 8 and 12 weeks and processed differently for different experiments.

3.2.2 Mammalian cell culture

3.2.2.1 Primary mouse cortical neuron culture

Primary cortical neurons from wild-type (C57BL/6) and p25Tg mice embryos (E16-18) were cultured in different densities (100,000 cells per 12-well plate/coverslip, 1×10^6 cells per 6-well plate and 6×10^6 cells per 10 cm dish) in coverslip/plates/dishes coated with poly-L-Lysine.

3.2.2.2 Primary mouse glia culture

Glial cells were extracted from P0-P2 pups of (C57BL/6) wild-type mice and cultured at 37°C with 5% CO_2.

3.2.3 Lentivirus production and transduction

Lentiviruses of empty vector (EV) and p25-enhanced green fluorescent protein (EGFP) were prepared from HEK293-FT cells using Virapower Packaging Mix and Lipofectamine 2000. Cortical neurons were treated with lentiviruses at optimal dilutions for 48 hours at 37°C with 5% CO_2 to get approximately 80 % transduction efficiency.

3.2.4 Co-culture and supernatant transfer experiments

EV-LV/p25-LV virus-transduced cortical neurons or primary neurons from p25Tg/control mice were co-cultured with glial cells using tissue culture

inserts in 6-well plates for 48 hours at 37°C with 5% CO_2. In parallel, culture media supernatants from p25 overexpressing/control neurons were transferred onto glial cells for 48 hours at 37°C with 5% CO_2. The glial cells from co-culture and supernatant transfer experiments were then processed individually for immunocytochemistry and Western blot analyses.

3.2.5 NMDA treatment

9 DIC (days in culture) cortical neurons in 6-well plates (1x 10^6 cells per well) were treated with NMDA + glycine (500 μM of NMDA (Tocris, 0114) and 100 μM of glycine (Sigma, 50046), glutamate + glycine (200 μM of glutamate (Sigma, G1251) and 100 μM of glycine) and NMDA + MK801+ glycine (500 μM of NMDA, 100 μM of glycine and 1 μM of MK801 (Tocris, 0924) for 12 hours at 37°C with 5% CO_2. Supernatants from these treatments were saved and transferred onto the glial cells in 6-well plates for 48 hours at 37°C with 5% CO_2. Cortical neurons were processed for Western blot analyses with anti-C19 antibody and glial cells were processed for both Western blot analyses and immunocytochemical staining experiments with anti-GFAP antibody.

3.2.6 Immunocytochemistry

Immunofluorescence staining was performed on glial cells from co-culture and supernatant transfer experiments using primary antibodies such as mouse anti-GFAP and anti-CD11b. Alexa Fluor 488 and Alexa Fluor 594 were used as secondary antibodies and nuclei were counterstained with DAPI. Immunofluorescence images were taken with Zeiss LSM-510 laser-scanning confocal microscope at 40X magnification.

3.2.7 Immunohistochemistry

16 μm brain sections collected from 1, 4, 8 and 12-week induced p25Tg/control mice were immunostained with primary antibodies such as mouse anti-GFAP, mouse monoclonal anti-GFP, mouse monoclonal anti-AT8, rabbit anti-beta-amyloid 1-42, mouse anti-CD11b, rabbit anti-tPA, mouse anti-CD4 and anti-CD8 antibodies. Later, sections were stained with Alexa Fluor 594 and 488 secondary antibodies followed by DAPI. Confocal

images were taken at 20X, 40X and 63X magnifications.

3.2.8 Western blot analyses

Brain lysates (from 1, 4, 8 and 12-week induced p25Tg/control mice), glial cell lysates (total cell lysates from co-culture and supernatant transfer experiments) and soluble cell lysates (from EV-LV/p25-LV virus-transduced cortical neurons and p25Tg/control mice neurons) were resolved on 4-20% polyacrylamide gels and transferred onto nitrocellulose membranes. Membranes were then immunoprobed with rabbit anti-GFAP, rabbit anti-Cdk5 (C-8) and rabbit anti-p35 (C-19) antibodies.

3.2.9 *In vitro* kinase assays

Changes in Cdk5 activity were investigated with kinase assays using brain lysates from 1, 4, 8 and 12-week induced p25Tg/control mice and EV-LV/p25-LV virus-transduced cortical neurons.

3.2.10 Real-Time PCR

Total RNA was extracted from 1, 4, 8 and 12-week induced p25Tg/control mice brains, EV-LV/p25-LV virus-transduced cortical neurons and p25Tg/control mice cortical neurons using RNeasy Mini Kit. cDNA was synthesized from RNA using High capacity cDNA reverse transcriptase kits and quantitative real-time PCR was performed with respective primers.

3.2.11 Statistical analyses

Data are expressed as the mean of at least three values ± standard error (s.e.m). Statistical significance was determined using student's *t*-test and P-value for statistical significance is defined as $P < 0.05$.

3.3 Results

3.3.1 p25 transgenic mice exhibit robust astrogliosis

Astrogliosis, a hypertrophy of astrocytes, is commonly observed during neuroinflammation (Sofroniew, 2009). In an effort to determine the onset of neuroinflammation in p25Tg mice, astrogliosis was evaluated at various time points such as 1, 4, 8 and 12-week induction of p25 expression in p25Tg mice and in age-matched control mice. Immunohistochemistry was performed on brain sections using anti-GFAP antibody to determine when astrogliosis commences in p25Tg mice and increased GFAP immunoreactivity was used as an indicative feature of astrogliosis. A substantial increase in GFAP immunoreactivity was observed especially in 2/3 layer of cortex of 1 week induced p25Tg mice compared to control mice (Figure 3.1A). Likewise, progressive and significant increase in GFAP expression was observed in 4, 8 and 12-week induced p25Tg mice. Moreover, a prominent increase in GFAP immunoreactivity was also observed in the CA3 region of hippocampus in 1-12 week induced p25Tg mice compared to the respective age-matched controls (Supplementary Figure 1 in Appendices).

Moreover, results from Western blot analyses using anti-GFAP antibody further confirmed immunohistochemistry results where robust elevation of GFAP expression levels was observed in brain lysates from 1 to 12-week induced p25Tg mice compared to the control mice (Figure 3.1B and 1C). In addition, kinase assay data and immunostaining experiments using anti-GFP antibody indicated a strong correlation between GFAP upregulation and p25/Cdk5 hyperactivation in 1 to 12-week induced p25Tg mice (Figure 3.1E and 1F). Cdk5 levels were found to be unaltered in all the time points of p25 induction in p25Tg mice (Figure 3.1D).
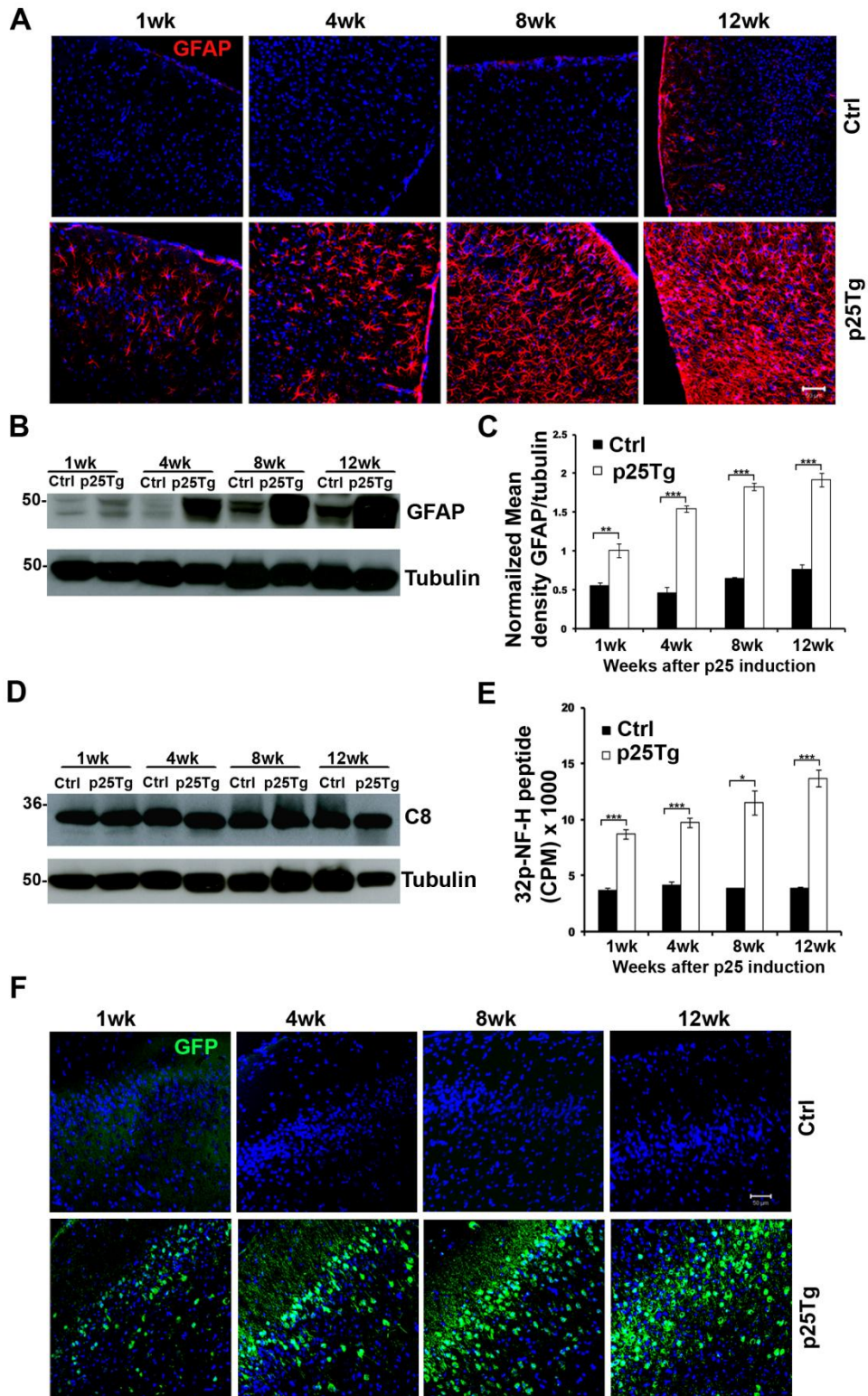
Figure 3.1: Astrogliosis is an early event in p25 transgenic mice

(**A**) Representative immunofluorescence images of 2/3 layer of cortex from 1, 4, 8 and 12-week induced p25Tg and their respective age-matched control (Ctrl) mice brain sections stained with anti-GFAP antibody (red) and nuclei were stained with DAPI (blue). (**B**) Immunoblot analyses results for the brain lysates of 1, 4, 8 and 12-week induced p25Tg/Ctrl mice using anti-GFAP antibody (top panel). Membranes were re-probed with anti-tubulin antibody (bottom panel) which acts as a loading control. (**C**) Quantification of immunoblot analyses in **B** by densitometric scanning (** p-value < 0.01 and *** p-value < 0.001). (**D**) Western blot analyses results from p25Tg/control mice using anti-Cdk5 (C8) antibody. (**E**) Representative *in vitro* kinase assay graph using active kinase (Cdk5) from p25Tg/control mice brain lysates (*** p-value < 0.001 and * p-value < 0.05) (student's *t*-test). Error bars indicate ± s.e.m. (**F**) Immunofluorescence images of the cortex from samples same as in **A** using anti-GFP antibody. Scale bars represent 50µm and images are representative of n=3 mice.

RT-PCR analyses were performed to observe changes in chemokines/cytokines such as MIP-1α, TNF-α, TGF-β and IL-1β expression levels in brain samples from 1, 4, 8 and 12-week induced p25Tg/control mice. Results identified a remarkable increase in chemokines/cytokines expression levels in the brain samples from p25Tg mice compared to the controls (Figure 3.2A-D). Specifically, MIP-1α, TGF-β and IL-1β expression levels peaked at 4 weeks of induction, whereas TNF-α expression peaked at 8 weeks of induction of p25 expression.

Together, these results determined that astrogliosis and the subsequent release of cytokines/chemokines were early events in the neurodegenerative process in p25Tg mice.
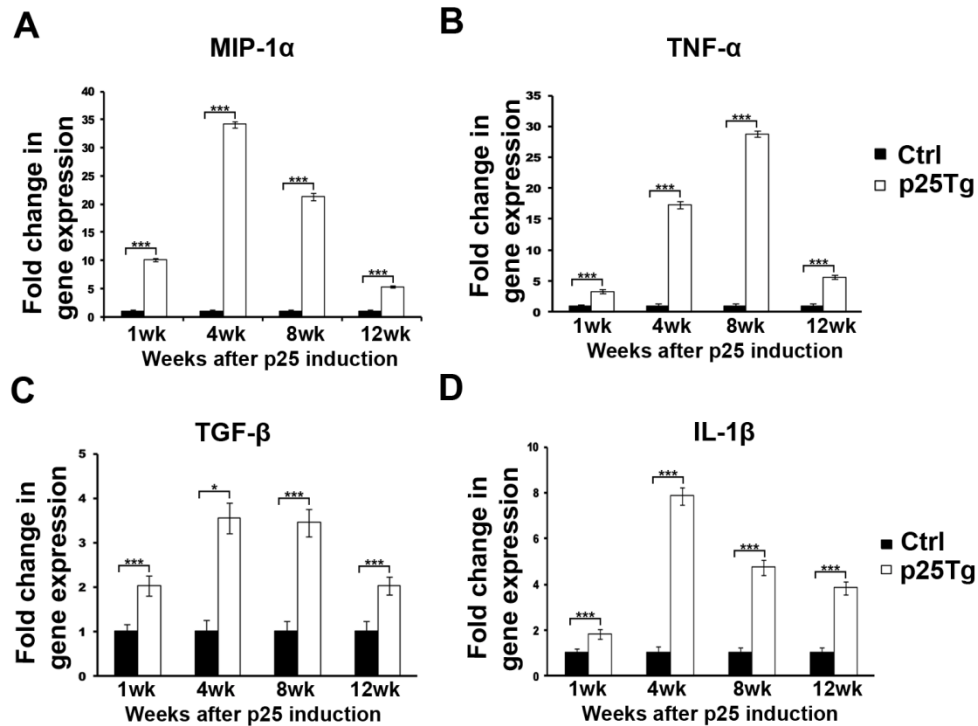
Figure 3.2: Chemokine/cytokine expression levels in p25 transgenic mice

Real-time PCR results for (**A**) MIP-1α, (**B**) TNF-α, (**C**) TGF-β and (**D**) IL-1β expression levels in 1, 4, 8 and 12-week induced p25Tg/control mice (*** p-value < 0.001 and * p-value < 0.05) (student's *t*-test). Error bars indicate ± s.e.m.

3.3.2 Reactive microgliosis is a late event in p25Tg mice

To facilitate the study of microglial activation status in p25Tg mice, immunohistochemistry was carried out with the brain sections from p25Tg/control mice using a specific marker for activated microglia, anti-Cd11b antibody. The results showed that microgliosis was absent at 1 week induction and only became evident after 4-week induction of p25 expression (Figure 3.3A). Thus, noticeable GFAP upregulation without microglial activation in 1 week induction of p25 expression (Figure 3.1) suggested that astrogliosis preceded microgliosis in p25-mediated neurodegenerative process in p25Tg mice.

Previous studies reported that the non-proteolytic action of tissue plasminogen activator (tPA) could mediate microglial activation and increases in tPA levels would be an indication for microglial activation during neurodegeneration (Siao and Tsirka, 2002; Pineda et al., 2012). To further confirm the findings about the onset of microgliosis in p25Tg mice, immunohistochemistry was performed and results using anti-tPA antibody were identical to the Cd11b findings (Figure 3.3B). Together, immunostaining results suggested that reactive microgliosis may occur secondary to astroglial activation in p25-mediated neuroinflammation.
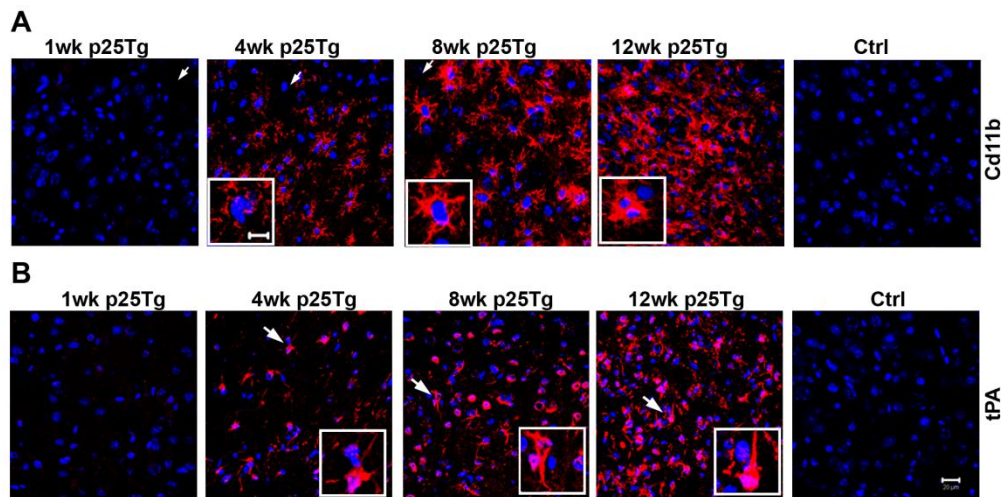
Figure 3.3: Reactive microgliosis in p25 overexpression-mediated neuroinflammation

Representative immunofluorescence images of the cortex from 1, 4, 8 and 12-week induced p25Tg/control mice using (**A**) anti-Cd11b, (**B**) anti-tPA antibodies (red). Nuclei were stained with DAPI (blue). White arrows show the region that is magnified in boxed insets (n=3). Scale bars: 20 µm (main panel) and 10 µm (insets).

3.3.3 p25Tg mice exhibit prominent infiltration of peripheral immune cells

Infiltration of peripheral immune cells into the central nervous system (CNS) is a critical phase in the progression of several neurodegenerative diseases such AD, PD and ALS (Town et al., 2005; Chiu et al., 2008; Brochard et al., 2009). However, the involvement of peripheral cell infiltration in p25-induced neuroinflammation has not been fully explored. Hence, the presence of peripheral immune cells in p25Tg mice brains was investigated using lymphocyte subset markers, CD4 and CD8. A dramatic increase in CD4 and CD8 immunostaining after 4 weeks of induction strongly suggested that peripheral cell infiltration was evident during p25-mediated neuroinflammation (Figure 3.4).
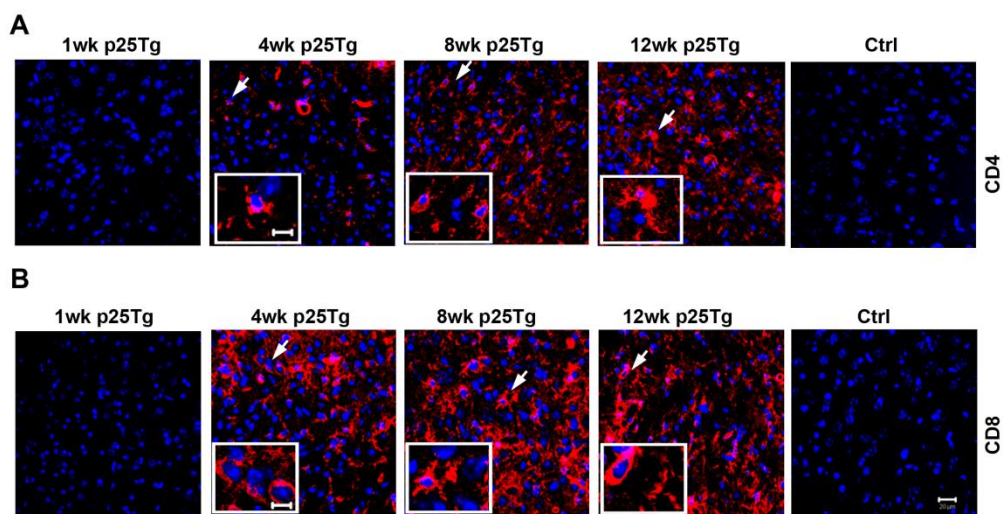
Figure 3.4: CNS infiltration of leukocytes in p25Tg mice

Confocal images of the cortex from p25Tg/control mice brain sections using (**A**) anti-CD4 and (**B**) anti-CD8 antibodies (red). Nuclei were stained with DAPI (blue). White arrows show the region that is magnified in boxed insets. Scale bars: 20 μm (main panel) and 10 μm (insets) (n=3).

3.3.4 Astrogliosis precedes amyloid-β/phospho-tau pathology in p25Tg mice

The onset of neurodegenerative hallmarks such as hyperphosphorylated tau and intraneuronal amyloid-β accumulation in p25Tg mice were examined at different time points such as 1, 4, 8 and 12-week induction of p25 expression in order to determine whether the p25-mediated astrogliosis is triggered by amyloid-β or phospho-tau accumulation. Immunostaining analyses were performed using AT8 (marker for hyperphosphorylated tau) & Aβ 1-42 antibodies and results indicated that phospho-tau production and amyloid accumulation were observed only after 4-week and 8-week induction of p25 expression respectively (Figure 3.5). However, astrogliosis and chemokines/cytokines upregulation were found even in 1 week of p25 induction (Figure 3.1 and 3.2). Thus, results identified that p25-mediated astrogliosis was not triggered either by phospho-tau or by amyloid-β pathology in p25Tg mice.
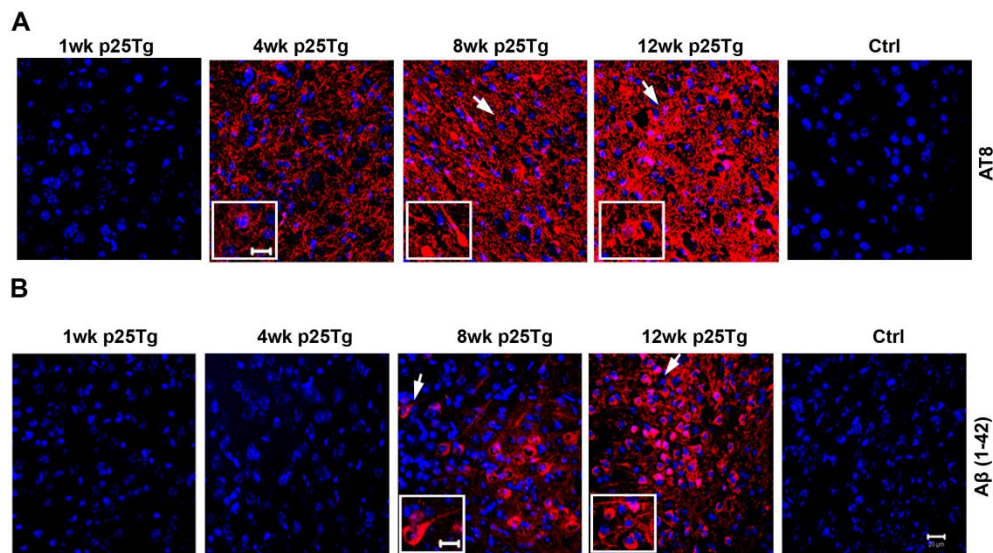
Figure 3.5: Initiation of neuroinflammation is independent of amyloid-β and tau phosphorylation in p25 transgenic mice

Confocal images of the cortex from p25Tg/control mice brain sections using (**A**) anti-AT8 and (**B**) anti-Aβ (1-42) antibodies (red). Nuclei were stained with DAPI (blue). White arrows show the region that is magnified in boxed insets. Scale bars: 20 μm (main panel) and 10 μm (insets) (n=3).

3.3.5 p25-induced glial activation is mediated by a soluble factor

Results from Figure 3.5 strongly suggested a possibility of an alternate trigger produced very early during p25 overexpression to mediate astrogliosis. Nonetheless, it was unclear what this trigger was. Hence, p25 overexpressing neurons and primary glial cells were used to investigate how p25 overexpression mediates this astrogliosis. Glial cells in 6-well plates were co-cultured with neurons transduced with p25-LV/EV-LV and primary neurons from p25Tg/control mice. Interestingly, immunostaining results indicated that GFAP immunostaining was significantly elevated in glial cells that were co-cultured with neurons transduced with p25-LV and neurons from p25Tg mice compared to the respective controls. Thus, these results suggested a possibility of the involvement of soluble factors in p25 overexpression-mediated astrocytes activation, since neurons and glial cells were not in direct contact with each other in co-culture experiments (Figure 3.6A). Subsequently, Western blot analyses were carried out on lysates from glial cells that were co-cultured with neurons transduced with EV-LV/p25-LV or neurons from p25Tg/control mice and results confirmed the findings of immunostaining results described above (Figure 3.6B).

Furthermore, RT-PCR analyses were performed to determine changes in chemokines/cytokines levels during the p25 overexpression-mediated activation of glia *in vitro*. Significant increases in inflammatory cytokines/chemokines levels such as MIP-1α, TNF-α, TGF-β and IL-1β were observed in glial cells that were co-cultured with neurons transduced with p25-LV and neurons from p25Tg mice compared to the respective controls (Figure 3.6C and D). In addition, cell-free supernatant transfer experiments were carried out between p25-overexpressing neurons and glial cells and results from immunostaining and Western blot analyses supported the findings from the co-culture experiments where soluble signals from p25 overexpressed neuron caused glial activation (Figure 3.7A and B). In parallel, kinase assays and Western blot analyses were carried out to determine the hyperactivation of Cdk5 in p25 overexpressing cortical neurons (Figure 3.7C and D).

In addition, to investigate the effects of p25-mediated soluble factor production on microgliosis, immunostaining using anti-Cd11b antibody was performed on glial cells that were incubated with cell-supernatants from p25 overexpressing neurons and results showed that there were no significant changes in microglial numbers compared to controls (Figure 3.7E).
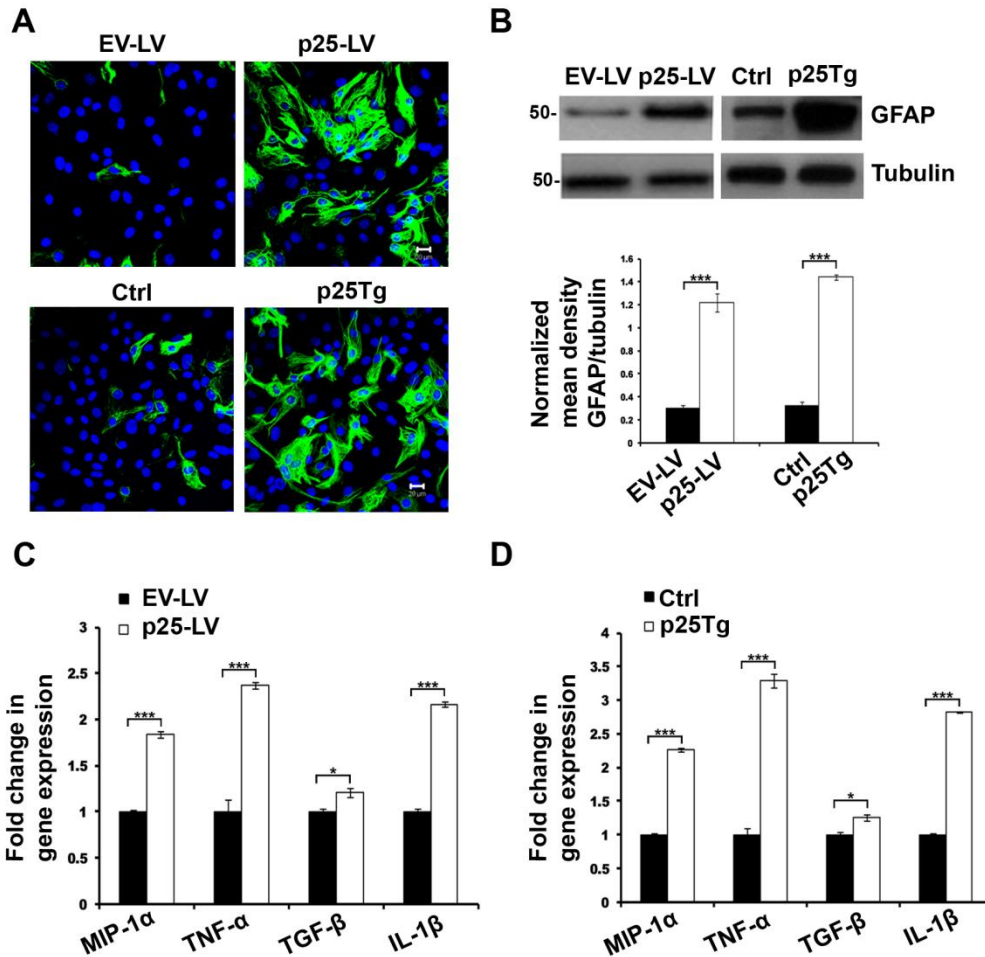
Figure 3.6: Characterization of p25 overexpression-mediated glial activation using co-culture system

(**A**) Immunofluorescence images from glial cells that were co-cultured with EV-LV/p25-LV transduced neurons (top panel) and primary neurons from control/p25Tg mice (bottom panel) using anti-GFAP antibody (green) and DAPI (blue). Scale bars: 20µm. (**B**) Western blots with glial cell lysates that were co-cultured with EV-LV/p25-LV transduced neurons and neurons from control/p25Tg mice using anti-GFAP antibody. Bar graph below the blots shows GFAP expression level quantification (*** p-value < 0.001). RT-PCR results for the expression of MIP-1α, TNF-α, TGF-β and IL-1β in glia co-cultured with (**C**) p25 overexpressing cortical neurons and (**D**) primary cortical neurons from p25Tg/control mice (*** p-values < 0.001 and * p-value <0.05).
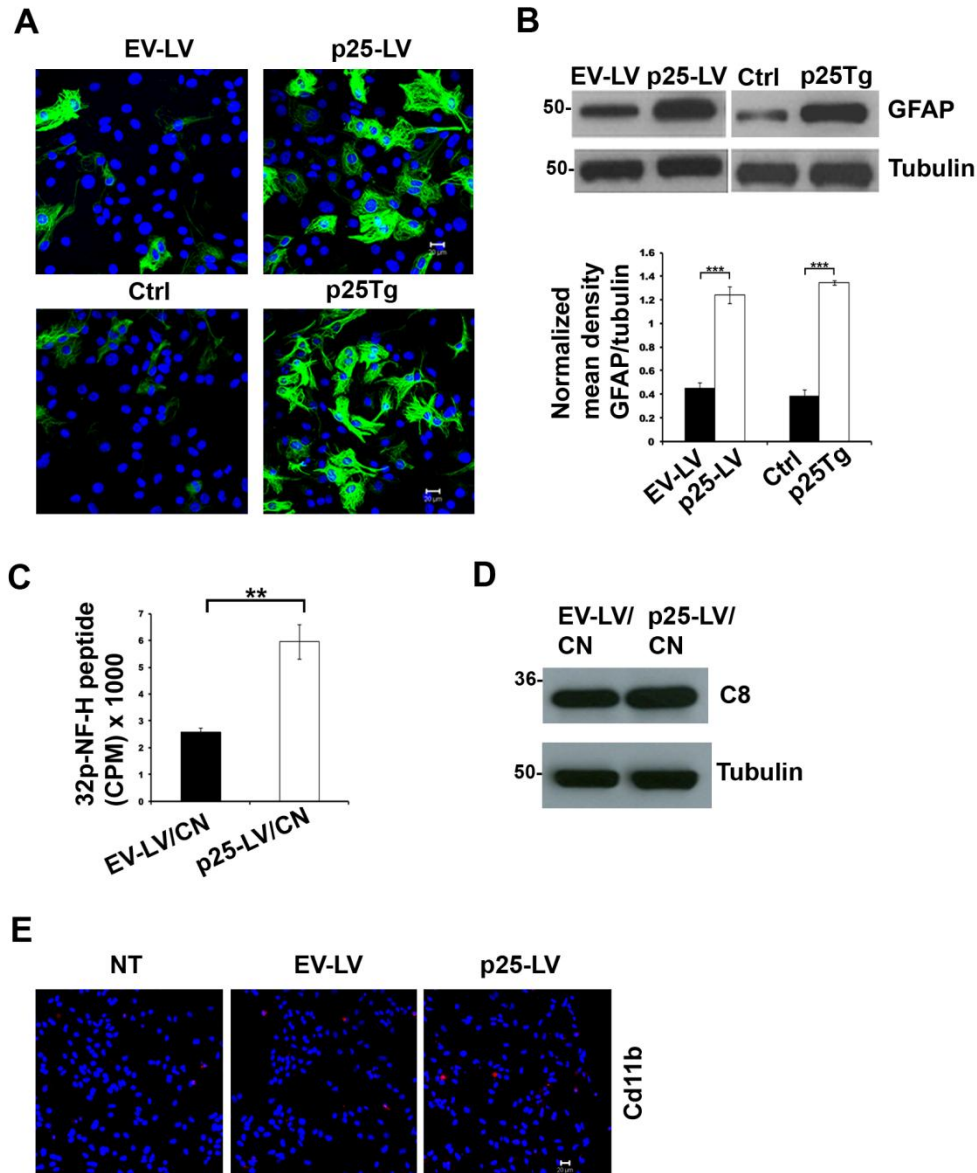
Figure 3.7: Characterization of p25 overexpression-mediated glial activation using supernatant transfer system

(**A**) Glial cells that received cell-free supernatants from EV-LV/p25-LV transduced neurons (top panel) and neurons from control/p25Tg mice (bottom panel) were immunostained with anti-GFAP antibody (green) and DAPI (blue). Scale bars: 20μm. (**B**) Western blots for samples same as in **A** using anti-GFAP antibody. Bar graph below the blots shows GFAP expression level quantification (*** p-value< 0.001). (**C**) Kinase assay results for cortical neurons transduced with EV-LV/p25-LV (** p-values < 0.01) (student's *t*-test). Error bars indicate ± s.e.m. (**D**) Western blot analyses results of cortical neurons transduced with EV-LV/p25-LV using anti-Cdk5 (C8) antibody. (**E**) Confocal images of glial cells treated with supernatants from p25 overexpressing /control neurons stained with anti-CD11b antibody (red) and DAPI (blue). Scale bars: 20μm.

3.3.6 Endogenously produced p25 induces astrogliosis through a soluble factor

NMDA has previously been shown to produce p25 from p35 through the activation of the calcium-dependent protease calpain (Kerokoski et al., 2002; Wei et al., 2005; Hosokawa et al., 2006). To investigate the effects of endogenously produced p25 on neuroinflammation, cortical neurons were treated with NMDA in the presence and absence of NMDA blocker MK180. Results from Western blot analyses confirmed the production of significant amounts of p25 from p35 in the presence of NMDA alone, whereas no change in p35 levels were observed in the presence of NMDR blocker MK180 (Figure 3.8A). Subsequently, cell-free supernatants from NMDA treated cortical neurons were transferred to glial cells and incubated for 48 hours. Immunocytochemical staining and Western blot analyses indicated that glial cells incubated with supernatants from cortical neurons with endogenously produced p25 were activated at about the same level as those incubated with supernatants from p25 overexpressed neurons (Figure 3.8B-E). Therefore, these data indicated that p25 caused neuroinflammation not only when overexpressed, but also when endogenously produced during neurotoxicity. In addition, results clearly demonstrated that endogenously-produced p25 also mediated astrogliosis through the production of soluble factors.
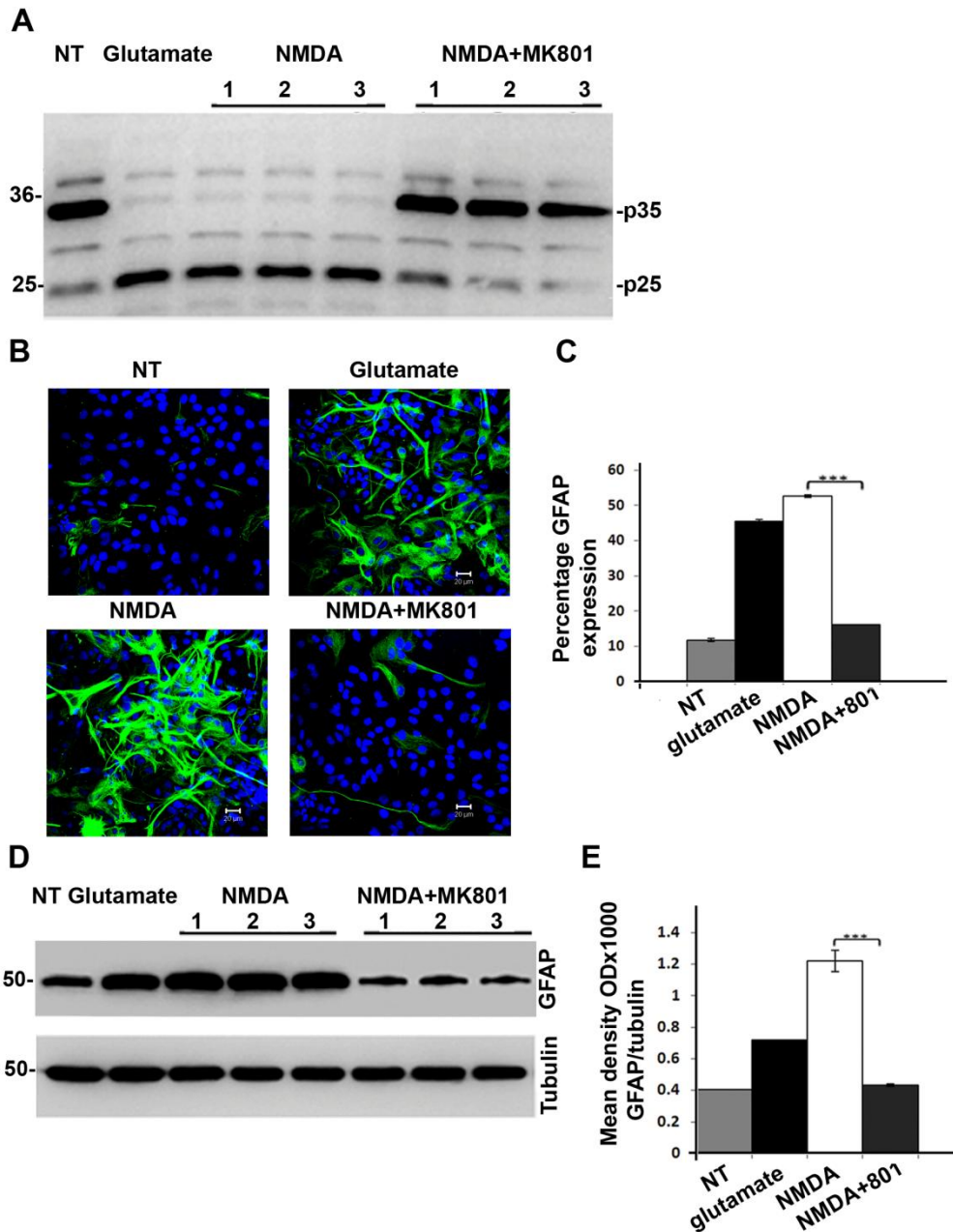
Figure 3.8: Endogenous p25 expression mimics the p25 overexpression induced effect on astrogliosis

(**A**) Western blot analyses results from non-treated neurons (NT), neurons treated with glutamate (positive control), NMDA and NMDA+MK801 using C-19 antibody. (**B**) Representative immunostaining images from glial cells treated with supernatants from NT neurons or neurons treated with glutamate, NMDA and NMDA+MK801 using anti-GFAP antibody. Scale bars represent 20μm. (**C**) Quantification of GFAP expression in **B** (*** p-value < 0.001). (**D**) Immunoblot analyses of lysates from glial cells treated with supernatants from NT neurons and neurons treated with glutamate, NMDA or NMDA+MK801 using GFAP antibody. (**E**) Quantification of Western blot analyses in **D** (*** p-value < 0.001) (student's *t*-test). Error bars indicate ± s.e.m.

3.4 Discussion

Results from this chapter uncover novel aspects of the mechanism behind p25/Cdk5-mediated neuroinflammation. Results showed that p25-mediated astrogliosis was an early as well as amyloid-independent event in p25Tg mice. However, microgliosis was observed secondary to astrogliosis in these mice. In addition, results indicated for the first time that p25 overexpression initiated peripheral cell recruitment into p25Tg mice brain and exacerbated neuroinflammation. Additionally, co-culture and supernatant experiments results strongly suggested that p25 expression (either by endogenous production or by overexpression) in neurons induced the release of a soluble factor to mediate astrocyte activation.

Although various experimental animal models of AD have been available to study the pathological changes, p25 transgenic (p25Tg) mouse is one of the well-studied mouse model of AD which recapitulates most of the neurological deficits reminiscent of AD (Cruz et al., 2003; Cruz et al., 2006; Muyllaert et al., 2008). p25Tg mice overexpress human p25 in the forebrain under the control of an inducible CaM Kinase IIA promoter. Astrogliosis, neurofibrillary tangles with hyperphosphorylated tau and intraneuronal accumulation of amyloid-β were evidently observed in these mice (Cruz et al., 2003; Cruz et al., 2006). Interestingly, a recent study reported the occurrence of intense neuroinflammation and its association between neurodegeneration in inducible p25Tg mice (Muyllaert et al., 2008). However, the onset of neuroinflammation and the actual mechanism behind how p25 causes robust increases in neuroinflammation were not fully described. To date, very limited evidence is available to decipher the link between p25-induced neuroinflammation and neurodegenerative disease progression. This study adds on to current knowledge by delineating key aspects that regulate the early phase of p25-mediated neuroinflammation and neurodegeneration.

3.4.1 Astrogliosis is an early event in p25 transgenic mice

Preliminary results from microarray analyses conducted by our group using brain samples of 4-week induced p25Tg mice suggested that neuroinflammation was an early incident in p25Tg mice (data not shown).

Inflammatory markers such as GFAP and pro-inflammatory cytokines expression were found to be robustly elevated in 4-week induced p25Tg mice. In addition, this interesting finding shed light on our further investigations to establish the mechanism behind the early changes in p25-mediated neuroinflammation. Results from immunohistochemistry, Western blot and RT-PCR analyses clearly demonstrated that GFAP expression and pro-inflammatory chemokines/cytokines such as TNF-α, MIP-1α, TGF-β and IL-1β levels were significantly increased even in 1 week induced p25Tg mice (Figure 3.1 and 3.2). The role of astrocytes in the progression of dementia was initially indicated by Dr. Alois Alzheimer himself (in 1910). Occurrence of reactive astrocytes in the animal models for AD, PD and ALS has also been reported previously (Nagele et al., 2004; Chiu et al., 2009; Ciesielska et al., 2009). Although the presence of GFAP immunoreactive astrocytes has previously been reported in p25 transgenic mice (Cruz et al., 2003; Muyllaert et al., 2008), results from this study identified astrogliosis and inflammatory cytokines production as very early events occurring before any neuropathological changes in p25Tg mice. Our findings are consistent with a recent clinical study where prominent astrogliosis was found in the cortex at early stages of patients with frontotemporal dementia (Kersaitis et al., 2004). In another study, astrocytes activation was observed as the first event that occurred before any neurodegenerative changes (Wu et al., 2011). In summary, results collectively suggested that targeting astrocytes could be a potential early intervention strategy for the treatment of neuroinflammation-associated neurodegenerative diseases including AD. Moreover, this interesting finding of early astrogliosis in p25Tg mice became a stepping stone for further investigations to understand the mechanism behind the p25/Cdk5 hyperactivation-mediated neuroinflammation.

3.4.2 p25-induced astrogliosis occurs prior to microgliosis in p25Tg mice

Reactive microgliosis has long been implicated as a key aspect in the development of neuropathology in various neurodegenerative diseases (McGeer et al., 1988; Hall et al., 1998). Hence, the role of microgliosis in p25-mediated neuroinflammation was studied using immunostaining experiments in 1, 4, 8 and 12-week induced p25Tg mice using anti-CD11b & anti-tPA

antibodies and results showed that reactive microgliosis appeared after 4 weeks of induction of p25 expression in p25Tg mice (Figure 3.3). However, astrogliosis was found even at 1 week of induction (Figure 3.1). In addition, results from conditioned media transfer experiments between p25 overexpressed neurons and glia further determined that astrocyte activation was observed primarily with substantially lower or no microglial activation (Figure 3.7E). Collectively, results showed that astrogliosis preceded microgliosis in p25-mediated neuroinflammation.

Recently, astrocyte activation was reported as a first response to α-synuclein release from degenerating neurons in a transgenic mouse model of PD (Sekiyama et al., 2012). Reactive astrocytes-mediated microglial activation was also reported in another recent study using a cuprizone-induced rodent model of demyelination (Skripuletz et al., 2012). Furthermore, results from various studies suggested that activated astrocytes released inflammatory chemokines/cytokines (mainly MIP-1α or TNF-α) to attract microglia and contributed further to neuronal damage (Hurwitz et al., 1995; Janelsins et al., 2005; Tuppo and Arias, 2005). Accordingly, findings of upregulated MIP-1α and TNF-α expression in 1 week induced p25Tg mice indicated that cytokines produced by p25-induced reactive astrocytes might be involved in the regulation of recruitment and activation of microglia and which might serve to further intensify neuroinflammation.

3.4.3 Peripheral cell infiltration is evident in p25Tg mice

Although, CNS recruitment of CD4+ and CD8+ T cells has been observed as a neuroinflammatory response in various neurodegenerative diseases (Brisebois et al., 2006; Brochard et al., 2009), there have been no clear evidence about the involvement of these peripheral immune cells in p25-mediated neuroinflammation. Results from immunostaining experiments using brain sections from p25Tg mice determined that there was a significant level of CNS infiltration of CD4+ and CD8+ T cells in p25Tg mice after 4 weeks of induction of p25 expression (Figure 3.4). However, this finding of late leukocyte infiltration suggested that early astrogliosis and cytokines upregulation might have a role in the induction of leukocyte infiltration during

neurodegeneration. A number of reports have suggested that inflammatory mediators secreted by injured neurons or cytokines produced by activated astrocytes, especially MIP-1α and TNF-α could trigger peripheral cell infiltration (Ousman and David, 2001; Garcia-Ramallo et al., 2002).

Recent studies on mouse models of neurodegenerative diseases suggested that CNS leukocyte traffic could be detrimental or beneficial depending on the disease state. Peripheral monocytes were found to be efficient in clearing amyloid-β plaques in a mouse model of AD (Town et al., 2008). CNS infiltration of CD4+ T lymphocytes promoted a neuroprotective microenvironment in a mouse model of ALS (Chiu et al., 2008). However, deleterious effects of CNS leukocyte traffic was also observed in a mouse model of multiple sclerosis (MS) and in experimental autoimmune encephalomyelitis (EAE) (Fletcher et al., 2010). Therefore, more studies are required to determine the significance of peripheral cell recruitment in p25-mediated neuroinflammation. Proper understanding of the mechanisms behind the role of peripheral immune cells in p25-mediated neuroinflammation may lead to novel therapeutics in the future.

3.4.4 p25-induced astrogliosis is an amyloid-β and phospho-tau independent event in p25Tg mice

Amyloid accumulation was thought to be a major contributing factor for the induction of neuroinflammation in various neurodegenerative models (Combs et al., 2001; White et al., 2005). Moreover, induction of neuroinflammation by tau protein abnormalities has also been reported earlier (Yoshiyama et al., 2007). Therefore, the onset of phospho-tau production and amyloid-β accumulation in p25Tg mice was investigated to determine the role of phospho-tau and amyloid-β in the induction of astrogliosis during p25 overexpression. Immunostaining results showed that phospho-tau and amyloid accumulation became evident after 4 and 8 weeks of p25 expression respectively (Figure 3.5). However, intense astrogliosis after 1 week of p25 expression clearly suggested that astrogliosis was an amyloid-independent event in p25Tg mice (Figure 3.1). Our findings have been supported by a study using APP [V717I] mice where activated astrocytes were detected

before any amyloid deposition (Heneka et al., 2005). In another study, GFAP upregulation was identified before the onset of many pronounced AD neuropathologies (Zhu et al., 2008). Together, results found that there might be an alternate trigger for astrogliosis that occurs even before any evidence of amyloid and tau pathology in p25Tg mice.

3.4.5 p25-induced astrocytes activation is mediated by a soluble factor

Subsequently, *in vitro* co-cultures as well as conditioned media transfer systems were employed to uncover the mechanism behind p25-mediated astrocyte activation. Results identified a robust increase in GFAP expression in glial cells co-cultured with p25-LV transduced neurons or with p25Tg mice neurons compared to control neurons (Figure 3.6). Hence, this finding demonstrated that p25 overexpression was involved in neuroinflammation *in vitro* where a soluble signal secreted by the p25 overexpressed neurons activated glial cells. This soluble factor-dependent activation was further investigated using cell-free supernatants experiments, where there is no direct physical contact between glia and neurons. Significant increases in GFAP levels in glial cells that received the cell-free supernatants from p25-overexpressed neurons further confirmed the findings from the co-culture experiments (Figure 3.7). Although studies indicated that signals from injured neurons could activate glial cells, (Salmina, 2009), the exact mechanism behind this link has not yet been fully elucidated.

3.5 Summary

The onset of neuroinflammation in p25Tg mice was well documented in this study. Furthermore, astrocyte activation was found to be triggered by soluble factors secreted by the p25-overexpressed neurons. In light of our findings above, it is immensely important to elucidate the nature of these soluble factors and the pathway behind the production of these factors. Together, the novel findings from this chapter which has been published (Sundaram et al., 2012) strongly indicated the need to establish the critical role played by the key inflammatory mediators so as to target them early to reduce neuroinflammation and subsequent neurodegeneration. As such, it is crucial to identify the nature of the soluble trigger in p25-mediated neuroinflammation and it is the aim of the next chapter.

CHAPTER 4

Chapter 4: Identification of pathway involved in induction of p25/Cdk5 hyperactivation-mediated astrogliosis: its significance in initiation of neurodegeneration

4.1 Introduction

The results in Chapter 3 revealed the role of soluble factors secreted by p25 overexpressing neurons in the induction of astrocytes activation. It is therefore important to elucidate the nature of these soluble factors and the pathway behind their production. Furthermore, identifying the mechanism as well as the trigger for neurodegeneration will help in early detection of neurodegenerative diseases and may provide novel therapeutic avenues to reduce the progression of neurodegenerative diseases where neuroinflammation is implicated in the pathogenesis.

The first part of this chapter details the experiments conducted to identify the nature of the soluble factors involved in p25-mediated neuroinflammation using sequential factor removal strategies in coordination with high performance liquid chromatography-mass spectrometry (LC-MS). Additionally, confirmation of gene expression changes was made using Real-time PCR and gene silencing experiments. The second part of this chapter focuses on the experiments conducted to determine whether the inflammatory mediators produced during p25 expression could initiate the progression of pathological changes in the brain. Together, results from this chapter identified a novel pathway behind p25-induced neuroinflammation and subsequent neurodegeneration.

4.2 Methods

4.2.1 Factor removal experiments

Culture media supernatants from p25 overexpressing neurons (EV-LV/p25-LV transduced neurons and p25Tg/control mice neurons) were treated with DNAse (8μg/ml), RNAse (50μg/ml) and Proteinase K (50μg/ml) (Sigma) for 60 minutes at 37°C. In parallel, supernatants were passed through the SPE C-18 (solid phase extraction) columns under vacuum in order to remove major lipids. Glial cells were incubated with enzyme-treated as well as lipid-free supernatants for 48 hours at 37°C. Later, glial cells were processed differently for Western blotting, immunocytochemistry and RT-PCR analyses.

4.2.2 Lipid analysis using High-Performance Liquid Chromatography/Mass Spectrometry

(This work was done in collaboration with Assoc Prof Markus Wenk's Lipidomics lab)

Individual lipids derived from the supernatants of EV-LV/p25-LV transduced cortical neurons and brain samples of p25Tg/control mice were separated and quantified using an Agilent 1200 high-performance liquid chromatography (HPLC) system and a 3200 Q-Trap mass spectrometer.

4.2 3 Lipid treatment experiments

Glial cells were incubated either with the lipids extracted from the cell-free supernatants of EV-LV/p25-LV transduced cortical neurons or with the commercially available LPC species 16:0, 18:0 and 18:1 (20 μM) for 24/48 hours at 37°C. Lipids treated glial cells were then processed individually for Western blotting and immunocytochemistry analyses.

4.2.4 cPLA2 activity assay

cPLA2 activity was determined for the samples from EV-LV/p25-LV transduced neurons and p25Tg/control mice neurons using the cPLA2 activity assay kit.

4.2.5 *cPLA2* gene silencing analyses

cPLA2 gene silencing analyses were performed in p25-overexpressing cortical neurons using cPLA2 shRNA lentivirus and cortical neurons were then processed for RT-PCR and Western blot analyses to confirm the gene silencing. Subsequently, cell-free supernatants from these neurons were then transferred to glial cells and incubated for 48 hours at 37°C.

4.2.6 Inhibitor studies

Cortical neurons transduced with p25-LV/EV-LV were incubated with 0.3 μM of bromoenol lactone (BEL) (iPLA2 inhibitor) or 10 μM of arachidonyl trifluoromethyl ketone (AACOCF3) (cPLA2 inhibitor) for 48 hours at 37°C. Neurons were then fixed and processed for immunocytochemistry.

4.2.7 Real-Time PCR

RNA samples were extracted from the glial cells incubated with enzyme-treated/lipid-free supernatants from p25 overexpressing neurons using RNeasy Mini Kit. Using high capacity cDNA reverse transcriptase kit, cDNA was synthesized from RNA and subsequently used for quantitative real-time PCR.

4.2.8 Stereotactic injection of lipids into mouse brain

1 μl of solution containing lipids (2 μM) were injected into anesthetized WT (C57BL/6) mice brains using a Hamilton microsyringe through a small hole drilled using the coordinates: caudal to bregma 2 mm, 2 mm lateral to the midline and 1.8 mm from the surface of the cortex at a constant rate for 5 minutes. After 10 minutes, needle was withdrawn and the scalp was sutured.

4.2.9 Immunohistochemistry

16 μm of mice brain sections were immunostained with mouse anti-GFAP antibody overnight at 4°C. Sections were washed with PBS before and after incubation with Alexa Fluor 594 secondary antibody for one hour at room temperature and nuclei were counterstained with DAPI. Immunofluorescence images were taken with Zeiss LSM-510 laser-scanning confocal microscope at 20X, 40X and 63X magnifications.

4.2.10 Immunocytochemical analyses

Immunofluorescence staining was performed on glial cells using mouse anti-GFAP (primary) and Alexa Fluor 488 (secondary) antibodies. Nuclei were counterstained with DAPI and fluorescent confocal images were taken at 40X magnification.

4.2.11 Western blot analyses

Total cell lysates (from glial cells) and soluble cell lysates (from EV-LV/p25-LV virus-transduced cortical neurons and p25Tg/control mice neurons) were resolved on 4-20% polyacrylamide gels, blotted onto nitrocellulose membranes and then immunoprobed with rabbit anti-GFAP and mouse anti-cPLA2 antibodies.

4.2.12 TUNEL assay

TUNEL staining was performed on 4% formaldehyde-fixed cortical neurons and 4% PFA-perfused mice brain sections using In Situ Cell Death Detection Kit, TMR red.

4.2.13 Statistical analysis

Data are expressed as the mean of at least three values ± standard error (s.e.m). Statistical significance was determined using student's *t*-test and P-value for statistical significance is defined as $P < 0.05$.

4.3 Results

4.3.1 p25-mediated neuroinflammation is caused by a lipid

Findings from Chapter 3 strongly suggested that p25-overexpressing cortical neurons regulated astrogliosis by secreting a soluble mediator. It has previously been demonstrated that neurons regulate astrocytes differentiation and activation through soluble factors (Alvarez-Maubecin et al., 2000; Benz et al., 2004). However, the exact nature of the soluble factor was not well characterized. Hence, experiments in this chapter aimed to determine the biochemical nature of the secreted factor from the p25 overexpressing neurons based on the protocols published earlier (Lauber et al., 2003).

To determine the possible factors that could be secreted during inflammation, supernatants of p25-LV/EV-LV transduced neurons were incubated with DNAse, RNAse and Proteinase K for 60 minutes at 37°C and then transferred onto glial cells for 48 hours. Later, glial cells were processed for immunostaining (Figure 4.1A and C) and Western blotting analyses (Figure 4.1B and D) using anti-GFAP antibody in order to analyze the changes in glial activation during each enzymatic treatments. Results specified that there was no significant change in GFAP upregulation in glial cells incubated with supernatants treated with DNAse, RNAse and Proteinase K compared to the non-treated supernatants from the p25-LV transduced neurons. Thus, the above findings clearly demonstrated that the factor causing astrocyte activation was neither DNA/RNA nor protein in nature.

In order to further characterize the soluble factor nature, the major lipids from the supernatants of p25 overexpressing neurons were removed by solid phase extraction column (SPE-C18) elution. Later, glial cells were treated with column-eluted supernatants of p25 overexpressing neurons and a change in glial activation was investigated using immunocytochemistry and Western blotting analyses. An interesting finding of marked reduction in GFAP levels in glial cells that received the SPE-C18 column-eluted supernatants demonstrated that the factor released during p25 overexpression could be lipid in nature (Figure 4.1A-D).
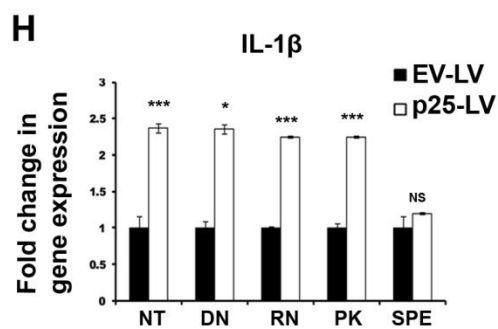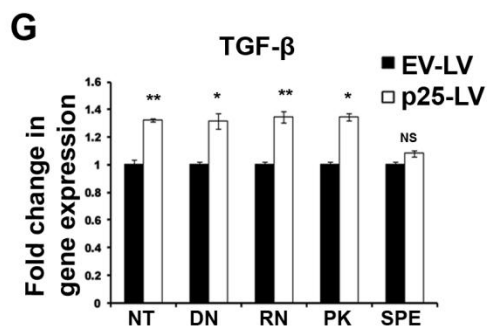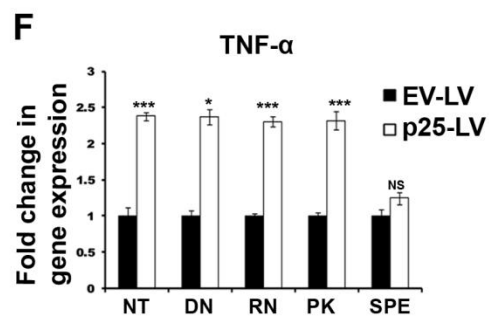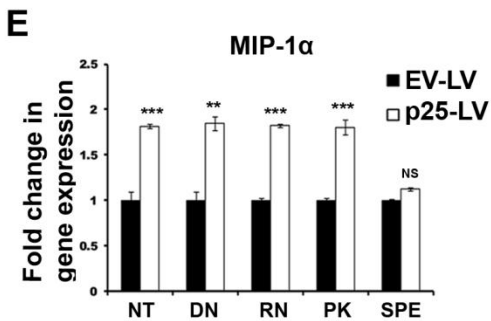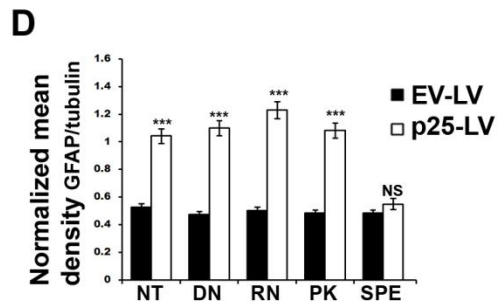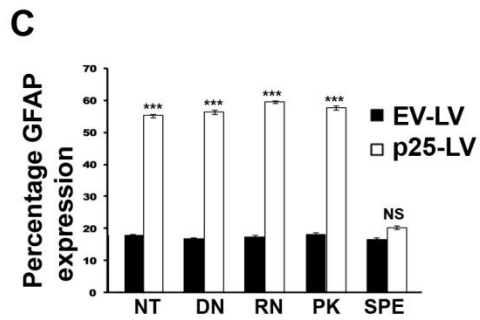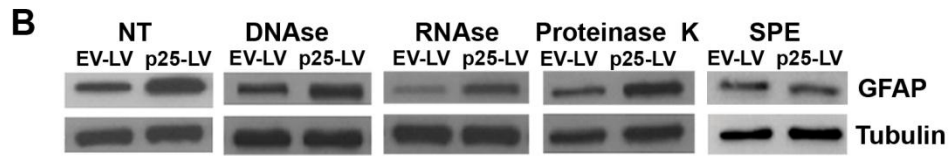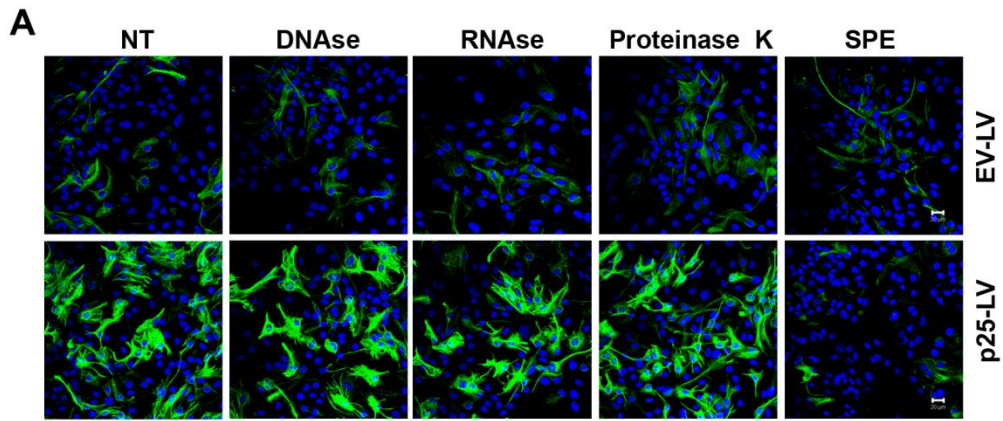
Figure 4.1: Elucidation of the nature of soluble factor secreted by p25-LV transduced neurons

(**A**) Glial cells incubated with DNAse, RNAse and Proteinase K treated or SPE-C18 column-eluted culture media supernatants from EV-LV/p25-LV transduced neurons were immunostained with anti-GFAP antibody (green) and DAPI (blue). Scale bars: 20μm (n=3 for each group). (**B**) Lysates of glia samples that were incubated with supernatants from same treatment as in **A** were resolved by SDS-PAGE and immunoprobed with anti-GFAP antibody (n=3 for each group). (**C**) Graph represent the percentage of GFAP expression in **A** (*** p-value < 0.001 and NS > 0.05). (**D**) Quantification of Western blots in **B** (*** p-value < 0.001 and NS > 0.05). RT-PCR results for the expression of (**E**) MIP-1α, (**F**) TNF-α, (**G**) TGF-β and (**H**) IL-1β in glial cells incubated with supernatants from the same treatment as in **A** (*** p-values < 0.001, ** p-values < 0.01, * p-values < 0.05 and NS > 0.05). Error bars indicate ± s.e.m (student's *t*-test).

The results from RT-PCR analyses for chemokines/cytokines expression from the glial cells that were incubated with SPE-C18 column-eluted or DNAse, RNAse and Proteinase K treated supernatants from p25 overexpressing neurons further supported the above findings and a remarkable reduction in MIP-1α, TNF-α, TGF-β and IL-1β expression levels was observed in glial cells treated with SPE-C18-eluted supernatants (Figure 4.1E-H). In addition, these findings were further confirmed by the results from the same factor elucidation experiments carried out in neurons from p25Tg/control mice (Figure 4.2A-D). Together, these results determined that the soluble factor secreted by the p25-overexpressing neurons to induce astrogliosis is lipid in nature.
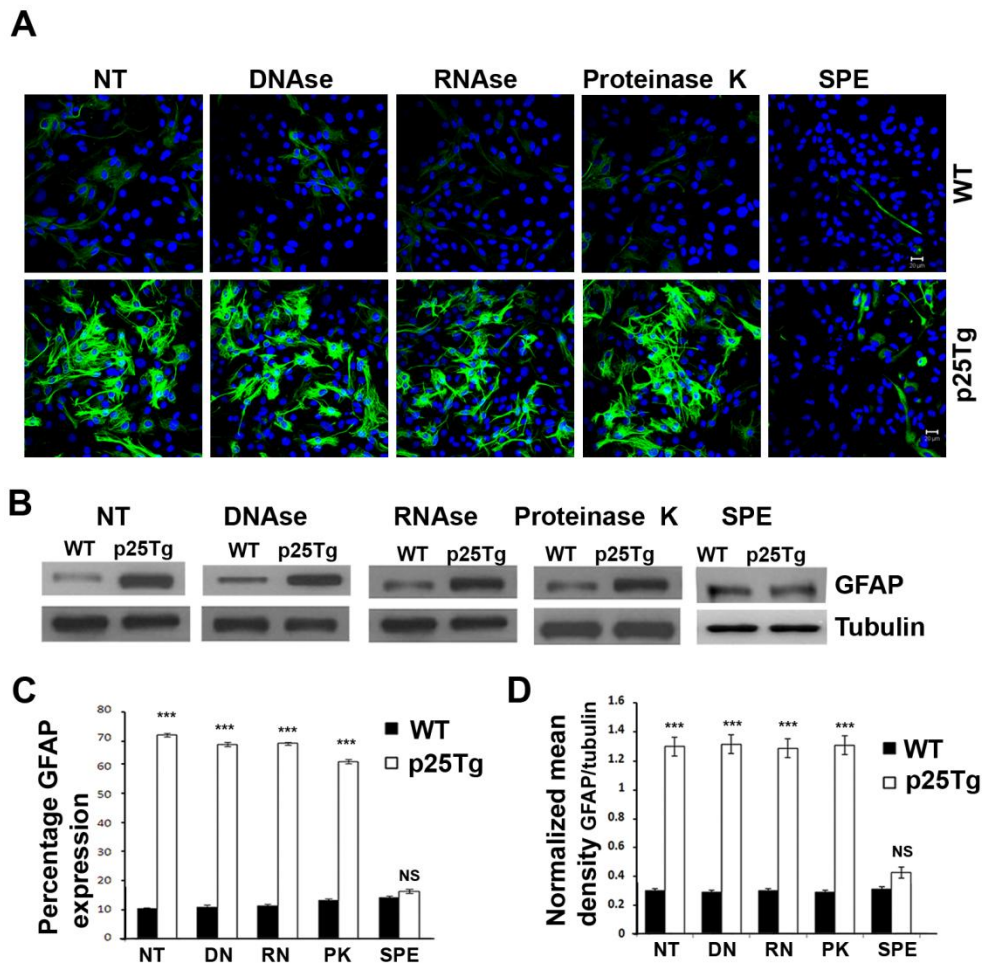
Figure 4.2: Elucidation of the nature of soluble factor secreted by neurons from p25Tg mice

Immunostaining (**A**) and Western blot analyses (**B**) results for the glial cells incubated with DNAse, RNAse and Proteinase K treated or SPE-C18 column-eluted culture media supernatants from primary neurons of p25Tg/control mice. (**C**) Graph represent the percentage of GFAP expression in **A** (*** p-value < 0.001 and NS > 0.05). (**D**) Quantification of Western blots in **B** (*** p-value < 0.001 and NS > 0.05). Error bars indicate ± s.e.m (student's *t*-test).

4.3.2 A lipid signal triggers the p25/Cdk5-mediated inflammatory cascade

To facilitate further investigation to confirm the lipid nature of the factor behind p25-mediated astrogliosis, total lipid extraction was performed using supernatants of neurons transduced with EV-LV/p25-LV and extracted lipids were then transferred onto glial cells for 24 and 48 hours. Results from immunocytochemical staining (Figure 4.3A) and Western blot analyses

(Figure 4.3B and C) showed a significant increase in GFAP expression in the glial cells treated with the lipids from p25 overexpressing neurons. Moreover, these lipid treatment results were found indistinguishable from the supernatant transfer experiments results in Chapter 3 (Figure 3.7). Subsequently, lipids from p25-LV transduced neurons were stereotactically injected into WT mice brains in order to validate the above finding *in vivo*. Results from immunohistochemical analyses showed robust increases in GFAP staining in brain sections from mice that received an injection with lipids from p25-LV transduced neurons compared to control (Figure 4.3D). Together, both *in vitro* and *in vivo* results showed that the factor behind the p25-induced astrogliosis was a soluble lipid.
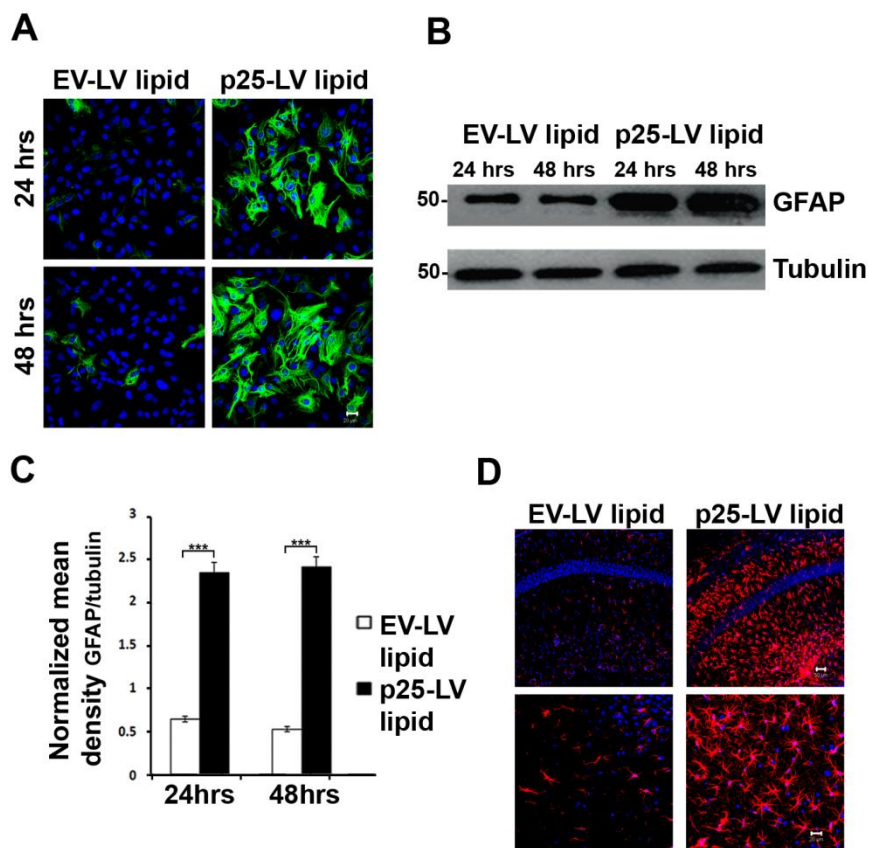
Figure 4.3: p25 overexpressing cells secrete soluble lipids to mediate astrogliosis

(**A**) Glial cells incubated with lipids from supernatants of EV-LV/p25-LV transduced neurons were stained with anti-GFAP antibody (green) and DAPI (blue). Scale bars: 20μm (n=3 for each group). (**B**) Immunoblot analyses of lysates from glial cells received same treatment as in **A** using anti-GFAP antibody (**C**) Quantification of

immunoblots in **B** (*** p-value < 0.001). Error bars indicate ± s.e.m (student's *t*-test). (**D**) Brain sections from mice received injection of lipids from supernatants of EV-LV/p25-LV transduced neurons were immunostained with anti-GFAP (red) and DAPI (blue). Images in top panel: 20X magnification (scale bars: 50μm) and images in bottom panel: 40X magnification (scale bars: 20μm) (n=3 for each group).

4.3.3 Lysophosphatidylcholine (LPC) is the lipid mediator involved in p25-mediated neuroinflammation

To identity the particular lipid present in the supernatants of p25 overexpressing neurons, lipidomic mass spectrometric analyses were carried out and results showed that lysophosphatidylcholine (LPC) levels were found to be significantly increased among the major lipids in supernatants from p25-LV transduced neurons compared to the control neurons (Figure 4.4A). Although lysophosphatidylinositol (LysoPI) levels were also increased, the difference was not statistically significant (P value = 0.223).

Likewise, LPC levels were again found to be significantly elevated among the major lipids in the brain samples from p25Tg mice compared to the controls (Figure 4.4B). Furthermore, progressive elevation of LPC levels from 1 to 12-week induction of p25 expression clearly demonstrated a strong correlation with the progressive elevation of GFAP expression in p25Tg mice (Figure 4.4C and Figure 3.1). Together, these data determined that LPC was the major lipid factor released by the p25 overexpressing neurons which resulted in astrogliosis.
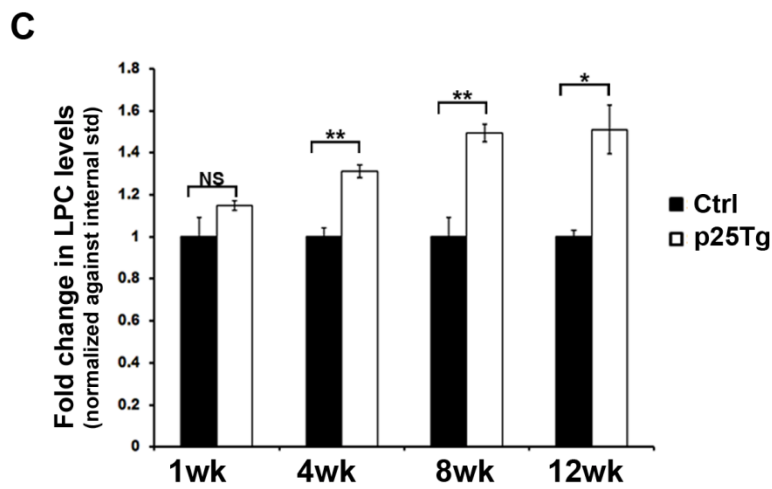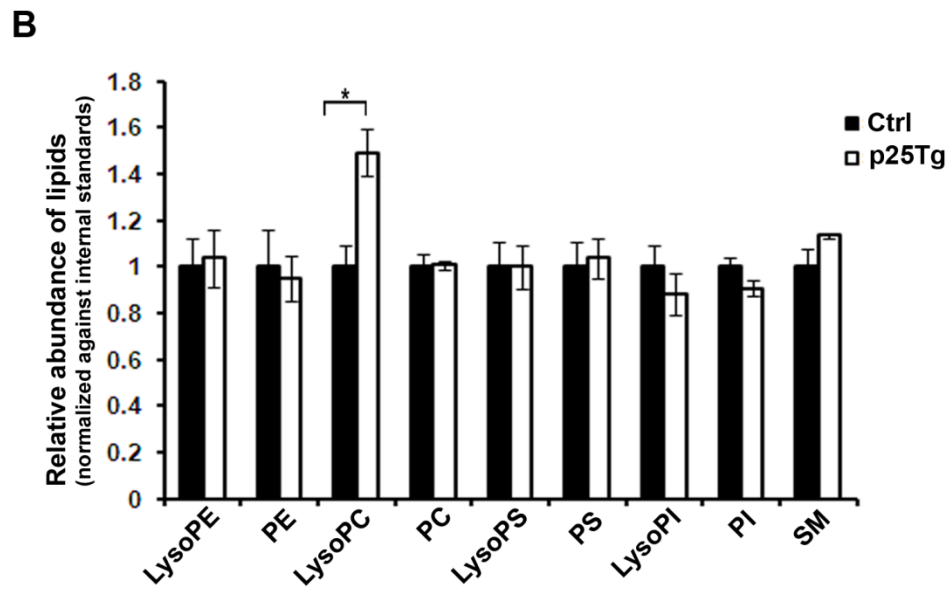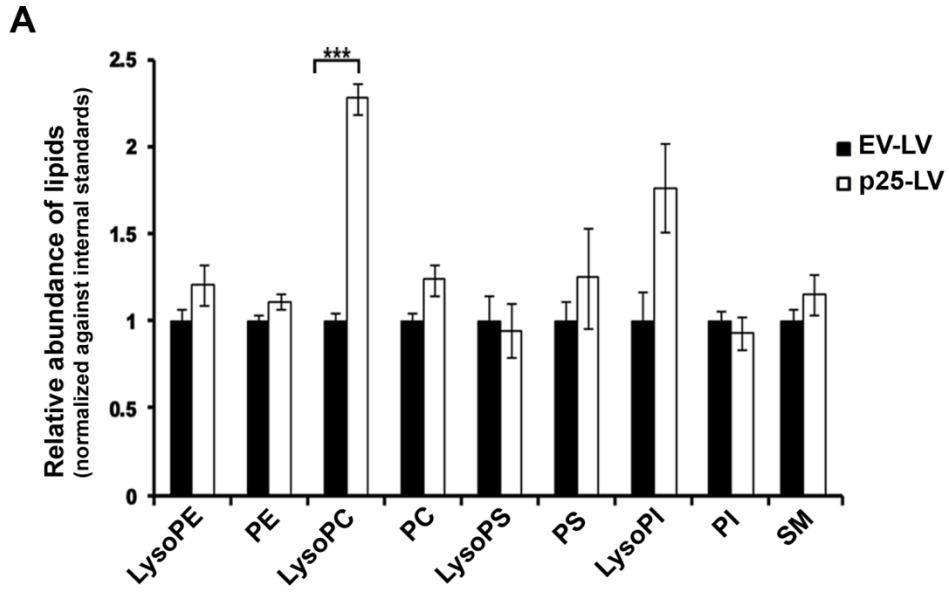
Figure 4.4: p25 overexpression causes lysophosphatidylcholine (LPC) production to induce astrogliosis

Results from mass spectrometric analyses using lipids from supernatants of (**A**) neurons transduced with EV-LV/p25-LV, (**B**) brain samples from 12-week induced p25Tg/control mice and (**C**) brain samples from 1, 4, 8 and 12-week induced p25Tg/age-matched control mice. Results were normalized against the internal standards of the respective lipids (*** p-values < 0.001, ** p-values < 0.01, * p-values < 0.05 and NS > 0.05). Error bars indicate ± s.e.m (student's *t*-test).

4.3.4 LPC 18:1 is the more potent species that effectively causes astrogliosis

LPC has many species based on variations in the acyl chain and potency of LPC is mainly determined by the acyl side chain (Ojala et al., 2007). To determine the role of different LPC species in the induction of astrogliosis, Lipidomics mass spectrometry analysis was carried out and results identified LPC 16:0, 18:0 and 18:1 as the main LPC species increased in p25-LV derived lipids compared to the control (Figure 4.5A). In addition, glial cells were treated with commercially available LPC species 16:0, 18:0 and 18:1 for 24 and 48 hours in order to determine which LPC species was more effective in stimulating GFAP expression. Results showed greater GFAP elevation in glial cells treated with LPC 18:1 in both 24 and 48 hours incubation. In contrast, LPC 16:0 didn't cause any changes in GFAP expression and LPC 18:0 effect was found only at 48 hour time point (Figure 4.5B-D). To further validate the above finding *in vivo*, commercial LPC 18:1 was stereotactically injected into WT mouse brains (Figure 4.5E) and results mirrored the *in vitro* experiment findings. Collectively, results determined that LPC 18:1 was one of the major lipids secreted by the p25 expressing neurons that induced astrogliosis.
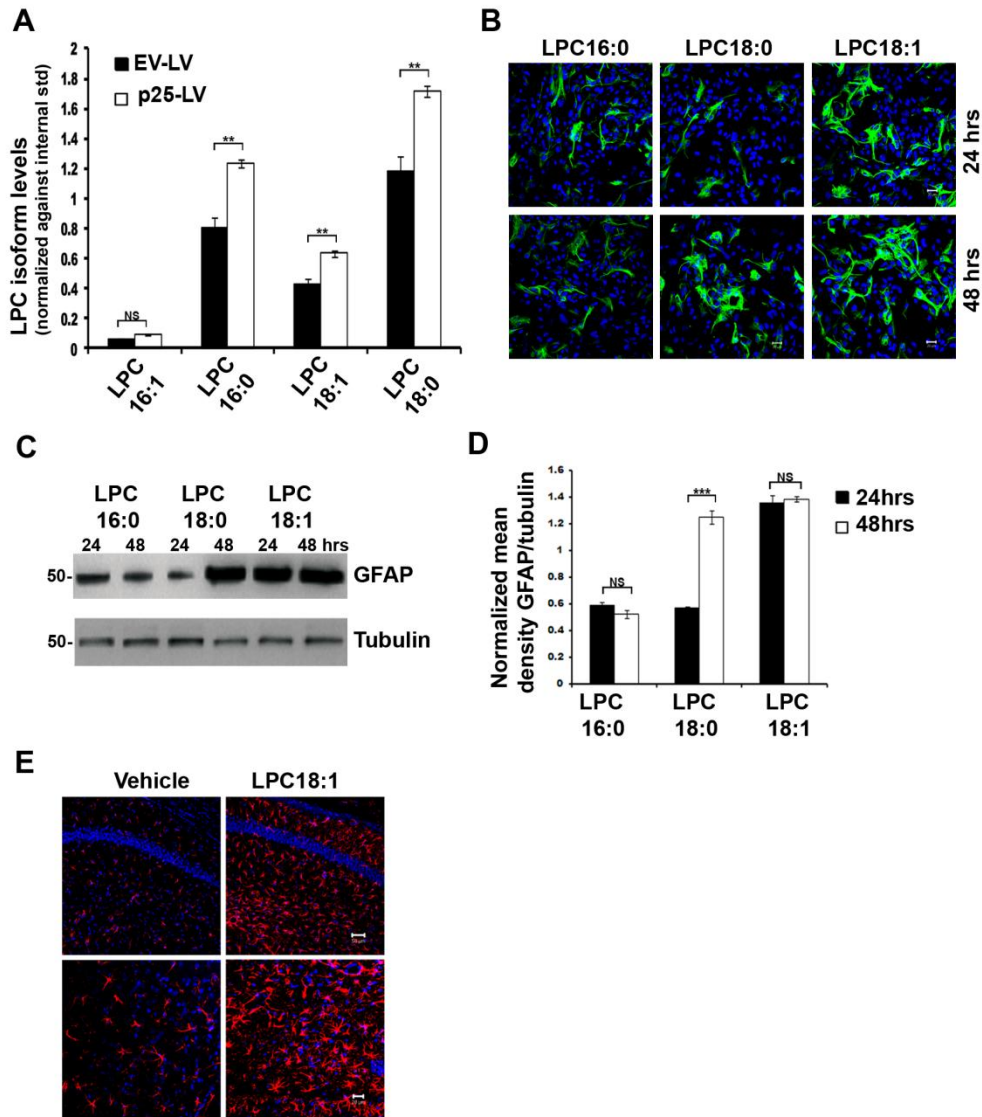
Figure 4.5: p25 overexpression mediates astrocytes activation through LPC 18:1

(**A**) Mass spectrometric analyses results for the lipids derived from supernatants of neurons transduced with EV-LV/p25-LV (** p-value < 0.01 and NS p-value > 0.05). (**B**) Glial cells incubated with media containing 20 μM of LPC species 16:0, 18:0 or 18:1 were immunostained using anti-GFAP antibody (green) and DAPI (blue). Scale bars represent 20 μm (n=3 for each group). (**C**) Representative Western blots of glial cells treated with 20 μM of LPC species 16:0, 18:0 or 18:1 using anti-GFAP antibody (n=3 for each group). (**D**) Quantification of immunoblots in **C** (*** p < 0.001 and NS p-value > 0.05). Error bars indicate ± s.e.m (student's *t*-test). (**E**) Brain sections from mice injected stereotactically with LPC 18:1/vehicle (chloroform/methanol) were immunostained with anti-GFAP (red) and DAPI (blue). Images in top panel: 20X magnification (scale bars: 50μm) and images in bottom panel: 40X magnification (scale bars: 20μm) (n=3 for each group).

4.3.5 p25 overexpression upregulates cPLA2 expression and activity

Lysophosphatidylcholine (LPC) is generated from phosphatidylcholine (PC) by phospholipase A2 (PLA2)-mediated hydrolysis (Steinbrecher et al., 1984). Recent studies have focused on characterizing the three major groups of PLA2: cytosolic PLA2 (cPLA2-IV), Ca^{2+}-dependent PLA2 (iPLA2-VI) and secretory PLA2 (sPLA2-II) due to their important roles in inflammatory-mediated neurodegeneration (Sun et al., 2010). To facilitate investigation of the role of these three major PLA2 enzymes in p25-mediated neuroinflammation, RT-PCR analyses were carried out on the p25-LV transduced neurons. CT values in RT-PCR using sPLA2 primers were found undetermined or not detected after 40 cycles of PCR and these results clearly indicated that the sPLA2-II mRNA is not present in an amount that is detectable in all the samples. In addition, results did not identify any obvious increase in iPLA2 expression between p25 overexpressing and control neurons. However, robust elevation of cPLA2 expression was observed in p25 overexpressing neurons compared to controls (Figure 4.6A). Together, RT-PCR results determined that only cPLA2 expression was significantly elevated among that of the three major PLA2 enzymes during p25 overexpression in neurons. Subsequently, the role of PLA2 isoforms in p25-mediated astrogliosis was investigated using bromoenol lactone (BEL) (iPLA2 inhibitor) and arachidonyl trifluoromethyl ketone (AACOCF3) (cPLA2 inhibitor). Obvious reductions in GFAP expression was observed in glial cells incubated with AACOCF3-treated supernatants compared to the BEL-treated supernatants from p25 overexpressing neurons (Figure 4.6B). Therefore, results confirmed that cPLA2 was the principal enzyme involved in p25-mediated astrogliosis.
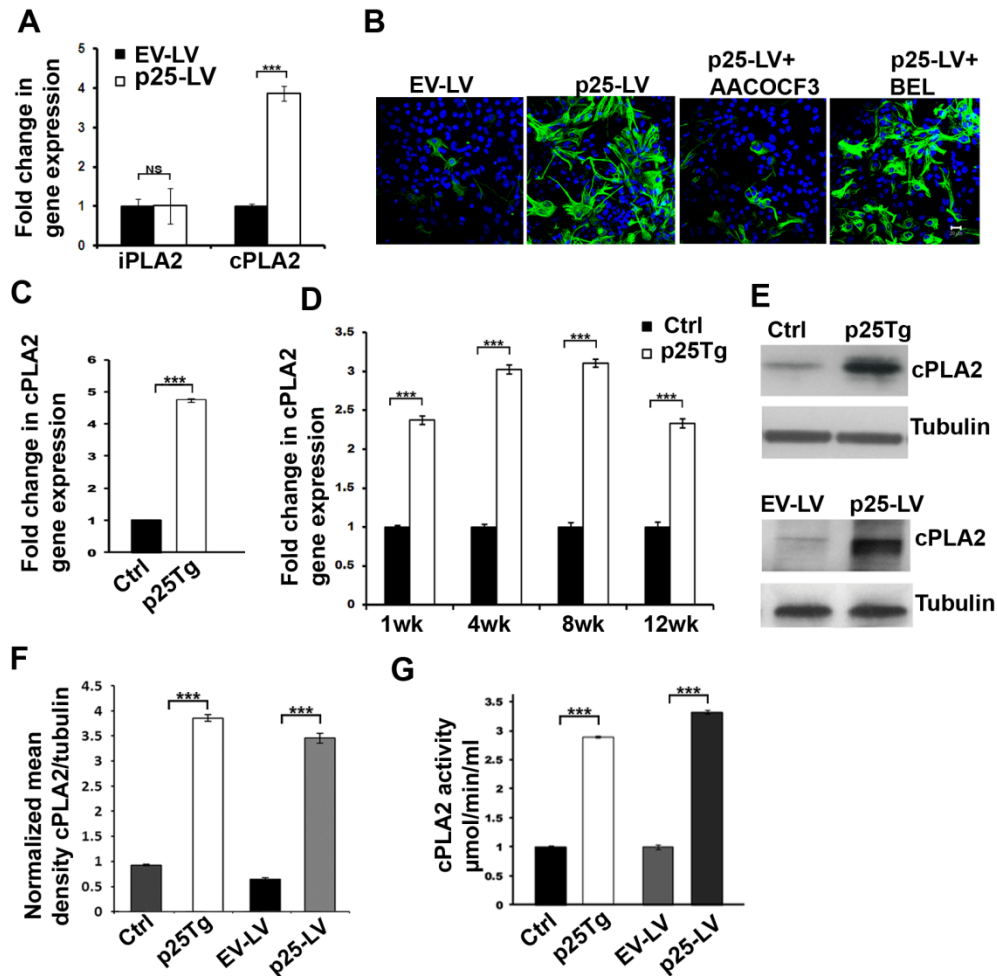
Figure 4.6: p25-induced upregulation of cPLA2 causes LPC production

(**A**) Graph represent the RT-PCR results of *iPLA2* and *cPLA2* gene expression from EV-LV/p25-LV transduced cortical neurons (NS p-value > 0.1 and *** p values < 0.001). (**B**) Immunocytochemistry results from glial cells treated with supernatants from cortical neurons transduced with EV-LV, p25-LV, p25-LV+cPLA2 inhibitor (AACOCF3) and p25–LV+iPLA2 inhibitor (BEL) using anti-GFAP antibody (green) and DAPI (blue). Scale bars represent 20 μm. RT-PCR results of *cPLA2* gene expression in (**C**) five days induced primary neurons from p25Tg/WT mice and (**D**) 1, 4, 8 and 12-week induced p25Tg mice/age-matched control mice (*** p values < 0.001) (n=3 for each group). (**E**) Western blots for lysates from five days induced primary neurons from p25Tg/control mice (top panel) and neurons transduced with EV-LV/p25-LV (bottom panel) using anti-cPLA2 antibody (n=3). (**F**) Quantification of immunoblots in **E** (*** p-values < 0.001). (**G**) cPLA2 activity assay results for neurons transduced with EV-LV/p25-LV and lysates from primary neurons from p25Tg/control mice (*** p values < 0.001) (n=3). Error bars indicate ± s.e.m (student's *t*-test).

Next, experiments focused on investigating cPLA2 expression in both *in vitro* (p25-LV transduced neurons and primary neurons from p25Tg mice) and *in vivo* (brain samples from p25Tg mice) p25 overexpression systems using RT-PCR as well as Western blot analyses (Figure 4.6C-F). Results showed a significant increase in cPLA2 expression in p25-LV transduced neurons and in primary neurons from p25Tg mice (Figure 4.6A, C and E). Moreover, the finding of the progressive increases in cPLA2 expression from 1 to 12-week induced p25Tg mice brain samples supported the above *in vitro* results (Figure 4.6D). Subsequently, cPLA2 activity assays were performed and results confirmed the robust elevation of cPLA2 activity in both *in vitro* and *in vivo* p25 overexpressing neurons (Figure 4.6G). Together, results suggested that p25 overexpression upregulated both cPLA2 expression and activity to produce LPC that in turn induced astrogliosis.

4.3.6 cPLA2 knock-down reduces p25-induced glial activation

To further define the role of cPLA2 activity on the glial activation, *cPLA2* gene silencing experiments were performed on the p25-LV transduced neurons using cPLA2 shRNA lentiviral particles. Silencing of the *cPLA2* gene was confirmed by RT-PCR, Western blot analyses and cPLA2 activity assays where cPLA2 levels and activity were reduced in cPLA2-silenced p25 overexpressed neurons compared to controls (Figure 4.7A-D). Later, mass spectrometric analyses were performed to determine the effect of *cPLA2* gene silencing on p25 expression-stimulated LPC production. Results showed significantly decreased total LPC and specific LPC species 18:0 and 18:1 levels from the p25-LV+cPLA2 shRNA transduced neurons compared to controls (Figure 4.7E). Thus, results clearly indicated that p25-mediated cPLA2 overexpression was crucial for the generation of the inflammatory mediator, LPC.
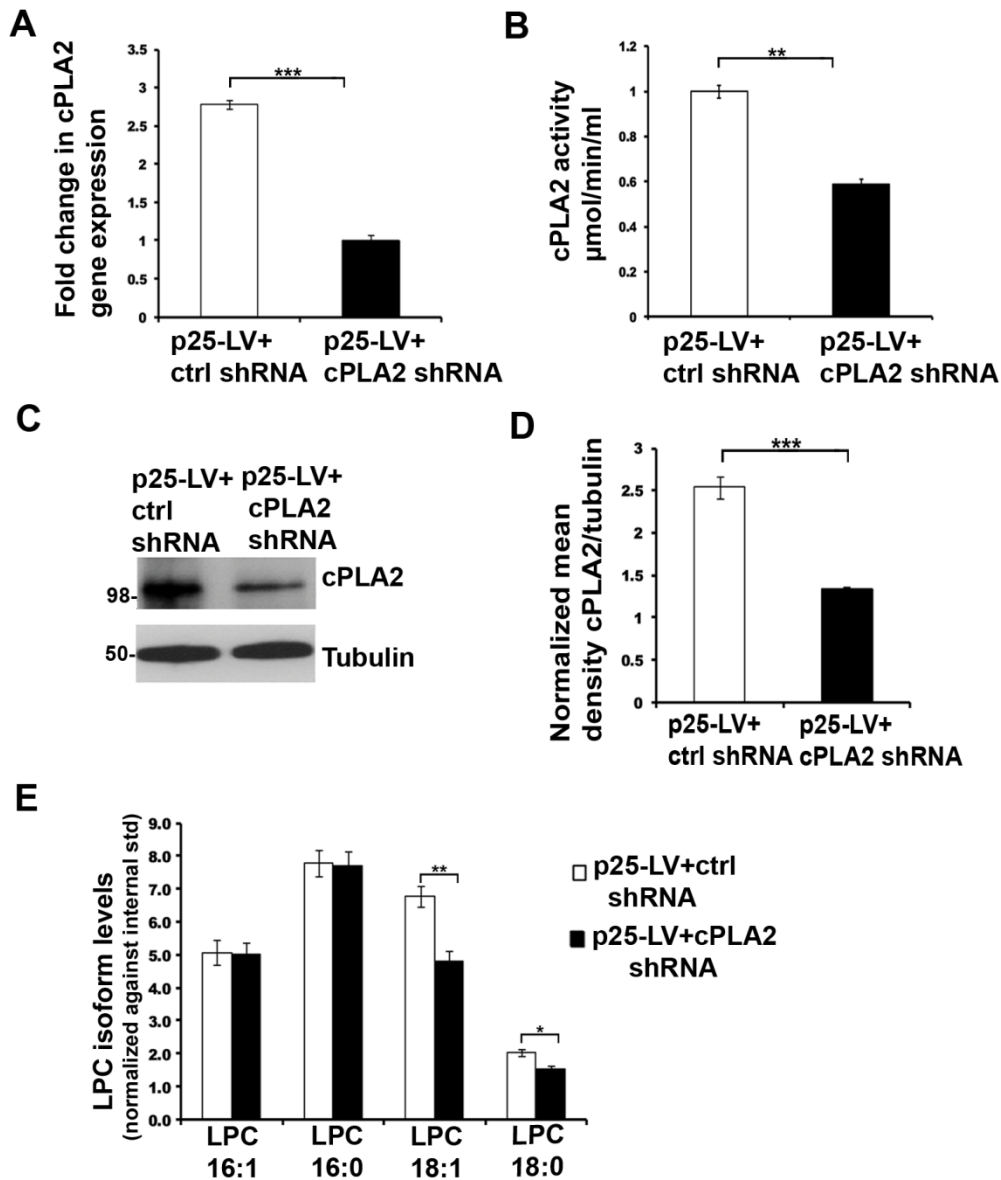
Figure 4.7: shRNA-mediated silencing of *cPLA2* gene reduces LPC production

(**A**) RT-PCR results for cPLA2 expression and (**B**) cPLA2 activity assay results for 7-DIC cortical neurons transduced with p25-LV+cPLA2 shRNA or p25-LV+control (ctrl) shRNA (*** p-values < 0.001 and ** p-values < 0.01). (**C**) Immunoblots for neurons transduced with p25-LV+cPLA2 shRNA or p25-LV+control shRNA using anti-cPLA2 antibody. (**D**) Quantification of immunoblots in **C** (*** p-values < 0.001). (**E**) Mass spectrometric analyses results of lipids from the supernatants of p25-LV+control shRNA/p25-LV+cPLA2 shRNA transduced neurons (** p-value < 0.01 and * p-value < 0.05).

To further investigate the role of cPLA2 knock-down in p25-mediated astrogliosis, glial cells were treated with supernatants from p25-LV+cPLA2 shRNA/p25-LV+control shRNA transduced neurons and then processed for Western blot analyses to determine changes in GFAP expression levels. Dramatic reductions in GFAP immunostaining were observed in glial cells treated with the supernatants from p25-LV+cPLA2 shRNA transduced neurons compared to controls (Figure 4.8A-C). In addition, RT-PCR analyses were carried out with RNA samples extracted from glial cells treated with cell-free supernatants from p25-LV+cPLA2 shRNA/p25-LV+control shRNA transduced neurons to detect for changes in chemokines/cytokines expression levels. Results showed a marked reduction in MIP-1α, TNF-α, TGF-β and IL-1β expression levels in glia that received supernatants from cPLA2 silenced neurons compared to controls (Figure 4.8D). Subsequently, total lipids extracted from the supernatants of p25-LV+control shRNA or p25-LV+cPLA2 shRNA transduced neurons were transferred onto the glial cells for 48 hours in order to further determine the significance of cPLA2 expression in the induction of astrocytes activation. Immunostaining and Western blot analyses results showed approximately 4 to 5-fold reductions in GFAP expression in glial cells incubated with lipids from p25-LV+cPLA2 shRNA transduced neurons compared to controls (Figure 4.8E-G).

In order to perform *in vivo* validation of findings from the above *in vitro* studies, lipids from the supernatants of p25-LV+control shRNA and p25-LV+cPLA2 shRNA transduced neurons were injected stereotactically into WT mice brains and immunohistochemical staining was performed with the brain sections using antibody specific to GFAP. Mice that received injection with lipids from p25-LV+cPLA2 shRNA transduced neurons exhibited reduced GFAP expression compared to controls (Figure 4.8H). Collectively, results from the *cPLA2* gene silencing experiments strongly indicated that cPLA2 upregulation is crucial in triggering the initiation of p25-mediated neuroinflammation.
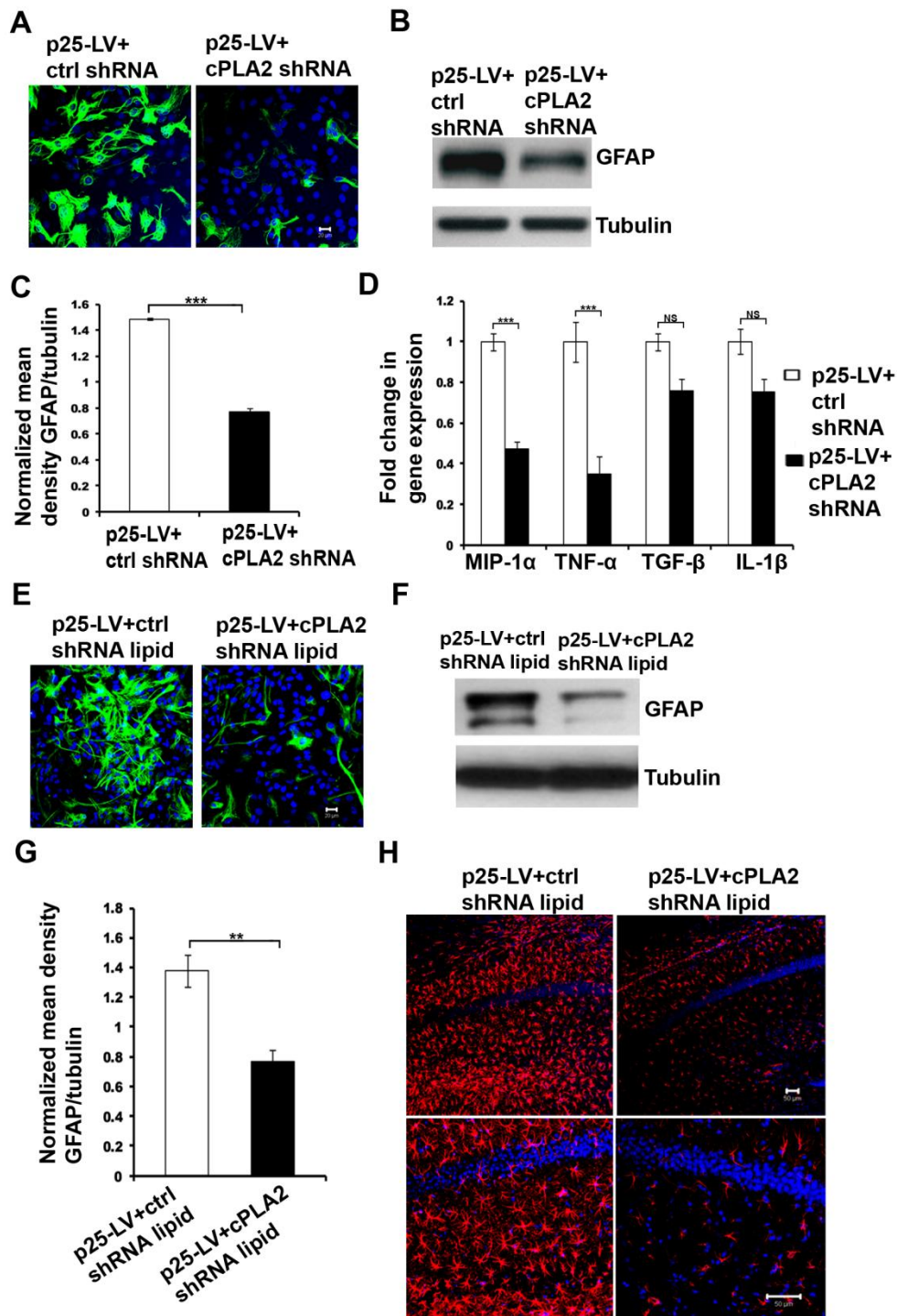
Figure 4.8: *cPLA2* **gene silencing attenuates p25-induced astrocyte activation**

(**A**) Immunocytochemistry results on glial cells treated with supernatants of neurons transduced with p25-LV+cPLA2 shRNA or p25-LV+control shRNA using anti-GFAP antibody (green) and DAPI (blue). Scale bars represent 20 μm. (**B**) Immunoblot analyses were performed on glial cells that received identical treatment as in **A** using anti-GFAP antibody. (**C**) Quantification of immunoblots in **B** (*** p-values < 0.001). (**D**) RT-PCR results showing the expression of chemokines MIP-1α, TNF-α, TGF-β and IL-1β in lysates from glial cells treated with supernatants from neurons transduced with p25-LV+cPLA2 shRNA or p25-LV+control shRNA (***p

value < 0.001, NS- p value >0 .1). (**E**) Immunostaining images from the glial cells treated with lipids from the supernatants of neurons transduced with p25-LV+cPLA2 shRNA or p25-LV+control shRNA using anti-GFAP antibody (green) and DAPI (blue). Scale bars represent 20 μm. (**F**) Western blot analyses using antibody specific to GFAP were performed on glial cells that received the same treatment as **E**. (**G**) Quantification of immunoblots in **F** (** p-values < 0.01). Error bars indicate ± s.e.m (student's *t*-test). (**H**) Brain sections from mice injected stereotactically with lipids from the supernatants of neurons transduced with p25-LV+cPLA2 shRNA or p25-LV+control shRNA were immunostained with anti-GFAP (red) and DAPI (blue). Images in top panel: 20X magnification (scale bars: 50μm) and images in bottom panel: 40X magnification (scale bars: 20μm) (n=3 for each group).

4.3.7 The inflammatory mediator LPC produced during p25 overexpression triggers amyloid and tau neuropathological changes

To discover the significance of p25-mediated neuroinflammation in the induction of neurodegeneration, 7 DIC healthy cortical neurons were treated with conditioned media supernatants from glial cells that were incubated with lipids from EV-LV, p25-LV+control shRNA and p25-LV+cPLA2 shRNA transduced neurons. Results from immunostaining analyses using phospho-tau (AT8 and AT270) and amyloid-β (6E10 and Aβ 1-42) antibodies showed increases in neurodegenerative markers mentioned above in healthy cortical neurons that have been incubated with supernatants from glial cells activated by p25 overexpressed neurons, compared to controls (Figure 4.9A and B).
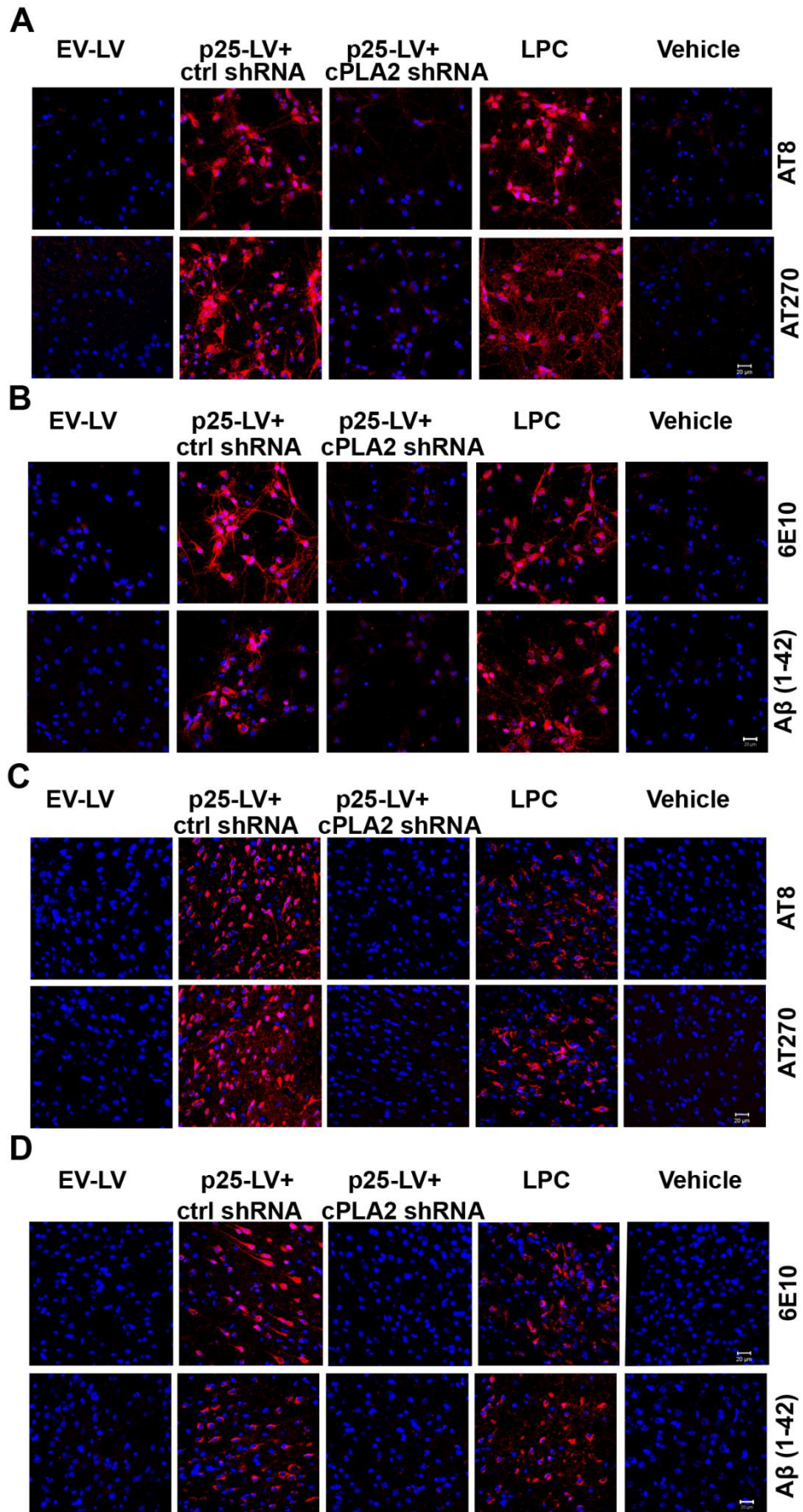
Figure 4.9: p25-mediated neuroinflammation is a trigger for neurodegeneration

7 DIC healthy cortical neurons incubated with supernatants from glial cells treated with either lipids derived from p25+control shRNA/p25+cPLA2 shRNA transduced neurons or with LPC18:1/vehicle were immunostained with (**A**) phospho-tau antibodies AT8 & AT270 and (**B**) Aβ antibodies 6E10 & Aβ (1-42) (red). Brain sections from mice stereotactically injected with the above mentioned lipids were immunostained with (**C**) phospho-tau antibodies AT8 & AT270 and (**D**) Aβ antibodies 6E10 & Aβ (1-42) (red). The nuclei were stained with DAPI (blue) (n=3). Scale bars represent 20 μm.

In addition, obvious reductions in phospho-tau and Aβ 1-42 staining intensities were observed in neurons treated with supernatants from glial cells that have been incubated with lipids derived from cPLA2 silenced p25 overexpressing neurons and this finding strongly indicated the importance of cPLA2 activity in the initiation of p25-mediated neurodegeneration (Figure 4.9A and B). In parallel, WT mice were stereotactically injected in the brain with lipids from EV-LV, p25-LV+control shRNA and p25-LV+cPLA2 shRNA transduced neurons and results showed nearly identical findings corroborated with the above *in vitro* analyses (Figure 4.9C and D).

TUNEL staining was performed in order to further investigate the role of p25-mediated inflammatory mediators in the induction of neuronal cell death and results showed statistically significant increases in cell death in neurons incubated with supernatants from glial cells that have been treated with lipids from cPLA2-upregulated p25 overexpressing neurons compared to the cPLA2-silenced p25 overexpressing neurons (Figure 4.10A and B). In contrast, there was no significant increase in cell death found in the *in vivo* experiments (Figure 4.10C). This suggested that single dose of lipid injection may not be strong enough to induce neuronal death in mice. Together, the results confirmed that the inflammatory components released during p25-mediated inflammatory events triggered the initiation of neurodegenerative changes described in AD.
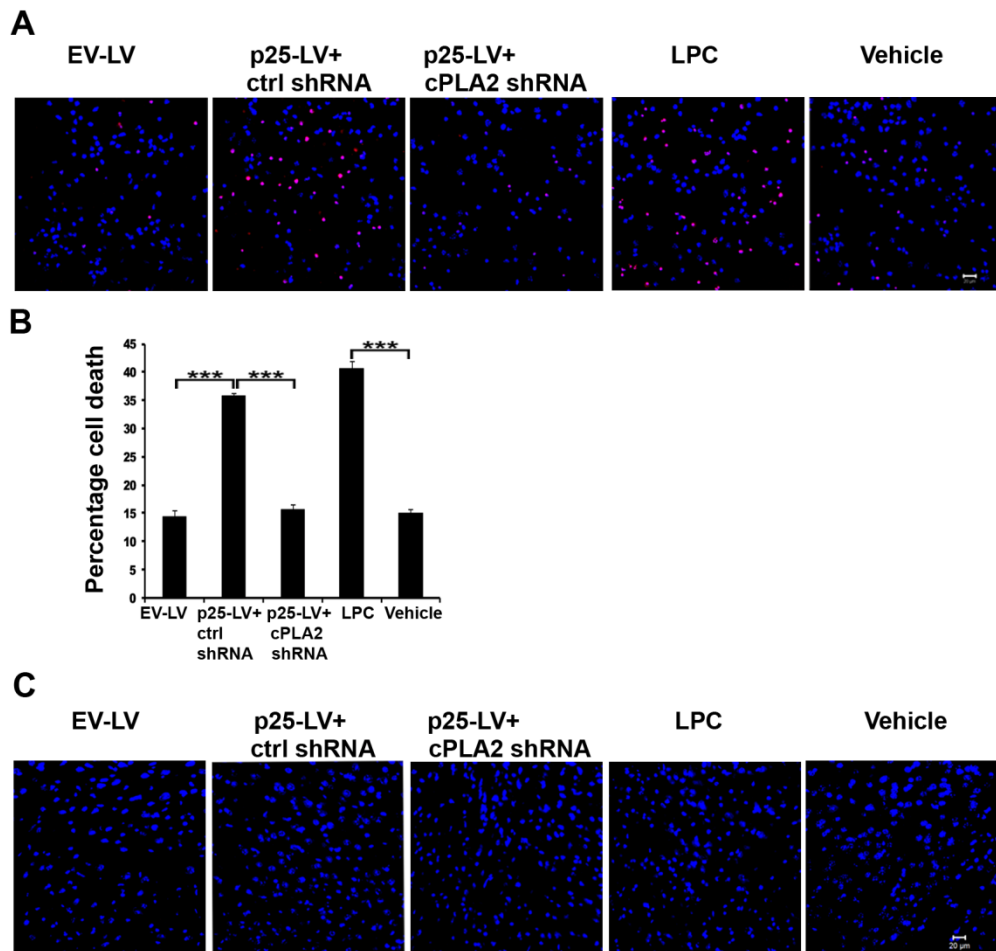
Figure 4.10: p25-mediated neuroinflammation is a trigger for neuronal cell death

(**A**) TUNEL staining images of cortical neurons incubated with supernatants from glial cells treated with vehicle, LPC 18:1 and lipids extracted from EV-LV, p25-LV+control shRNA/p25-LV+cPLA2 shRNA treated neurons. Scale bars: 20 µm. (**B**) Percentage cell death in panel **A** was determined by counting the number of TUNEL positive cells and normalized against DAPI signals from 10 independent fields (*** p-value < 0.001). Error bars indicate ± s.e.m (student's *t*-test). (**C**) TUNEL staining images from brain sections of WT mice injected with lipids samples same as in **A**. Scale bars: 20 µm.

4.4 DISCUSSION

The previous chapter (Chapter 3) described the finding of soluble factors triggering neuroinflammation. This chapter focuses on the identification of the factor as well as the pathways involved in its production. It is crucial to investigate the above-mentioned knowledge gaps to understand the mechanism behind p25/Cdk5 hyperactivation, neuroinflammation and subsequent neurodegeneration. Results from this chapter demonstrated that the overexpression of cPLA2 regulated glial activation through the production of LPC, a soluble lipid factor. The results further determined that the lipids from p25 overexpressing neurons could trigger neuropathological disease progression both *in vivo* and *in vitro*. Furthermore, results suggested that inhibition of cPLA2 early in the process of neurodegeneration could be a possible therapeutic target to decrease or slow down neurodegeneration.

4.4.1 p25-induced neuroinflammation is mediated by a soluble lipid factor, Lysophosphatidylcholine (LPC)

Biochemical characterization of the supernatants from p25 overexpressed cells determined the soluble signal secreted by p25 overexpressing cells to glial cells to be lipid in nature (Figure 4.1 and 4.2). This finding was further validated by *in vitro* as well as *in vivo* treatments of glial cells with lipids extracted from p25 overexpressing neurons (Figure 4.3). Although the involvement of lipids in neurodegeneration has been reported previously (Wells et al., 1995; Bassett et al., 1999; Grimm et al., 2005), the exact changes in lipid profiles during neuroinflammation were not fully studied. Hence, mass spectrometry analyses were carried out on the total lipids extracted from p25 overexpressing neurons and results showed that the neuroinflammation induced by p25 overexpression was caused by a polar phospholipid, Lysophosphatidylcholine (LPC) (Figure 4.4). Moreover, the progressive increase in LPC levels from 1 to 12 weeks of induction of p25 expression in mice hinted at the role of LPC in the induction of astrogliosis, T cell infiltration and further progression of neurodegeneration in p25Tg mice. A possible mechanism behind the induction of neuroinflammation by LPC was reported earlier where LPC treatment activated resident astrocytes via a Rho

kinase-mediated inflammatory response (Sheikh et al., 2009). In addition, G-protein coupled receptor, G2A has been recognized as the receptor for LPC, through which LPC functions as a chemo-attractant for T cells and macrophages (Radu et al., 2004). It has been reported earlier that LPC could regulate the expressions of various inflammation-related genes that encode chemokines, adhesion molecules, growth factors and pro-inflammatory enzymes in macrophages and T cells (Cieslik et al., 1998).

To further characterize the particular subtype of LPC responsible for p25-mediated astrogliosis, mass spectrometry analyses were performed using internal standards of individual LPC species and results identified that LPC 16:0, 18:0 and 18:1 were robustly increased when p25 was overexpressed. However, further studies on glial cells treated with commercially available LPC species indicated that LPC 18:1 was the most effective species in causing cause GFAP upregulation and astrogliosis (Figure 4.5). Previous studies already suggested that the effect of LPC might differ based on the unsaturation of acyl chain. Another important factor that can modify LPC effects is the capability to generate active micelles (Lauber et al., 2003; Ojala et al., 2007). Hence, it is understandable that the unsaturated nature of the LPC species 18:1 aids in the formation of active micelles compared to the other saturated species. This could be the reason behind the increased potency of LPC 18:1 in the activation of astrocytes. Although increased levels of LPC have been observed previously during neuropathological changes (Andreoli et al., 1973; Wender et al., 1988), the actual mechanism behind the role of LPC in the induction of neuroinflammation was not fully described. This study is the first to link p25/Cdk5 hyperactivation with LPC production and subsequent neuroinflammation.

4.4.2 p25 overexpression induces LPC production through the upregulation of cytosolic PLA2 (cPLA2)

LPC is produced from phosphatidylcholine by the action of phospholipase A2 (PLA2) (Steinbrecher et al., 1984). Previous studies indicated that increased PLA2 activity and PLA2-generated pro-inflammatory mediators play a major role in the induction of inflammatory changes in numerous neurological

disorders such as ischemia, AD, PD, and MS (Stephenson et al., 1996; Tariq et al., 2001; Yagami et al., 2002; Kalyvas and David, 2004; Farooqui et al., 2006). So far, cytosolic PLA2 (cPLA2-IV), Ca^{2+}-independent PLA2 (iPLA2-VI) and secretory PLA2 (sPLA2-II), the three main PLA2 types, have been studied extensively due to their significant role in inflammation-associated neurodegeneration (Sun et al., 2010). However, sPLA2-II is absent in our primary neuron culture and our mice model, because of a naturally-occurring frame shift mutation in the C57BL/6 inbred mice strain (Kennedy et al., 1995). Undetermined Ct values from RT-PCR studies using sPLA2-II primers further confirmed the absence of sPLA2-II mRNA in our experimental system. In addition, studies have suggested that sPLA2 action might be dependent on an active cPLA2 (Balsinde et al., 1998). Therefore, cPLA2 is likely to be the key enzyme for lysophospholipid metabolism even when sPLA2 is present. This essential role of cPLA2 in lysophospholipid signaling pathways was emphasized by a study using cPLA2 knock-out mice where the rate of inflammatory mediators release was significantly reduced (Uozumi et al., 1997). The iPLA2 subtype is one of the common housekeeping enzymes that usually maintain constant membrane phospholipids contents. Activity of iPLA2 has been reported previously to be involved in the process of vascular smooth muscle contraction and apoptosis (Guo et al., 2003). RT-PCR data from this chapter confirmed that there was no obvious difference in iPLA2 levels between the control and the p25 overexpressing neurons (Figure 4.6A). It has been found earlier that AACOCF3 is a more potent inhibitor for cPLA2 (500-fold higher) than for sPLA2, and BEL is 1,000-fold more selective for iPLA2 than for cPLA2 (Riendeau et al., 1994; Jenkins et al., 2002; Farooqui et al., 2006). Results from experiments in this chapter using AACOCF3 and BEL further determined that the p25 overexpression did not affect iPLA2 levels, but increased cPLA2 expression and activity (Figure 4.6). Together, these results identified a robust increase in *cPLA2* gene expression, protein level and activity in various p25 overexpression systems including p25 overexpressing transgenic mice model, primary neurons from the p25 transgenic mice and the neurons transduced with p25-LV.

In order to study whether the reduction of p25-induced cPLA2 overexpression could ameliorate the progression of pathological changes, *cPLA2* gene silencing experiments were carried out and the results demonstrated a dramatic reduction in LPC 18:1 level as well as the expression of downstream neuroinflammatory markers (Figure 4.7 and 4.8). Previous studies have reported the involvement of cPLA2 in neurodegeneration and cPLA2 expression has been shown to be abundant in AD brains especially in the hippocampal regions (Stephenson et al., 1996; Farooqui et al., 1997; Colangelo et al., 2002; Farooqui et al., 2003). Elevated cPLA2 expression levels have also been observed in injured cervical neurons and dorsal root ganglia (Hornfelt et al., 1999). In addition, studies also reported that NMDA infusion into rat hippocampus caused striking increases in cPLA2 activity (Pepicelli et al., 2002). Moreover, increased levels of cPLA2 activity were observed in hAPP mice (Sanchez-Mejia et al., 2008). However, the neuroinflammatory role of cPLA2 was not fully investigated yet. Findings from this chapter strongly suggest that cPLA2 activity has a critical role in the p25/Cdk5 hyperactivation-mediated neuroinflammation and neurodegeneration.

Previous studies reported an association between the Aβ toxicity and increased cPLA2 activity in AD brains (Stephenson et al., 1996; Farooqui et al., 1997; Kriem et al., 2005). However, findings from this chapter suggested that cPLA2 upregulation might occur before the induction of tau hyperphosphorylation or amyloid accumulations (Figure 4.6 and Figure 3.5). Thus, there must be an alternate trigger for this upregulation of cPLA2. The next important question to be answered is how p25 regulate this cPLA2 expression. p25/Cdk5 activity has been observed earlier in the nuclei of neurons (Patrick et al., 1999; O'Hare et al., 2005; Saito et al., 2007). In addition, it was reported that p25/Cdk5 complex may interact with nuclear machineries to modulate gene transcription (Yin et al., 2005). Therefore, evidence from various studies led to a hypothesis that p25/Cdk5 hyperactivation may possibly mediate this effect through the transcriptional regulation of *cPLA2* gene expression. Previous studies showed that *cPLA2* gene expression could be regulated by the transcription factors p300 and NF-

κB (Luo et al., 2006; Lee et al., 2010; Lee et al., 2011). Furthermore, AKT-mediated phosphorylation was found to be critical for the regulation of p300 and NF-κB activity (Kane et al., 2002; Huang and Chen, 2005). p25/Cdk5-mediated AKT activation (Liu et al., 2008) has also been reported previously. However, more studies are needed to understand the actual mechanism behind the p25/Cdk5 hyperactivation-mediated cPLA2 upregulation. Although the occurrence of neuroinflammation during p25 overexpression has been reported previously (Cruz et al., 2003; Muyllaert et al., 2008), this is the first study to not only provide a crucial link between the two processes, but also identify the pathway behind the initiation of neuroinflammation where upregulation of cPLA2 caused the production of LPC.

4.4.3 p25-mediated neuroinflammation triggers neurodegenerative changes

Astrocytes can respond to factors released by neurons at the synaptic cleft by releasing glutamate back to neurons (Sonnewald et al., 2002). To investigate the involvement of p25-induced production of inflammatory mediators in the initiation of neurodegeneration, conditional media transfer experiments were performed between activated glial cells and healthy cortical neurons. The results showed noticeable increases in neurodegenerative markers, phospho-tau and intracellular Aβ (1-42) accumulation in neurons treated with supernatants from glial cells that were previously incubated with lipids from p25 overexpressing neurons and commercially obtained LPC 18:1. The above finding was further confirmed by *in vivo* injection of mice brain with lipids from p25 overexpressing neurons and commercially obtained LPC18:1. Thus, results collectively indicated that p25-mediated inflammatory changes could trigger the initiation of neurodegeneration (Figure 4.9). TUNEL staining experiments further suggested a significant increase, compared to control, in cell death when neurons treated with supernatants from glial cells that have been treated with lipids from p25 overexpressing neurons. In contrast, there was no TUNEL staining in the *in vivo* experiments (Figure 4.10). This could be due to the single dose injection of lipids and following clearance of lipids. Moreover, one-time injection of lipids into mice was just sufficient to trigger

the pathological hallmark production, but subsequent induction of the neuronal death cascade might require sustained LPC levels. In addition, marked reduction in the expression of neurodegenerative markers with cPLA2 knock-down condition supported strongly the above findings.

Together, results indicated that cPLA2 is elevated when p25 is produced, resulting in subsequent neuroinflammation and neurodegeneration. Findings from this study are supported by various studies conducted on other neurodegenerative models where CDP-choline (a cPLA2 inhibitor) protected neurons from excitotoxicity (Mir et al., 2003). Moreover, AACOCF3, a potent inhibitor of cPLA2, reduced the release of arachidonic acid metabolites in MPP$^+$-mediated neurodegeneration, an *in vitro* model of PD (Yoshinaga et al., 2000).

We proposed a model based on the findings from this chapter to understand the mechanism behind p25-induced neuroinflammation-mediated neurodegeneration (Figure 4.11). p25/Cdk5 hyperactivation causes increases in cPLA2 expression and releases extracellular soluble LPC from PC which activate glial cells to produce chemokines/cytokines such as MIP-1α, TNF-α, TGF-β and IL-1β. This results in the CNS recruitment of peripheral immune cells which then instigates the next phase of neuroinflammatory response, causing further damage.
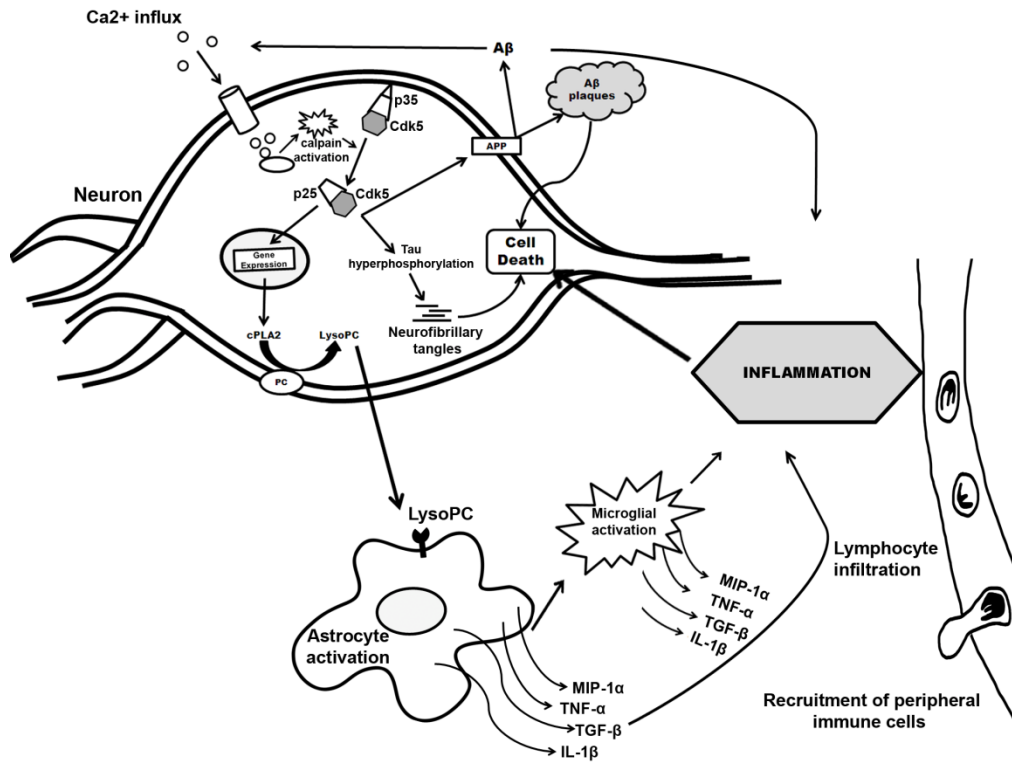
Figure 4.11: Schematic representation of neurodegeneration caused by p25/Cdk5-mediated neuroinflammation

Neurotoxic insults cause abnormal $Ca2^+$ influx and intense calpain activation. Calpain in turn cleaves Cdk5 activator, p35 into p25. p25 has increase stability and potential to hyperactivate Cdk5. p25/Cdk5 hyperactivation leads to intra cellular tangle formation and extra cellular Aβ plaque deposition through hyperphosphorylation of tau and APP. Moreover, p25/Cdk5 hyperactivation causes increase in cPLA2 production and activation which in turn releases extracellular soluble LPC from PC. LPC activate glial cells to produce chemokines such as MIP-1α, TNF-α, TGF-β and IL-1β. Furthermore, LPC and chemokines production cause microglial activation and CD4+/CD8+ lymphocytes infiltration, the main indicators for severe neuroinflammation and further cell death in neurons containing p25.

4.5 SUMMARY

In conclusion, findings from this chapter demonstrated that LPC was a soluble molecular signal released from stressed neurons to induce the activation of glial cells and the subsequent release of diverse inflammatory mediators that have been implicated in the progression of AD-like neuropathology in p25Tg mice. Results also identified cPLA2 and LPC species 18:1 as being responsible for the pathological effects caused by p25/Cdk5 hyperactivation. Thus, results suggested that targeting cPLA2 activity might be a viable therapeutic target to halt neurodegeneration caused by p25/Cdk5 hyperactivation. Development of a specific cPLA2 inhibitor for human clinical use could be a valuable therapeutic tool to treat neuroinflammation-associated neurodegenerative diseases.

Although some studies have explained the role of anti-inflammatory drugs in the amelioration of neurodegenerative changes (Jantzen et al., 2002; Sastre et al., 2006), there have so far been no optimal approaches supporting the treatment of AD (Imbimbo, 2009). Hence, it is crucial to investigate the effect of various anti-inflammatory agents on the p25 overexpression-mediated cPLA2 upregulation and subsequent neurodegenerative disease progression. The next chapter will focus on the investigation of the effect of curcumin, a naturally occurring anti-inflammatory molecule on p25-mediated neuroinflammation and neurodegeneration. Moreover, the results from these studies will provide comprehensive evidence to uncover the mechanism behind the inflammatory-mediated neurodegenerative disease progression in various neurodegenerative diseases and open up avenues for intervention.

CHAPTER 5

Chapter 5: Curcumin (a natural polyphenol) blocks the neuroinflammatory cascade, attenuates neuropathological progression and offers neuroprotection against p25/Cdk5-mediated neurodegeneration

5.1 Introduction

The results in Chapter 3 and Chapter 4 revealed that the p25/Cdk5-mediated neuroinflammation was an early event and not a secondary consequence of amyloid or tau pathology in p25Tg mice. In addition, results indicated that the cPLA2 upregulation and the subsequent LPC production were the critical events that regulated the initiation of neuroinflammation as well as the progression of neurodegeneration in p25Tg mice. Hence, the most obvious next step is to extend the investigation on the p25-mediated neuroinflammation using reported anti-inflammatory agents such as curcumin and study their effects on the p25-mediated neuropathological changes including amyloid and tau pathology in p25Tg mice. Curcumin, the main component of turmeric (a spice present in Indian curries) is well known for its antioxidant, anti-amyloid, anti-inflammatory and anti-oncogenic properties (Menon and Sudheer, 2007; Sa and Das, 2008; Monroy et al., 2013). Moreover, recent studies indicated that this natural and inexpensive dietary supplement can cross the blood-brain barrier and offer neuroprotection (Garcia-Alloza et al., 2007). However, the major limitation in the use of curcumin is its low bioavailability due to poor oral adsorption (Anand et al., 2007). Fortunately, our collaborator in UCLA has formulated a novel curcumin formulation with solid lipid curcumin particle (SLCP) preparation, called "LONGVIDA", which effectively increased free curcumin levels in plasma as well as in brain (Begum et al., 2008; Gota et al., 2010; Dadhaniya et al., 2011). Therefore, it would be interesting to investigate the effect of curcumin (LONGVIDA) on the p25-mediated neuroinflammation and the subsequent neuropathology in p25Tg mice.

The first part of this chapter focuses on the experiments to determine the effects of curcumin on p25-mediated neuroinflammatory changes including

glial activation, cPLA2 upregulation and LPC production. The second part details the study on the neuroprotective ability of curcumin against p25-mediated neurodegenerative changes including tau and amyloid pathologies. Together, results from this chapter showed that early inhibition of p25-mediated neuroinflammation prevented the robust progression of neurodegeneration and provided neuroprotection against p25/Cdk5 hyperactivation and neurotoxicity.

5.2 Methods

5.2.1 Curcumin treatment in p25 transgenic mice

LONGVIDA, a novel curcumin formulation prepared using a novel method called SLCP (solid lipid curcumin particle) (Verdure Sciences), was used in this study under collaboration. p25Tg mice were treated with this special curcumin formulation orally via their feed (4 g/kg of feed, Harlan).

5.2.2 Western blot analyses

Brain lysates from 4 and 12-week induced p25Tg/control mice (with and without curcumin treatment) were resolved on 4-20% polyacrylamide gels, blotted onto nitrocellulose membranes and then immunoprobed with mouse anti-GFAP, mouse anti-GFP, mouse anti-CD11b, mouse anti-cPLA2, rabbit anti-NF-κB and mouse monoclonal anti-PHF-tau antibodies (clones AT8 and AT100).

5.2.3 *In vitro* kinase assays

(This work was done in collaboration with Dr. Tej Kumar Pareek, Case Western Reserve University, Cleveland, OH, USA)

Cdk5 activity levels were analyzed using kinase assays with brain lysates from 4 and 12-week induced p25Tg/control mice (with and without curcumin treatment).

5.2.4 Real-Time PCR

RNA samples were extracted from 4 and 12-week induced p25Tg/control mice brains (with and without curcumin treatment) using RNeasy Mini Kit. Quantitative real-time PCR for chemokines/cytokines expression levels was performed with cDNA synthesized from RNA using High capacity cDNA reverse transcriptase kits.

5.2.5 Immunohistochemistry

16 μm brain sections from 4 and 12-week induced p25Tg/control mice (with and without curcumin treatment) were immunostained with primary antibodies

such as mouse anti-GFAP, mouse monoclonal anti-GFP, mouse anti-CD11b, rabbit anti-tPA, mouse anti-CD4, mouse anti-CD8, mouse monoclonal anti-PHF-tau antibodies (clones AT8 and AT100), rabbit anti-beta-amyloid 1-42, mouse monoclonal anti-beta-amyloid 1-16 (6E10) and rabbit anti-cleaved caspase-3 antibodies. Secondary fluorescence-conjugated antibodies used were Alexa Fluor 488 and Alexa Fluor 594. Confocal images were taken at 40X magnification.

5.2.6 Thioflavin staining

Thioflavin staining was performed as described in section 2.2.11.3 using brain sections from 12-week induced p25Tg/control mice (with and without curcumin treatment) and confocal images were taken at 40X magnification.

5.2.7 Bielschowsky silver staining

Bielschowsky silver staining was performed as described in section 2.2.11.4 using brain sections from 12-week induced p25Tg/control mice (with and without curcumin treatment) and images were taken at 20X magnification.

5.2.8 cPLA2 activity assay

cPLA2 activity was analyzed using the brain samples from 4 and 12-week induced p25Tg/control mice (with and without curcumin treatment) using the cPLA2 activity assay kit.

5.2.9 Lipids analysis using High-Performance Liquid Chromatography/Mass Spectrometry

(This work was done in collaboration with A/Prof Markus Wenk's Lipidomics lab, NUS)

Lysophosphatidylcholine (LPC) levels were quantified from the total lipids extracted from brain samples of 4 and 12-week induced p25Tg/control mice (with and without curcumin treatment) with an Agilent 1200 high-performance liquid chromatography (HPLC) systems and a 3200 Q-Trap mass spectrometer.

5.2.10 Behavioural studies

The radial arm maze study was carried out using the 8 arm radial maze according to the protocol described in detail in section 2.2.15. The number of reference memory errors (entering a non-baited arm) and working memory errors (entering a baited arm but previously entered) were measured and analyzed for 12-week induced p25Tg/control mice groups (with and without curcumin treatment).

5.2.11 Statistical analyses

Data are expressed as the mean of at least three values $\pm$ standard error (s.e.m). Statistical significance was determined using one-way ANOVA followed by post-hoc tukey's test and repeated measures ANOVA followed by post-hoc tukey's test (Figure 12: reference memory errors). P-value for statistical significance is defined as $P < 0.05$.

5.3 Results

5.3.1 Curcumin reduces p25-mediated astrocyte activation in p25Tg mice

In order to investigate the effect of curcumin on p25-mediated neuroinflammation and the subsequent neurodegeneration, p25Tg mice were fed with curcumin-enriched feed for 4 and 12 weeks after the induction of p25 expression. There were no obvious side effects including weight loss and behavioural abnormalities observed after 4 and 12-week curcumin treatment. Curcumin-treated control mice were in good health with normal exploratory/foraging behaviours, smooth coat, and stable weight growth. Firstly, equivalent levels of p25 expression were confirmed in the curcumin-treated as well as non-treated p25Tg mice groups for both 4 and 12-week time points using immunohistochemistry (Figure 5.1A and B) and Western blot analyses with anti-GFP antibody (Figure 5.1C and D).

Subsequently, the effect of curcumin on p25-mediated astrocyte activation was investigated using anti-GFAP antibody. Results from immunohistochemistry analyses revealed that the intensity of GFAP staining was greatly reduced in the cortex as well as the hippocampus of 4 and 12-week induced curcumin-treated p25Tg mice group compared to the non-treated p25Tg mice group (Figure 5.2A and B).

Furthermore, Western blot analyses were performed to quantitate the rate of reduction of p25-mediated glial activation by curcumin treatment using anti-GFAP antibody and approximately 2-3 fold reduction in GFAP expression levels were observed in both 4 and 12-week induction groups in the forebrain of curcumin-treated p25Tg mice compared to the non-treated group (Figure 5.2C and D). Collectively, these results suggested that curcumin effectively reduced p25-mediated astrocyte activation.
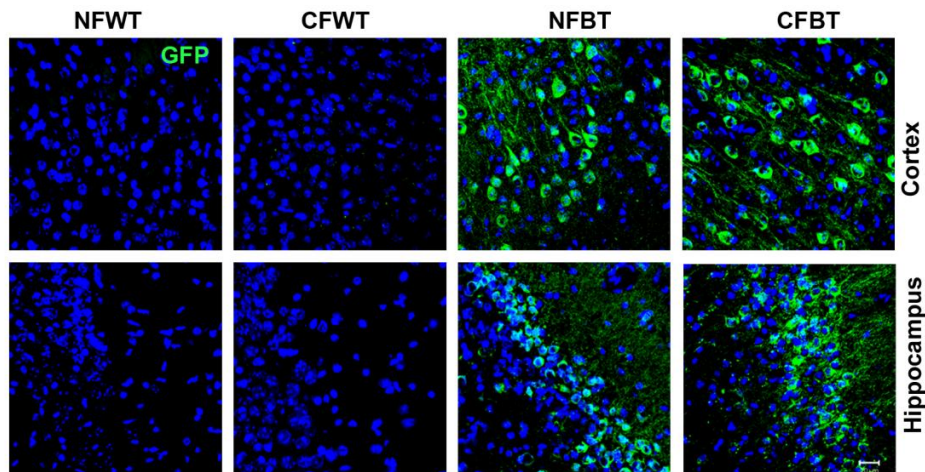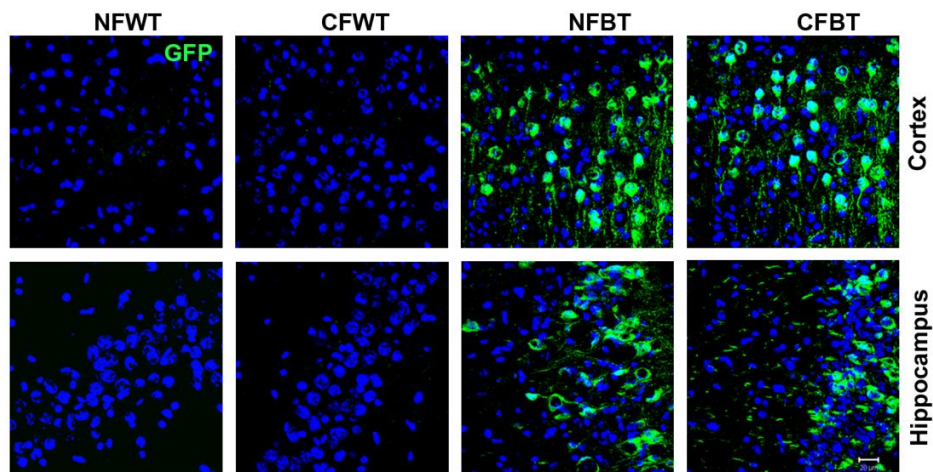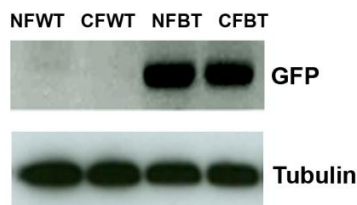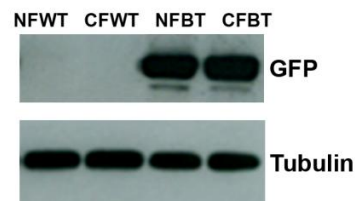
Figure 5.1: Expression levels of p25 in p25Tg mice

Representative confocal pictures of frontal cortex (layer 2/3) (top panels) and CA3 region of hippocampus (bottom panels) from the (**A**) 4-week and (**B**) 12-week induced p25Tg mice with normal feed (NFBT), p25Tg mice with curcumin feed (CFBT), respective age-matched WT mice with normal feed (NFWT) and WT mice with curcumin feed (CFWT) (n=3). Immunofluorescence staining was performed on the brain sections using anti-GFP antibody (green) and DAPI (blue). Scale bars represent 20 μm. Western blot results of the brain lysates from (**C**) 4-week and (**D**) 12-week induced NFBT, CFBT, NFWT, CFWT mice using anti-GFP antibody (top panels). Immunoblots were re-probed with anti-tubulin antibody (a loading control) (bottom panels).
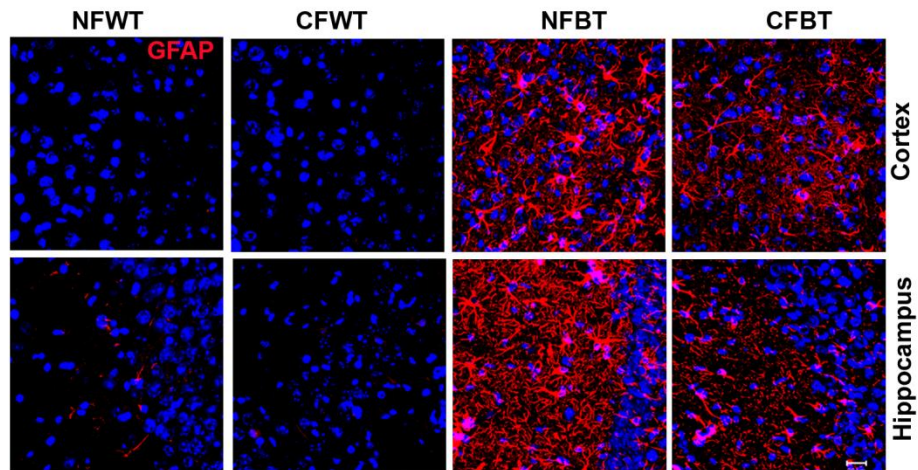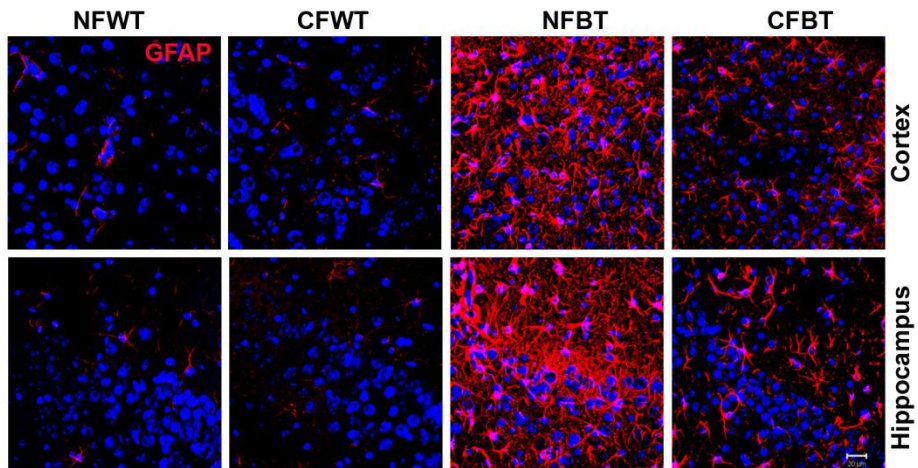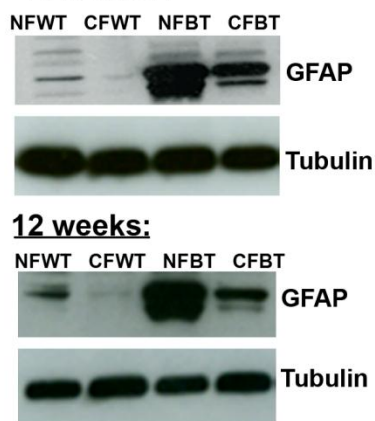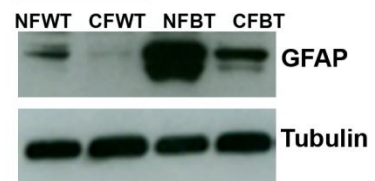
Figure 5.2: Reduced astrocyte activation in curcumin-treated p25Tg mice

Immunofluorescence images from the cortex (layer 2/3) (top panels) and hippocampus (CA3 region) (bottom panels) of the brain sections from (**A**) 4-week and (**B**) 12-week induced p25Tg mice with normal feed (NFBT), p25Tg mice with curcumin feed (CFBT), respective age-matched WT mice with normal feed (NFWT)

and WT mice with curcumin feed (CFWT) (n=3) using anti-GFAP antibody (red) and DAPI (blue). (**C**) GFAP levels were analyzed by immunoblot analyses with brain lysates from 4-week (top panel) and 12-week (bottom panel) induced p25Tg/control mice with/without curcumin treatment using anti-GFAP and anti-tubulin antibodies. (**D**) Quantification of immunoblots in **C** by densitometric scanning (*** p-value < 0.001, ** p-value < 0.01 and NS p-value > 0.05) (one-way ANOVA followed by post-hoc tukey's test). Scale bars represent 20 μm. Error bars indicate ± s.e.m.

To further investigate the role of curcumin on p25-mediated glial activation, chemokine/cytokine expression levels were analyzed using RT-PCR studies with RNA samples from curcumin-treated and non-treated p25Tg/control mice for both 4 and 12-week induction periods. p25-mediated upregulation of expression levels of pro-inflammatory chemokines/cytokines such as MIP-1α, TNF-α and IL-1β were significantly abolished by curcumin (Figure 5.3A, B and D). However, TGF-β levels were found to be unaltered by curcumin treatment in p25Tg mice (Figure 5.3C).
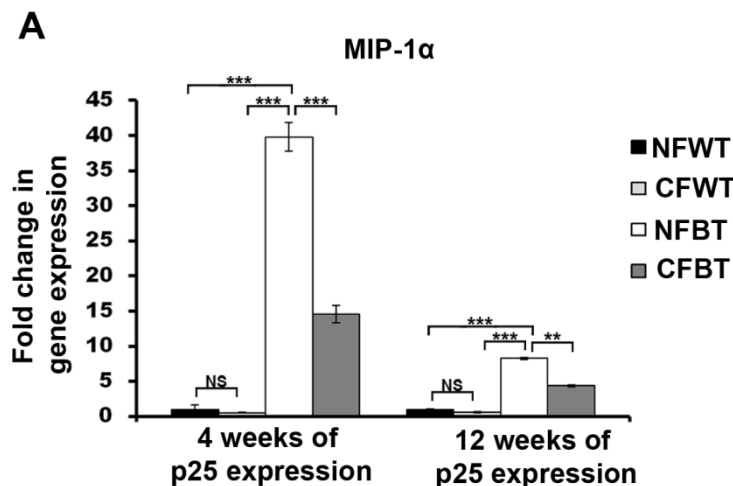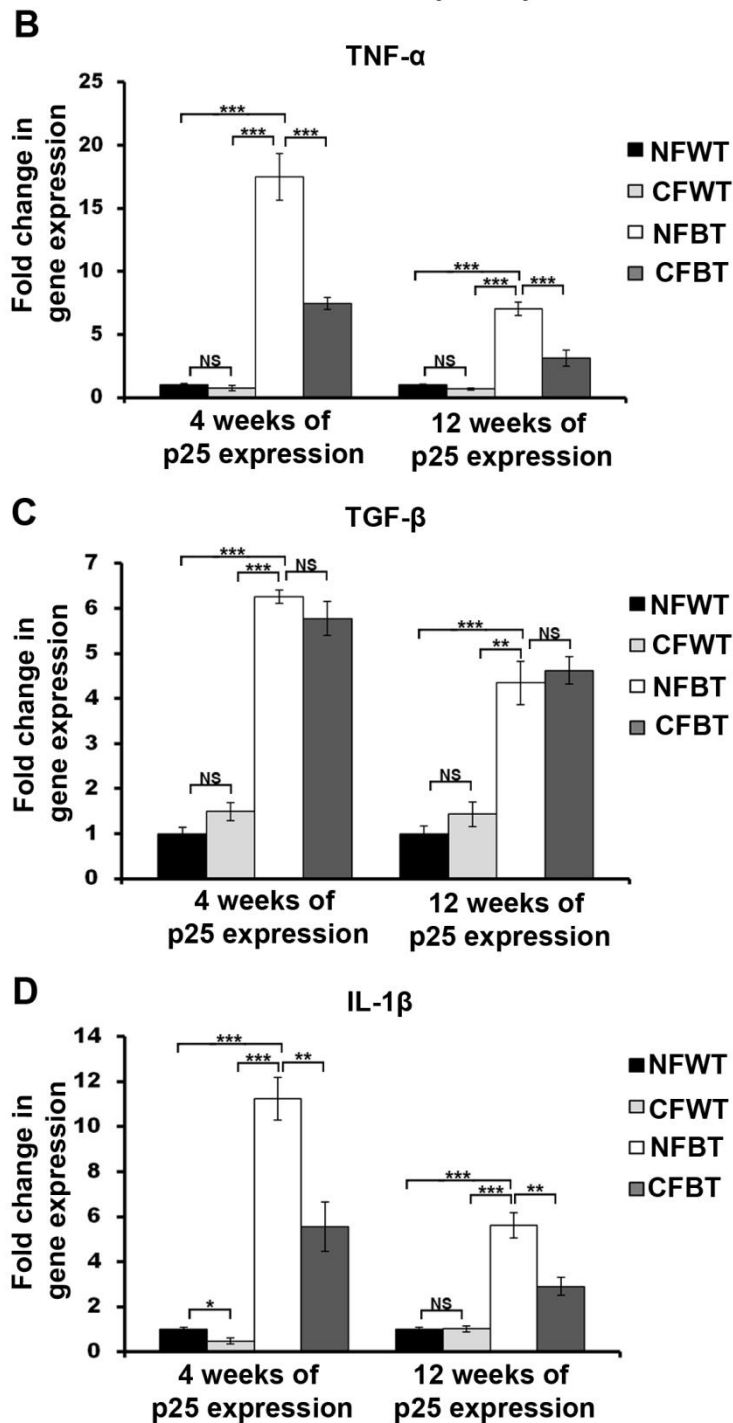
Figure 5.3: Chemokine/cytokine expression levels in curcumin-treated p25Tg mice

Real-Time PCR results for (**A**) MIP-1α, (**B**) TNF-α, (**C**) TGF-β and (**D**) IL-1β expression in 4-week/12-week induced p25Tg mice with normal feed (NFBT), p25Tg mice with curcumin feed (CFBT), respective age-matched WT mice with normal feed (NFWT) and WT mice with curcumin feed (CFWT) (n=3) (*** p-value < 0.001, ** p-value < 0.01, * p-value < 0.05 and NS p-value > 0.05) (one-way ANOVA followed by post-hoc tukey's test). Error bars indicate ± s.e.m.

5.3.2 Curcumin inhibits p25/Cdk5 hyperactivation in p25Tg mice

In order to investigate whether curcumin has any effect on p25/Cdk5 hyperactivation, kinase assays and immunoblots analyses were performed and results indicated that there was no obvious change in Cdk5 protein levels between the curcumin-treated and non-treated p25Tg mice groups in both 4 and 12-week induction groups (Figure 5.4A-C). However, p25-mediated Cdk5 hyperactivity was reduced significantly by curcumin treatment especially in the 12-week induced p25Tg mice (Figure 5.4D). Endogenous p35 and exogenous p25 expression levels were also determined using C19 antibody and results showed that there was no significant change in endogenous p35 expression levels in p25Tg mice with and without curcumin treatment (Supplementary Figure 2 in Appendices).
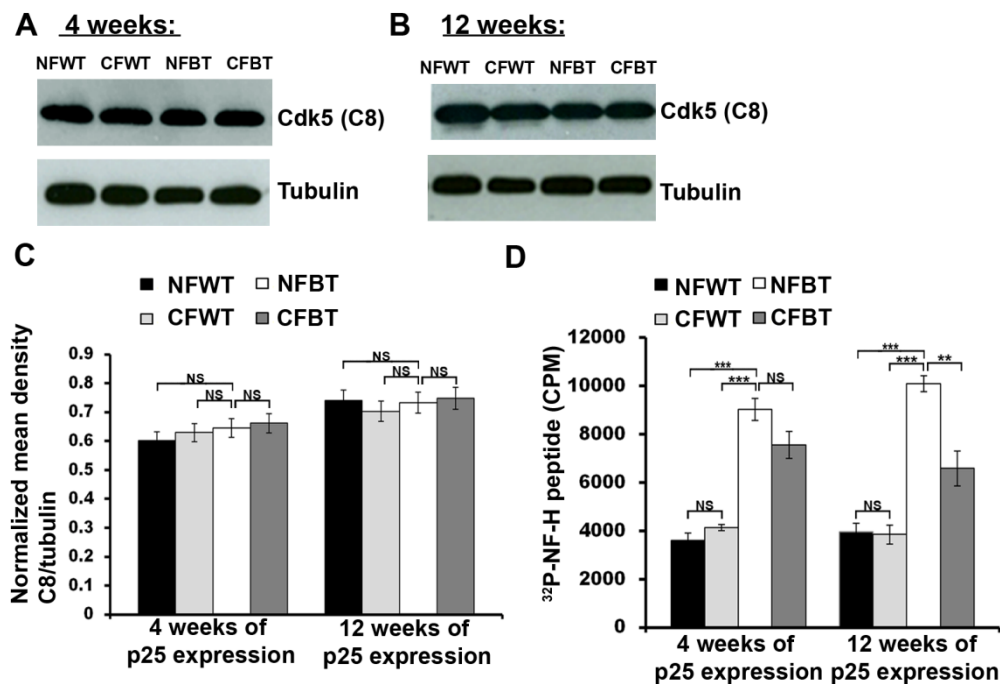
Figure 5.4: Reduced Cdk5 hyperactivity in curcumin-treated p25Tg mice

Western blot results of brain lysates from the (**A**) 4-week and (**B**) 12-week induced p25Tg mice with normal feed (NFBT), p25Tg mice with curcumin feed (CFBT), respective age-matched WT mice with normal feed (NFWT) and WT mice with curcumin feed (CFWT) using anti-C8 antibody (n=3). (**C**) Quantification of immunoblots in **A** & **B** by densitometric scanning. (**D**) Kinase assay results of the brain lysates from the samples same as in **A** and **B** (*** p-value < 0.001, * p-value < 0.05 and NS p-value > 0.05) (one-way ANOVA followed by post-hoc tukey's test). Error bars indicate ± s.e.m.

5.3.3 Curcumin regulates p25-induced microgliosis

In order to extend the investigation of curcumin effects on the p25-mediated neuroinflammation, the role of curcumin on p25-mediated microgliosis was examined by immunohistochemical studies and Western blot analyses using microglial activation markers anti-Cd11b and anti-tPA antibodies. Cd11b immunostaining was markedly decreased in both cortical and hippocampal regions of curcumin-treated 4-week induced p25Tg mice brain sections compared to those in the non-treated p25Tg mice (Figure 5.5A). However, there was only a moderate reduction in Cd11b staining in the 12-week induced curcumin-treated p25Tg mice (Figure 5.5B). Western blot results were identical to the immunostaining results and reduction in Cd11b expression levels were significant in 4-week induced curcumin-treated samples compared to 12-week induced curcumin-treated p25Tg mice brain samples (Figure 5.5C and D). Together, these results showed that the curcumin-mediated reduction in microglial activation was more significant in 4-week induced p25Tg mice compared to 12-week induced p25Tg mice.

A <u>4 weeks of p25 expression</u> :

NFWT   CFWT   NFBT   CFBT

Cd11b

Cortex

Hippocampus

20 µm

B <u>12 weeks of p25 expression</u> :

NFWT   CFWT   NFBT   CFBT

Cd11b

Cortex

Hippocampus

20 µm

C <u>4 weeks:</u>

NFWT CFWT NFBT CFBT

Cd11b

Tubulin

<u>12 weeks:</u>

NFWT CFWT NFBT CFBT

Cd11b

Tubulin

D

Normalized mean density Cd11b/tubulin

■ NFWT   □ NFBT
□ CFWT   ▨ CFBT
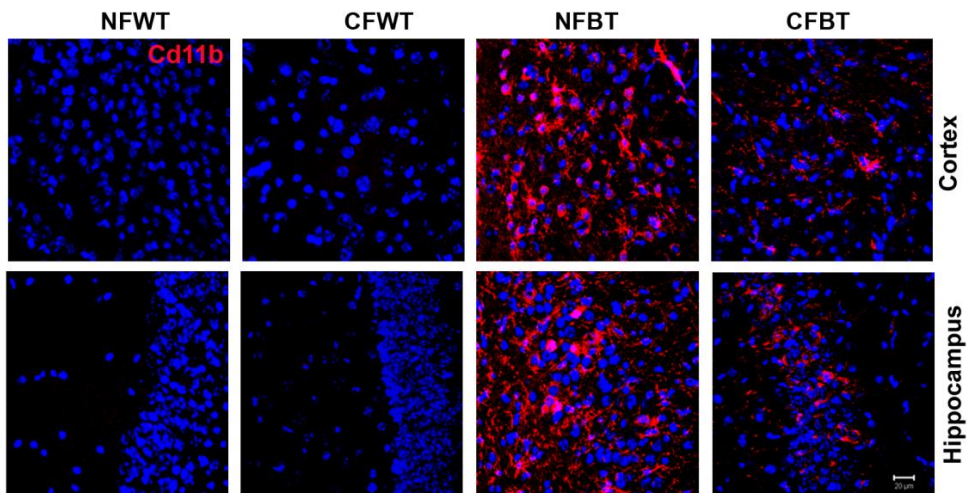
4 weeks of p25 expression   12 weeks of p25 expression
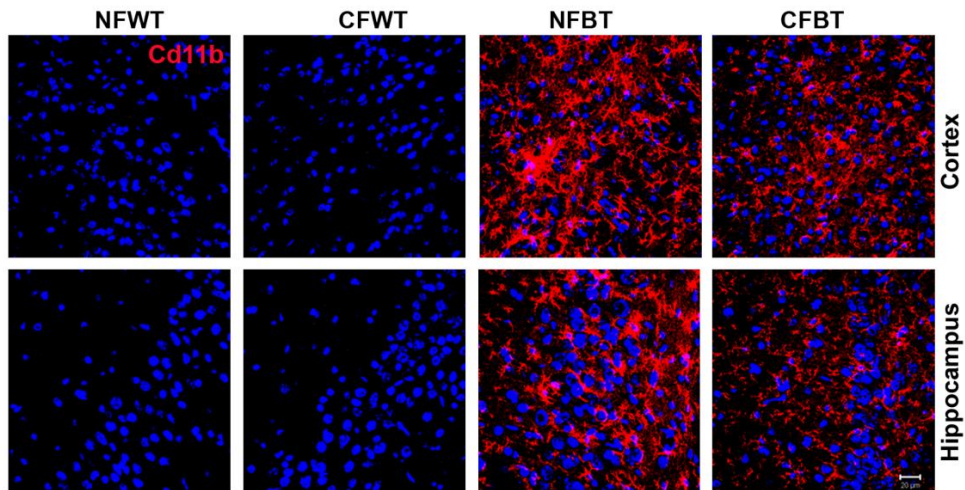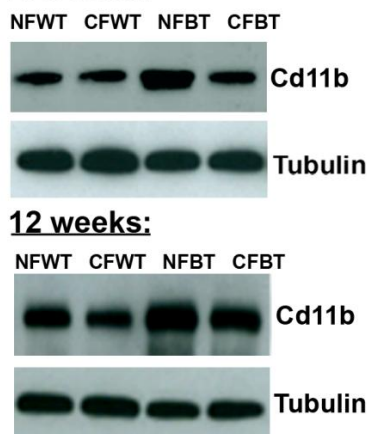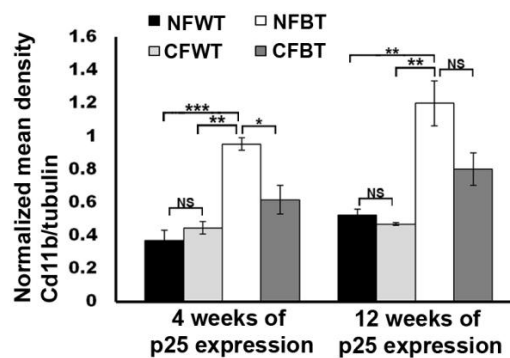
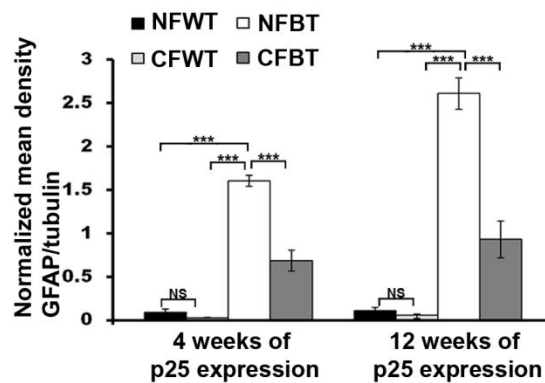**Figure 5.5: Reduced microgliosis in curcumin-treated p25Tg mice**

Immunofluorescence images from the cortex (layer 2/3) (top panels) and hippocampus (CA3 region) (bottom panels) of brain sections from (**A**) 4-week and (**B**) 12-week induced p25Tg mice with normal feed (NFBT), p25Tg mice with

146

curcumin feed (CFBT), respective age-matched WT mice with normal feed (NFWT) and WT mice with curcumin feed (CFWT) (n=3) using anti-Cd11b antibody (red) and DAPI (blue). (**C**) Cd11b levels were analyzed by immunoblot analyses with brain lysates from 4-week (top panel) and 12-week (bottom panel) induced p25Tg/control mice with/without curcumin treatment using anti-Cd11b antibody. (**D**) Quantification of immunoblots in **C** by densitometric scanning (*** p-value < 0.001, ** p-value < 0.01, * p-value < 0.05 and NS p-value > 0.05) (one-way ANOVA followed by post-hoc tukey's test). Scale bars represent 20 μm. Error bars indicate ± s.e.m.

As mentioned in Chapter 3 (section 3.3.2), tissue plasminogen activator (tPA) upregulation is an indicator for inflammatory-microglial activation (Siao and Tsirka, 2002; Pineda et al., 2012). In addition, results in Chapter 3 showed that tPA levels were elevated in p25Tg mice compared to the controls (Figure 3.3B) and it is important to study the changes in tPA levels after curcumin treatment in p25Tg mice. Interestingly, results from this chapter identified that tPA immuostaining was almost completely abolished in both 4 and 12-week induced curcumin-treated p25Tg mice brain sections compared to the non-treated p25Tg (Figure 5.6A and B). Thus, results collectively revealed that the pro-inflammatory state of microglial activation was efficiently blocked by curcumin in p25Tg mice.
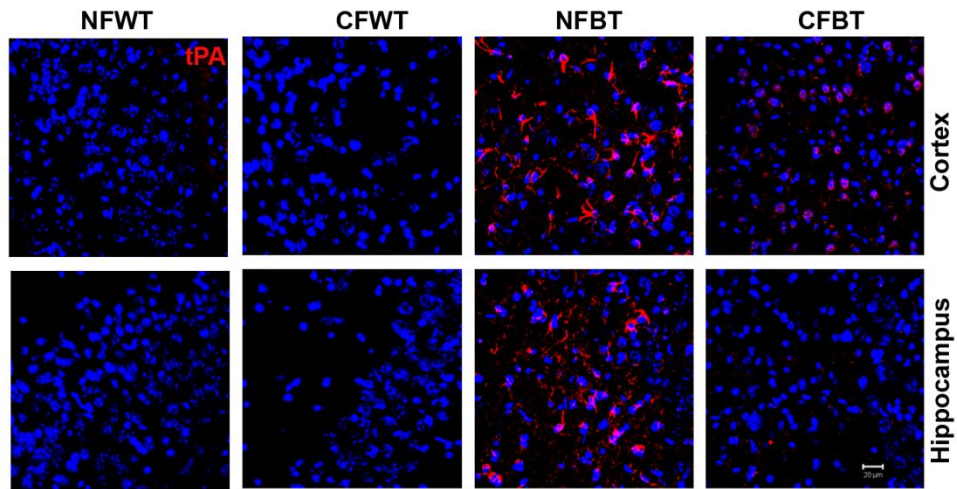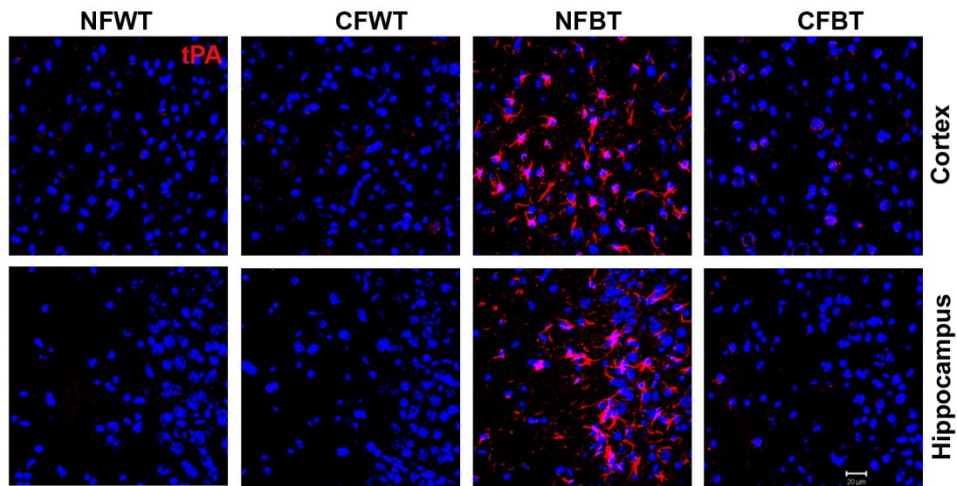
Figure 5.6: Reduced pro-inflammatory microglial activation in curcumin-treated p25Tg mice

Confocal images from the cortex (layer 2/3) (top panels) and hippocampus (CA3 region) (bottom panels) of the brain sections from (**A**) 4-week and (**B**) 12-week induced p25Tg mice with normal feed (NFBT), p25Tg mice with curcumin feed (CFBT), respective age-matched WT mice with normal feed (NFWT) and WT mice with curcumin feed (CFWT) (n=3) using anti-tPA antibody (red). Nuclei were stained with DAPI (blue). Scale bars represent 20 μm.

5.3.4 Curcumin induces temporal change in the rate of peripheral cells brain infiltration in p25Tg mice

Results in Chapter 3 showed that the infiltration of CD4- and CD8-positive peripherally-derived lymphocytes was very prominent in the p25Tg mice brain (Figure 3.4). Hence, experiments in this chapter were focused on studying the effects of curcumin on this event, using immunohistochemical staining. The results suggested that there was a noticeable reduction in CD4 (Figure 5.7A) and CD8 (Figure 5.7C) staining in 4-week treatment of curcumin in p25Tg mice. However, this curcumin-mediated reduction of peripheral cell infiltration was only moderate in 12-week induced p25Tg mice (Figure 5.7B and D). Moreover, these results were found almost identical to the effect of curcumin on microgliosis. Thus, these results suggested that curcumin was unable to effectively block the CNS infiltration of peripheral immune cells especially during chronic expression of p25 in 12-week induced p25Tg mice.
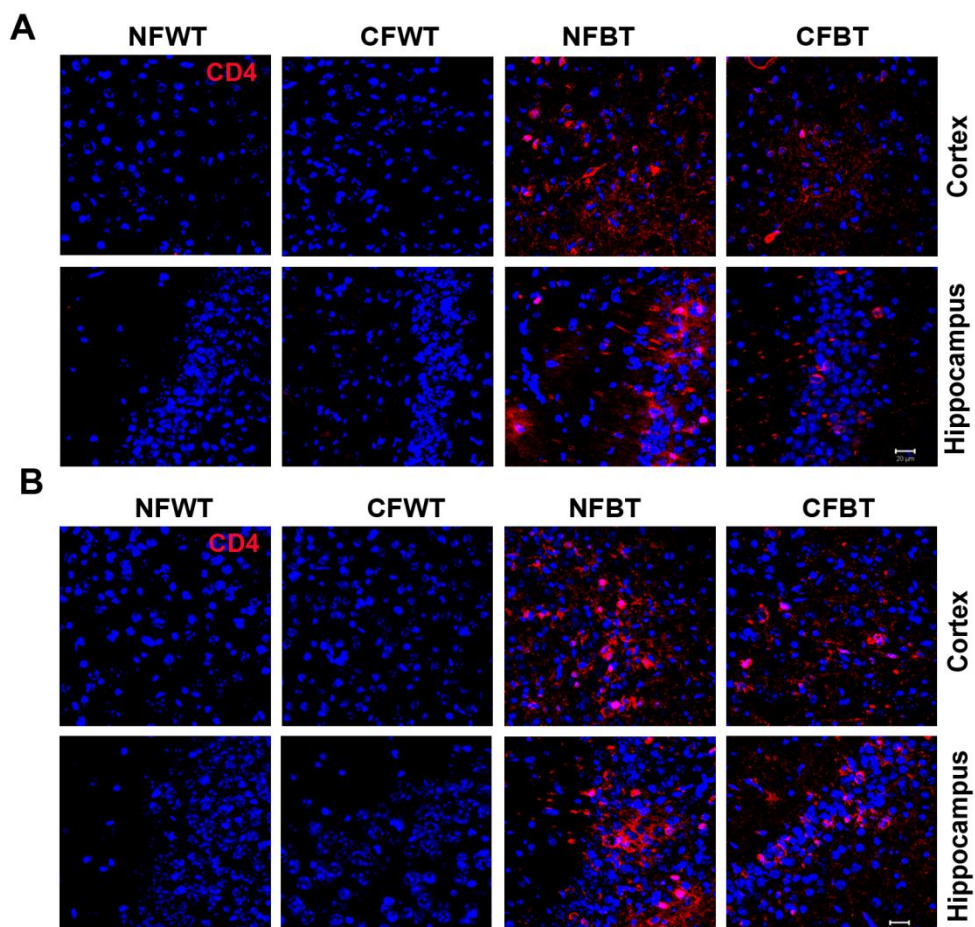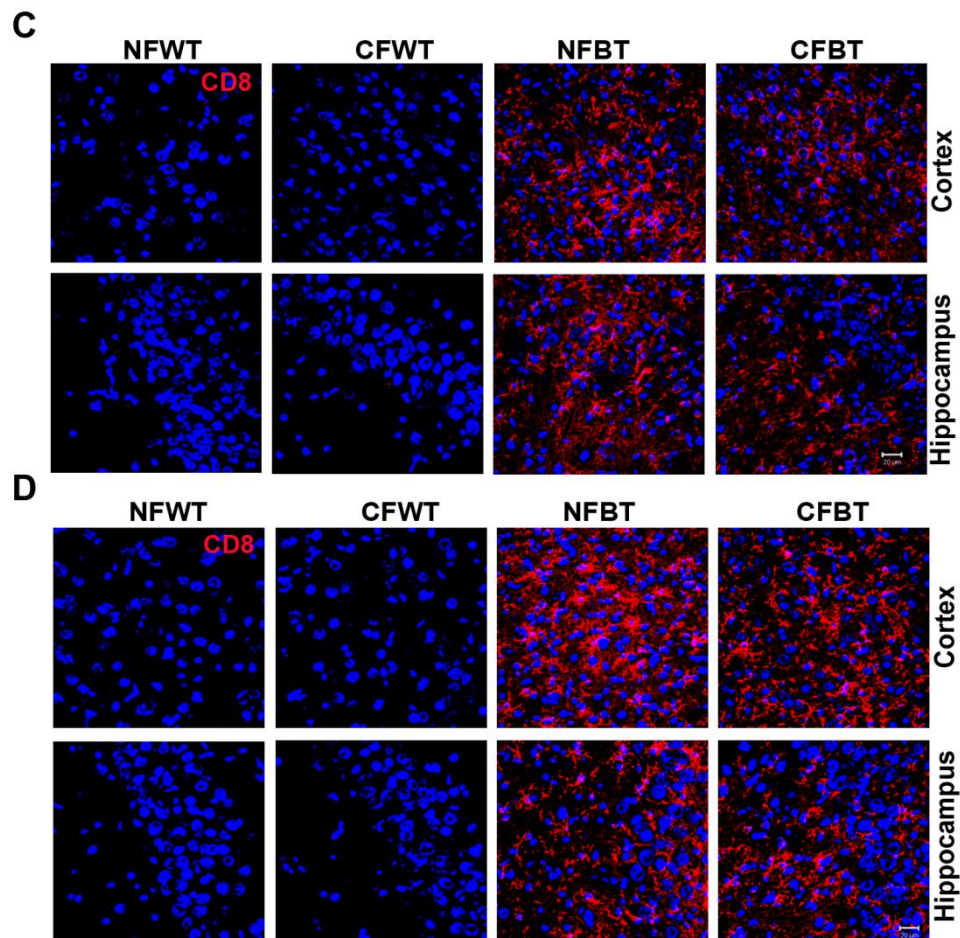
Figure 5.7: Peripheral cell infiltration in curcumin-treated p25Tg mice

Representative confocal images from the cortical (layer 2/3) (top panels) and hippocampal (CA3 region) (bottom panels) regions of the brain sections from p25Tg mice with normal feed (NFBT), p25Tg mice with curcumin feed (CFBT), respective age-matched WT mice with normal feed (NFWT) and WT mice with curcumin feed (CFWT) (n=3). Immunofluorescence staining was performed using anti-CD4 (red) (**A:** 4-week and **B:** 12-week) and anti-CD8 (red) (**C:** 4-week and **D:** 12-week) antibodies and nuclei were stained with DAPI (blue). Scale bars represent 20 μm.

5.3.5 Curcumin blocks p25-mediated neuroinflammatory cascade in p25Tg mice

Chapter 4 results concluded that cPLA2 upregulation and the subsequent LPC production are the crucial events behind p25-mediated neuroinflammation and neurodegeneration. Hence, experiments were next focused on analyzing the role of curcumin on the p25-mediated increase in cPLA2 expression and LPC production. Results from Western blot analyses using anti-cPLA2 antibody revealed approximately 3-fold reductions in p25-mediated cPLA2 upregulation in both the 4 and 12-week induced curcumin-treated p25Tg mice (Figure 5.8A top panel and B). In addition, cPLA2 activity was also significantly reduced in curcumin-treated p25Tg mice brain samples compared to the non-treated samples (Figure 5.8D). Furthermore, mass spectrometry analyses results specified that p25-mediated LPC production was markedly decreased by curcumin treatment in p25Tg mice (Figure 5.8E). Recently, it was shown that cPLA2 expression and activation were regulated by NF-κB (Cheng et al., 2009; Lee et al., 2010; Lee et al., 2011). The activation of NF-κB (transcription factor), the master switch of the inflammatory cascade, plays a critical role in the pathogenesis of many chronic inflammatory diseases (Salminen et al., 2008). Western blot results from this chapter determined that NF-κB expression levels were augmented during p25 overexpression in p25Tg mice. In addition, results further identified that curcumin effectively abolished the p25 overexpression-mediated NF-κB upregulation in both the 4 and 12-week induced p25Tg mice brain samples (Figure 5.8A second panel and C). Hence, the results collectively indicated that p25-mediated increases in cPLA2 levels/activity and LPC production via NF-κB upregulation were effectively reversed by curcumin treatment in p25Tg mice.
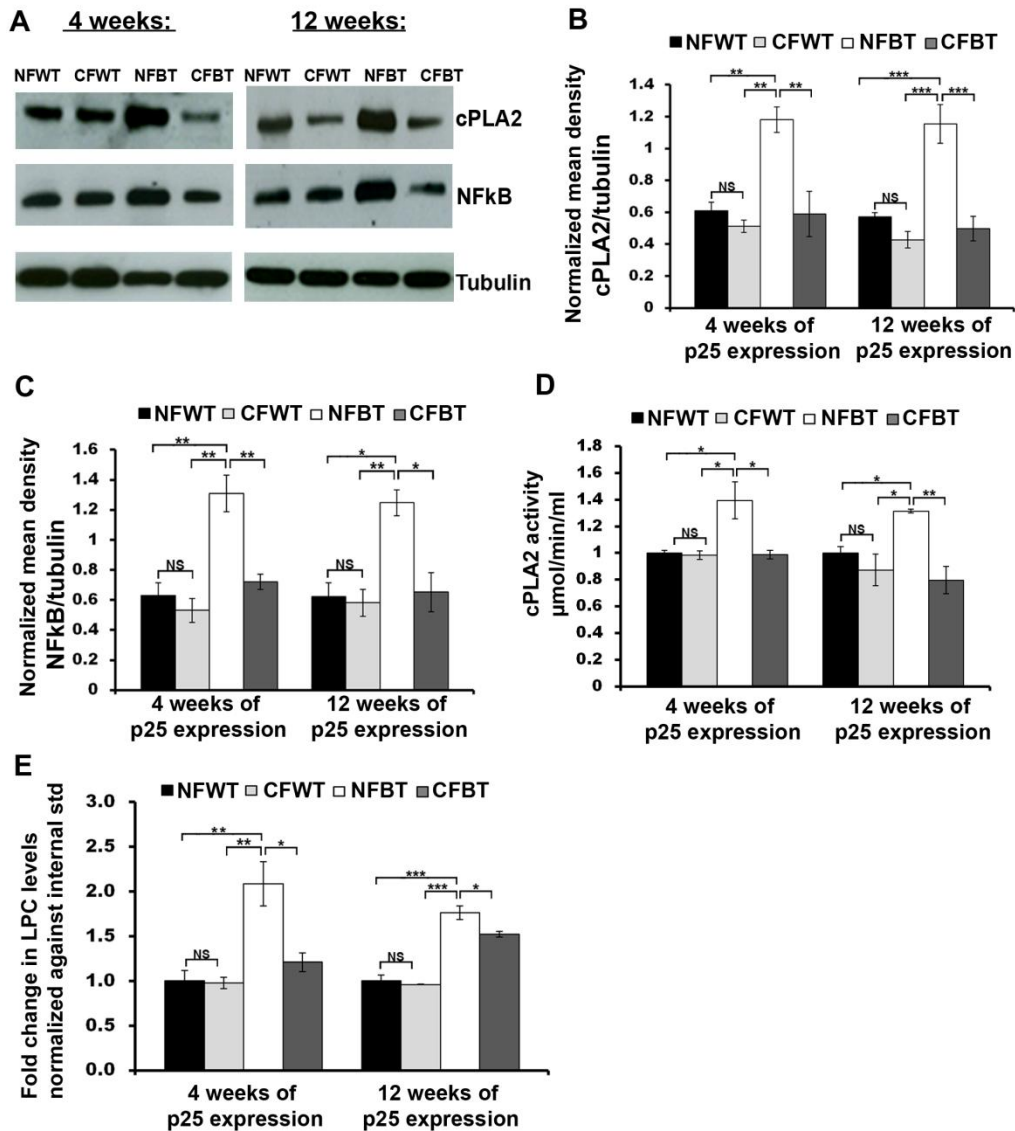
Figure 5.8: Curcumin effectively blocks the cPLA2/LPC pathway in p25Tg mice

(**A**) Immunoblots for brain lysates from 4-week (left) and 12-week (right) induced p25Tg mice with normal feed (NFBT), p25Tg mice with curcumin feed (CFBT), respective age-matched WT mice with normal feed (NFWT) and WT mice with curcumin feed (CFWT) (n=3) using anti-cPLA2 (top panel) and anti-NF-κB (second panel) and anti-tubulin (bottom panel) antibodies. Quantification of (**B**) cPLA2 immunoblots and (**C**) NF-κB immunoblots were performed by densitometric scanning. (**D**) cPLA2 activity assay results for the mice groups same as in **A**. (**E**) Mass spectrometric analyses results for lysophosphatidylcholine (LPC) levels in the forebrain samples from the mice groups same as in **A** (*** p-value < 0.001, ** p-value < 0.01, * p-value < 0.05 and NS p-value > 0.05) (one-way ANOVA followed by post-hoc tukey's test). Error bars indicate ± s.e.m.

5.3.6 Curcumin attenuates p25-mediated neurodegenerative pathology in p25Tg mice

To facilitate the investigation of the role of curcumin on p25-medited tau hyperphosphorylation, immunohistochemistry and Western blot analyses were performed using phospho-tau antibodies AT8 and AT100. Results showed that immunostaining intensities for both AT8 (Figure 5.9A and B) and AT100 (Figure 5.10A and B) antibodies were reduced in curcumin-treated p25Tg mice compared to non-treated p25Tg mice. This immunostaining finding was further confirmed by Western blot analyses where approximately 2-fold reductions in AT8 (Figure 5.9C and D) and AT100 levels (Figure 5.10C and D) were observed in curcumin-treated p25Tg mice compared to the non-treated p25Tg mice.
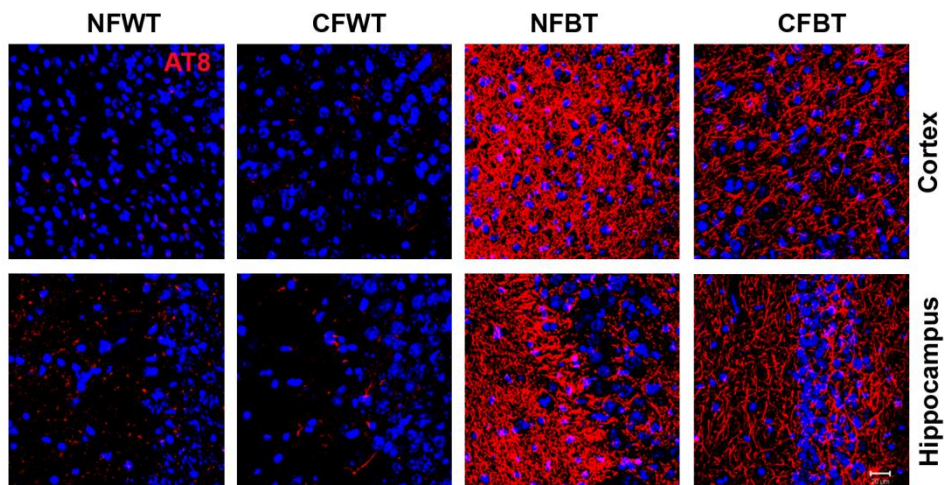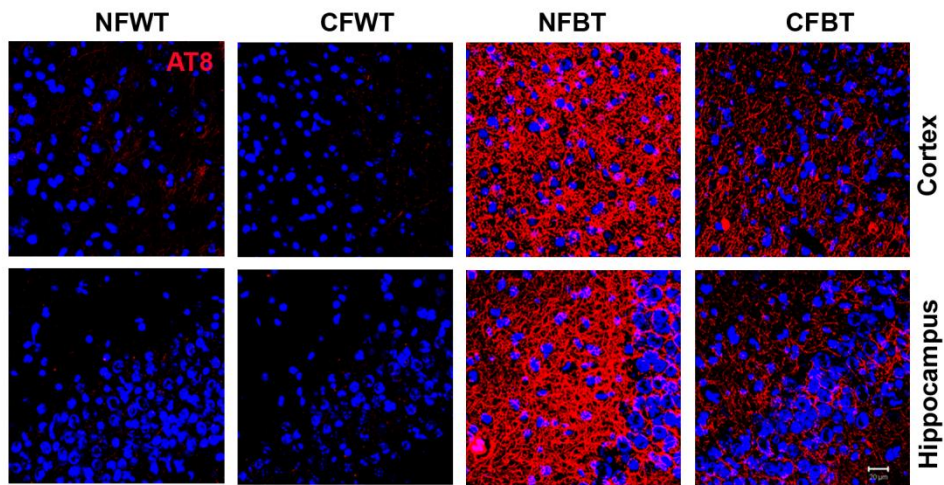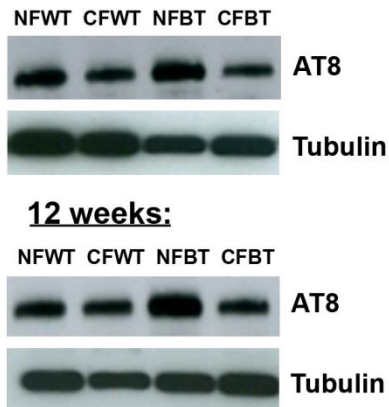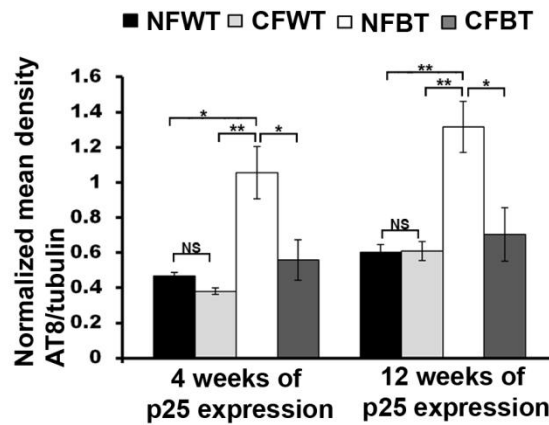
Figure 5.9: Curcumin attenuates p25-mediated tau hyperphosphorylation (AT8) in p25Tg mice

Immunofluorescence staining images from the cortex (layer 2/3) (top panels) and hippocampus (CA3 region) (bottom panels) of the brain sections from (**A**) 4-week and (**B**) 12-week induced p25Tg mice with normal feed (NFBT), p25Tg mice with curcumin feed (CFBT), respective age-matched WT mice with normal feed (NFWT) and WT mice with curcumin feed (CFWT) (n=3) using phospho-tau antibody AT8 (red) and DAPI (blue). (C) Phospho-tau levels were analyzed by immunoblot analyses with brain lysates from 4-week (top panel) and 12-week (bottom panel) induced p25Tg/control mice with/without curcumin treatment using anti-AT8 antibody. (**D**) Quantification of immunoblots in **C** by densitometric scanning (** p-value < 0.01, * p-value < 0.05 and NS p-value > 0.05) (one-way ANOVA followed by post-hoc tukey's test). Error bars indicate ± s.e.m. Scale bars represent 20 μm.

A <u>4 weeks of p25 expression :</u>

NFWT   CFWT   NFBT   CFBT

AT100

Cortex

Hippocampus

B <u>12 weeks of p25 expression</u> :

NFWT   CFWT   NFBT   CFBT

AT100

Cortex

Hippocampus

C   <u>4 weeks:</u>

NFWT CFWT NFBT CFBT

AT100

Tubulin

<u>12 weeks:</u>

NFWT CFWT NFBT CFBT

AT100

Tubulin
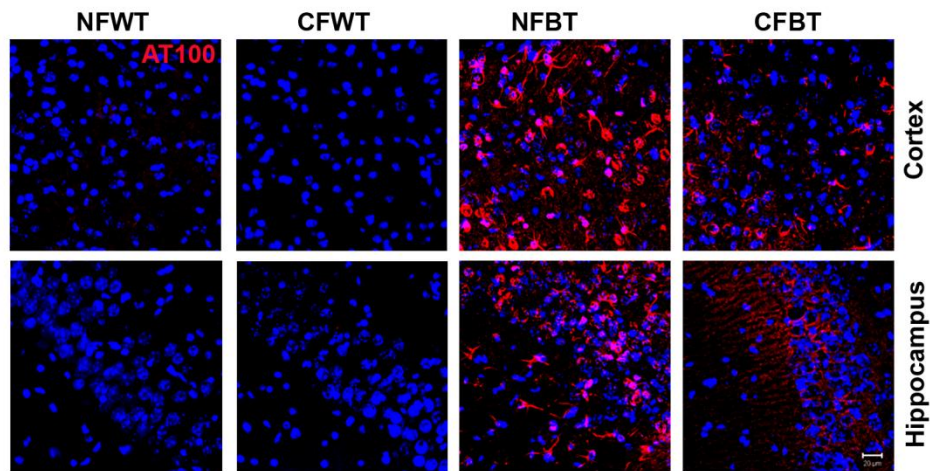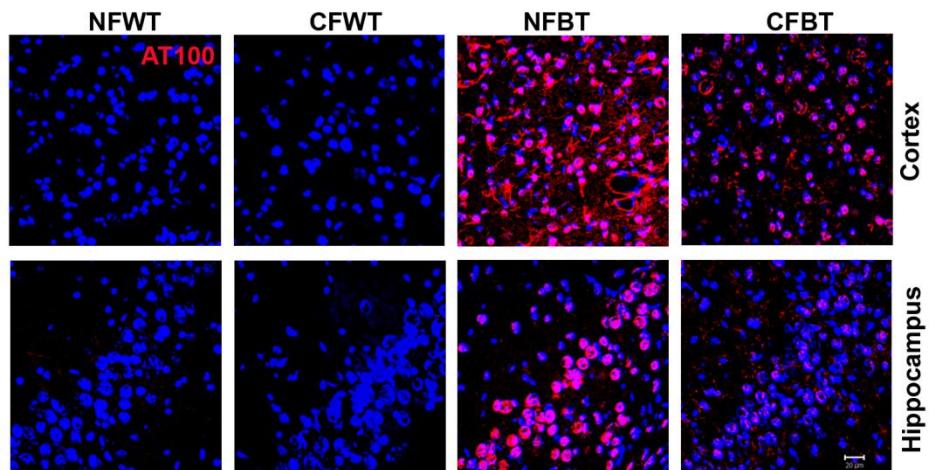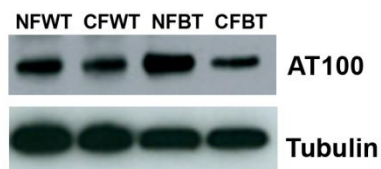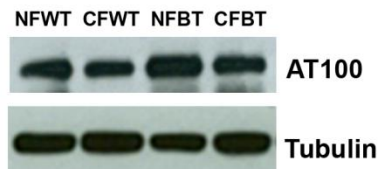
D
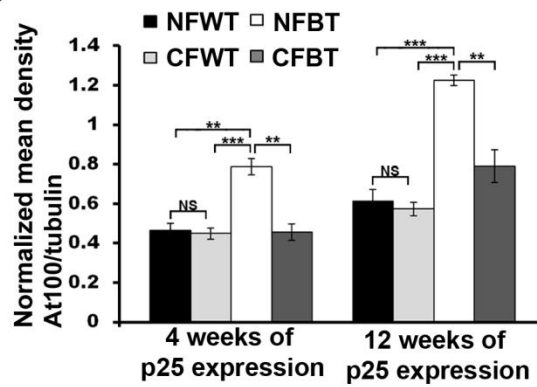
Figure 5.10: Curcumin reduces p25-mediated tau hyperphosphorylation (AT100) in p25Tg mice

Immunofluorescence staining images from cortex (layer 2/3) (top panels) and hippocampus (CA3 region) (bottom panels) of the brain sections from (**A**) 4-week and (**B**) 12-week induced p25Tg mice with normal feed (NFBT), p25Tg mice with curcumin feed (CFBT), respective age-matched WT mice with normal feed (NFWT) and WT mice with curcumin feed (CFWT) (n=3) using phospho-tau antibody AT100 (red). (**C**) Phospho-tau levels were analyzed by immunoblot analyses with brain lysates from 4-week (top panel) and 12-week (bottom panel) induced p25Tg/control mice with/without curcumin treatment using anti-AT100 antibody. (**D**) Quantification of immunoblots in **C** by densitometric scanning (*** p-value < 0.001, ** p-value < 0.01 and NS p-value > 0.05) (one-way ANOVA followed by post-hoc tukey's test). Error bars indicate ± s.e.m. Scale bars represent 20 μm.

Subsequently, immunofluorescence, thioflavin and Bielschowsky silver staining experiments were performed in order to examine whether curcumin treatment had any effects on p25-stimulated amyloid-β accumulation in p25Tg mice. Results identified remarkable reductions in 6E10 and Aβ (1-42) immunostaining in curcumin-treated p25Tg mice compared to the non-treated p25Tg mice (Figure 5.11A and B). Moreover, thioflavin and silver staining results were identical to the immunohistochemical staining findings (Figure 5.11C and D). Together, the results demonstrated that curcumin efficiently abrogated the progression of p25-induced tau hyperphosphorylation and amyloid aggregations in p25Tg mice.

A

NFWT CFWT NFBT CFBT

6E10

Cortex

Hippocampus

20 µm

B

NFWT CFWT NFBT CFBT

Aβ (1-42)

Cortex

Hippocampus

20 µm

C

NFWT CFWT NFBT CFBT

Thioflavin

Cortex

Hippocampus

20 µm

D

NFWT CFWT NFBT CFBT

Silver staining

Cortex

Hippocampus

157
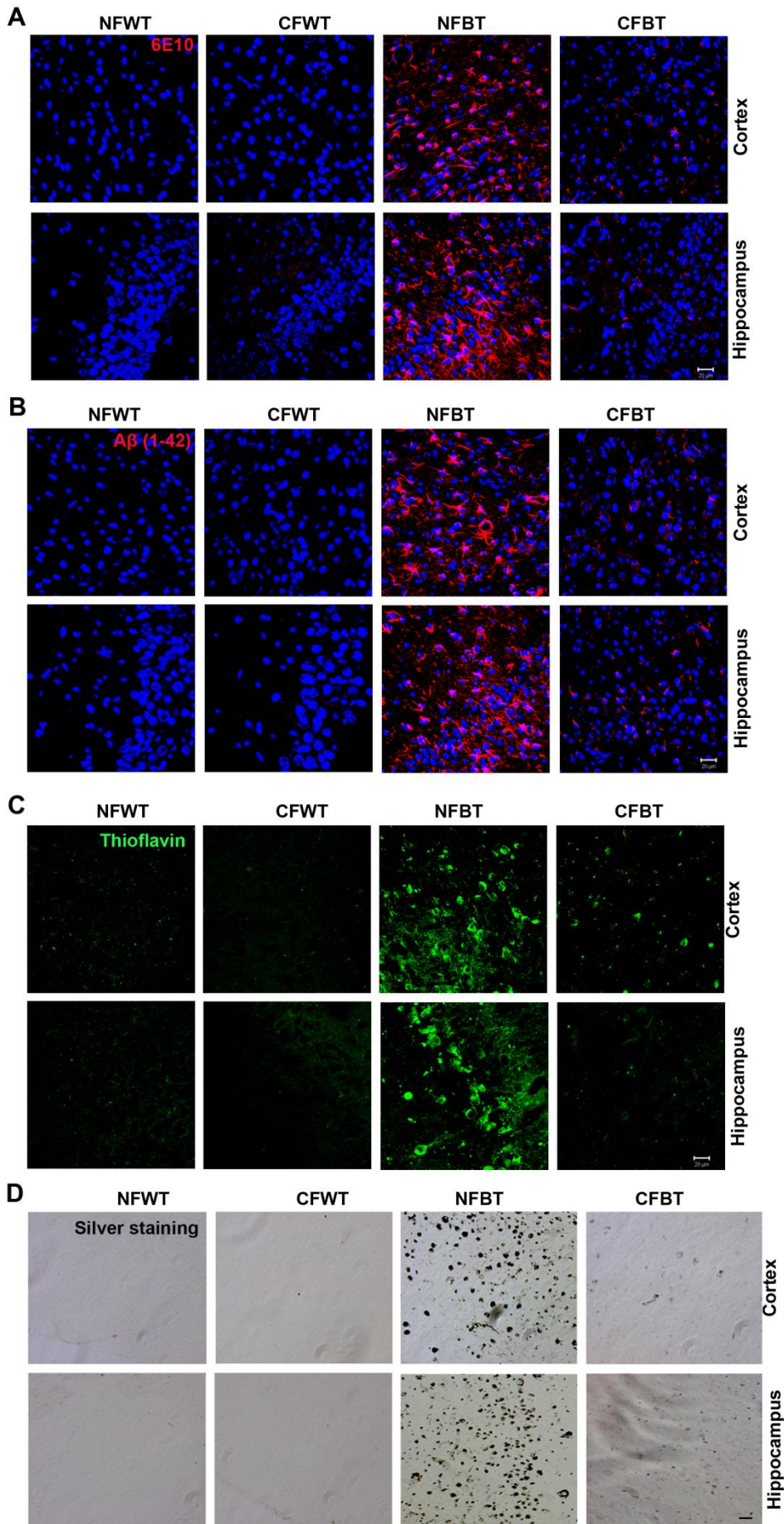
Figure 5.11: Robust amyloid accumulation reduction in curcumin-treated p25Tg mice

Brain sections from the 12-week induced p25Tg mice with normal feed (NFBT), p25Tg mice with curcumin feed (CFBT), respective age-matched WT mice with normal feed (NFWT) and WT mice with curcumin feed (CFWT) (n=3) were immunostained with (**A**) 6E10 (Aβ 1-16) and (**B**) Aβ (1-42) (red). Nuclei were stained with DAPI (blue). (**C**) Thioflavin-S staining and (**D**) Bielschowsky silver staining images from the brain sections of the mice groups same as in **A**. Scale bars represent 20 μm.

5.3.7 Curcumin reduces p25-mediated neuronal apoptosis and neurocognitive deficits in p25Tg mice

It has been shown previously that neuronal apoptosis and forebrain atrophy are significant between 8-12 weeks of p25 expression in p25Tg mice (Cruz et al., 2003). Hence, the next set of experiments was designed to detect whether curcumin has any effect on p25-induced neuronal death. Cleaved caspase-3 immunostaining was performed and results showed a noticeable increase in cleaved caspase-3 immunostaining in 12-week induced p25Tg mice, which were reduced after curcumin treatment (Figure 5.12A).

To further examine whether curcumin treatment has any beneficial role on p25 overexpression-stimulated neurocognitive deficits in p25Tg mice, spatial memory tasks were performed using the radial arm maze. Results confirmed that curcumin-treated p25Tg mice exhibited better performance compared to non-treated p25Tg mice. Working memory errors were reduced almost to normal levels (Figure 5.12B) and reference memory errors decreased robustly in curcumin-treated p25Tg mice (Figure 5.12C). Together, these results demonstrated that curcumin has the capability to restore p25-induced cognitive defects in p25Tg mice.
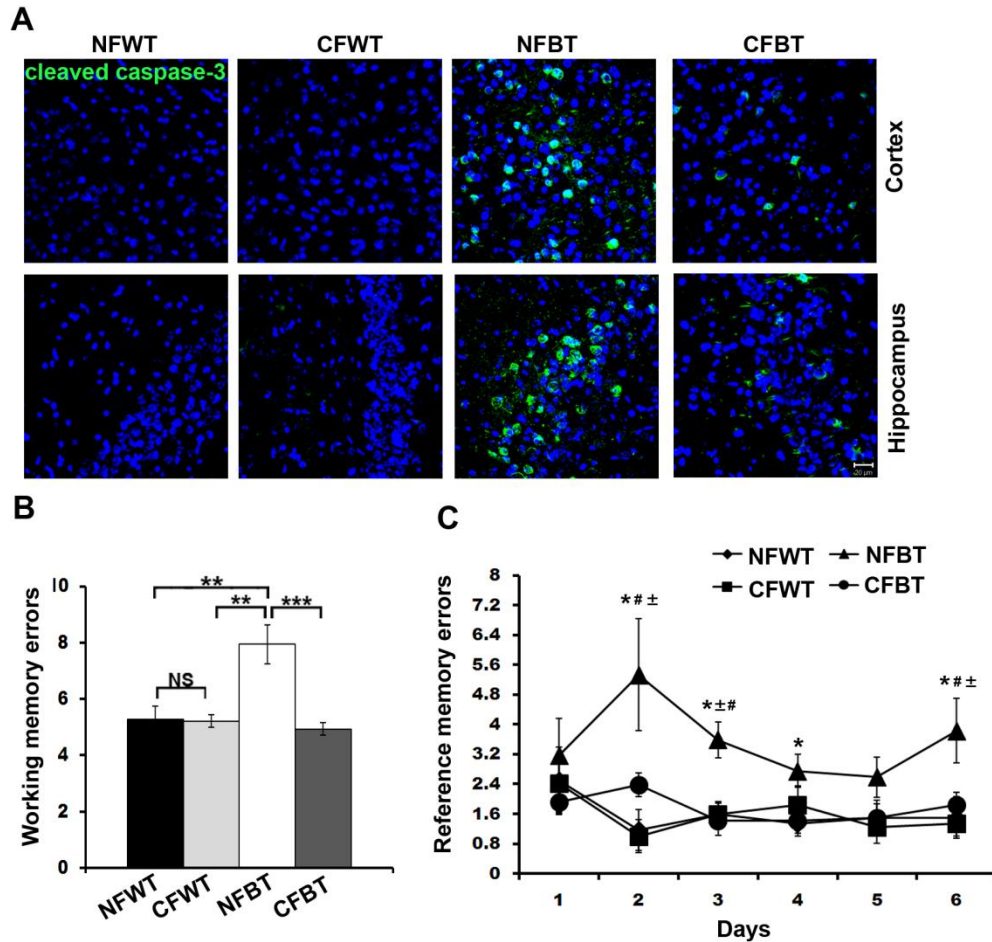
Figure 5.12: Curcumin rescues neuronal apoptosis and ameliorates cognitive deficits in p25Tg mice

(**A**) Immunofluorescence staining images using anti-cleaved caspase-3 antibody (green) and nuclei were stained with DAPI (blue) (n=3). Scale bars represent 20 μm. Eight-arm radial maze performance was analyzed for 12-week induced NFBT (n=5), CFBT (n=6), NFWT (n=5) and CFWT (n=6) mice. (**B**) Working memory errors (average of 10 sessions) (** p-value < 0.01) (one-way ANOVA followed by post-hoc tukey's test) and (**C**) reference memory errors (the average of sessions per day (10 sessions in 6 days)) (* p-value < 0.05 compared to NFWT mice, [#] p-value < 0.05 compared to CFWT mice and [±] p-value < 0.05 compared to CFBT mice) (repeated measures ANOVA followed by post hoc tukey's test). Error bars indicate ± s.e.m.

5.4 Discussion

Results from Chapter 3 and Chapter 4 facilitated the elucidation of the actual mechanism behind early changes in p25-mediated development of neurodegeneration where p25 overexpression induced neuroinflammation and triggered neurodegeneration via cPLA2 upregulation and LPC production. In addition, results from *in vitro* studies clearly demonstrated that the inhibition of early events of neuroinflammation could reverse the progression of p25-mediated neuropathology. Hence, the obvious extension of this study is to carry out *in vivo* investigation using p25Tg mice to explore the effects of inhibiting p25-mediated inflammatory triggers on the progression of the later events of neurodegeneration. To achieve this essential objective, p25Tg mice were treated with naturally available anti-inflammatory agent, curcumin, and results from 4-week treatment of curcumin in p25Tg mice showed an obvious reduction in the major events of p25-mediated inflammation. In particular, curcumin efficiently reduced p25 overexpression-induced astrocyte activation, chemokine/cytokine release, cPLA2 upregulation and LPC production. Moreover, results from curcumin-treated 12-week induced p25Tg mice revealed that the curcumin-mediated inhibition of neuroinflammation reversed the progression of p25-induced neurodegenerative changes including tau and amyloid pathology and rescued neurocognitive deficits.

5.4.1 Overview of therapeutic properties of curcumin

To date, there is no effective approach to treat neurodegenerative diseases including AD, using anti-inflammatory drugs (Imbimbo, 2009). Although some epidemiological studies have suggested that the use of nonsteroidal anti-inflammatory drugs (NSAIDs) could reduce AD incidence (McGeer et al., 1996), there have been numerous failures in clinical trials with NSAIDs in AD/MCI patient cohorts (Aisen et al., 2003; Pasqualetti et al., 2009). NSAIDs exert their anti-inflammatory properties through the inhibition of COX-2 (Masferrer et al., 1996). COX-2 is an inducible form of cyclooxygenase (COX), which catalyzes the initial step in the synthesis of pro-inflammatory arachidonic acid metabolites including prostaglandins (O'Banion, 1999). Although studies have suggested that COX-2 activity is upregulated in AD

brain and may contribute to the development of pathogenesis of AD (Ho et al., 2001), multiple failures of clinical trials with COX-2 inhibitors in human AD/MCI patients have brought up doubts about the involvement of COX-2 in Alzheimer's disease (Imbimbo, 2009). Moreover, studies indicated that these NSAIDs may be effective only in normal brains to prevent the production of Aβ (1-42) and may not be effective in AD/MCI patients where Aβ deposition have already begun (Imbimbo, 2009). In addition, long term use of NSAIDs may cause adverse side effects like gastrointestinal, cardiovascular and kidney toxicity (Armstrong and Blower, 1987; Al-Saeed, 2011).

Thus, there is a need for more studies to investigate potential for clinical use of natural compounds that do not overtly display severe side effects. One such potential candidate is curcumin (Diferuloylmethane), a natural polyphenolic component of the rhizome of the turmeric (Curcuma longa) plant that grows naturally in southeast Asia (Ammon and Wahl, 1991). Turmeric powder is a spice present in Indian curries and has also been used for thousands of years in Indian and Chinese medicine (Prasad and Aggarwal, 2011). Curcumin is well-known for its antioxidant, anti-arthritic, anti-ischemic, anti-amyloid, anti-inflammatory and anti-oncogenic properties (Ammon and Wahl, 1991; Menon and Sudheer, 2007; Mishra and Palanivelu, 2008; Sa and Das, 2008; Monroy et al., 2013). Clinical trials with curcumin for many inflammation-associated diseases including ulcerative colitis, suggested that the use of curcumin is relatively safe and even in larger quantities does not cause any severe side effects to humans (Hanai et al., 2006). Moreover, curcumin exerts beneficial effects in many diseases including cancer (Basnet and Skalko-Basnet, 2011), diabetes, atherosclerosis (Jagtap et al., 2009), arthritis (Chandran and Goel, ; Funk et al., 2006), stroke, peripheral neuropathy, inflammatory bowel, and brain trauma (Aggarwal et al., 2007; Begum et al., 2008).

However, the major limitation in the use of curcumin for treatment of neurodegenerative diseases is the low bioavailability of curcumin due to its low solubility in water and poor oral adsorption (Anand et al., 2007). Pharmacokinetic studies of curcumin showed that after administration, curcumin rapidly biotransformed into curcumin sulfate and curcumin glucuronide (Pan et al., 1999). Curcumin was also reduced to an unconjugated

active metabolite tetrahydrocurcumin. Moreover, evidence suggested that curcumin is able to cross the BBB mostly in unconjugated form. However, unconjugated curcumin is highly unstable with a shorter half-life and hence goes mostly undetected in clinical trials with regular unformulated curcumin (Baum et al., 2008). Numerous approaches have been undertaken to improve the bioavailability of curcumin and some of them have been successful. The laboratory of Sally Frautschy in UCLA has formulated a novel curcumin with solid lipid curcumin particle (SLCP) preparation, called "LONGVIDA". Studies with this new formulation showed increased concentration of curcumin in plasma as well as in brain compared to unformulated curcumin (Begum et al., 2008; Gota et al., 2010; Dadhaniya et al., 2011). A study with chronic administration of SLCP curcumin (4 months, 500-2000 ppm) to an AD mouse model (APPsw Tg2576) detected significant levels of unconjugated curcumin in plasma ((parent curcumin-0.095-0.465 μM) and (tetrahydrocurcumin-0.023-0.115 μM)) as well as in brain ((parent curcumin-1.276-1.428 μM) and (tetrahydrocurcumin-0.264-0.143 μM)) (Begum et al., 2008). In healthy volunteers, SLCP curcumin administration (650 mg) showed substantial levels of free curcumin in plasma compared to the 95% curcuminoids extracts. This enhanced bioavailability of SLCP curcumin could be either due to increased absorption or due to reduced conversion of free curcumin to conjugated products (Gota et al., 2010). Hence, in this study, p25Tg mice were fed with this special formulation in the form of curcumin supplemented feed pellets (1000 ppm) (SLCP-Longvida) after the induction of p25 expression (withdrawal of doxycycline water 6-week postnatal). Brain samples were collected at early (4-week) as well as late (12-week) time points of p25 expression for various analyses.

5.4.2 Curcumin counteracts p25-mediated neuroinflammation in p25Tg mice

Results from this chapter (Figure 5.2) clearly suggested that GFAP upregulation and astrogliosis were significantly reduced by curcumin treatment in p25Tg mice. It has been shown previously that curcumin reduces astrocytic activation in amyloid-β induced primary astrocytes (Wang et al., 2010), in APPsw mouse model (Lim et al., 2001), a hemiparkinsonian mouse

model (Tripanichkul and Jaroensuppaperch, 2013) and in an AD rat model (Wang et al., 2013). However, the exact mechanism behind this curcumin-mediated inhibition of astrocyte activation has not yet been clearly defined. Results in Chapter 4 identified that p25-induced glial activation was mediated through the upregulation of cPLA2 and LPC production. The results from this chapter (Figure 5.8) showed that curcumin significantly reduced the cPLA2 levels/activity and also significantly decreased LPC levels. Therefore, this curcumin-mediated reduction of p25-induced cPLA2 upregulation could be the reason behind the inhibition of glial activation in the curcumin-treated p25Tg mice.

The next important question to be answered was how curcumin regulates cPLA2 activity. Of late, it was shown that cPLA2 expression and activation are regulated by NF-κB (Cheng et al., 2009; Lee et al., 2010; Lee et al., 2011). Results from immunoblot analyses using NF-κB (p65) antibody showed that NF-κB expression was significantly elevated in p25Tg mice; however, this p25-mediated elevated NF-κB expression was reduced to WT/control levels by curcumin treatment in p25Tg mice (Figure 5.8). Inhibition of NF-κB is believed to be a central pathway behind the anti-inflammatory effects of curcumin (Jin et al., 2007). NF-κB (transcription factor), is thought to be a master switch controlling the inflammatory cascade and play a critical role in the inflammatory pathogenesis of many chronic diseases (Salminen et al., 2008). In 1995, Singh and Aggarwal reported this curcumin-mediated suppression of NF-κB (Singh and Aggarwal, 1995). It has previously been shown that curcumin blocked NF-κB activation via its inhibitory effects on IκB kinase, which subsequently resulted in the inhibition of the *NF-κB* gene products (Aggarwal and Sung, 2009).

Results from chemokine/cytokine RT-PCR analyses clearly demonstrated that curcumin treatment selectively downregulated pro-inflammatory chemokines/cytokines such as MIP-1α, TNF-α and IL-1β expression levels in p25Tg mice. In contrast, TGF-β levels were found unaltered between the two groups (Figure 5.3). TGF-β, an anti-inflammatory cytokine, was found to be elevated in AD as a regulatory response to maintain homeostasis in brain (Chao et al., 1994; Rota et al., 2006). Moreover, studies reported that TGF-β

was involved in the regulation of alternate activation of microglia which could be a protective adaption against chronic inflammation (Zhou et al., 2012). A number of studies have already reported that curcumin negatively regulated pro-inflammatory cytokine production especially that of TNF-α (Paul et al., 2006; Jain et al., 2009). Studies have also indicated that curcumin mediated this function through the inhibition of various inflammatory signaling pathways including NF-κB and Janus kinase-STAT (Kim et al., 2003; Park et al., 2012).

The main sources for chemokines/cytokines production are activated astrocytes and microglia. In light of this, experiments were then focused on analyzing the effect of curcumin on p25-mediated microglial activation. Different markers for microglial activation were used in immunostaining analyses and results demonstrated that the total activation of microglia was effectively reduced in curcumin-treated 4-week induced groups compared to non-treated groups. However, this curcumin-induced reduction in microglial activation was only moderate in 12-week induced curcumin-treated groups (Figure 5.5). Similarly, Iba-1 and F4/80 staining results were found identical to the Cd11b results (data not shown). In contrast, pro-inflammatory cytokines/chemokines expression levels were dramatically reduced in 12 induced curcumin-treated p25Tg mice (Figure 5.3). Moreover, CNS infiltration of peripheral immune cells was not significantly reduced in 12-week induced curcumin-treated group compared to the non-treated p25Tg mice (Figure 5.7). Hence, these results collectively suggested that curcumin selectively targeted the release of pro-inflammatory mediators without affecting microgliosis or CNS infiltration rate of peripherally-derived immune cells especially at the late time point of 12-week induction of p25 expression in p25Tg mice. This finding is supported by evidence from a previous study where curcumin effectively suppressed microglial activation in neuronal layers, but failed to prevent microgliosis near amyloid deposits. Furthermore, it has been suggested that curcumin might induce microglial-mediated phagocytosis of amyloid (Lim et al., 2001).

In general, resident microglial cells become activated during the early phase of neuroinflammation and this is followed by the recruitment of peripherally derived macrophages. In the later stage, these macrophages are subsequently transformed into microglial cells (Krause and Muller, 2010). In addition, studies also suggested that these newly recruited microglial cells have increased phagocytic ability compared to the intrinsic microglia (Majumdar et al., 2007). However, the phagocytic ability of this newly recruited microglia may be dampened by the expression of pro-inflammatory cytokines especially TNF-α (Koenigsknecht-Talboo and Landreth, 2005). It has also been demonstrated previously that TGF-β expression might promote the microglial-mediated clearance of Aβ (Wyss-Coray et al., 2001). Hence, results from this chapter and previous evidence indicated that curcumin treatment might inhibit the early activation of microglial cells that were committed to an inflammatory response in 4-week induced p25Tg mice via the regulation of NF-κB signaling pathways. On the other hand, curcumin facilitated the later recruitment and activation of peripherally-derived macrophages/leukocytes in 12-week induced p25Tg mice by regulating the pro- and anti-inflammatory cytokines signal mechanisms (Jobin et al., 1999; Koenigsknecht-Talboo and Landreth, 2005; Bisht et al., 2009). Moreover, this curcumin-mediated temporal regulation of microglial activation and subsequent CNS infiltration of immune cells resulted in the reduction of detrimental pro-inflammatory response and at the same time ameliorated amyloid pathology in p25Tg mice.

In addition, p25-induced upregulation of tissue plasminogen activator (tPA) was completely abolished by curcumin in both 4 and 12-week induced p25Tg mice (Figure 5.6). It has been reported previously that tPA is a potent stimulator of the conversion of microglial cells into a pro-inflammatory phenotype (Siao and Tsirka, 2002; Pineda et al., 2012). Thus, these results demonstrated that curcumin selectively changed the pro-inflammatory state of microglia into a beneficial anti-inflammatory phenotype via multiple ways. A recent report supported our finding and their microarray results indicated that curcumin can trigger a change in microglial phenotype from pro-inflammatory to anti-inflammatory with neuroprotective properties (Karlstetter et al., 2011). Furthermore, their transcriptomic analyses identified that curcumin inhibited

the gene expression of *NF-κB, STAT3* and *complement factor 3* which are main factors inducing the conversion of microglial cells to the pro-inflammatory state. In addition, curcumin was found to increase the gene expression of *peroxisome proliferator-activated receptor-gamma (PPARγ),* a primary inhibitor of the pro-inflammatory activation of the microglia (Karlstetter et al., 2011).

5.4.3 Curcumin attenuates p25-induced tau and amyloid pathology in p25Tg mice

Hyperphosphorylation of tau and amyloid accumulations are prominent events in p25-mediated neurodegeneration of p25Tg mice (Chapter 3 results and (Cruz et al., 2003; Cruz et al., 2006)). However, significant reduction in tau phosphorylation and clearance of amyloid accumulations were observed after treatment with curcumin in p25Tg mice (Figure 5.9, 5.10 and 5.11). Interestingly, these observations strongly supported the hypothesis of this study that early inhibition of neuroinflammation can slow down the progression of later pathological events. The finding of curcumin-mediated reduction in tau pathology in p25Tg mice was supported by a recent study using 3xTg-AD mice. Oral administration of 500 ppm curcumin decreased tau phosphorylation and mice showed improvement in Y-maze performance (Ma et al., 2009). In another study, approximately 80% reduction in tau phosphorylation was observed in curcumin-treated Tg2576 AD mice (Shytle et al., 2012). In addition, significant reductions in Cdk5 hyperactivation were observed after curcumin treatment in p25Tg mice (Figure 5.4). Hence, this suggested that curcumin-mediated reduction of neurodegenerative pathology may be achieved via multiple diverse mechanisms. Although, it has already been reported that curcumin inhibits GSK-3β (Bustanji et al., 2009), there was no previous evidence concerning curcumin-mediated inhibition of Cdk5 hyperactivity. Hence, further investigation is required to fully understand the actual mechanism behind the curcumin-mediated specific reduction in Cdk5 hyperactivity. However, previous reports showed that there was a feed-forward loop mechanism between amyloid and p25/Cdk5 hyperactivity (Lee et al., 2000; Lee et al., 2003; Cruz et al., 2006). Thus, curcumin-mediated reduction in neurotoxicity including oxidative stress and amyloid

accumulation might reduce the feed-forward mechanism-based upregulation of Cdk5 activity in p25Tg mice.

Numerous studies have determined that curcumin was a potent anti-amyloidogenic agent that inhibited Aβ aggregation, conferring protecting against Aβ-induced cell death (Yang et al., 2005; Zhang et al., 2010). Curcumin has been shown to reduce the amyloid-β burden in Tg2576 AD mice (Lim et al., 2001). Moreover, intravenous administration of curcumin cleared senile plaques in APPswe/PS1dE9 mice (Garcia-Alloza et al., 2007). In another study, Aβ infusion-induced cognitive deficits were corrected by curcumin treatment in Sprague-Dawley rats (Frautschy et al., 2001). In addition, it was reported recently that curcumin reduced amyloid production via inhibition of the BACE expression and activity (Shimmyo et al., 2008). Studies are now focused on finding out the mechanism behind the curcumin-mediated clearance of amyloid aggregations and it has been reported that curcumin cleared amyloid aggregates via the induction of phagocytosis by brain macrophages and microglia. It has been found that curcumin even at low doses effectively stimulates robust microglial phagocytosis both *in vitro* and *in vivo* (Cole et al., 2007). In addition, it has been reported that curcumin cleared amyloid burden via monocytic gene expression regulation (Gagliardi et al., 2011). In general, peripheral blood mononuclear cells (PBMC) from AD patients were found to be defective in Aβ phagocytosis (Cashman et al., 2008). However, curcumin treatment was shown to restore the amyloid phagocytic ability of AD PBMCs via the upregulation of some of the key genes that regulate macrophage activation including *TLRs* (Toll-like receptors) and *MGAT3* (β-1, 4-mannosyl-glycoprotein-4-β-N-acetylglucosaminyltransferase) (Gagliardi et al., 2011; Cashman et al., 2012). Therefore, based on evidences from previous reports, one can hypothesize that curcumin enhanced the phagocytic ability of p25-induced brain recruited PBMCs to clear the p25-mediated amyloid accumulations. However, more studies are needed to further support this theory. Thus, the results collectively suggested that curcumin-mediated selective activation of microglia/monocytes into a beneficial anti-inflammatory phenotype would be a valuable therapeutic tool to fight against the neuroinflammation-associated neurodegenerative diseases.

5.4.4 Curcumin rescues against p25-induced apoptosis and restores neurocognitive abilities in p25Tg mice

Results from immunostaining with cleaved caspase-3 antibody showed that p25-mediated neuronal apoptosis was reduced after curcumin treatment in p25Tg mice. In addition, radial arm maze task results clearly demonstrated that the p25-induced spatial memory deficits were corrected almost back to normal by curcumin treatment in p25Tg mice (Figure 5.12). Curcumin-mediated reductions in the p25-mediated pathologies including aberrant glial activation, upregulated pro-inflammatory cytokines especially TNF-α, and intraneuronal tau/amyloid accumulations could be the reasons behind this curcumin-mediated reversal of neuronal apoptosis and cognitive deficits. Moreover, previous studies reported that curcumin, a potent anti-oxidant prevented neuronal apoptosis through reduction in ROS production and oxidative damage (Zhu et al., 2004). Collectively, results confirmed that curcumin offered neuroprotection against p25-mediated neurotoxicity via its anti-inflammatory, anti-amyloidogenic and anti-oxidant properties.

5.5 Summary

The results from this chapter collectively showed that curcumin, a potent natural anti-inflammatory agent, effectively counteracted the p25-mediated glial activation and pro-inflammatory chemokines/cytokines production in p25Tg mice. In addition, curcumin significantly reduced p25/Cdk5 hyperactivation-mediated tau hyperphosphorylation, amyloid accumulations, neuronal apoptosis and neurocognitive deficits. Thus, results from this chapter strongly suggested that curcumin, a multipotent natural compound, could be a valuable tool to prevent the progression of neuroinflammation-associated neurodegenerative diseases including AD.

CHAPTER 6

CHAPTER 6: Final discussion, conclusions and future work

6.1 Discussion and conclusions

Although there are numerous AD intervention strategies currently being investigated, none of them have effectively translated into disease modification and clinical success. To date, drugs marketed for the treatment of AD are acetylcholinesterase (AChE) inhibitors (donepezil, galantamine, rivastigmine) and the glutamate receptor antagonist (memantine) (Noetzli and Eap, 2013). Despite this, these treatment strategies in AD do not have neuroprotective properties and even symptomatic relief is only temporary. Moreover, recent studies suggested that cholinergic deficit occur fairly late in the disease (Frolich, 2002), while it has also been acknowledged that to treat AD, one must target the early-stage pathological changes and protect neurons from irreversible damage (Sperling et al., 2011). Although epidemiological evidence suggested that NSAIDs have beneficial effects in AD treatment (McGeer et al., 1996), increasing failures in clinical trials for AD with NSAIDs clearly indicate that they are either not effective in late stage patients or not able to combat the multifactorial nature of AD pathology (Aisen et al., 2003; Imbimbo, 2009). Moreover, recent failures reported in clinical trials with anti-Aβ immunization strategies have brought the Aβ hypothesis into some question. In a recent clinical trial, bapineuzimab (initially co-developed by Elan/Wyeth and then acquired by Johnson & Johnson/Pfizer) has been reported to be effective in decreasing the amyloid burden. However, primary clinical endpoints (improved cognitive ability) were not met in the phase II clinical trial (Salloway et al., 2009). Hence, it is evident that a better understanding of the initiation and progression of AD, a complex and multifactorial syndrome, is needed to allow future treatments to be developed with novel drug targets. Moreover, finding a multi-target approach that can hit the early events of neuropathology may be more important in AD therapeutics (Figure 6.1). Hence, targeting the pathological hallmarks such as amyloid-β and tau may not be an effective strategy due to its late timeline of development.
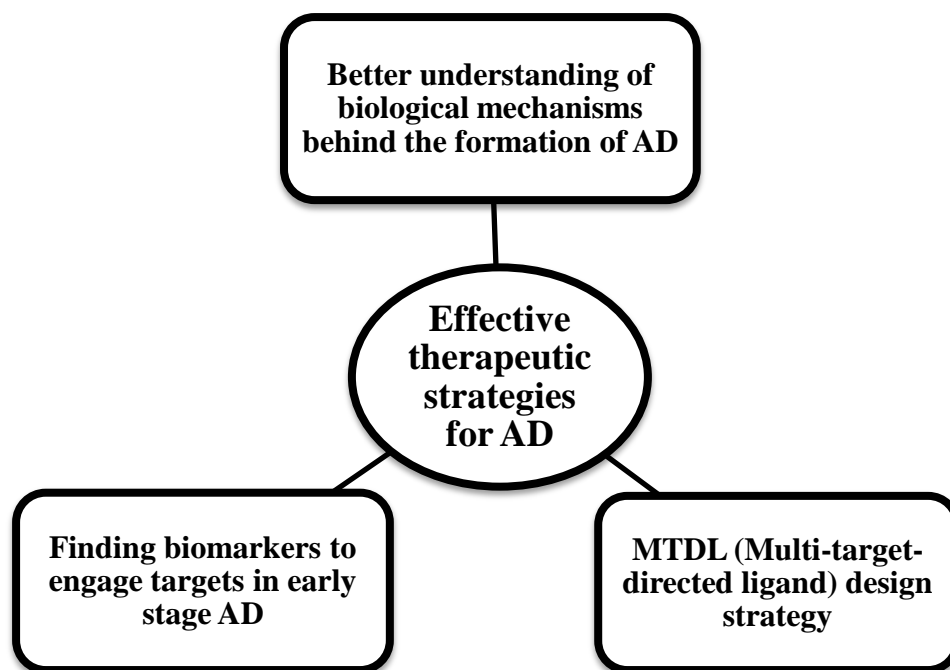
Figure 6.1: Schematic description showing key points behind the development of effective drugs to treat AD

The Alzheimer's Disease Research Summit 2012 strongly recommended the use of experimental models that better simulate the multifactorial nature of AD to more accurately identify disease modifying pathways and to assess effective treatment strategies (National Institute on Aging, 2013). Although there are numerous available AD mouse models based on genetic mutations found in AD patients (Hall and Roberson, 2012), not all the models develop pathological features reminiscent of AD. Some models develop amyloid plaques without tau hyperphosphorylation and some exhibit only tau pathology (Duff and Suleman, 2004). Very few models exist that recapitulate most of the AD pathologic features and one such mouse model is the p25 transgenic mouse model which exhibits robust astrogliosis, substantial tau hyperphosphorylation, intraneuronal amyloid accumulations, and extensive neuronal loss especially in the forebrain. Moreover, these mice exhibit cognitive defects in addition to the pathology (Cruz et al., 2003; Fischer et al., 2005; Cruz et al., 2006; Sundaram et al., 2013). Deregulation of Cdk5 activity has previously been shown to be a contributory factor in the pathogenesis of various neurological disorders such as AD, PD and ALS (Nguyen et al., 2001;

Lee and Tsai, 2003; Smith et al., 2006). Although there have been some conflicting data about the elevation of p25 levels in post-mortem samples of AD patients (Tandon et al., 2003), subsequent studies have confirmed the occurrence of increased p25 expression and altered Cdk5 activity in the human AD cases (Patrick et al., 1999; Tseng et al., 2002). Mechanistically, abnormal calcium influx-induced, calpain-mediated p25 production and subsequent Cdk5 deregulation results in the hyperphosphorylation of microtubule protein tau, neurofilaments and amyloid precursor protein (APP), which ultimately leads to the production of NFTs and amyloid accumulations (Patrick et al., 1999; Ahlijanian et al., 2000; Noble et al., 2003). Although there is considerable evidence to support the role of Cdk5 in neurodegeneration, there has not been a clear demonstration for the actual mechanism behind the initiation of p25/Cdk5 hyperactivation-mediated neuroinflammation and its role in the progression of neurodegeneration. Finding out this piece of puzzle will certainly add more value to the field. Hence, this study was designed to investigate p25/Cdk5-mediated neuroinflammatory mechanisms using the CamK2a-p25 inducible transgenic (p25Tg) mice and *in vitro* lentivirus-based overexpression of p25 in cortical neurons.

Experiments were initially focused to gain more information about the onset of major inflammatory events like astrogliosis, microgliosis and chemokines/cytokines production in p25Tg mice. Results from multi-platform experiments such as immunohistochemistry, Western blots and RT-PCR clearly indicated that astrogliosis was an early event in p25-mediated neuroinflammation where GFAP expression and pro-inflammatory chemokines/cytokines such as TNF-α, MIP-1α, TGF-β and IL-1β levels were significantly elevated even in 1 week induced p25Tg mice (Figures 3.1 and 3.2). In addition, the finding of astrogliosis preceding microgliosis in the p25-mediated inflammatory paradigm suggested that microglial activation may possibly be dependent on chemokine/cytokine release by activated astrocytes (Figure 3.3). Moreover, results showed that this early event of astrogliosis occurred prior to any neuropathological changes such as tau and amyloid pathology (Figure 3.5). Hence, results collectively suggested that targeting astrocytes could be a potential early intervention strategy for AD therapeutics.

For some time, astrocytes were just considered as the "brain glue" and the role of astrocytes during AD progression have not received as much attention as the role of microglia (Miller, 2005; Ralay Ranaivo et al., 2006). Earlier studies indicated that the development of a drug that is able to specifically target glia and reduce inflammation in the brain without weakening the immune system may be extremely valuable in AD therapeutics (Miller, 2005).

Furthermore, immunostaining results in Chapter 3 identified the presence of brain infiltration of peripherally-derived CD4+ and CD8+ T cells in p25Tg mice especially after 4 weeks of induction of p25 expression (Figure 3.4). However, the role and significance of these CNS infiltrating T cells are unclear in these mice. Recent studies demonstrated that leukocytes translocating into the CNS could be detrimental (in multiple sclerosis) or beneficial (in ALS) depending upon the disease state (Chiu et al., 2008; Fletcher et al., 2010). Detection of CNS infiltration of leukocytes in p25Tg mice suggested that further investigation into this field might provide new ways to elucidate the complex mechanisms and consequences of neuroinflammation. Subsequently, results from *in vitro* co-cultures as well as conditioned media transfer systems in Chapter 3 showed that there was a soluble signal secreted by the p25 expressing neurons (via both overexpression and endogenous production) that caused the activation of glial cells (Figures 3.6, 3.7 and 3.8). Together, results in Chapter 3 showed that astrogliosis was a principal event in the p25-mediated neuroinflammation that began very early in the absence of microgliosis, tau and amyloid pathology. Further findings indicated that there was a soluble trigger behind this p25-induced astrocyte activation. Hence, these results have emphasized the importance of further characterization of this soluble trigger and experiments in Chapter 4 aimed to uncover the mechanism behind the production of this soluble trigger.

Results from factor removal experiments and high performance mass spectrometry lipidomics in Chapter 4 identified that lysophosphatidylcholine (LPC) was the soluble lipid signal secreted from the p25 expressing neurons that mediated astrogliosis (Figures 4.1, 4.2, 4.3 and 4.4). Gradual increases in LPC levels from 1 to 12-week expression of p25 in p25Tg mice clearly showed that production of LPC could be a critical event in the initiation and as

well as progression of p25-mediated neuroinflammation (Figure 4.4C). Further characterization using *in vitro* experiments identified the particular LPC species that most effectively induced the astrocyte activation as LPC 18:0 and 18:1 (Figure 4.5). Moreover, this exciting finding is supported by considerable evidence from previous studies where LPC was found to be involved in the regulation of astrocyte activation, T cell migration and transcriptional activation of genes relevant to inflammation (Cieslik et al., 1998; Radu et al., 2004; Sheikh et al., 2009).

Real-time PCR, enzyme activity assays and cPLA2 inhibitor experiments were carried out to trace this pathway back into the neurons and results identified that cytosolic Phospholipase A2 (cPLA2) was the enzyme responsible for this lipid signal production (Figure 4.6). Furthermore, gene silencing experiments indicated that cPLA2 upregulation was crucial for the production of LPC and subsequent astrocyte activation during p25 overexpression (Figures 4.7 and 4.8). cPLA2 expression has been reported previously in neurons and the activation of cPLA2 under normal conditions resulted in the generation of arachidonic acid and lysophospholipids which in turn regulated membrane dynamics, signal transduction and cell proliferation. However, prolonged activation of cPLA2 under pathological conditions may contribute to neurodegeneration via neuronal membrane degradation and overproduction of inflammatory mediators including LPC, platelet-activating factors and 4-hydroxynonenal. Thus, cPLA2 activity must be tightly regulated in order to maintain cellular homeostasis (Katsuki and Okuda, 1995; Farooqui et al., 2006; Sun et al., 2010). Moreover, there are data demonstrating an obvious change in cPLA2 mRNA expression as well as cPLA2 immunoreactivity in the AD brain as compared to age-matched controls (Stephenson et al., 1996; Colangelo et al., 2002).

In addition, it is crucial to find out the link between p25 overexpression and cPLA2 elevation. It has been reported previously that p25/Cdk5 activity may act on nuclear machinery to regulate gene transcription (Patrick et al., 1999; O'Hare et al., 2005; Saito et al., 2007) and recent reports showed that *cPLA2* gene expression can be regulated by the transcription factors p300 and NF-κB (Luo et al., 2006; Lee et al., 2010; Lee et al., 2011). Adding on to that, it was

reported that p25/Cdk5 interacts with CREB1 binding protein (CBP), the co-activator protein for p300, through the binding with C53. Moreover, evidence from various studies have led to a hypothesis that p25/Cdk5 might regulate NF-κB activity via AKT-mediated phosphorylation (Kane et al., 2002; Huang and Chen, 2005; Liu et al., 2008). Furthermore, the hypothesis of Cdk5-mediated regulation of NF-κB activity is further supported by the Western blot results in this thesis where NF-κB expression was noticeably increased in both 4-week and 12-week expression of p25 in p25Tg mice compared to the controls (Figure 5.8). However, further studies would be needed to fully understand the mechanism behind the p25-mediated cPLA2 elevation.

Subsequently, results from Chapter 4 also determined that the inflammatory mediators released during the p25-mediated neuroinflammation might trigger the progression of neuropathological changes including hyperphosphorylation of tau and amyloid production. Of further significance, reducing LPC production by silencing cPLA2 attenuated glial activation and subsequent development of tau and amyloid pathology (Figure 4.9). Previous studies have shown that cPLA2 activity mediated amyloid-β-induced mitochondrial dysfunction and neuronal apoptosis (Kriem et al., 2005; Shelat et al., 2008). Moreover, the pathological breakdown of phosphatidylcholine and production of LPC by cPLA2 could induce neuronal sheath demyelination, axonal degeneration and neuronal apoptosis (Hall, 1972; Jean et al., 2002). In addition, reports have shown the direct effect of LPC on Aβ-induced neuronal apoptosis to be occurring through signal pathways of orphan G protein-coupled receptors (Hall, 1972; Kabarowski et al., 2001; Qin et al., 2009). Hence, this study strongly suggested that cPLA2 activity may be a viable molecular target to halt the progression of neurodegeneration caused by p25/Cdk5 hyperactivation. Indeed, the novel findings from this study will assist the identification of early detection and possible therapeutic targets for various neurodegenerative diseases especially AD. Key findings from Chapter 3 and 4 are summarized in Figure 6.2.
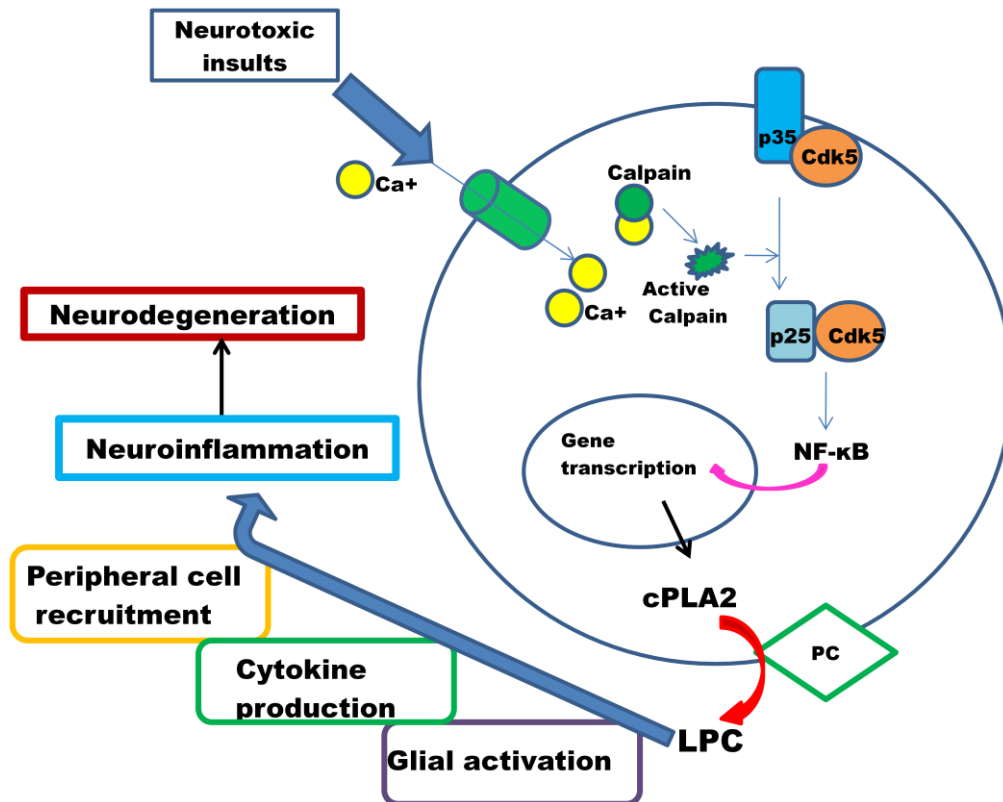
Figure 6.2: Schematic representation of the mechanism behind the p25/Cdk5-mediated neuroinflammation

Neurotoxic insults-induced Ca2$^+$ influx and subsequent intense calpain activation cause Cdk5 hyperactivation via the abnormal production of p25 from p35. Successively, p25/Cdk5 hyperactivation causes increase in cytosolic phospholipase A2 (cPLA2) production/activation which in turn releases extracellular soluble lysophosphatidylcholine (LPC) from phosphatidylcholine (PC). LPC activates astrocytes/microglial cells to release pro-inflammatory cytokines and then causes CD4$^+$ and CD8+ lymphocytes infiltration which are the main indicators for severe neuroinflammation. Subsequently, these inflammatory mediators induce progression of neurodegeneration in neurons expressing p25.

Results from *in vitro* studies in chapter 4 showed that inhibiting early events of neuroinflammation during p25 overexpression could prevent the progression of p25-mediated neuropathology. Therefore, extension of this study using *in vivo* experiments is vital to further support the research in AD therapy development. Moreover, it is important to select a compound that is chronically active against the sustained neuroinflammation and can cross the BBB without any adverse side effects. One such candidate is curcumin, a naturally available multipotent polyphenol present in turmeric, a spice

commonly found in the Indian diet. Various clinical trials with curcumin have been conducted for inflammation-associated diseases and curcumin was found to be effective against cancer, diabetes, stroke, atherosclerosis and brain trauma (Aggarwal et al., 2007; Begum et al., 2008; Jagtap et al., 2009; Basnet and Skalko-Basnet, 2011). Therefore, experiments in Chapter 5 aimed to determine the effects of early intervention of p25-mediated neuroinflammation in the progression of neurodegeneration in p25Tg mice by using a special formulation of curcumin ("LONGVIDA") prepared under a novel SLCP (solid lipid curcumin particle preparation) technology. Studies with this new formulation have shown increased free curcumin levels in plasma as well as in brain in both human and mice models (Begum et al., 2008; Gota et al., 2010; Dadhaniya et al., 2011).

Results from Chapter 5 showed that curcumin attenuated the p25-mediated neuroinflammatory events, in particular astrocyte activation and pro-inflammatory chemokines/cytokines production, in p25Tg mice (Figures 5.2 and 5.3). Results also suggested that the actual mechanism behind this curcumin effect might be through the inhibition of p25-mediated cPLA2 upregulation and LPC production (Figure 5.8). In addition, curcumin efficiently reduced p25-mediated over-production of NF-κB, the master regulator for various inflammatory events including cPLA2 expression (Figure 5.8). Furthermore, experiments were next focused on examining whether this curcumin-mediated attenuation of p25-induced neuroinflammatory triggers has any effect on the neurodegenerative progression in p25Tg mice. Interestingly, there was a marked reduction in tau hyperphosphorylation and amyloid accumulations after curcumin treatment in 12-week induced p25Tg mice (Figures 5.9, 5.10 and 5.11). Curcumin treatment might mediate these effects via multiple ways and should be investigated carefully. This thesis proposed a few hypotheses. Firstly, curcumin might inhibit the neuroinflammation-triggered initiation of neurodegeneration. Secondly, results in Chapter 5 showed that curcumin may act directly at the level of Cdk5 and reduce its hyperactivation (Figure 5.4). Curcumin-mediated reduction in neurotoxicity could lead to the decrease in feed-forward mechanism-based elevation of Cdk5 activity in p25Tg mice. Furthermore, results in Chapter 5

also indicated that curcumin altered the microglia/macrophage phenotype from a pro-inflammatory to an anti-inflammatory state (Figures 5.5, 5.6 and 5.7). Previous studies reported that curcumin clears amyloid burden via the regulation of phagocytic ability of microglia, macrophages and monocytes (Cole et al., 2007; Gagliardi et al., 2011) and hence one hypothesis could be that curcumin treatment may alter or improve the phagocytic ability of microglia and CNS-infiltrating immune cells in p25Tg mice. However, further investigation should be undertaken to fully validate this concept. Results in Chapter 5 also showed that curcumin effectively reversed the p25-mediated neuronal apoptosis and memory deficits in p25Tg mice via its anti-inflammatory, anti-amyloidogenic and anti-oxidant properties (Figure 5.12). The neuroprotective effects of curcumin against the p25-mediated neuroinflammation and subsequent neurodegeneration is summarized in Figure 6.3. Collectively, results in Chapter 5 demonstrated that curcumin; a multipotent natural compound, could be a promising tool to treat neuroinflammation-associated neurodegenerative diseases including AD.
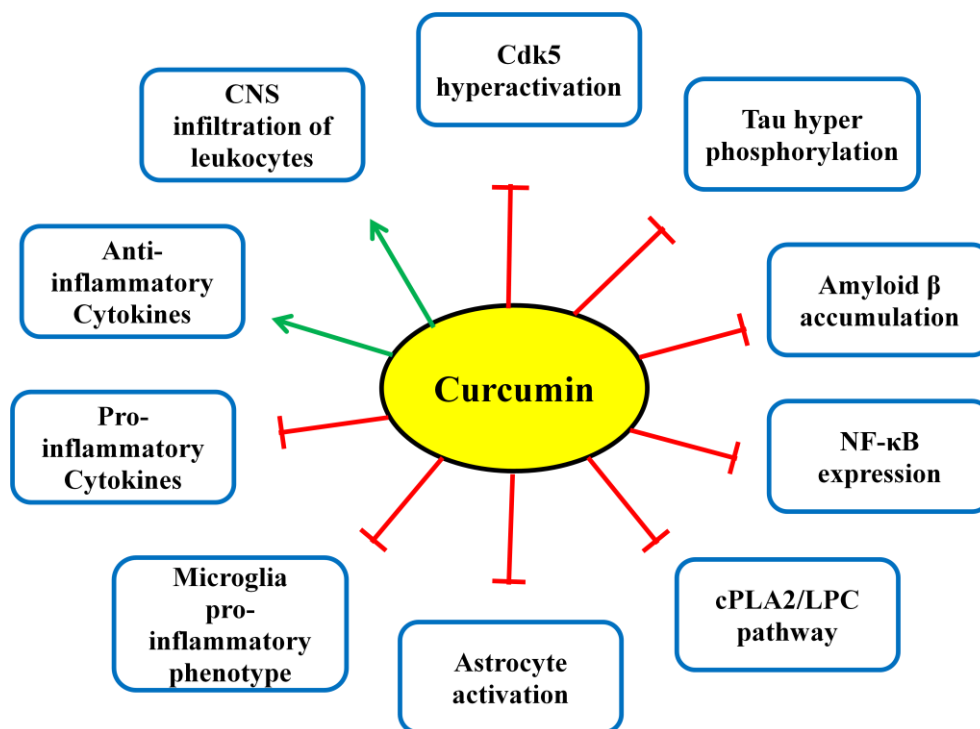
Figure 6.3: Summary of effects of curcumin on p25/Cdk5-mediated neuroinflammation and subsequent neurodegeneration

Red indicator symbolizes the inhibitory effect of curcumin and green arrow represents the positive effect of curcumin

6.2 Caveats and Future works

Results from this thesis identified that cPLA2 overexpression is a crucial event in p25/Cdk5-associated neurodegeneration and inhibition of cPLA2 activity could be a viable therapeutic approach in AD. However, further experimental investigations in this area are necessary in order to achieve a clear understanding of the mechanism behind neuroinflammation. Firstly, it is essential to extend the investigation to study the effects of specific inhibition of cPLA2 on the progression of neurodegeneration in p25Tg mice. However, *cPLA2* gene silencing using shRNA lentiviruses in p25Tg mice would be challenging and would probably require many injections with shRNA virus to achieve extended *in vivo* knock-down of cPLA2 overexpression caused by p25 elevation. Therefore, another possible way to do this *in vivo* investigation could be to use a cPLA2 inhibitor with adequate potency to inhibit the early inflammatory changes during p25 overexpression in p25Tg mice. However, currently there are no chronically active and brain-penetrant specific inhibitors of cPLA2 (Farooqui et al., 2006). Hence, it is critical to develop small molecule inhibitors specific to cPLA2 and investigate the effect of those compounds in p25Tg mice. Our laboratory has recently been involved in the development of such small molecule specific inhibitors for cPLA2 based on the knowledge of the structure of commercially available cPLA2 inhibitors and a cPLA2 X-ray structure. Molecules will be tested *in vitro* (p25-LV transduced cortical neurons) and then *in vivo* in various AD mouse models including p25Tg mice and results from this future project will certainly pave the way to the discovery of an effective drug against the neuroinflammation-associated neurodegenerative diseases.

The next key area that requires further investigation is the link between p25 overexpression and cPLA2 upregulation. Although Western blot results from this thesis supported the hypothesis that p25 might regulate cPLA2 expression via the NF-κB pathway, it is important to delineate the exact interaction between p25/Cdk5 hyperactivation and the NF-kB pathway. In addition, it would be interesting to find out the possibility of involvement and interaction of other major transcription factors in the p25/Cdk5-mediated cPLA2 upregulation. One possible way to do this investigation could be to perform

chromatin immunoprecipitation assay coupled with DNA microarrays (ChIP-on-chip assay) using RNA samples from p25 overexpressing neurons. Results from this study will certainly add more value to the future development of effective biomarkers for the early detection and prevention of AD.

The aberrant p25/Cdk5 complex which is involved in the formation of major AD pathological hallmarks such as Aβ plaques, NFTs, and neuroinflammatory changes, can be a good candidate for the disease modifying therapies. Therefore, targeting either the Cdk5 hyperactivation directly or the secondary events mediated by Cdk5 hyperactivation could be a viable avenue for developing effective treatment strategies to combat the early events of pathological changes in various neurodegenerative diseases. More recently, studies have shown that silencing Cdk5 using lentiviral or adeno-associated viral vectors markedly reduced the formation of neurofibrillary tangles in AD mouse models (Piedrahita et al., 2010). Furthermore, the effects of Cdk5 kinase inhibitors that target ATP binding sites have also been studied recently (Helal et al., 2004; Helal et al., 2009). However, these compounds not only do not specifically target p25/Cdk5, but they also inhibit p35/Cdk5 activity, interfering with normal Cdk5 activity and causing deleterious side effects. In recent years, Dr. Harish C. Pant and his colleagues have successfully generated truncated peptides of p35 including Cdk5 inhibitor peptide (CIP) (a 125-residue peptide) and p5 (a 24-residue peptide) and previous *in vitro* studies demonstrated that both CIP and p5 were specific inhibitors against p25/Cdk5-mediated neuropathological developments, without affecting normal p35/Cdk5 activity (Zheng et al., 2002; Zheng et al., 2005; Kesavapany et al., 2007; Zheng et al., 2010). Moreover, a recent *in vivo* study by our group further supported the above *in vitro* findings using transgenic mice that overexpress both CIP and p25 in the forebrain. Results confirmed a remarkable reduction in hyperphosphorylated tau, amyloid accumulations and brain atrophy in these mice (Sundaram et al., 2013). However, neuroinflammation was not completely reversed as compared to the amyloid pathology in these mice. Therefore, it would be interesting to investigate whether curcumin can be additive to this protection in addition to the CIP effect to bring about a complete reversal of p25-mediated neurotoxicity.

Furthermore, this combinational therapy could be effective against multi-factorial neurodegenerative diseases. Since p5, the further truncated product of CIP was also found to be effective specifically against p25/Cdk5 hyperactivation, it would be interesting to extend the investigation with the combination of p5 peptide and curcumin in p25 transgenic mice. Together, consistent progress in the investigation of independent treatment strategies such as specific inhibition of p25/Cdk5 hyperactivation, and early inhibition of neuroinflammation using curcumin in the field of Cdk5-associated neurodegenerative diseases strongly recommend the use of combinational therapy to target both events simultaneously so as to promote an improved therapeutic approach. Furthermore, careful and stringent evaluation of these promising candidates in other AD transgenic mouse models or in other neurodegenerative disease models would afford the necessary pre-clinical validation before progression.

BIBLIOGRAPHY

BIBLIOGRAPHY

Addae JI, Youssef FF, Stone TW (2003) Neuroprotective role of learning in dementia: a biological explanation. J Alzheimers Dis 5:91-104.

Aggarwal BB, Sung B (2009) Pharmacological basis for the role of curcumin in chronic diseases: an age-old spice with modern targets. Trends Pharmacol Sci 30:85-94.

Aggarwal BB, Sundaram C, Malani N, Ichikawa H (2007) Curcumin: the Indian solid gold. Adv Exp Med Biol 595:1-75.

Agostinho P, Cunha RA, Oliveira C (2010) Neuroinflammation, oxidative stress and the pathogenesis of Alzheimer's disease. Curr Pharm Des 16:2766-2778.

Ahlijanian MK, Barrezueta NX, Williams RD, Jakowski A, Kowsz KP, McCarthy S, Coskran T, Carlo A, Seymour PA, Burkhardt JE, Nelson RB, McNeish JD (2000) Hyperphosphorylated tau and neurofilament and cytoskeletal disruptions in mice overexpressing human p25, an activator of cdk5. Proc Natl Acad Sci U S A 97:2910-2915.

Aisen PS (1996) Inflammation and Alzheimer disease. Mol Chem Neuropathol 28:83-88.

Aisen PS, Schafer KA, Grundman M, Pfeiffer E, Sano M, Davis KL, Farlow MR, Jin S, Thomas RG, Thal LJ (2003) Effects of rofecoxib or naproxen vs placebo on Alzheimer disease progression: a randomized controlled trial. Jama 289:2819-2826.

Ajami B, Bennett JL, Krieger C, Tetzlaff W, Rossi FM (2007) Local self-renewal can sustain CNS microglia maintenance and function throughout adult life. Nat Neurosci 10:1538-1543.

Akiyama H, Barger S, Barnum S, Bradt B, Bauer J, Cole GM, Cooper NR, Eikelenboom P, Emmerling M, Fiebich BL, Finch CE, Frautschy S, Griffin WS, Hampel H, Hull M, Landreth G, Lue L, Mrak R, Mackenzie IR, McGeer PL, O'Banion MK, Pachter J, Pasinetti G, Plata-Salaman C, Rogers J, Rydel R, Shen Y, Streit W, Strohmeyer R, Tooyoma I, Van Muiswinkel FL, Veerhuis R, Walker D, Webster S,

Wegrzyniak B, Wenk G, Wyss-Coray T (2000) Inflammation and Alzheimer's disease. Neurobiol Aging 21:383-421.

Al-Saeed A (2011) Gastrointestinal and Cardiovascular Risk of Nonsteroidal Anti-inflammatory Drugs. Oman Med J 26:385-391.

Alberdi E, Sanchez-Gomez MV, Cavaliere F, Perez-Samartin A, Zugaza JL, Trullas R, Domercq M, Matute C (2010) Amyloid beta oligomers induce Ca2+ dysregulation and neuronal death through activation of ionotropic glutamate receptors. Cell Calcium 47:264-272.

Albert MS, DeKosky ST, Dickson D, Dubois B, Feldman HH, Fox NC, Gamst A, Holtzman DM, Jagust WJ, Petersen RC, Snyder PJ, Carrillo MC, Thies B, Phelps CH (2011) The diagnosis of mild cognitive impairment due to Alzheimer's disease: recommendations from the National Institute on Aging-Alzheimer's Association workgroups on diagnostic guidelines for Alzheimer's disease. Alzheimers Dement 7:270-279.

Alonso G, Privat A (1993) Reactive astrocytes involved in the formation of lesional scars differ in the mediobasal hypothalamus and in other forebrain regions. J Neurosci Res 34:523-538.

Alvarez-Maubecin V, Garcia-Hernandez F, Williams JT, Van Bockstaele EJ (2000) Functional coupling between neurons and glia. J Neurosci 20:4091-4098.

Alvira D, Ferrer I, Gutierrez-Cuesta J, Garcia-Castro B, Pallas M, Camins A (2008) Activation of the calpain/cdk5/p25 pathway in the girus cinguli in Parkinson's disease. Parkinsonism Relat Disord 14:309-313.

Alvira D, Tajes M, Verdaguer E, Acuna-Castroviejo D, Folch J, Camins A, Pallas M (2006) Inhibition of the cdk5/p25 fragment formation may explain the antiapoptotic effects of melatonin in an experimental model of Parkinson's disease. J Pineal Res 40:251-258.

Alzheimer's Disease Association Singapore In.

Alzheimer A (1911) Über eigenartige Krankheitsfälle des späteren Alters. Zeitschrift für die. Gesamte Neurologie und sychiatrie 4:356–385.

Amieva H, Le Goff M, Millet X, Orgogozo JM, Peres K, Barberger-Gateau P, Jacqmin-Gadda H, Dartigues JF (2008) Prodromal Alzheimer's

disease: successive emergence of the clinical symptoms. Ann Neurol 64:492-498.

Amin ND, Albers W, Pant HC (2002) Cyclin-dependent kinase 5 (cdk5) activation requires interaction with three domains of p35. J Neurosci Res 67:354-362.

Ammon HP, Wahl MA (1991) Pharmacology of Curcuma longa. Planta Med 57:1-7.

Anand P, Kunnumakkara AB, Newman RA, Aggarwal BB (2007) Bioavailability of curcumin: problems and promises. Mol Pharm 4:807-818.

Andreoli VM, Maffei F, Tonon GC, Zibetti A (1973) Significance of plasma lysolecithin in patients with multiple sclerosis: a longitudinal study. J Neurol Neurosurg Psychiatry 36:661-667.

Angelo M, Plattner F, Irvine EE, Giese KP (2003) Improved reversal learning and altered fear conditioning in transgenic mice with regionally restricted p25 expression. Eur J Neurosci 18:423-431.

Anne SL, Saudou F, Humbert S (2007) Phosphorylation of huntingtin by cyclin-dependent kinase 5 is induced by DNA damage and regulates wild-type and mutant huntingtin toxicity in neurons. J Neurosci 27:7318-7328.

Araujo IM, Carreira BP, Carvalho CM, Carvalho AP (2010) Calpains and delayed calcium deregulation in excitotoxicity. Neurochem Res 35:1966-1969.

Arendt T, Bigl V, Arendt A, Tennstedt A (1983) Loss of neurons in the nucleus basalis of Meynert in Alzheimer's disease, paralysis agitans and Korsakoff's Disease. Acta Neuropathol 61:101-108.

Armstrong CP, Blower AL (1987) Non-steroidal anti-inflammatory drugs and life threatening complications of peptic ulceration. Gut 28:527-532.

Arriagada PV, Growdon JH, Hedley-Whyte ET, Hyman BT (1992) Neurofibrillary tangles but not senile plaques parallel duration and severity of Alzheimer's disease. Neurology 42:631-639.

Asada A, Yamamoto N, Gohda M, Saito T, Hayashi N, Hisanaga S (2008) Myristoylation of p39 and p35 is a determinant of cytoplasmic or

nuclear localization of active cyclin-dependent kinase 5 complexes. J Neurochem 106:1325-1336.

Avraham E, Rott R, Liani E, Szargel R, Engelender S (2007) Phosphorylation of Parkin by the cyclin-dependent kinase 5 at the linker region modulates its ubiquitin-ligase activity and aggregation. J Biol Chem 282:12842-12850.

Ayoub AE, Salm AK (2003) Increased morphological diversity of microglia in the activated hypothalamic supraoptic nucleus. J Neurosci 23:7759-7766.

Baba M, Nakajo S, Tu PH, Tomita T, Nakaya K, Lee VM, Trojanowski JQ, Iwatsubo T (1998) Aggregation of alpha-synuclein in Lewy bodies of sporadic Parkinson's disease and dementia with Lewy bodies. Am J Pathol 152:879-884.

Bajaj NP, al-Sarraj ST, Leigh PN, Anderson V, Miller CC (1999) Cyclin dependent kinase-5 (CDK-5) phosphorylates neurofilament heavy (NF-H) chain to generate epitopes for antibodies that label neurofilament accumulations in amyotrophic lateral sclerosis (ALS) and is present in affected motor neurones in ALS. Prog Neuropsychopharmacol Biol Psychiatry 23:833-850.

Balsinde J, Balboa MA, Dennis EA (1998) Functional coupling between secretory phospholipase A2 and cyclooxygenase-2 and its regulation by cytosolic group IV phospholipase A2. Proc Natl Acad Sci U S A 95:7951-7956.

Basnet P, Skalko-Basnet N (2011) Curcumin: an anti-inflammatory molecule from a curry spice on the path to cancer treatment. Molecules 16:4567-4598.

Bassett CN, Neely MD, Sidell KR, Markesbery WR, Swift LL, Montine TJ (1999) Cerebrospinal fluid lipoproteins are more vulnerable to oxidation in Alzheimer's disease and are neurotoxic when oxidized ex vivo. Lipids 34:1273-1280.

Bateman RJ, Xiong C, Benzinger TL, Fagan AM, Goate A, Fox NC, Marcus DS, Cairns NJ, Xie X, Blazey TM, Holtzman DM, Santacruz A, Buckles V, Oliver A, Moulder K, Aisen PS, Ghetti B, Klunk WE, McDade E, Martins RN, Masters CL, Mayeux R, Ringman JM, Rossor

MN, Schofield PR, Sperling RA, Salloway S, Morris JC (2012) Clinical and biomarker changes in dominantly inherited Alzheimer's disease. N Engl J Med 367:795-804.

Baum L, Lam CW, Cheung SK, Kwok T, Lui V, Tsoh J, Lam L, Leung V, Hui E, Ng C, Woo J, Chiu HF, Goggins WB, Zee BC, Cheng KF, Fong CY, Wong A, Mok H, Chow MS, Ho PC, Ip SP, Ho CS, Yu XW, Lai CY, Chan MH, Szeto S, Chan IH, Mok V (2008) Six-month randomized, placebo-controlled, double-blind, pilot clinical trial of curcumin in patients with Alzheimer disease. J Clin Psychopharmacol 28:110-113.

Beaudette KN, Lew J, Wang JH (1993) Substrate specificity characterization of a cdc2-like protein kinase purified from bovine brain. J Biol Chem 268:20825-20830.

Beaulieu C (2002) The basis of anisotropic water diffusion in the nervous system - a technical review. NMR Biomed 15:435-455.

Beauquis J, Pavia P, Pomilio C, Vinuesa A, Podlutskaya N, Galvan V, Saravia F (2012) Environmental enrichment prevents astroglial pathological changes in the hippocampus of APP transgenic mice, model of Alzheimer's disease. Exp Neurol 239:28-37.

Begum AN, Jones MR, Lim GP, Morihara T, Kim P, Heath DD, Rock CL, Pruitt MA, Yang F, Hudspeth B, Hu S, Faull KF, Teter B, Cole GM, Frautschy SA (2008) Curcumin structure-function, bioavailability, and efficacy in models of neuroinflammation and Alzheimer's disease. J Pharmacol Exp Ther 326:196-208.

Bentham P, Gray R, Sellwood E, Raftery J (1999) Effectiveness of rivastigmine in Alzheimer's disease. Improvements in functional ability remain unestablished. Bmj 319:640-641.

Benz B, Grima G, Do KQ (2004) Glutamate-induced homocysteic acid release from astrocytes: possible implication in glia-neuron signaling. Neuroscience 124:377-386.

Benzi G, Moretti A (1998) Is there a rationale for the use of acetylcholinesterase inhibitors in the therapy of Alzheimer's disease? Eur J Pharmacol 346:1-13.

Berger AK, Fratiglioni L, Forsell Y, Winblad B, Backman L (1999) The occurrence of depressive symptoms in the preclinical phase of AD: a population-based study. Neurology 53:1998-2002.

Bertram L, McQueen MB, Mullin K, Blacker D, Tanzi RE (2007) Systematic meta-analyses of Alzheimer disease genetic association studies: the AlzGene database. Nat Genet 39:17-23.

Bian F, Nath R, Sobocinski G, Booher RN, Lipinski WJ, Callahan MJ, Pack A, Wang KK, Walker LC (2002) Axonopathy, tau abnormalities, and dyskinesia, but no neurofibrillary tangles in p25-transgenic mice. J Comp Neurol 446:257-266.

Bibb JA (2003) Role of Cdk5 in neuronal signaling, plasticity, and drug abuse. Neurosignals 12:191-199.

Bibb JA, Chen J, Taylor JR, Svenningsson P, Nishi A, Snyder GL, Yan Z, Sagawa ZK, Ouimet CC, Nairn AC, Nestler EJ, Greengard P (2001) Effects of chronic exposure to cocaine are regulated by the neuronal protein Cdk5. Nature 410:376-380.

Bird TD (1993) Alzheimer Disease Overview.

Bisht K, Choi WH, Park SY, Chung MK, Koh WS (2009) Curcumin enhances non-inflammatory phagocytic activity of RAW264.7 cells. Biochem Biophys Res Commun 379:632-636.

Blennow K, Zetterberg H (2009) Cerebrospinal fluid biomarkers for Alzheimer's disease. J Alzheimers Dis 18:413-417.

Block ML, Zecca L, Hong JS (2007) Microglia-mediated neurotoxicity: uncovering the molecular mechanisms. Nat Rev Neurosci 8:57-69.

Blurton-Jones M, Laferla FM (2006) Pathways by which Abeta facilitates tau pathology. Curr Alzheimer Res 3:437-448.

Boje KM, Arora PK (1992) Microglial-produced nitric oxide and reactive nitrogen oxides mediate neuronal cell death. Brain Res 587:250-256.

Bornemann KD, Wiederhold KH, Pauli C, Ermini F, Stalder M, Schnell L, Sommer B, Jucker M, Staufenbiel M (2001) Abeta-induced inflammatory processes in microglia cells of APP23 transgenic mice. Am J Pathol 158:63-73.

Braak H, Braak E (1991) Neuropathological stageing of Alzheimer-related changes. Acta Neuropathol 82:239-259.

Breitner JC, Folstein MF, Murphy EA (1986) Familial aggregation in Alzheimer dementia--I. A model for the age-dependent expression of an autosomal dominant gene. J Psychiatr Res 20:31-43.

Bremer J, Norum KR (1982) Metabolism of very long-chain monounsaturated fatty acids (22:1) and the adaptation to their presence in the diet. J Lipid Res 23:243-256.

Brisebois M, Zehntner SP, Estrada J, Owens T, Fournier S (2006) A pathogenic role for CD8+ T cells in a spontaneous model of demyelinating disease. J Immunol 177:2403-2411.

Brochard V, Combadiere B, Prigent A, Laouar Y, Perrin A, Beray-Berthat V, Bonduelle O, Alvarez-Fischer D, Callebert J, Launay JM, Duyckaerts C, Flavell RA, Hirsch EC, Hunot S (2009) Infiltration of CD4+ lymphocytes into the brain contributes to neurodegeneration in a mouse model of Parkinson disease. J Clin Invest 119:182-192.

Brown NR, Noble ME, Lawrie AM, Morris MC, Tunnah P, Divita G, Johnson LN, Endicott JA (1999) Effects of phosphorylation of threonine 160 on cyclin-dependent kinase 2 structure and activity. J Biol Chem 274:8746-8756.

Buee L, Bussiere T, Buee-Scherrer V, Delacourte A, Hof PR (2000) Tau protein isoforms, phosphorylation and role in neurodegenerative disorders. Brain Res Brain Res Rev 33:95-130.

Bustanji Y, Taha MO, Almasri IM, Al-Ghussein MA, Mohammad MK, Alkhatib HS (2009) Inhibition of glycogen synthase kinase by curcumin: Investigation by simulated molecular docking and subsequent in vitro/in vivo evaluation. J Enzyme Inhib Med Chem 24:771-778.

Butterfield DA (1997) beta-Amyloid-associated free radical oxidative stress and neurotoxicity: implications for Alzheimer's disease. Chem Res Toxicol 10:495-506.

Cameron B, Landreth GE (2010) Inflammation, microglia, and Alzheimer's disease. Neurobiol Dis 37:503-509.

Camins A, Verdaguer E, Folch J, Canudas AM, Pallas M (2006) The role of CDK5/P25 formation/inhibition in neurodegeneration. Drug News Perspect 19:453-460.

Cashman JR, Ghirmai S, Abel KJ, Fiala M (2008) Immune defects in Alzheimer's disease: new medications development. BMC Neurosci 9 Suppl 2:S13.

Cashman JR, Gagliardi S, Lanier M, Ghirmai S, Abel KJ, Fiala M (2012) Curcumins promote monocytic gene expression related to beta-amyloid and superoxide dismutase clearance. Neurodegener Dis 10:274-276.

Castano EM, Prelli F, Wisniewski T, Golabek A, Kumar RA, Soto C, Frangione B (1995) Fibrillogenesis in Alzheimer's disease of amyloid beta peptides and apolipoprotein E. Biochem J 306 (Pt 2):599-604.

Castell JV, Andus T, Kunz D, Heinrich PC (1989) Interleukin-6. The major regulator of acute-phase protein synthesis in man and rat. Ann N Y Acad Sci 557:87-99; discussion 100-101.

Chandran B, Goel A A randomized, pilot study to assess the efficacy and safety of curcumin in patients with active rheumatoid arthritis. Phytother Res 26:1719-1725.

Chao CC, Hu S, Frey WH, 2nd, Ala TA, Tourtellotte WW, Peterson PK (1994) Transforming growth factor beta in Alzheimer's disease. Clin Diagn Lab Immunol 1:109-110.

Chen G, Chen KS, Knox J, Inglis J, Bernard A, Martin SJ, Justice A, McConlogue L, Games D, Freedman SB, Morris RG (2000) A learning deficit related to age and beta-amyloid plaques in a mouse model of Alzheimer's disease. Nature 408:975-979.

Cheng SE, Luo SF, Jou MJ, Lin CC, Kou YR, Lee IT, Hsieh HL, Yang CM (2009) Cigarette smoke extract induces cytosolic phospholipase A2 expression via NADPH oxidase, MAPKs, AP-1, and NF-kappaB in human tracheal smooth muscle cells. Free Radic Biol Med 46:948-960.

Cheung ZH, Ip NY (2012) Cdk5: a multifaceted kinase in neurodegenerative diseases. Trends Cell Biol 22:169-175.

Cheung ZH, Gong K, Ip NY (2008) Cyclin-dependent kinase 5 supports neuronal survival through phosphorylation of Bcl-2. J Neurosci 28:4872-4877.

Ching YP, Pang AS, Lam WH, Qi RZ, Wang JH (2002) Identification of a neuronal Cdk5 activator-binding protein as Cdk5 inhibitor. J Biol Chem 277:15237-15240.

Chishti MA, Yang DS, Janus C, Phinney AL, Horne P, Pearson J, Strome R, Zuker N, Loukides J, French J, Turner S, Lozza G, Grilli M, Kunicki S, Morissette C, Paquette J, Gervais F, Bergeron C, Fraser PE, Carlson GA, George-Hyslop PS, Westaway D (2001) Early-onset amyloid deposition and cognitive deficits in transgenic mice expressing a double mutant form of amyloid precursor protein 695. J Biol Chem 276:21562-21570.

Chiu IM, Chen A, Zheng Y, Kosaras B, Tsiftsoglou SA, Vartanian TK, Brown RH, Jr., Carroll MC (2008) T lymphocytes potentiate endogenous neuroprotective inflammation in a mouse model of ALS. Proc Natl Acad Sci U S A 105:17913-17918.

Chiu IM, Phatnani H, Kuligowski M, Tapia JC, Carrasco MA, Zhang M, Maniatis T, Carroll MC (2009) Activation of innate and humoral immunity in the peripheral nervous system of ALS transgenic mice. Proc Natl Acad Sci U S A 106:20960-20965.

Chow VW, Mattson MP, Wong PC, Gleichmann M (2010) An overview of APP processing enzymes and products. Neuromolecular Med 12:1-12.

Ciesielska A, Joniec I, Kurkowska-Jastrzebska I, Cudna A, Przybylkowski A, Czlonkowska A, Czlonkowski A (2009) The impact of age and gender on the striatal astrocytes activation in murine model of Parkinson's disease. Inflamm Res 58:747-753.

Cieslik K, Zembowicz A, Tang JL, Wu KK (1998) Transcriptional regulation of endothelial nitric-oxide synthase by lysophosphatidylcholine. J Biol Chem 273:14885-14890.

Cleveland DW (1999) From Charcot to SOD1: mechanisms of selective motor neuron death in ALS. Neuron 24:515-520.

Colangelo V, Schurr J, Ball MJ, Pelaez RP, Bazan NG, Lukiw WJ (2002) Gene expression profiling of 12633 genes in Alzheimer hippocampal CA1: transcription and neurotrophic factor down-regulation and up-regulation of apoptotic and pro-inflammatory signaling. J Neurosci Res 70:462-473.

Cole GM, Teter B, Frautschy SA (2007) Neuroprotective effects of curcumin. Adv Exp Med Biol 595:197-212.

Combs CK (2009) Inflammation and microglia actions in Alzheimer's disease. J Neuroimmune Pharmacol 4:380-388.

Combs CK, Karlo JC, Kao SC, Landreth GE (2001) beta-Amyloid stimulation of microglia and monocytes results in TNFalpha-dependent expression of inducible nitric oxide synthase and neuronal apoptosis. J Neurosci 21:1179-1188.

Croisile B, Auriacombe S, Etcharry-Bouyx F, Vercelletto M (2012) [The new 2011 recommendations of the National Institute on Aging and the Alzheimer's Association on diagnostic guidelines for Alzheimer's disease: Preclinal stages, mild cognitive impairment, and dementia]. Rev Neurol (Paris) 168:471-482.

Cruz JC, Tsai LH (2004) Cdk5 deregulation in the pathogenesis of Alzheimer's disease. Trends Mol Med 10:452-458.

Cruz JC, Tseng HC, Goldman JA, Shih H, Tsai LH (2003) Aberrant Cdk5 activation by p25 triggers pathological events leading to neurodegeneration and neurofibrillary tangles. Neuron 40:471-483.

Cruz JC, Kim D, Moy LY, Dobbin MM, Sun X, Bronson RT, Tsai LH (2006) p25/cyclin-dependent kinase 5 induces production and intraneuronal accumulation of amyloid beta in vivo. J Neurosci 26:10536-10541.

Cuchillo-Ibanez I, Seereeram A, Byers HL, Leung KY, Ward MA, Anderton BH, Hanger DP (2008) Phosphorylation of tau regulates its axonal transport by controlling its binding to kinesin. Faseb J 22:3186-3195.

Cudkowicz ME, McKenna-Yasek D, Sapp PE, Chin W, Geller B, Hayden DL, Schoenfeld DA, Hosler BA, Horvitz HR, Brown RH (1997) Epidemiology of mutations in superoxide dismutase in amyotrophic lateral sclerosis. Ann Neurol 41:210-221.

Dadhaniya P, Patel C, Muchhara J, Bhadja N, Mathuria N, Vachhani K, Soni MG (2011) Safety assessment of a solid lipid curcumin particle preparation: acute and subchronic toxicity studies. Food Chem Toxicol 49:1834-1842.

Dahm R (2006) Alzheimer's discovery. Curr Biol 16:R906-910.

Das P, Golde T (2006) Dysfunction of TGF-beta signaling in Alzheimer's disease. J Clin Invest 116:2855-2857.

Dauer W, Przedborski S (2003) Parkinson's disease: mechanisms and models. Neuron 39:889-909.

David DC, Hauptmann S, Scherping I, Schuessel K, Keil U, Rizzu P, Ravid R, Drose S, Brandt U, Muller WE, Eckert A, Gotz J (2005) Proteomic and functional analyses reveal a mitochondrial dysfunction in P301L tau transgenic mice. J Biol Chem 280:23802-23814.

Delalle I, Bhide PG, Caviness VS, Jr., Tsai LH (1997) Temporal and spatial patterns of expression of p35, a regulatory subunit of cyclin-dependent kinase 5, in the nervous system of the mouse. J Neurocytol 26:283-296.

Demetrick DJ, Zhang H, Beach DH (1994) Chromosomal mapping of human CDK2, CDK4, and CDK5 cell cycle kinase genes. Cytogenet Cell Genet 66:72-74.

Dhavan R, Tsai LH (2001) A decade of CDK5. Nat Rev Mol Cell Biol 2:749-759.

Dickson DW (1997) Neuropathological diagnosis of Alzheimer's disease: a perspective from longitudinal clinicopathological studies. Neurobiol Aging 18:S21-26.

Doraiswamy PM (2002) Non-cholinergic strategies for treating and preventing Alzheimer's disease. CNS Drugs 16:811-824.

Duff K, Suleman F (2004) Transgenic mouse models of Alzheimer's disease: how useful have they been for therapeutic development? Brief Funct Genomic Proteomic 3:47-59.

Eimer WA, Vassar R (2013) Neuron loss in the 5XFAD mouse model of Alzheimer's disease correlates with intraneuronal Abeta42 accumulation and Caspase-3 activation. Mol Neurodegener 8:2.

Eng LF, Ghirnikar RS (1994) GFAP and astrogliosis. Brain Pathol 4:229-237.

Engelhardt B (2008) The blood-central nervous system barriers actively control immune cell entry into the central nervous system. Curr Pharm Des 14:1555-1565.

Farooqui AA, Rapoport SI, Horrocks LA (1997) Membrane phospholipid alterations in Alzheimer's disease: deficiency of ethanolamine plasmalogens. Neurochem Res 22:523-527.

Farooqui AA, Ong WY, Horrocks LA (2003) Plasmalogens, docosahexaenoic acid and neurological disorders. Adv Exp Med Biol 544:335-354.

Farooqui AA, Ong WY, Horrocks LA (2006) Inhibitors of brain phospholipase A2 activity: their neuropharmacological effects and therapeutic importance for the treatment of neurologic disorders. Pharmacol Rev 58:591-620.

Fischer A, Sananbenesi F, Pang PT, Lu B, Tsai LH (2005) Opposing roles of transient and prolonged expression of p25 in synaptic plasticity and hippocampus-dependent memory. Neuron 48:825-838.

Fischer A, Sananbenesi F, Wang X, Dobbin M, Tsai LH (2007) Recovery of learning and memory is associated with chromatin remodelling. Nature 447:178-182.

Flaherty DB, Soria JP, Tomasiewicz HG, Wood JG (2000) Phosphorylation of human tau protein by microtubule-associated kinases: GSK3beta and cdk5 are key participants. J Neurosci Res 62:463-472.

Fletcher JM, Lalor SJ, Sweeney CM, Tubridy N, Mills KH (2010) T cells in multiple sclerosis and experimental autoimmune encephalomyelitis. Clin Exp Immunol 162:1-11.

Floden AM, Li S, Combs CK (2005) Beta-amyloid-stimulated microglia induce neuron death via synergistic stimulation of tumor necrosis factor alpha and NMDA receptors. J Neurosci 25:2566-2575.

Folstein MF, Folstein SE, McHugh PR (1975) "Mini-mental state". A practical method for grading the cognitive state of patients for the clinician. J Psychiatr Res 12:189-198.

Forsberg A, Engler H, Almkvist O, Blomquist G, Hagman G, Wall A, Ringheim A, Langstrom B, Nordberg A (2008) PET imaging of amyloid deposition in patients with mild cognitive impairment. Neurobiol Aging 29:1456-1465.

Forstl H, Kurz A (1999) Clinical features of Alzheimer's disease. Eur Arch Psychiatry Clin Neurosci 249:288-290.

Frank-Cannon TC, Alto LT, McAlpine FE, Tansey MG (2009) Does neuroinflammation fan the flame in neurodegenerative diseases? Mol Neurodegener 4:47.

Frautschy SA, Cole GM (2010) Why pleiotropic interventions are needed for Alzheimer's disease. Mol Neurobiol 41:392-409.

Frautschy SA, Yang F, Irrizarry M, Hyman B, Saido TC, Hsiao K, Cole GM (1998) Microglial response to amyloid plaques in APPsw transgenic mice. Am J Pathol 152:307-317.

Frautschy SA, Hu W, Kim P, Miller SA, Chu T, Harris-White ME, Cole GM (2001) Phenolic anti-inflammatory antioxidant reversal of Abeta-induced cognitive deficits and neuropathology. Neurobiol Aging 22:993-1005.

Frolich L (2002) The cholinergic pathology in Alzheimer's disease--discrepancies between clinical experience and pathophysiological findings. J Neural Transm 109:1003-1013.

Fu AK, Fu WY, Cheung J, Tsim KW, Ip FC, Wang JH, Ip NY (2001) Cdk5 is involved in neuregulin-induced AChR expression at the neuromuscular junction. Nat Neurosci 4:374-381.

Funk JL, Frye JB, Oyarzo JN, Kuscuoglu N, Wilson J, McCaffrey G, Stafford G, Chen G, Lantz RC, Jolad SD, Solyom AM, Kiela PR, Timmermann BN (2006) Efficacy and mechanism of action of turmeric supplements in the treatment of experimental arthritis. Arthritis Rheum 54:3452-3464.

Gagliardi S, Ghirmai S, Abel KJ, Lanier M, Gardai SJ, Lee C, Cashman JR (2011) Evaluation in vitro of synthetic curcumins as agents promoting monocytic gene expression related to beta-amyloid clearance. Chem Res Toxicol 25:101-112.

Games D, Adams D, Alessandrini R, Barbour R, Berthelette P, Blackwell C, Carr T, Clemens J, Donaldson T, Gillespie F, et al. (1995) Alzheimer-type neuropathology in transgenic mice overexpressing V717F beta-amyloid precursor protein. Nature 373:523-527.

Gao CY, Zakeri Z, Zhu Y, He H, Zelenka PS (1997) Expression of Cdk5, p35, and Cdk5-associated kinase activity in the developing rat lens. Dev Genet 20:267-275.

Garcia-Alloza M, Borrelli LA, Rozkalne A, Hyman BT, Bacskai BJ (2007) Curcumin labels amyloid pathology in vivo, disrupts existing plaques, and partially restores distorted neurites in an Alzheimer mouse model. J Neurochem 102:1095-1104.

Garcia-Ramallo E, Marques T, Prats N, Beleta J, Kunkel SL, Godessart N (2002) Resident cell chemokine expression serves as the major mechanism for leukocyte recruitment during local inflammation. J Immunol 169:6467-6473.

Garwood CJ, Pooler AM, Atherton J, Hanger DP, Noble W (2011) Astrocytes are important mediators of Abeta-induced neurotoxicity and tau phosphorylation in primary culture. Cell Death Dis 2:e167.

Giannakopoulos P, Herrmann FR, Bussiere T, Bouras C, Kovari E, Perl DP, Morrison JH, Gold G, Hof PR (2003) Tangle and neuron numbers, but not amyloid load, predict cognitive status in Alzheimer's disease. Neurology 60:1495-1500.

Giese KP, Ris L, Plattner F (2005) Is there a role of the cyclin-dependent kinase 5 activator p25 in Alzheimer's disease? Neuroreport 16:1725-1730.

Gilmore EC, Ohshima T, Goffinet AM, Kulkarni AB, Herrup K (1998) Cyclin-dependent kinase 5-deficient mice demonstrate novel developmental arrest in cerebral cortex. J Neurosci 18:6370-6377.

Goate A, Chartier-Harlin MC, Mullan M, Brown J, Crawford F, Fidani L, Giuffra L, Haynes A, Irving N, James L, et al. (1991) Segregation of a missense mutation in the amyloid precursor protein gene with familial Alzheimer's disease. Nature 349:704-706.

Gong X, Tang X, Wiedmann M, Wang X, Peng J, Zheng D, Blair LA, Marshall J, Mao Z (2003) Cdk5-mediated inhibition of the protective effects of transcription factor MEF2 in neurotoxicity-induced apoptosis. Neuron 38:33-46.

Gota VS, Maru GB, Soni TG, Gandhi TR, Kochar N, Agarwal MG (2010) Safety and pharmacokinetics of a solid lipid curcumin particle formulation in osteosarcoma patients and healthy volunteers. J Agric Food Chem 58:2095-2099.

Gotz J, Chen F, Barmettler R, Nitsch RM (2001a) Tau filament formation in transgenic mice expressing P301L tau. J Biol Chem 276:529-534.

Gotz J, Chen F, van Dorpe J, Nitsch RM (2001b) Formation of neurofibrillary tangles in P301l tau transgenic mice induced by Abeta 42 fibrils. Science 293:1491-1495.

Gountouna VE, Job DE, McIntosh AM, Moorhead TW, Lymer GK, Whalley HC, Hall J, Waiter GD, Brennan D, McGonigle DJ, Ahearn TS, Cavanagh J, Condon B, Hadley DM, Marshall I, Murray AD, Steele JD, Wardlaw JM, Lawrie SM (2010) Functional Magnetic Resonance Imaging (fMRI) reproducibility and variance components across visits and scanning sites with a finger tapping task. Neuroimage 49:552-560.

Granic I, Nyakas C, Luiten PG, Eisel UL, Halmy LG, Gross G, Schoemaker H, Moller A, Nimmrich V (2010) Calpain inhibition prevents amyloid-beta-induced neurodegeneration and associated behavioral dysfunction in rats. Neuropharmacology 59:334-342.

Grant P, Sharma P, Pant HC (2001) Cyclin-dependent protein kinase 5 (Cdk5) and the regulation of neurofilament metabolism. Eur J Biochem 268:1534-1546.

Grimm MO, Grimm HS, Patzold AJ, Zinser EG, Halonen R, Duering M, Tschape JA, De Strooper B, Muller U, Shen J, Hartmann T (2005) Regulation of cholesterol and sphingomyelin metabolism by amyloid-beta and presenilin. Nat Cell Biol 7:1118-1123.

Guillozet AL, Weintraub S, Mash DC, Mesulam MM (2003) Neurofibrillary tangles, amyloid, and memory in aging and mild cognitive impairment. Arch Neurol 60:729-736.

Guo Q, Fu W, Sopher BL, Miller MW, Ware CB, Martin GM, Mattson MP (1999) Increased vulnerability of hippocampal neurons to excitotoxic necrosis in presenilin-1 mutant knock-in mice. Nat Med 5:101-106.

Guo Z, Su W, Ma Z, Smith GM, Gong MC (2003) Ca2+-independent phospholipase A2 is required for agonist-induced Ca2+ sensitization of contraction in vascular smooth muscle. J Biol Chem 278:1856-1863.

Guo Z, Cupples LA, Kurz A, Auerbach SH, Volicer L, Chui H, Green RC, Sadovnick AD, Duara R, DeCarli C, Johnson K, Go RC, Growdon JH,

Haines JL, Kukull WA, Farrer LA (2000) Head injury and the risk of AD in the MIRAGE study. Neurology 54:1316-1323.

Hall AM, Roberson ED (2012) Mouse models of Alzheimer's disease. Brain Res Bull 88:3-12.

Hall ED, Oostveen JA, Gurney ME (1998) Relationship of microglial and astrocytic activation to disease onset and progression in a transgenic model of familial ALS. Glia 23:249-256.

Hall SM (1972) The effect of injections of lysophosphatidyl choline into white matter of the adult mouse spinal cord. J Cell Sci 10:535-546.

Hampel H, Lista S (2012) Alzheimer disease: From inherited to sporadic AD-crossing the biomarker bridge. Nat Rev Neurol 8:598-600.

Hanai H, Iida T, Takeuchi K, Watanabe F, Maruyama Y, Andoh A, Tsujikawa T, Fujiyama Y, Mitsuyama K, Sata M, Yamada M, Iwaoka Y, Kanke K, Hiraishi H, Hirayama K, Arai H, Yoshii S, Uchijima M, Nagata T, Koide Y (2006) Curcumin maintenance therapy for ulcerative colitis: randomized, multicenter, double-blind, placebo-controlled trial. Clin Gastroenterol Hepatol 4:1502-1506.

Hardy J, Selkoe DJ (2002) The amyloid hypothesis of Alzheimer's disease: progress and problems on the road to therapeutics. Science 297:353-356.

Harpin ML, Delaere P, Javoy-Agid F, Bock E, Jacque C, Delpech B, Villarroya H, Duyckaerts C, Hauw JJ, Baumann N (1990) Glial fibrillary acidic protein and beta A4 protein deposits in temporal lobe of aging brain and senile dementia of the Alzheimer type: relation with the cognitive state and with quantitative studies of senile plaques and neurofibrillary tangles. J Neurosci Res 27:587-594.

Harrison J, Minassian SL, Jenkins L, Black RS, Koller M, Grundman M (2007) A neuropsychological test battery for use in Alzheimer disease clinical trials. Arch Neurol 64:1323-1329.

Hart AD, Wyttenbach A, Perry VH, Teeling JL (2012) Age related changes in microglial phenotype vary between CNS regions: grey versus white matter differences. Brain Behav Immun 26:754-765.

Hashiguchi M, Saito T, Hisanaga S, Hashiguchi T (2002) Truncation of CDK5 activator p35 induces intensive phosphorylation of Ser202/Thr205 of human tau. J Biol Chem 277:44525-44530.

Hawasli AH, Benavides DR, Nguyen C, Kansy JW, Hayashi K, Chambon P, Greengard P, Powell CM, Cooper DC, Bibb JA (2007) Cyclin-dependent kinase 5 governs learning and synaptic plasticity via control of NMDAR degradation. Nat Neurosci 10:880-886.

Hawkes CA, McLaurin J (2009) Selective targeting of perivascular macrophages for clearance of beta-amyloid in cerebral amyloid angiopathy. Proc Natl Acad Sci U S A 106:1261-1266.

Hebert LE, Beckett LA, Scherr PA, Evans DA (2001) Annual incidence of Alzheimer disease in the United States projected to the years 2000 through 2050. Alzheimer Dis Assoc Disord 15:169-173.

Hebert LE, Weuve J, Scherr PA, Evans DA (2013) Alzheimer disease in the United States (2010-2050) estimated using the 2010 census. Neurology.

Helal CJ, Sanner MA, Cooper CB, Gant T, Adam M, Lucas JC, Kang Z, Kupchinsky S, Ahlijanian MK, Tate B, Menniti FS, Kelly K, Peterson M (2004) Discovery and SAR of 2-aminothiazole inhibitors of cyclin-dependent kinase 5/p25 as a potential treatment for Alzheimer's disease. Bioorg Med Chem Lett 14:5521-5525.

Helal CJ, Kang Z, Lucas JC, Gant T, Ahlijanian MK, Schachter JB, Richter KE, Cook JM, Menniti FS, Kelly K, Mente S, Pandit J, Hosea N (2009) Potent and cellularly active 4-aminoimidazole inhibitors of cyclin-dependent kinase 5/p25 for the treatment of Alzheimer's disease. Bioorg Med Chem Lett 19:5703-5707.

Hellmich MR, Pant HC, Wada E, Battey JF (1992) Neuronal cdc2-like kinase: a cdc2-related protein kinase with predominantly neuronal expression. Proc Natl Acad Sci U S A 89:10867-10871.

Hellmich MR, Kennison JA, Hampton LL, Battey JF (1994) Cloning and characterization of the Drosophila melanogaster CDK5 homolog. FEBS Lett 356:317-321.

Heneka MT, O'Banion MK (2007) Inflammatory processes in Alzheimer's disease. J Neuroimmunol 184:69-91.

Heneka MT, Sastre M, Dumitrescu-Ozimek L, Dewachter I, Walter J, Klockgether T, Van Leuven F (2005) Focal glial activation coincides with increased BACE1 activation and precedes amyloid plaque deposition in APP[V717I] transgenic mice. J Neuroinflammation 2:22.

Hengst L, Dulic V, Slingerland JM, Lees E, Reed SI (1994) A cell cycle-regulated inhibitor of cyclin-dependent kinases. Proc Natl Acad Sci U S A 91:5291-5295.

Herholz K (2011) Perfusion SPECT and FDG-PET. Int Psychogeriatr 23 Suppl 2:S25-31.

Hirohata M, Ono K, Yamada M (2008) Non-steroidal anti-inflammatory drugs as anti-amyloidogenic compounds. Curr Pharm Des 14:3280-3294.

Hisanaga S, Ishiguro K, Uchida T, Okumura E, Okano T, Kishimoto T (1993) Tau protein kinase II has a similar characteristic to cdc2 kinase for phosphorylating neurofilament proteins. J Biol Chem 268:15056-15060.

Ho L, Purohit D, Haroutunian V, Luterman JD, Willis F, Naslund J, Buxbaum JD, Mohs RC, Aisen PS, Pasinetti GM (2001) Neuronal cyclooxygenase 2 expression in the hippocampal formation as a function of the clinical progression of Alzheimer disease. Arch Neurol 58:487-492.

Hornfelt M, Edstrom A, Ekstrom PA (1999) Upregulation of cytosolic phospholipase A2 correlates with apoptosis in mouse superior cervical and dorsal root ganglia neurons. Neurosci Lett 265:87-90.

Hosokawa T, Saito T, Asada A, Ohshima T, Itakura M, Takahashi M, Fukunaga K, Hisanaga S (2006) Enhanced activation of Ca2+/calmodulin-dependent protein kinase II upon downregulation of cyclin-dependent kinase 5-p35. J Neurosci Res 84:747-754.

Hou ST, MacManus JP (2002) Molecular mechanisms of cerebral ischemia-induced neuronal death. Int Rev Cytol 221:93-148.

Hsiao K, Chapman P, Nilsen S, Eckman C, Harigaya Y, Younkin S, Yang F, Cole G (1996) Correlative memory deficits, Abeta elevation, and amyloid plaques in transgenic mice. Science 274:99-102.

Huang D, Patrick G, Moffat J, Tsai LH, Andrews B (1999) Mammalian Cdk5 is a functional homologue of the budding yeast Pho85 cyclin-dependent protein kinase. Proc Natl Acad Sci U S A 96:14445-14450.

Huang WC, Chen CC (2005) Akt phosphorylation of p300 at Ser-1834 is essential for its histone acetyltransferase and transcriptional activity. Mol Cell Biol 25:6592-6602.

Hughes V (2012) Microglia: The constant gardeners. Nature 485:570-572.

Hurwitz AA, Lyman WD, Berman JW (1995) Tumor necrosis factor alpha and transforming growth factor beta upregulate astrocyte expression of monocyte chemoattractant protein-1. J Neuroimmunol 57:193-198.

Ihara Y, Nukina N, Miura R, Ogawara M (1986) Phosphorylated tau protein is integrated into paired helical filaments in Alzheimer's disease. J Biochem 99:1807-1810.

Iijima K, Ando K, Takeda S, Satoh Y, Seki T, Itohara S, Greengard P, Kirino Y, Nairn AC, Suzuki T (2000) Neuron-specific phosphorylation of Alzheimer's beta-amyloid precursor protein by cyclin-dependent kinase 5. J Neurochem 75:1085-1091.

Imbimbo BP (2009) An update on the efficacy of non-steroidal anti-inflammatory drugs in Alzheimer's disease. Expert Opin Investig Drugs 18:1147-1168.

Iqbal K, Liu F, Gong CX, Alonso Adel C, Grundke-Iqbal I (2009) Mechanisms of tau-induced neurodegeneration. Acta Neuropathol 118:53-69.

Ito T, Meguro K, Akanuma K, Meguro M, Lee E, Kasuya M, Ishii H, Mori E (2007) Behavioral and psychological symptoms assessed with the BEHAVE-AD-FW are differentially associated with cognitive dysfunction in Alzheimer's disease. J Clin Neurosci 14:850-855.

Jacobson SA, Sabbagh MN (2008) Donepezil: potential neuroprotective and disease-modifying effects. Expert Opin Drug Metab Toxicol 4:1363-1369.

Jagtap S, Meganathan K, Wagh V, Winkler J, Hescheler J, Sachinidis A (2009) Chemoprotective mechanism of the natural compounds, epigallocatechin-3-O-gallate, quercetin and curcumin against cancer and cardiovascular diseases. Curr Med Chem 16:1451-1462.

Jagust W, Thisted R, Devous MD, Sr., Van Heertum R, Mayberg H, Jobst K, Smith AD, Borys N (2001) SPECT perfusion imaging in the diagnosis of Alzheimer's disease: a clinical-pathologic study. Neurology 56:950-956.

Jain SK, Rains J, Croad J, Larson B, Jones K (2009) Curcumin supplementation lowers TNF-alpha, IL-6, IL-8, and MCP-1 secretion in high glucose-treated cultured monocytes and blood levels of TNF-alpha, IL-6, MCP-1, glucose, and glycosylated hemoglobin in diabetic rats. Antioxid Redox Signal 11:241-249.

Janelsins MC, Mastrangelo MA, Oddo S, LaFerla FM, Federoff HJ, Bowers WJ (2005) Early correlation of microglial activation with enhanced tumor necrosis factor-alpha and monocyte chemoattractant protein-1 expression specifically within the entorhinal cortex of triple transgenic Alzheimer's disease mice. J Neuroinflammation 2:23.

Jantzen PT, Connor KE, DiCarlo G, Wenk GL, Wallace JL, Rojiani AM, Coppola D, Morgan D, Gordon MN (2002) Microglial activation and beta -amyloid deposit reduction caused by a nitric oxide-releasing nonsteroidal anti-inflammatory drug in amyloid precursor protein plus presenilin-1 transgenic mice. J Neurosci 22:2246-2254.

Jean I, Allamargot C, Barthelaix-Pouplard A, Fressinaud C (2002) Axonal lesions and PDGF-enhanced remyelination in the rat corpus callosum after lysolecithin demyelination. Neuroreport 13:627-631.

Jenkins CM, Han X, Mancuso DJ, Gross RW (2002) Identification of calcium-independent phospholipase A2 (iPLA2) beta, and not iPLA2gamma, as the mediator of arginine vasopressin-induced arachidonic acid release in A-10 smooth muscle cells. Enantioselective mechanism-based discrimination of mammalian iPLA2s. J Biol Chem 277:32807-32814.

Jia J, Sun B, Guo Z, Zhang J, Tian J, Tang H, Wang L (2011) Positron emission tomography with Pittsburgh compound B in diagnosis of early stage Alzheimer's disease. Cell Biochem Biophys 59:57-62.

Jin CY, Lee JD, Park C, Choi YH, Kim GY (2007) Curcumin attenuates the release of pro-inflammatory cytokines in lipopolysaccharide-stimulated BV2 microglia. Acta Pharmacol Sin 28:1645-1651.

Jobin C, Bradham CA, Russo MP, Juma B, Narula AS, Brenner DA, Sartor RB (1999) Curcumin blocks cytokine-mediated NF-kappa B activation and proinflammatory gene expression by inhibiting inhibitory factor I-kappa B kinase activity. J Immunol 163:3474-3483.

Johnston H, Boutin H, Allan SM (2011) Assessing the contribution of inflammation in models of Alzheimer's disease. Biochem Soc Trans 39:886-890.

Jolas T, Zhang XS, Zhang Q, Wong G, Del Vecchio R, Gold L, Priestley T (2002) Long-term potentiation is increased in the CA1 area of the hippocampus of APP(swe/ind) CRND8 mice. Neurobiol Dis 11:394-409.

Jones TA, Hawrylak N, Greenough WT (1996) Rapid laminar-dependent changes in GFAP immunoreactive astrocytes in the visual cortex of rats reared in a complex environment. Psychoneuroendocrinology 21:189-201.

Jucker M (2010) The benefits and limitations of animal models for translational research in neurodegenerative diseases. Nat Med 16:1210-1214.

Kabarowski JH, Zhu K, Le LQ, Witte ON, Xu Y (2001) Lysophosphatidylcholine as a ligand for the immunoregulatory receptor G2A. Science 293:702-705.

Kaether C, Haass C (2004) A lipid boundary separates APP and secretases and limits amyloid beta-peptide generation. J Cell Biol 167:809-812.

Kalaria RN, Maestre GE, Arizaga R, Friedland RP, Galasko D, Hall K, Luchsinger JA, Ogunniyi A, Perry EK, Potocnik F, Prince M, Stewart R, Wimo A, Zhang ZX, Antuono P (2008) Alzheimer's disease and vascular dementia in developing countries: prevalence, management, and risk factors. Lancet Neurol 7:812-826.

Kalyvas A, David S (2004) Cytosolic phospholipase A2 plays a key role in the pathogenesis of multiple sclerosis-like disease. Neuron 41:323-335.

Kane LP, Mollenauer MN, Xu Z, Turck CW, Weiss A (2002) Akt-dependent phosphorylation specifically regulates Cot induction of NF-kappa B-dependent transcription. Mol Cell Biol 22:5962-5974.

Karlstetter M, Lippe E, Walczak Y, Moehle C, Aslanidis A, Mirza M, Langmann T (2011) Curcumin is a potent modulator of microglial gene expression and migration. J Neuroinflammation 8:125.

Katsuki H, Okuda S (1995) Arachidonic acid as a neurotoxic and neurotrophic substance. Prog Neurobiol 46:607-636.

Kennedy BP, Payette P, Mudgett J, Vadas P, Pruzanski W, Kwan M, Tang C, Rancourt DE, Cromlish WA (1995) A natural disruption of the secretory group II phospholipase A2 gene in inbred mouse strains. J Biol Chem 270:22378-22385.

Kerokoski P, Suuronen T, Salminen A, Soininen H, Pirttila T (2002) Cleavage of the cyclin-dependent kinase 5 activator p35 to p25 does not induce tau hyperphosphorylation. Biochem Biophys Res Commun 298:693-698.

Kersaitis C, Halliday GM, Kril JJ (2004) Regional and cellular pathology in frontotemporal dementia: relationship to stage of disease in cases with and without Pick bodies. Acta Neuropathol 108:515-523.

Kesavapany S, Zheng YL, Amin N, Pant HC (2007) Peptides derived from Cdk5 activator p35, specifically inhibit deregulated activity of Cdk5. Biotechnol J 2:978-987.

Kesavapany S, Lau KF, McLoughlin DM, Brownlees J, Ackerley S, Leigh PN, Shaw CE, Miller CC (2001) p35/cdk5 binds and phosphorylates beta-catenin and regulates beta-catenin/presenilin-1 interaction. Eur J Neurosci 13:241-247.

Kesavapany S, Pareek TK, Zheng YL, Amin N, Gutkind JS, Ma W, Kulkarni AB, Grant P, Pant HC (2006) Neuronal nuclear organization is controlled by cyclin-dependent kinase 5 phosphorylation of Ras Guanine nucleotide releasing factor-1. Neurosignals 15:157-173.

Kesavapany S, Amin N, Zheng YL, Nijhara R, Jaffe H, Sihag R, Gutkind JS, Takahashi S, Kulkarni A, Grant P, Pant HC (2004) p35/cyclin-dependent kinase 5 phosphorylation of ras guanine nucleotide releasing factor 2 (RasGRF2) mediates Rac-dependent Extracellular Signal-regulated kinase 1/2 activity, altering RasGRF2 and microtubule-associated protein 1b distribution in neurons. J Neurosci 24:4421-4431.

Khachaturian ZS (1985) Diagnosis of Alzheimer's disease. Arch Neurol 42:1097-1105.

Khatoon S, Grundke-Iqbal I, Iqbal K (1992) Brain levels of microtubule-associated protein tau are elevated in Alzheimer's disease: a radioimmuno-slot-blot assay for nanograms of the protein. J Neurochem 59:750-753.

Kim D, Frank CL, Dobbin MM, Tsunemoto RK, Tu W, Peng PL, Guan JS, Lee BH, Moy LY, Giusti P, Broodie N, Mazitschek R, Delalle I, Haggarty SJ, Neve RL, Lu Y, Tsai LH (2008) Deregulation of HDAC1 by p25/Cdk5 in neurotoxicity. Neuron 60:803-817.

Kim HY, Park EJ, Joe EH, Jou I (2003) Curcumin suppresses Janus kinase-STAT inflammatory signaling through activation of Src homology 2 domain-containing tyrosine phosphatase 2 in brain microglia. J Immunol 171:6072-6079.

Kirkitadze MD, Bitan G, Teplow DB (2002) Paradigm shifts in Alzheimer's disease and other neurodegenerative disorders: the emerging role of oligomeric assemblies. J Neurosci Res 69:567-577.

Ko J, Humbert S, Bronson RT, Takahashi S, Kulkarni AB, Li E, Tsai LH (2001) p35 and p39 are essential for cyclin-dependent kinase 5 function during neurodevelopment. J Neurosci 21:6758-6771.

Koenigsknecht-Talboo J, Landreth GE (2005) Microglial phagocytosis induced by fibrillar beta-amyloid and IgGs are differentially regulated by proinflammatory cytokines. J Neurosci 25:8240-8249.

Kofuji P, Newman EA (2004) Potassium buffering in the central nervous system. Neuroscience 129:1045-1056.

Koistinaho M, Lin S, Wu X, Esterman M, Koger D, Hanson J, Higgs R, Liu F, Malkani S, Bales KR, Paul SM (2004) Apolipoprotein E promotes astrocyte colocalization and degradation of deposited amyloid-beta peptides. Nat Med 10:719-726.

Komarova NL, Thalhauser CJ (2011) High degree of heterogeneity in Alzheimer's disease progression patterns. PLoS Comput Biol 7:e1002251.

Kosik KS, Joachim CL, Selkoe DJ (1986) Microtubule-associated protein tau (tau) is a major antigenic component of paired helical filaments in Alzheimer disease. Proc Natl Acad Sci U S A 83:4044-4048.

Kraepelin E (1910) Psychiatrie: Ein Lehrbuch für Studierende und Árzte. Barth, Leipzig 593–632.

Krause DL, Muller N (2010) Neuroinflammation, microglia and implications for anti-inflammatory treatment in Alzheimer's disease. Int J Alzheimers Dis 2010.

Kriem B, Sponne I, Fifre A, Malaplate-Armand C, Lozac'h-Pillot K, Koziel V, Yen-Potin FT, Bihain B, Oster T, Olivier JL, Pillot T (2005) Cytosolic phospholipase A2 mediates neuronal apoptosis induced by soluble oligomers of the amyloid-beta peptide. Faseb J 19:85-87.

Kriz J, Gowing G, Julien JP (2003) Efficient three-drug cocktail for disease induced by mutant superoxide dismutase. Ann Neurol 53:429-436.

Kroner Z (2009) The relationship between Alzheimer's disease and diabetes: Type 3 diabetes? Altern Med Rev 14:373-379.

Kusakawa G, Saito T, Onuki R, Ishiguro K, Kishimoto T, Hisanaga S (2000) Calpain-dependent proteolytic cleavage of the p35 cyclin-dependent kinase 5 activator to p25. J Biol Chem 275:17166-17172.

Kuwako K, Nishimura I, Uetsuki T, Saido TC, Yoshikawa K (2002) Activation of calpain in cultured neurons overexpressing Alzheimer amyloid precursor protein. Brain Res Mol Brain Res 107:166-175.

Kwon YT, Tsai LH (1998) A novel disruption of cortical development in p35(-/-) mice distinct from reeler. J Comp Neurol 395:510-522.

Lace GL, Wharton SB, Ince PG (2007) A brief history of tau: the evolving view of the microtubule-associated protein tau in neurodegenerative diseases. Clin Neuropathol 26:43-58.

Lai KO, Ip NY (2009) Recent advances in understanding the roles of Cdk5 in synaptic plasticity. Biochim Biophys Acta 1792:741-745.

Larson EB, Wang L, Bowen JD, McCormick WC, Teri L, Crane P, Kukull W (2006) Exercise is associated with reduced risk for incident dementia among persons 65 years of age and older. Ann Intern Med 144:73-81.

Lau LF, Seymour PA, Sanner MA, Schachter JB (2002) Cdk5 as a drug target for the treatment of Alzheimer's disease. J Mol Neurosci 19:267-273.

Lauber K, Bohn E, Krober SM, Xiao YJ, Blumenthal SG, Lindemann RK, Marini P, Wiedig C, Zobywalski A, Baksh S, Xu Y, Autenrieth IB, Schulze-Osthoff K, Belka C, Stuhler G, Wesselborg S (2003) Apoptotic cells induce migration of phagocytes via caspase-3-mediated release of a lipid attraction signal. Cell 113:717-730.

Lautner R, Mattsson N, Scholl M, Augutis K, Blennow K, Olsson B, Zetterberg H (2011) Biomarkers for microglial activation in Alzheimer's disease. Int J Alzheimers Dis 2011:939426.

Le Prince G, Delaere P, Fages C, Duyckaerts C, Hauw JJ, Tardy M (1993) Alterations of glial fibrillary acidic protein mRNA level in the aging brain and in senile dementia of the Alzheimer type. Neurosci Lett 151:71-73.

Lee CW, Lin CC, Lee IT, Lee HC, Yang CM (2011) Activation and induction of cytosolic phospholipase A2 by TNF-alpha mediated through Nox2, MAPKs, NF-kappaB, and p300 in human tracheal smooth muscle cells. J Cell Physiol 226:2103-2114.

Lee CW, Lee IT, Lin CC, Lee HC, Lin WN, Yang CM (2010) Activation and induction of cytosolic phospholipase A2 by IL-1beta in human tracheal smooth muscle cells: role of MAPKs/p300 and NF-kappaB. J Cell Biochem 109:1045-1056.

Lee KY, Clark AW, Rosales JL, Chapman K, Fung T, Johnston RN (1999) Elevated neuronal Cdc2-like kinase activity in the Alzheimer disease brain. Neurosci Res 34:21-29.

Lee MS, Tsai LH (2003) Cdk5: one of the links between senile plaques and neurofibrillary tangles? J Alzheimers Dis 5:127-137.

Lee MS, Kwon YT, Li M, Peng J, Friedlander RM, Tsai LH (2000) Neurotoxicity induces cleavage of p35 to p25 by calpain. Nature 405:360-364.

Lee MS, Kao SC, Lemere CA, Xia W, Tseng HC, Zhou Y, Neve R, Ahlijanian MK, Tsai LH (2003) APP processing is regulated by cytoplasmic phosphorylation. J Cell Biol 163:83-95.

Lew J, Winkfein RJ, Paudel HK, Wang JH (1992) Brain proline-directed protein kinase is a neurofilament kinase which displays high sequence homology to p34cdc2. J Biol Chem 267:25922-25926.

Lew J, Huang QQ, Qi Z, Winkfein RJ, Aebersold R, Hunt T, Wang JH (1994) A brain-specific activator of cyclin-dependent kinase 5. Nature 371:423-426.

Lew J, Qi Z, Huang QQ, Paudel H, Matsuura I, Matsushita M, Zhu X, Wang JH (1995) Structure, function, and regulation of neuronal Cdc2-like protein kinase. Neurobiol Aging 16:263-268; discussion 268-270.

Lewis J, Dickson DW, Lin WL, Chisholm L, Corral A, Jones G, Yen SH, Sahara N, Skipper L, Yager D, Eckman C, Hardy J, Hutton M, McGowan E (2001) Enhanced neurofibrillary degeneration in transgenic mice expressing mutant tau and APP. Science 293:1487-1491.

Li B, Chohan MO, Grundke-Iqbal I, Iqbal K (2007) Disruption of microtubule network by Alzheimer abnormally hyperphosphorylated tau. Acta Neuropathol 113:501-511.

Li BS, Zhang L, Takahashi S, Ma W, Jaffe H, Kulkarni AB, Pant HC (2002) Cyclin-dependent kinase 5 prevents neuronal apoptosis by negative regulation of c-Jun N-terminal kinase 3. Embo J 21:324-333.

Li BS, Ma W, Jaffe H, Zheng Y, Takahashi S, Zhang L, Kulkarni AB, Pant HC (2003) Cyclin-dependent kinase-5 is involved in neuregulin-dependent activation of phosphatidylinositol 3-kinase and Akt activity mediating neuronal survival. J Biol Chem 278:35702-35709.

Li BS, Sun MK, Zhang L, Takahashi S, Ma W, Vinade L, Kulkarni AB, Brady RO, Pant HC (2001) Regulation of NMDA receptors by cyclin-dependent kinase-5. Proc Natl Acad Sci U S A 98:12742-12747.

Li F, Calingasan NY, Yu F, Mauck WM, Toidze M, Almeida CG, Takahashi RH, Carlson GA, Flint Beal M, Lin MT, Gouras GK (2004) Increased plaque burden in brains of APP mutant MnSOD heterozygous knockout mice. J Neurochem 89:1308-1312.

Lilja L, Yang SN, Webb DL, Juntti-Berggren L, Berggren PO, Bark C (2001) Cyclin-dependent kinase 5 promotes insulin exocytosis. J Biol Chem 276:34199-34205.

Lim AC, Hou Z, Goh CP, Qi RZ (2004) Protein kinase CK2 is an inhibitor of the neuronal Cdk5 kinase. J Biol Chem 279:46668-46673.

Lim GP, Chu T, Yang F, Beech W, Frautschy SA, Cole GM (2001) The curry spice curcumin reduces oxidative damage and amyloid pathology in an Alzheimer transgenic mouse. J Neurosci 21:8370-8377.

Lin MT, Beal MF (2006) Mitochondrial dysfunction and oxidative stress in neurodegenerative diseases. Nature 443:787-795.

Lipton SA, Rosenberg PA (1994) Excitatory amino acids as a final common pathway for neurologic disorders. N Engl J Med 330:613-622.

Liu F, Iqbal K, Grundke-Iqbal I, Rossie S, Gong CX (2005) Dephosphorylation of tau by protein phosphatase 5: impairment in Alzheimer's disease. J Biol Chem 280:1790-1796.

Liu R, Tian B, Gearing M, Hunter S, Ye K, Mao Z (2008) Cdk5-mediated regulation of the PIKE-A-Akt pathway and glioblastoma cell invasion. Proc Natl Acad Sci U S A 105:7570-7575.

Locascio JJ, Growdon JH, Corkin S (1995) Cognitive test performance in detecting, staging, and tracking Alzheimer's disease. Arch Neurol 52:1087-1099.

Lopes JP, Oliveira CR, Agostinho P (2007) Role of cyclin-dependent kinase 5 in the neurodegenerative process triggered by amyloid-Beta and prion peptides: implications for Alzheimer's disease and prion-related encephalopathies. Cell Mol Neurobiol 27:943-957.

Lopes JP, Oliveira CR, Agostinho P (2010) Neurodegeneration in an Abeta-induced model of Alzheimer's disease: the role of Cdk5. Aging Cell 9:64-77.

Lopez-Tobon A, Castro-Alvarez JF, Piedrahita D, Boudreau RL, Gallego-Gomez JC, Cardona-Gomez GP (2011) Silencing of CDK5 as potential therapy for Alzheimer's disease. Rev Neurosci 22:143-152.

Lu Y, Li T, Qureshi HY, Han D, Paudel HK (2011) Early growth response 1 (Egr-1) regulates phosphorylation of microtubule-associated protein tau in mammalian brain. J Biol Chem 286:20569-20581.

Lue LF, Kuo YM, Beach T, Walker DG (2010) Microglia activation and anti-inflammatory regulation in Alzheimer's disease. Mol Neurobiol 41:115-128.

Lue LF, Rydel R, Brigham EF, Yang LB, Hampel H, Murphy GM, Jr., Brachova L, Yan SD, Walker DG, Shen Y, Rogers J (2001)

Inflammatory repertoire of Alzheimer's disease and nondemented elderly microglia in vitro. Glia 35:72-79.

Luo S, Vacher C, Davies JE, Rubinsztein DC (2005) Cdk5 phosphorylation of huntingtin reduces its cleavage by caspases: implications for mutant huntingtin toxicity. J Cell Biol 169:647-656.

Luo SF, Lin WN, Yang CM, Lee CW, Liao CH, Leu YL, Hsiao LD (2006) Induction of cytosolic phospholipase A2 by lipopolysaccharide in canine tracheal smooth muscle cells: involvement of MAPKs and NF-kappaB pathways. Cell Signal 18:1201-1211.

Luo XG, Chen SD (2012) The changing phenotype of microglia from homeostasis to disease. Transl Neurodegener 1:9.

Luster AD (1998) Chemokines--chemotactic cytokines that mediate inflammation. N Engl J Med 338:436-445.

Ma QL, Yang F, Rosario ER, Ubeda OJ, Beech W, Gant DJ, Chen PP, Hudspeth B, Chen C, Zhao Y, Vinters HV, Frautschy SA, Cole GM (2009) Beta-amyloid oligomers induce phosphorylation of tau and inactivation of insulin receptor substrate via c-Jun N-terminal kinase signaling: suppression by omega-3 fatty acids and curcumin. J Neurosci 29:9078-9089.

Mahley RW (1988) Apolipoprotein E: cholesterol transport protein with expanding role in cell biology. Science 240:622-630.

Majumdar A, Cruz D, Asamoah N, Buxbaum A, Sohar I, Lobel P, Maxfield FR (2007) Activation of microglia acidifies lysosomes and leads to degradation of Alzheimer amyloid fibrils. Mol Biol Cell 18:1490-1496.

Mandelkow EM, Biernat J, Drewes G, Gustke N, Trinczek B, Mandelkow E (1995) Tau domains, phosphorylation, and interactions with microtubules. Neurobiol Aging 16:355-362; discussion 362-353.

Maragakis NJ, Rothstein JD (2006) Mechanisms of Disease: astrocytes in neurodegenerative disease. Nat Clin Pract Neurol 2:679-689.

Mariani E, Monastero R, Mecocci P (2007) Mild cognitive impairment: a systematic review. J Alzheimers Dis 12:23-35.

Masferrer JL, Isakson PC, Seibert K (1996) Cyclooxygenase-2 inhibitors: a new class of anti-inflammatory agents that spare the gastrointestinal tract. Gastroenterol Clin North Am 25:363-372.

Maurer K, Volk S, Gerbaldo H (1997) Auguste D and Alzheimer's disease. Lancet 349:1546-1549.

McCool MF, Varty GB, Del Vecchio RA, Kazdoba TM, Parker EM, Hunter JC, Hyde LA (2003) Increased auditory startle response and reduced prepulse inhibition of startle in transgenic mice expressing a double mutant form of amyloid precursor protein. Brain Res 994:99-106.

McGeer PL, Schulzer M, McGeer EG (1996) Arthritis and anti-inflammatory agents as possible protective factors for Alzheimer's disease: a review of 17 epidemiologic studies. Neurology 47:425-432.

McGeer PL, Itagaki S, Boyes BE, McGeer EG (1988) Reactive microglia are positive for HLA-DR in the substantia nigra of Parkinson's and Alzheimer's disease brains. Neurology 38:1285-1291.

McGowan E, Sanders S, Iwatsubo T, Takeuchi A, Saido T, Zehr C, Yu X, Uljon S, Wang R, Mann D, Dickson D, Duff K (1999) Amyloid phenotype characterization of transgenic mice overexpressing both mutant amyloid precursor protein and mutant presenilin 1 transgenes. Neurobiol Dis 6:231-244.

McKhann G, Drachman D, Folstein M, Katzman R, Price D, Stadlan EM (1984) Clinical diagnosis of Alzheimer's disease: report of the NINCDS-ADRDA Work Group under the auspices of Department of Health and Human Services Task Force on Alzheimer's Disease. Neurology 34:939-944.

McKhann GM, Knopman DS, Chertkow H, Hyman BT, Jack CR, Jr., Kawas CH, Klunk WE, Koroshetz WJ, Manly JJ, Mayeux R, Mohs RC, Morris JC, Rossor MN, Scheltens P, Carrillo MC, Thies B, Weintraub S, Phelps CH (2011) The diagnosis of dementia due to Alzheimer's disease: recommendations from the National Institute on Aging-Alzheimer's Association workgroups on diagnostic guidelines for Alzheimer's disease. Alzheimers Dement 7:263-269.

McLellan ME, Kajdasz ST, Hyman BT, Bacskai BJ (2003) In vivo imaging of reactive oxygen species specifically associated with thioflavine S-positive amyloid plaques by multiphoton microscopy. J Neurosci 23:2212-2217.

Meda L, Baron P, Scarlato G (2001) Glial activation in Alzheimer's disease: the role of Abeta and its associated proteins. Neurobiol Aging 22:885-893.

Mehta SL, Manhas N, Raghubir R (2007) Molecular targets in cerebral ischemia for developing novel therapeutics. Brain Res Rev 54:34-66.

Menon VP, Sudheer AR (2007) Antioxidant and anti-inflammatory properties of curcumin. Adv Exp Med Biol 595:105-125.

Meyerson M, Enders GH, Wu CL, Su LK, Gorka C, Nelson C, Harlow E, Tsai LH (1992) A family of human cdc2-related protein kinases. Embo J 11:2909-2917.

Mildner A, Schmidt H, Nitsche M, Merkler D, Hanisch UK, Mack M, Heikenwalder M, Bruck W, Priller J, Prinz M (2007) Microglia in the adult brain arise from Ly-6ChiCCR2+ monocytes only under defined host conditions. Nat Neurosci 10:1544-1553.

Miller G (2005) Neuroscience. The dark side of glia. Science 308:778-781.

Mir C, Clotet J, Aledo R, Durany N, Argemi J, Lozano R, Cervos-Navarro J, Casals N (2003) CDP-choline prevents glutamate-mediated cell death in cerebellar granule neurons. J Mol Neurosci 20:53-60.

Mishra S, Palanivelu K (2008) The effect of curcumin (turmeric) on Alzheimer's disease: An overview. Ann Indian Acad Neurol 11:13-19.

Miyoshi K (2009) What is 'early onset dementia'? Psychogeriatrics 9:67-72.

Mizuno K, Plattner F, Peter Giese K (2006) Expression of p25 impairs contextual learning but not latent inhibition in mice. Neuroreport 17:1903-1905.

Mohajeri MH, Saini KD, Nitsch RM (2004) Transgenic BACE expression in mouse neurons accelerates amyloid plaque pathology. J Neural Transm 111:413-425.

Moller HJ, Graeber MB (1998) The case described by Alois Alzheimer in 1911. Historical and conceptual perspectives based on the clinical record and neurohistological sections. Eur Arch Psychiatry Clin Neurosci 248:111-122.

Monastero R, Mangialasche F, Camarda C, Ercolani S, Camarda R (2009) A systematic review of neuropsychiatric symptoms in mild cognitive impairment. J Alzheimers Dis 18:11-30.

Monroy A, Lithgow GJ, Alavez S (2013) Curcumin and neurodegenerative diseases. Biofactors 39:122-132.

Moorthamer M, Chaudhuri B (1999) Identification of ribosomal protein L34 as a novel Cdk5 inhibitor. Biochem Biophys Res Commun 255:631-638.

Morgan DO (1997) Cyclin-dependent kinases: engines, clocks, and microprocessors. Annu Rev Cell Dev Biol 13:261-291.

Mrak RE, Griffin WS (2001) Interleukin-1, neuroinflammation, and Alzheimer's disease. Neurobiol Aging 22:903-908.

Mrak RE, Griffin WS (2005) Glia and their cytokines in progression of neurodegeneration. Neurobiol Aging 26:349-354.

Musa FR, Tokuda M, Kuwata Y, Ogawa T, Tomizawa K, Konishi R, Takenaka I, Hatase O (1998) Expression of cyclin-dependent kinase 5 and associated cyclins in Leydig and Sertoli cells of the testis. J Androl 19:657-666.

Muyllaert D, Terwel D, Kremer A, Sennvik K, Borghgraef P, Devijver H, Dewachter I, Van Leuven F (2008) Neurodegeneration and neuroinflammation in cdk5/p25-inducible mice: a model for hippocampal sclerosis and neocortical degeneration. Am J Pathol 172:470-485.

Nagele RG, Wegiel J, Venkataraman V, Imaki H, Wang KC, Wegiel J (2004) Contribution of glial cells to the development of amyloid plaques in Alzheimer's disease. Neurobiol Aging 25:663-674.

Nakka VP, Gusain A, Mehta SL, Raghubir R (2008) Molecular mechanisms of apoptosis in cerebral ischemia: multiple neuroprotective opportunities. Mol Neurobiol 37:7-38.

Naslund J, Haroutunian V, Mohs R, Davis KL, Davies P, Greengard P, Buxbaum JD (2000) Correlation between elevated levels of amyloid beta-peptide in the brain and cognitive decline. Jama 283:1571-1577.

National Institute on Aging (2013) The Alzheimer's Disease Research Summit 2012 In: National Institue on Aging.

National Institute on Aging, Health and Human Services Department NIHNIA (2003) Alzheimer's Disease: Unraveling the Mystery: U.S. Government Printing Office.

Nguyen MD, Lariviere RC, Julien JP (2001) Deregulation of Cdk5 in a mouse model of ALS: toxicity alleviated by perikaryal neurofilament inclusions. Neuron 30:135-147.

Nguyen MD, Boudreau M, Kriz J, Couillard-Despres S, Kaplan DR, Julien JP (2003) Cell cycle regulators in the neuronal death pathway of amyotrophic lateral sclerosis caused by mutant superoxide dismutase 1. J Neurosci 23:2131-2140.

Niethammer M, Smith DS, Ayala R, Peng J, Ko J, Lee MS, Morabito M, Tsai LH (2000) NUDEL is a novel Cdk5 substrate that associates with LIS1 and cytoplasmic dynein. Neuron 28:697-711.

Nikolic M, Dudek H, Kwon YT, Ramos YF, Tsai LH (1996) The cdk5/p35 kinase is essential for neurite outgrowth during neuronal differentiation. Genes Dev 10:816-825.

Nikolic M, Chou MM, Lu W, Mayer BJ, Tsai LH (1998) The p35/Cdk5 kinase is a neuron-specific Rac effector that inhibits Pak1 activity. Nature 395:194-198.

Nimmerjahn A, Kirchhoff F, Helmchen F (2005) Resting microglial cells are highly dynamic surveillants of brain parenchyma in vivo. Science 308:1314-1318.

Noble W, Olm V, Takata K, Casey E, Mary O, Meyerson J, Gaynor K, LaFrancois J, Wang L, Kondo T, Davies P, Burns M, Veeranna, Nixon R, Dickson D, Matsuoka Y, Ahlijanian M, Lau LF, Duff K (2003) Cdk5 is a key factor in tau aggregation and tangle formation in vivo. Neuron 38:555-565.

Noetzli M, Eap CB (2013) Pharmacodynamic, pharmacokinetic and pharmacogenetic aspects of drugs used in the treatment of Alzheimer's disease. Clin Pharmacokinet 52:225-241.

O'Banion MK (1999) Cyclooxygenase-2: molecular biology, pharmacology, and neurobiology. Crit Rev Neurobiol 13:45-82.

O'Hare MJ, Kushwaha N, Zhang Y, Aleyasin H, Callaghan SM, Slack RS, Albert PR, Vincent I, Park DS (2005) Differential roles of nuclear and cytoplasmic cyclin-dependent kinase 5 in apoptotic and excitotoxic neuronal death. J Neurosci 25:8954-8966.

O'Keefe GM, Nguyen VT, Benveniste EN (1999) Class II transactivator and class II MHC gene expression in microglia: modulation by the cytokines TGF-beta, IL-4, IL-13 and IL-10. Eur J Immunol 29:1275-1285.

Oakley H, Cole SL, Logan S, Maus E, Shao P, Craft J, Guillozet-Bongaarts A, Ohno M, Disterhoft J, Van Eldik L, Berry R, Vassar R (2006) Intraneuronal beta-amyloid aggregates, neurodegeneration, and neuron loss in transgenic mice with five familial Alzheimer's disease mutations: potential factors in amyloid plaque formation. J Neurosci 26:10129-10140.

Oddo S (2008) The ubiquitin-proteasome system in Alzheimer's disease. J Cell Mol Med 12:363-373.

Oddo S, Caccamo A, Kitazawa M, Tseng BP, LaFerla FM (2003) Amyloid deposition precedes tangle formation in a triple transgenic model of Alzheimer's disease. Neurobiol Aging 24:1063-1070.

Oh KJ, Perez SE, Lagalwar S, Vana L, Binder L, Mufson EJ (2010) Staging of Alzheimer's pathology in triple transgenic mice: a light and electron microscopic analysis. Int J Alzheimers Dis 2010.

Ohshima T, Gilmore EC, Longenecker G, Jacobowitz DM, Brady RO, Herrup K, Kulkarni AB (1999) Migration defects of cdk5(-/-) neurons in the developing cerebellum is cell autonomous. J Neurosci 19:6017-6026.

Ohshima T, Ward JM, Huh CG, Longenecker G, Veeranna, Pant HC, Brady RO, Martin LJ, Kulkarni AB (1996) Targeted disruption of the cyclin-dependent kinase 5 gene results in abnormal corticogenesis, neuronal pathology and perinatal death. Proc Natl Acad Sci U S A 93:11173-11178.

Ohshima T, Ogura H, Tomizawa K, Hayashi K, Suzuki H, Saito T, Kamei H, Nishi A, Bibb JA, Hisanaga S, Matsui H, Mikoshiba K (2005) Impairment of hippocampal long-term depression and defective spatial learning and memory in p35 mice. J Neurochem 94:917-925.

Ojala PJ, Hirvonen TE, Hermansson M, Somerharju P, Parkkinen J (2007) Acyl chain-dependent effect of lysophosphatidylcholine on human neutrophils. J Leukoc Biol 82:1501-1509.

Olabarria M, Noristani HN, Verkhratsky A, Rodriguez JJ (2010) Concomitant astroglial atrophy and astrogliosis in a triple transgenic animal model of Alzheimer's disease. Glia 58:831-838.

Ousman SS, David S (2001) MIP-1alpha, MCP-1, GM-CSF, and TNF-alpha control the immune cell response that mediates rapid phagocytosis of myelin from the adult mouse spinal cord. J Neurosci 21:4649-4656.

Ozmen L, Woolley M, Albientz A, Miss MT, Nelboeck P, Malherbe P, Czech C, Gruninger-Leitch F, Brockhaus M, Ballard T, Jacobsen H (2005) BACE/APPV717F double-transgenic mice develop cerebral amyloidosis and inflammation. Neurodegener Dis 2:284-298.

Paglini G, Pigino G, Kunda P, Morfini G, Maccioni R, Quiroga S, Ferreira A, Caceres A (1998) Evidence for the participation of the neuron-specific CDK5 activator P35 during laminin-enhanced axonal growth. J Neurosci 18:9858-9869.

Pan MH, Huang TM, Lin JK (1999) Biotransformation of curcumin through reduction and glucuronidation in mice. Drug Metab Dispos 27:486-494.

Paradisi S, Sacchetti B, Balduzzi M, Gaudi S, Malchiodi-Albedi F (2004) Astrocyte modulation of in vitro beta-amyloid neurotoxicity. Glia 46:252-260.

Pareek TK, Keller J, Kesavapany S, Pant HC, Iadarola MJ, Brady RO, Kulkarni AB (2006) Cyclin-dependent kinase 5 activity regulates pain signaling. Proc Natl Acad Sci U S A 103:791-796.

Park SY, Jin ML, Kim YH, Kim Y, Lee SJ (2012) Anti-inflammatory effects of aromatic-turmerone through blocking of NF-kappaB, JNK, and p38 MAPK signaling pathways in amyloid beta-stimulated microglia. Int Immunopharmacol 14:13-20.

Pasqualetti P, Bonomini C, Dal Forno G, Paulon L, Sinforiani E, Marra C, Zanetti O, Rossini PM (2009) A randomized controlled study on effects of ibuprofen on cognitive progression of Alzheimer's disease. Aging Clin Exp Res 21:102-110.

Patrick GN, Zhou P, Kwon YT, Howley PM, Tsai LH (1998) p35, the neuronal-specific activator of cyclin-dependent kinase 5 (Cdk5) is

degraded by the ubiquitin-proteasome pathway. J Biol Chem 273:24057-24064.

Patrick GN, Zukerberg L, Nikolic M, de la Monte S, Dikkes P, Tsai LH (1999) Conversion of p35 to p25 deregulates Cdk5 activity and promotes neurodegeneration. Nature 402:615-622.

Patzke H, Tsai LH (2002a) Cdk5 sinks into ALS. Trends Neurosci 25:8-10.

Patzke H, Tsai LH (2002b) Calpain-mediated cleavage of the cyclin-dependent kinase-5 activator p39 to p29. J Biol Chem 277:8054-8060.

Patzke H, Maddineni U, Ayala R, Morabito M, Volker J, Dikkes P, Ahlijanian MK, Tsai LH (2003) Partial rescue of the p35-/- brain phenotype by low expression of a neuronal-specific enolase p25 transgene. J Neurosci 23:2769-2778.

Paul AT, Gohil VM, Bhutani KK (2006) Modulating TNF-alpha signaling with natural products. Drug Discov Today 11:725-732.

Pavletich NP (1999) Mechanisms of cyclin-dependent kinase regulation: structures of Cdks, their cyclin activators, and Cip and INK4 inhibitors. J Mol Biol 287:821-828.

Pei JJ, Grundke-Iqbal I, Iqbal K, Bogdanovic N, Winblad B, Cowburn RF (1998) Accumulation of cyclin-dependent kinase 5 (cdk5) in neurons with early stages of Alzheimer's disease neurofibrillary degeneration. Brain Res 797:267-277.

Pekny M, Nilsson M (2005) Astrocyte activation and reactive gliosis. Glia 50:427-434.

Pepicelli O, Fedele E, Bonanno G, Raiteri M, Ajmone-Cat MA, Greco A, Levi G, Minghetti L (2002) In vivo activation of N-methyl-D-aspartate receptors in the rat hippocampus increases prostaglandin E(2) extracellular levels and triggers lipid peroxidation through cyclooxygenase-mediated mechanisms. J Neurochem 81:1028-1034.

Perrin RJ, Fagan AM, Holtzman DM (2009) Multimodal techniques for diagnosis and prognosis of Alzheimer's disease. Nature 461:916-922.

Piedrahita D, Hernandez I, Lopez-Tobon A, Fedorov D, Obara B, Manjunath BS, Boudreau RL, Davidson B, Laferla F, Gallego-Gomez JC, Kosik KS, Cardona-Gomez GP (2010) Silencing of CDK5 reduces

neurofibrillary tangles in transgenic alzheimer's mice. J Neurosci 30:13966-13976.

Pineda D, Ampurdanes C, Medina MG, Serratosa J, Tusell JM, Saura J, Planas AM, Navarro P (2012) Tissue plasminogen activator induces microglial inflammation via a noncatalytic molecular mechanism involving activation of mitogen-activated protein kinases and Akt signaling pathways and AnnexinA2 and Galectin-1 receptors. Glia 60:526-540.

Poon RY, Lew J, Hunter T (1997) Identification of functional domains in the neuronal Cdk5 activator protein. J Biol Chem 272:5703-5708.

Prasad S, Aggarwal BB (2011) Turmeric, the Golden Spice: From Traditional Medicine to Modern Medicine.

Pratico D, Sung S (2004) Lipid peroxidation and oxidative imbalance: early functional events in Alzheimer's disease. J Alzheimers Dis 6:171-175.

Qin ZX, Zhu HY, Hu YH (2009) Effects of lysophosphatidylcholine on beta-amyloid-induced neuronal apoptosis. Acta Pharmacol Sin 30:388-395.

Qu D, Li Q, Lim HY, Cheung NS, Li R, Wang JH, Qi RZ (2002) The protein SET binds the neuronal Cdk5 activator p35nck5a and modulates Cdk5/p35nck5a activity. J Biol Chem 277:7324-7332.

Qu D, Rashidian J, Mount MP, Aleyasin H, Parsanejad M, Lira A, Haque E, Zhang Y, Callaghan S, Daigle M, Rousseaux MW, Slack RS, Albert PR, Vincent I, Woulfe JM, Park DS (2007) Role of Cdk5-mediated phosphorylation of Prx2 in MPTP toxicity and Parkinson's disease. Neuron 55:37-52.

Radu CG, Yang LV, Riedinger M, Au M, Witte ON (2004) T cell chemotaxis to lysophosphatidylcholine through the G2A receptor. Proc Natl Acad Sci U S A 101:245-250.

Ralay Ranaivo H, Craft JM, Hu W, Guo L, Wing LK, Van Eldik LJ, Watterson DM (2006) Glia as a therapeutic target: selective suppression of human amyloid-beta-induced upregulation of brain proinflammatory cytokine production attenuates neurodegeneration. J Neurosci 26:662-670.

Ramos CD, Canetti C, Souto JT, Silva JS, Hogaboam CM, Ferreira SH, Cunha FQ (2005) MIP-1alpha[CCL3] acting on the CCR1 receptor mediates

neutrophil migration in immune inflammation via sequential release of TNF-alpha and LTB4. J Leukoc Biol 78:167-177.

Reaux-Le Goazigo A, Van Steenwinckel J, Rostene W, Melik Parsadaniantz S (2013) Current status of chemokines in the adult CNS. Prog Neurobiol 104:67-92.

Rezai-Zadeh K, Gate D, Town T (2009) CNS infiltration of peripheral immune cells: D-Day for neurodegenerative disease? J Neuroimmune Pharmacol 4:462-475.

Riendeau D, Guay J, Weech PK, Laliberte F, Yergey J, Li C, Desmarais S, Perrier H, Liu S, Nicoll-Griffith D, et al. (1994) Arachidonyl trifluoromethyl ketone, a potent inhibitor of 85-kDa phospholipase A2, blocks production of arachidonate and 12-hydroxyeicosatetraenoic acid by calcium ionophore-challenged platelets. J Biol Chem 269:15619-15624.

Rodgers AB, National Institute on A, National Institutes of H (2002) Alzheimer's disease: unraveling the mystery: National Institutes of Health.

Rogers J, Webster S, Lue LF, Brachova L, Civin WH, Emmerling M, Shivers B, Walker D, McGeer P (1996) Inflammation and Alzheimer's disease pathogenesis. Neurobiol Aging 17:681-686.

Rogers J, Kirby LC, Hempelman SR, Berry DL, McGeer PL, Kaszniak AW, Zalinski J, Cofield M, Mansukhani L, Willson P, et al. (1993) Clinical trial of indomethacin in Alzheimer's disease. Neurology 43:1609-1611.

Rohan de Silva HA, Patel AJ (1997) Presenilins and early-onset familial Alzheimer's disease. Neuroreport 8:i-xii.

Rosen WG, Mohs RC, Davis KL (1984) A new rating scale for Alzheimer's disease. Am J Psychiatry 141:1356-1364.

Rossner S, Lange-Dohna C, Zeitschel U, Perez-Polo JR (2005) Alzheimer's disease beta-secretase BACE1 is not a neuron-specific enzyme. J Neurochem 92:226-234.

Rota E, Bellone G, Rocca P, Bergamasco B, Emanuelli G, Ferrero P (2006) Increased intrathecal TGF-beta1, but not IL-12, IFN-gamma and IL-10 levels in Alzheimer's disease patients. Neurol Sci 27:33-39.

Rothstein JD, Dykes-Hoberg M, Pardo CA, Bristol LA, Jin L, Kuncl RW, Kanai Y, Hediger MA, Wang Y, Schielke JP, Welty DF (1996) Knockout of glutamate transporters reveals a major role for astroglial transport in excitotoxicity and clearance of glutamate. Neuron 16:675-686.

Rubinsztein DC, Carmichael J (2003) Huntington's disease: molecular basis of neurodegeneration. Expert Rev Mol Med 5:1-21.

Rubio de la Torre E, Luzon-Toro B, Forte-Lago I, Minguez-Castellanos A, Ferrer I, Hilfiker S (2009) Combined kinase inhibition modulates parkin inactivation. Hum Mol Genet 18:809-823.

Russo AA, Jeffrey PD, Pavletich NP (1996) Structural basis of cyclin-dependent kinase activation by phosphorylation. Nat Struct Biol 3:696-700.

Sa G, Das T (2008) Anti cancer effects of curcumin: cycle of life and death. Cell Div 3:14.

Saez TE, Pehar M, Vargas M, Barbeito L, Maccioni RB (2004) Astrocytic nitric oxide triggers tau hyperphosphorylation in hippocampal neurons. In Vivo 18:275-280.

Sahadevan S, Saw SM, Gao W, Tan LC, Chin JJ, Hong CY, Venketasubramanian N (2008) Ethnic differences in Singapore's dementia prevalence: the stroke, Parkinson's disease, epilepsy, and dementia in Singapore study. J Am Geriatr Soc 56:2061-2068.

Saito K, Elce JS, Hamos JE, Nixon RA (1993) Widespread activation of calcium-activated neutral proteinase (calpain) in the brain in Alzheimer disease: a potential molecular basis for neuronal degeneration. Proc Natl Acad Sci U S A 90:2628-2632.

Saito T, Konno T, Hosokawa T, Asada A, Ishiguro K, Hisanaga S (2007) p25/cyclin-dependent kinase 5 promotes the progression of cell death in nucleus of endoplasmic reticulum-stressed neurons. J Neurochem 102:133-140.

Salloway S, Sperling R, Gilman S, Fox NC, Blennow K, Raskind M, Sabbagh M, Honig LS, Doody R, van Dyck CH, Mulnard R, Barakos J, Gregg KM, Liu E, Lieberburg I, Schenk D, Black R, Grundman M (2009) A

phase 2 multiple ascending dose trial of bapineuzumab in mild to moderate Alzheimer disease. Neurology 73:2061-2070.

Salmina AB (2009) Neuron-glia interactions as therapeutic targets in neurodegeneration. J Alzheimers Dis 16:485-502.

Salminen A, Huuskonen J, Ojala J, Kauppinen A, Kaarniranta K, Suuronen T (2008) Activation of innate immunity system during aging: NF-kB signaling is the molecular culprit of inflamm-aging. Ageing Res Rev 7:83-105.

Sanchez-Mejia RO, Newman JW, Toh S, Yu GQ, Zhou Y, Halabisky B, Cisse M, Scearce-Levie K, Cheng IH, Gan L, Palop JJ, Bonventre JV, Mucke L (2008) Phospholipase A2 reduction ameliorates cognitive deficits in a mouse model of Alzheimer's disease. Nat Neurosci 11:1311-1318.

Sastre M, Dewachter I, Rossner S, Bogdanovic N, Rosen E, Borghgraef P, Evert BO, Dumitrescu-Ozimek L, Thal DR, Landreth G, Walter J, Klockgether T, van Leuven F, Heneka MT (2006) Nonsteroidal anti-inflammatory drugs repress beta-secretase gene promoter activity by the activation of PPARgamma. Proc Natl Acad Sci U S A 103:443-448.

Sato K, Minegishi S, Takano J, Plattner F, Saito T, Asada A, Kawahara H, Iwata N, Saido TC, Hisanaga S (2008) Calpastatin, an endogenous calpain-inhibitor protein, regulates the cleavage of the Cdk5 activator p35 to p25. J Neurochem 117:504-515.

Satyanarayana A, Kaldis P (2009) Mammalian cell-cycle regulation: several Cdks, numerous cyclins and diverse compensatory mechanisms. Oncogene 28:2925-2939.

Schlachetzki JC, Hull M (2009) Microglial activation in Alzheimer's disease. Curr Alzheimer Res 6:554-563.

Schmitt WB, Deacon RM, Seeburg PH, Rawlins JN, Bannerman DM (2003) A within-subjects, within-task demonstration of intact spatial reference memory and impaired spatial working memory in glutamate receptor-A-deficient mice. J Neurosci 23:3953-3959.

Sekiyama K, Sugama S, Fujita M, Sekigawa A, Takamatsu Y, Waragai M, Takenouchi T, Hashimoto M (2012) Neuroinflammation in Parkinson's

Disease and Related Disorders: A Lesson from Genetically Manipulated Mouse Models of alpha-Synucleinopathies. Parkinsons Dis 2012:271732.

Sharma P, Veeranna, Sharma M, Amin ND, Sihag RK, Grant P, Ahn N, Kulkarni AB, Pant HC (2002) Phosphorylation of MEK1 by cdk5/p35 down-regulates the mitogen-activated protein kinase pathway. J Biol Chem 277:528-534.

Sharman MJ, Shui G, Fernandis AZ, Lim WL, Berger T, Hone E, Taddei K, Martins IJ, Ghiso J, Buxbaum JD, Gandy S, Wenk MR, Martins RN (2010) Profiling brain and plasma lipids in human APOE epsilon2, epsilon3, and epsilon4 knock-in mice using electrospray ionization mass spectrometry. J Alzheimers Dis 20:105-111.

Sheikh AM, Nagai A, Ryu JK, McLarnon JG, Kim SU, Masuda J (2009) Lysophosphatidylcholine induces glial cell activation: role of rho kinase. Glia 57:898-907.

Shelat PB, Chalimoniuk M, Wang JH, Strosznajder JB, Lee JC, Sun AY, Simonyi A, Sun GY (2008) Amyloid beta peptide and NMDA induce ROS from NADPH oxidase and AA release from cytosolic phospholipase A2 in cortical neurons. J Neurochem 106:45-55.

Shimmyo Y, Kihara T, Akaike A, Niidome T, Sugimoto H (2008) Epigallocatechin-3-gallate and curcumin suppress amyloid beta-induced beta-site APP cleaving enzyme-1 upregulation. Neuroreport 19:1329-1333.

Shoji M, Golde TE, Ghiso J, Cheung TT, Estus S, Shaffer LM, Cai XD, McKay DM, Tintner R, Frangione B, et al. (1992) Production of the Alzheimer amyloid beta protein by normal proteolytic processing. Science 258:126-129.

Shytle RD, Tan J, Bickford PC, Rezai-Zadeh K, Hou L, Zeng J, Sanberg PR, Sanberg CD, Alberte RS, Fink RC, Roschek B, Jr. (2012) Optimized turmeric extract reduces beta-Amyloid and phosphorylated Tau protein burden in Alzheimer's transgenic mice. Curr Alzheimer Res 9:500-506.

Siao CJ, Tsirka SE (2002) Tissue plasminogen activator mediates microglial activation via its finger domain through annexin II. J Neurosci 22:3352-3358.

Simard AR, Soulet D, Gowing G, Julien JP, Rivest S (2006) Bone marrow-derived microglia play a critical role in restricting senile plaque formation in Alzheimer's disease. Neuron 49:489-502.

Simard M, Nedergaard M (2004) The neurobiology of glia in the context of water and ion homeostasis. Neuroscience 129:877-896.

Singh S, Aggarwal BB (1995) Activation of transcription factor NF-kappa B is suppressed by curcumin (diferuloylmethane) [corrected]. J Biol Chem 270:24995-25000.

Skripuletz T, Hackstette D, Bauer K, Gudi V, Pul R, Voss E, Berger K, Kipp M, Baumgartner W, Stangel M (2012) Astrocytes regulate myelin clearance through recruitment of microglia during cuprizone-induced demyelination. Brain 136:147-167.

Slevin M, Krupinski J (2009) Cyclin-dependent kinase-5 targeting for ischaemic stroke. Curr Opin Pharmacol 9:119-124.

Smith CD, Carney JM, Starke-Reed PE, Oliver CN, Stadtman ER, Floyd RA, Markesbery WR (1991) Excess brain protein oxidation and enzyme dysfunction in normal aging and in Alzheimer disease. Proc Natl Acad Sci U S A 88:10540-10543.

Smith PD, Mount MP, Shree R, Callaghan S, Slack RS, Anisman H, Vincent I, Wang X, Mao Z, Park DS (2006) Calpain-regulated p35/cdk5 plays a central role in dopaminergic neuron death through modulation of the transcription factor myocyte enhancer factor 2. J Neurosci 26:440-447.

Smith PD, Crocker SJ, Jackson-Lewis V, Jordan-Sciutto KL, Hayley S, Mount MP, O'Hare MJ, Callaghan S, Slack RS, Przedborski S, Anisman H, Park DS (2003) Cyclin-dependent kinase 5 is a mediator of dopaminergic neuron loss in a mouse model of Parkinson's disease. Proc Natl Acad Sci U S A 100:13650-13655.

Smits HA, Rijsmus A, van Loon JH, Wat JW, Verhoef J, Boven LA, Nottet HS (2002) Amyloid-beta-induced chemokine production in primary human macrophages and astrocytes. J Neuroimmunol 127:160-168.

Sobue K, Agarwal-Mawal A, Li W, Sun W, Miura Y, Paudel HK (2000) Interaction of neuronal Cdc2-like protein kinase with microtubule-associated protein tau. J Biol Chem 275:16673-16680.

Sofroniew MV (2005) Reactive astrocytes in neural repair and protection. Neuroscientist 11:400-407.

Sofroniew MV (2009) Molecular dissection of reactive astrogliosis and glial scar formation. Trends Neurosci 32:638-647.

Solfrizzi V, Panza F, Frisardi V, Seripa D, Logroscino G, Imbimbo BP, Pilotto A (2011) Diet and Alzheimer's disease risk factors or prevention: the current evidence. Expert Rev Neurother 11:677-708.

Sonnewald U, Qu H, Aschner M (2002) Pharmacology and toxicology of astrocyte-neuron glutamate transport and cycling. J Pharmacol Exp Ther 301:1-6.

Sperling RA, Aisen PS, Beckett LA, Bennett DA, Craft S, Fagan AM, Iwatsubo T, Jack CR, Jr., Kaye J, Montine TJ, Park DC, Reiman EM, Rowe CC, Siemers E, Stern Y, Yaffe K, Carrillo MC, Thies B, Morrison-Bogorad M, Wagster MV, Phelps CH (2011) Toward defining the preclinical stages of Alzheimer's disease: recommendations from the National Institute on Aging-Alzheimer's Association workgroups on diagnostic guidelines for Alzheimer's disease. Alzheimers Dement 7:280-292.

Spillantini MG, Van Swieten JC, Goedert M (2000) Tau gene mutations in frontotemporal dementia and parkinsonism linked to chromosome 17 (FTDP-17). Neurogenetics 2:193-205.

Spillantini MG, Schmidt ML, Lee VM, Trojanowski JQ, Jakes R, Goedert M (1997) Alpha-synuclein in Lewy bodies. Nature 388:839-840.

Spires TL, Hyman BT (2005) Transgenic models of Alzheimer's disease: learning from animals. NeuroRx 2:423-437.

Stalder AK, Ermini F, Bondolfi L, Krenger W, Burbach GJ, Deller T, Coomaraswamy J, Staufenbiel M, Landmann R, Jucker M (2005) Invasion of hematopoietic cells into the brain of amyloid precursor protein transgenic mice. J Neurosci 25:11125-11132.

Steinbrecher UP, Parthasarathy S, Leake DS, Witztum JL, Steinberg D (1984) Modification of low density lipoprotein by endothelial cells involves lipid peroxidation and degradation of low density lipoprotein phospholipids. Proc Natl Acad Sci U S A 81:3883-3887.

Stephenson DT, Lemere CA, Selkoe DJ, Clemens JA (1996) Cytosolic phospholipase A2 (cPLA2) immunoreactivity is elevated in Alzheimer's disease brain. Neurobiol Dis 3:51-63.

Strittmatter WJ, Saunders AM, Schmechel D, Pericak-Vance M, Enghild J, Salvesen GS, Roses AD (1993) Apolipoprotein E: high-avidity binding to beta-amyloid and increased frequency of type 4 allele in late-onset familial Alzheimer disease. Proc Natl Acad Sci U S A 90:1977-1981.

Stutzmann GE, Smith I, Caccamo A, Oddo S, Laferla FM, Parker I (2006) Enhanced ryanodine receptor recruitment contributes to Ca2+ disruptions in young, adult, and aged Alzheimer's disease mice. J Neurosci 26:5180-5189.

Sudoh S, Kawamura Y, Sato S, Wang R, Saido TC, Oyama F, Sakaki Y, Komano H, Yanagisawa K (1998) Presenilin 1 mutations linked to familial Alzheimer's disease increase the intracellular levels of amyloid beta-protein 1-42 and its N-terminally truncated variant(s) which are generated at distinct sites. J Neurochem 71:1535-1543.

Sun A, Nguyen XV, Bing G (2002) Comparative analysis of an improved thioflavin-s stain, Gallyas silver stain, and immunohistochemistry for neurofibrillary tangle demonstration on the same sections. J Histochem Cytochem 50:463-472.

Sun GY, Shelat PB, Jensen MB, He Y, Sun AY, Simonyi A (2010) Phospholipases A2 and inflammatory responses in the central nervous system. Neuromolecular Med 12:133-148.

Sundaram JR, Chan ES, Poore CP, Pareek TK, Cheong WF, Shui G, Tang N, Low CM, Wenk MR, Kesavapany S (2012) Cdk5/p25-induced cytosolic PLA2-mediated lysophosphatidylcholine production regulates neuroinflammation and triggers neurodegeneration. J Neurosci 32:1020-1034.

Sundaram JR, Poore CP, Sulaimee NH, Pareek T, Asad AB, Rajkumar R, Cheong WF, Wenk MR, Dawe GS, Chuang KH, Pant HC, Kesavapany S (2013) Specific inhibition of p25/Cdk5 activity by the Cdk5 inhibitory peptide reduces neurodegeneration in vivo. J Neurosci 33:334-343.

Takano T, Tian GF, Peng W, Lou N, Libionka W, Han X, Nedergaard M (2006) Astrocyte-mediated control of cerebral blood flow. Nat Neurosci 9:260-267.

Takashima A, Murayama M, Yasutake K, Takahashi H, Yokoyama M, Ishiguro K (2001) Involvement of cyclin dependent kinase5 activator p25 on tau phosphorylation in mouse brain. Neurosci Lett 306:37-40.

Tan TC, Valova VA, Malladi CS, Graham ME, Berven LA, Jupp OJ, Hansra G, McClure SJ, Sarcevic B, Boadle RA, Larsen MR, Cousin MA, Robinson PJ (2003) Cdk5 is essential for synaptic vesicle endocytosis. Nat Cell Biol 5:701-710.

Tandon A, Yu H, Wang L, Rogaeva E, Sato C, Chishti MA, Kawarai T, Hasegawa H, Chen F, Davies P, Fraser PE, Westaway D, St George-Hyslop PH (2003) Brain levels of CDK5 activator p25 are not increased in Alzheimer's or other neurodegenerative diseases with neurofibrillary tangles. J Neurochem 86:572-581.

Tandon R, Adak S, Kaye JA (2006) Neural networks for longitudinal studies in Alzheimer's disease. Artif Intell Med 36:245-255.

Tang D, Wang JH (1996) Cyclin-dependent kinase 5 (Cdk5) and neuron-specific Cdk5 activators. Prog Cell Cycle Res 2:205-216.

Tang D, Yeung J, Lee KY, Matsushita M, Matsui H, Tomizawa K, Hatase O, Wang JH (1995) An isoform of the neuronal cyclin-dependent kinase 5 (Cdk5) activator. J Biol Chem 270:26897-26903.

Tannoch VJ, Hinds PW, Tsai LH (2000) Cell cycle control. Adv Exp Med Biol 465:127-140.

Tariq M, Khan HA, Al Moutaery K, Al Deeb S (2001) Protective effect of quinacrine on striatal dopamine levels in 6-OHDA and MPTP models of Parkinsonism in rodents. Brain Res Bull 54:77-82.

Tarkowski E, Liljeroth AM, Minthon L, Tarkowski A, Wallin A, Blennow K (2003) Cerebral pattern of pro- and anti-inflammatory cytokines in dementias. Brain Res Bull 61:255-260.

Tarricone C, Dhavan R, Peng J, Areces LB, Tsai LH, Musacchio A (2001) Structure and regulation of the CDK5-p25(nck5a) complex. Mol Cell 8:657-669.

Teipel SJ, Ewers M, Wolf S, Jessen F, Kolsch H, Arlt S, Luckhaus C, Schonknecht P, Schmidtke K, Heuser I, Frolich L, Ende G, Pantel J, Wiltfang J, Rakebrandt F, Peters O, Born C, Kornhuber J, Hampel H (2010) Multicentre variability of MRI-based medial temporal lobe volumetry in Alzheimer's disease. Psychiatry Res 182:244-250.

Thies W, Bleiler L (2013) 2013 Alzheimer's disease facts and figures. Alzheimers Dement 9:208-245.

Thinakaran G, Koo EH (2008) Amyloid precursor protein trafficking, processing, and function. J Biol Chem 283:29615-29619.

Tokuoka H, Saito T, Yorifuji H, Wei F, Kishimoto T, Hisanaga S (2000) Brain-derived neurotrophic factor-induced phosphorylation of neurofilament-H subunit in primary cultures of embryo rat cortical neurons. J Cell Sci 113 (Pt 6):1059-1068.

Tomizawa K, Ohta J, Matsushita M, Moriwaki A, Li ST, Takei K, Matsui H (2002) Cdk5/p35 regulates neurotransmitter release through phosphorylation and downregulation of P/Q-type voltage-dependent calcium channel activity. J Neurosci 22:2590-2597.

Tomizawa K, Sunada S, Lu YF, Oda Y, Kinuta M, Ohshima T, Saito T, Wei FY, Matsushita M, Li ST, Tsutsui K, Hisanaga S, Mikoshiba K, Takei K, Matsui H (2003) Cophosphorylation of amphiphysin I and dynamin I by Cdk5 regulates clathrin-mediated endocytosis of synaptic vesicles. J Cell Biol 163:813-824.

Torres-Aleman I (2008) Mouse models of Alzheimer's dementia: current concepts and new trends. Endocrinology 149:5952-5957.

Town T, Tan J, Flavell RA, Mullan M (2005) T-cells in Alzheimer's disease. Neuromolecular Med 7:255-264.

Town T, Laouar Y, Pittenger C, Mori T, Szekely CA, Tan J, Duman RS, Flavell RA (2008) Blocking TGF-beta-Smad2/3 innate immune signaling mitigates Alzheimer-like pathology. Nat Med 14:681-687.

Tripanichkul W, Jaroensuppaperch EO (2013) Ameliorating effects of curcumin on 6-OHDA-induced dopaminergic denervation, glial response, and SOD1 reduction in the striatum of hemiparkinsonian mice. Eur Rev Med Pharmacol Sci 17:1360-1368.

Tsai LH, Lee MS, Cruz J (2004) Cdk5, a therapeutic target for Alzheimer's disease? Biochim Biophys Acta 1697:137-142.

Tsai LH, Delalle I, Caviness VS, Jr., Chae T, Harlow E (1994) p35 is a neural-specific regulatory subunit of cyclin-dependent kinase 5. Nature 371:419-423.

Tseng HC, Zhou Y, Shen Y, Tsai LH (2002) A survey of Cdk5 activator p35 and p25 levels in Alzheimer's disease brains. FEBS Lett 523:58-62.

Tuppo EE, Arias HR (2005) The role of inflammation in Alzheimer's disease. Int J Biochem Cell Biol 37:289-305.

Uozumi N, Kume K, Nagase T, Nakatani N, Ishii S, Tashiro F, Komagata Y, Maki K, Ikuta K, Ouchi Y, Miyazaki J, Shimizu T (1997) Role of cytosolic phospholipase A2 in allergic response and parturition. Nature 390:618-622.

van der Worp HB, Howells DW, Sena ES, Porritt MJ, Rewell S, O'Collins V, Macleod MR (2010) Can animal models of disease reliably inform human studies? PLoS Med 7:e1000245.

Venda LL, Cragg SJ, Buchman VL, Wade-Martins R (2010) alpha-Synuclein and dopamine at the crossroads of Parkinson's disease. Trends Neurosci 33:559-568.

Vesce S, Rossi D, Brambilla L, Volterra A (2007) Glutamate release from astrocytes in physiological conditions and in neurodegenerative disorders characterized by neuroinflammation. Int Rev Neurobiol 82:57-71.

Vina J, Lloret A (2010) Why women have more Alzheimer's disease than men: gender and mitochondrial toxicity of amyloid-beta peptide. J Alzheimers Dis 20 Suppl 2:S527-533.

Vosler PS, Brennan CS, Chen J (2008) Calpain-mediated signaling mechanisms in neuronal injury and neurodegeneration. Mol Neurobiol 38:78-100.

Wang H, Yu SW, Koh DW, Lew J, Coombs C, Bowers W, Federoff HJ, Poirier GG, Dawson TM, Dawson VL (2004) Apoptosis-inducing factor substitutes for caspase executioners in NMDA-triggered excitotoxic neuronal death. J Neurosci 24:10963-10973.

Wang HM, Zhao YX, Zhang S, Liu GD, Kang WY, Tang HD, Ding JQ, Chen SD (2010) PPARgamma agonist curcumin reduces the amyloid-beta-stimulated inflammatory responses in primary astrocytes. J Alzheimers Dis 20:1189-1199.

Wang JZ, Grundke-Iqbal I, Iqbal K (2007) Kinases and phosphatases and tau sites involved in Alzheimer neurofibrillary degeneration. Eur J Neurosci 25:59-68.

Wang Q, Wu J, Rowan MJ, Anwyl R (2005) Beta-amyloid inhibition of long-term potentiation is mediated via tumor necrosis factor. Eur J Neurosci 22:2827-2832.

Wang Y, Yin H, Wang L, Shuboy A, Lou J, Han B, Zhang X, Li J (2013) Curcumin as a potential treatment for Alzheimer's disease: a study of the effects of curcumin on hippocampal expression of glial fibrillary acidic protein. Am J Chin Med 41:59-70.

Wei FY, Tomizawa K, Ohshima T, Asada A, Saito T, Nguyen C, Bibb JA, Ishiguro K, Kulkarni AB, Pant HC, Mikoshiba K, Matsui H, Hisanaga S (2005) Control of cyclin-dependent kinase 5 (Cdk5) activity by glutamatergic regulation of p35 stability. J Neurochem 93:502-512.

Wells K, Farooqui AA, Liss L, Horrocks LA (1995) Neural membrane phospholipids in Alzheimer disease. Neurochem Res 20:1329-1333.

Wen Y, Yang SH, Liu R, Perez EJ, Brun-Zinkernagel AM, Koulen P, Simpkins JW (2007) Cdk5 is involved in NFT-like tauopathy induced by transient cerebral ischemia in female rats. Biochim Biophys Acta 1772:473-483.

Wen Y, Yu WH, Maloney B, Bailey J, Ma J, Marie I, Maurin T, Wang L, Figueroa H, Herman M, Krishnamurthy P, Liu L, Planel E, Lau LF, Lahiri DK, Duff K (2008) Transcriptional regulation of beta-secretase by p25/cdk5 leads to enhanced amyloidogenic processing. Neuron 57:680-690.

Wender M, Adamczewska-Goncerzewicz Z, Szczech J, Godlewski A (1988) Myelin lipids in aging human brain. Neurochem Pathol 8:121-130.

Westerman MA, Cooper-Blacketer D, Mariash A, Kotilinek L, Kawarabayashi T, Younkin LH, Carlson GA, Younkin SG, Ashe KH (2002) The

relationship between Abeta and memory in the Tg2576 mouse model of Alzheimer's disease. J Neurosci 22:1858-1867.

White JA, Manelli AM, Holmberg KH, Van Eldik LJ, Ladu MJ (2005) Differential effects of oligomeric and fibrillar amyloid-beta 1-42 on astrocyte-mediated inflammation. Neurobiol Dis 18:459-465.

Whitehouse PJ, Price DL, Clark AW, Coyle JT, DeLong MR (1981) Alzheimer disease: evidence for selective loss of cholinergic neurons in the nucleus basalis. Ann Neurol 10:122-126.

Wisniewski T, Castano EM, Golabek A, Vogel T, Frangione B (1994) Acceleration of Alzheimer's fibril formation by apolipoprotein E in vitro. Am J Pathol 145:1030-1035.

Wortmann M (2012) Dementia: a global health priority - highlights from an ADI and World Health Organization report. Alzheimers Res Ther 4:40.

Wu W, Li M, Liu L, Gao J, Kong H, Ding J, Hu G, Xiao M (2011) Astrocyte activation but not neuronal impairment occurs in the hippocampus of mice after 2 weeks of d-galactose exposure. Life Sci 89:355-363.

Wyss-Coray T, Lin C, Yan F, Yu GQ, Rohde M, McConlogue L, Masliah E, Mucke L (2001) TGF-beta1 promotes microglial amyloid-beta clearance and reduces plaque burden in transgenic mice. Nat Med 7:612-618.

Xia MQ, Hyman BT (1999) Chemokines/chemokine receptors in the central nervous system and Alzheimer's disease. J Neurovirol 5:32-41.

Xiong W, Pestell R, Rosner MR (1997) Role of cyclins in neuronal differentiation of immortalized hippocampal cells. Mol Cell Biol 17:6585-6597.

Yagami T, Ueda K, Asakura K, Hata S, Kuroda T, Sakaeda T, Takasu N, Tanaka K, Gemba T, Hori Y (2002) Human group IIA secretory phospholipase A2 induces neuronal cell death via apoptosis. Mol Pharmacol 61:114-126.

Yamaguchi H, Ishiguro K, Uchida T, Takashima A, Lemere CA, Imahori K (1996) Preferential labeling of Alzheimer neurofibrillary tangles with antisera for tau protein kinase (TPK) I/glycogen synthase kinase-3 beta and cyclin-dependent kinase 5, a component of TPK II. Acta Neuropathol 92:232-241.

Yang F, Lim GP, Begum AN, Ubeda OJ, Simmons MR, Ambegaokar SS, Chen PP, Kayed R, Glabe CG, Frautschy SA, Cole GM (2005) Curcumin inhibits formation of amyloid beta oligomers and fibrils, binds plaques, and reduces amyloid in vivo. J Biol Chem 280:5892-5901.

Yao M, Nguyen TV, Pike CJ (2005) Beta-amyloid-induced neuronal apoptosis involves c-Jun N-terminal kinase-dependent downregulation of Bcl-w. J Neurosci 25:1149-1158.

Yin X, Warner DR, Roberts EA, Pisano MM, Greene RM (2005) Novel interaction between nuclear co-activator CBP and the CDK5 activator binding protein - C53. Int J Mol Med 16:251-256.

Yoo BC, Lubec G (2001) p25 protein in neurodegeneration. Nature 411:763-764; discussion 764-765.

Yoshinaga N, Yasuda Y, Murayama T, Nomura Y (2000) Possible involvement of cytosolic phospholipase A(2) in cell death induced by 1-methyl-4-phenylpyridinium ion, a dopaminergic neurotoxin, in GH3 cells. Brain Res 855:244-251.

Yoshiyama Y, Higuchi M, Zhang B, Huang SM, Iwata N, Saido TC, Maeda J, Suhara T, Trojanowski JQ, Lee VM (2007) Synapse loss and microglial activation precede tangles in a P301S tauopathy mouse model. Neuron 53:337-351.

Yuan J, Yankner BA (2000) Apoptosis in the nervous system. Nature 407:802-809.

Zempel H, Thies E, Mandelkow E, Mandelkow EM (2010) Abeta oligomers cause localized Ca(2+) elevation, missorting of endogenous Tau into dendrites, Tau phosphorylation, and destruction of microtubules and spines. J Neurosci 30:11938-11950.

Zhang C, Browne A, Child D, Tanzi RE (2010) Curcumin decreases amyloid-beta peptide levels by attenuating the maturation of amyloid-beta precursor protein. J Biol Chem 285:28472-28480.

Zhang J, Krishnamurthy PK, Johnson GV (2002) Cdk5 phosphorylates p53 and regulates its activity. J Neurochem 81:307-313.

Zhang S, Edelmann L, Liu J, Crandall JE, Morabito MA (2008) Cdk5 regulates the phosphorylation of tyrosine 1472 NR2B and the surface expression of NMDA receptors. J Neurosci 28:415-424.

Zhang YW, Thompson R, Zhang H, Xu H (2011) APP processing in Alzheimer's disease. Mol Brain 4:3.

Zhao J, O'Connor T, Vassar R (2011) The contribution of activated astrocytes to Abeta production: implications for Alzheimer's disease pathogenesis. J Neuroinflammation 8:150.

Zheng YL, Li BS, Amin ND, Albers W, Pant HC (2002) A peptide derived from cyclin-dependent kinase activator (p35) specifically inhibits Cdk5 activity and phosphorylation of tau protein in transfected cells. Eur J Biochem 269:4427-4434.

Zheng YL, Kesavapany S, Gravell M, Hamilton RS, Schubert M, Amin N, Albers W, Grant P, Pant HC (2005) A Cdk5 inhibitory peptide reduces tau hyperphosphorylation and apoptosis in neurons. Embo J 24:209-220.

Zheng YL, Amin ND, Hu YF, Rudrabhatla P, Shukla V, Kanungo J, Kesavapany S, Grant P, Albers W, Pant HC (2010) A 24-residue peptide (p5), derived from p35, the Cdk5 neuronal activator, specifically inhibits Cdk5-p25 hyperactivity and tau hyperphosphorylation. J Biol Chem 285:34202-34212.

Zhou X, Spittau B, Krieglstein K (2012) TGFbeta signalling plays an important role in IL4-induced alternative activation of microglia. J Neuroinflammation 9:210.

Zhu M, Gu F, Shi J, Hu J, Hu Y, Zhao Z (2008) Increased oxidative stress and astrogliosis responses in conditional double-knockout mice of Alzheimer-like presenilin-1 and presenilin-2. Free Radic Biol Med 45:1493-1499.

Zhu YG, Chen XC, Chen ZZ, Zeng YQ, Shi GB, Su YH, Peng X (2004) Curcumin protects mitochondria from oxidative damage and attenuates apoptosis in cortical neurons. Acta Pharmacol Sin 25:1606-1612.

Zilka N, Ferencik M, Hulin I (2006) Neuroinflammation in Alzheimer's disease: protector or promoter? Bratisl Lek Listy 107:374-383.

Zonta M, Angulo MC, Gobbo S, Rosengarten B, Hossmann KA, Pozzan T, Carmignoto G (2003) Neuron-to-astrocyte signaling is central to the dynamic control of brain microcirculation. Nat Neurosci 6:43-50.

Zou JY, Crews FT (2005) TNF alpha potentiates glutamate neurotoxicity by inhibiting glutamate uptake in organotypic brain slice cultures: neuroprotection by NF kappa B inhibition. Brain Res 1034:11-24.

Zou LB, Yamada K, Tanaka T, Kameyama T, Nabeshima T (1998) Nitric oxide synthase inhibitors impair reference memory formation in a radial arm maze task in rats. Neuropharmacology 37:323-330.

Zukerberg LR, Patrick GN, Nikolic M, Humbert S, Wu CL, Lanier LM, Gertler FB, Vidal M, Van Etten RA, Tsai LH (2000) Cables links Cdk5 and c-Abl and facilitates Cdk5 tyrosine phosphorylation, kinase upregulation, and neurite outgrowth. Neuron 26:633-646.

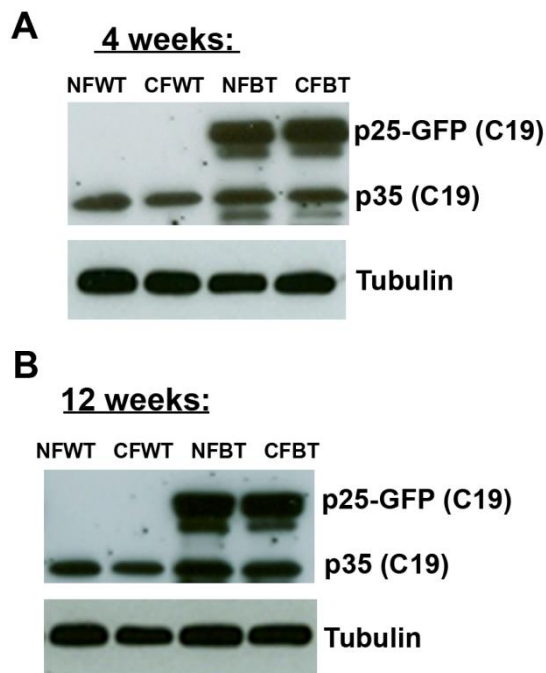# APPENDICES

Supplementary Figures

Supplementary Figure 1:
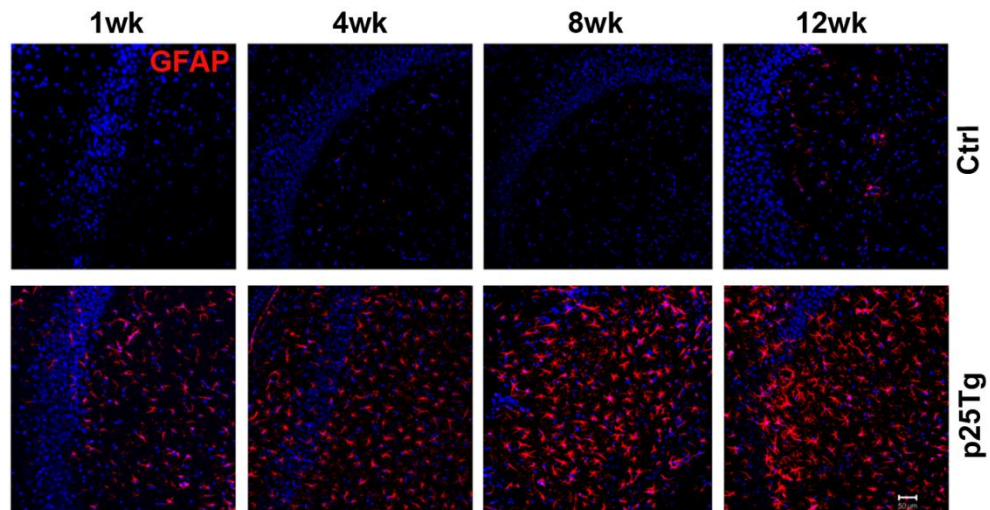
Astrogliosis in p25 transgenic mice

Representative immunofluorescence images of hippocampus (CA3 region) from 1, 4, 8 and 12-week induced p25Tg and their respective age-matched control (Ctrl) mice brain sections stained with anti-GFAP antibody (red) and nuclei were stained with DAPI (blue). Scale bars represent 50µm and images are representative of n=3 mice.

Supplementary Figure 2:

A   4 weeks:

NFWT CFWT NFBT CFBT

p25-GFP (C19)

p35 (C19)

Tubulin

B
12 weeks:

NFWT CFWT NFBT CFBT

p25-GFP (C19)

p35 (C19)

Tubulin

Endogenous p35 expression and exogenous p25 expression levels in p25Tg mice

Western blot results of brain lysates from the (**A**) 4-week and (**B**) 12-week induced p25Tg mice with normal feed (NFBT), p25Tg mice with curcumin feed (CFBT), respective age-matched WT mice with normal feed (NFWT) and WT mice with curcumin feed (CFWT) using anti-C19 antibody (n=3). Membranes were re-probed with anti-tubulin antibody which acts as a loading control.